On the Geochemical Study of Carbon 14. I. The Ozegahara Peat

By Makoto SHIMA

(Received November 9, 1955)

Introduction

It is well known that ^{14}C is continuously produced in the atomsphere by the action of neutrons produced by cosmic-rays, involving the reaction $^{14}N(n, p) \rightarrow {}^{14}C$. Libby[1], with a number of associates, for the first time recognized that atmospheric carbon dioxide, including those present in hydrosphere and biosphere, showed radio-activity of the order of 15.3 dpm. per g, (about $1.5 \times 10^{-10}\%$). He also found that the age of substances containing carbon can be calculated from the half-life of ^{14}C (5568±30 years). Since these pioneering experiments[2,3], Libby and Arnold measured and published the ages of more than 100 specimens, including neary every conceivable kind of relic of the past. In Japan, T. Hamada and F. Yamazaki set up a counter of Libby's type and mainly measured the amount of ^{14}C in the biological and archaeological substances[4].

The present author took up this method to determine the age of peat in Ozegahara in his study of geochemistry with special reference to the sedimentation of coal. It was found that the layer of 2 m. beneath the surface is about 1000 years old and that of 3 to 4 m. is about 5000 years old. The rate of sedimentation is about 1.6 mm. per year at present and appears to have been 1 mm. and 0.25 mm. per year when the layers 2 m. and 3–4 m. beneath the surfaces were formed, respectively. This fact suggests that the apparent volume of the peat has been changed to such an extent in the course of the years concerned.

Sample Occurrence

Ozegahara exists on the boundary of Tochigi, Fukushima, Niigata and Gumma prefectures. It is a famous subtundra. The peat of Ozegahara had been formed upon the lake sediments of the old Ozegahara lake.

1) W.F. Libby et al., *Science*, **109**, 227 (1949); ibid, **110**, 678 (1949); *Phys. Rev.*, **81**, 64 (1951); *R. S. I.*, **22**, 225 (1951).
2) W. F. Libby, "Radiocarbon Dating", Univ. of Chicago Press (1952).
3) T.P. Kohman and N. Saito, *Ann. Review of Nuclear Sci.*, **4**, 401 (1954).
4) T. Hamada, *Nuclear Study*, **1**, No. 3, 187 (1954) (in Japanese).

The samples at Nakatashiro (P11) are illustrated in the column section (Fig. 1). At

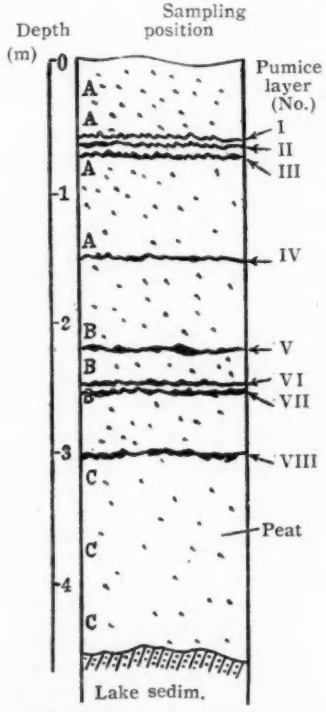

Fig. 1. The column section of peat occurence.

480 cm. depth there are sand and clay layers of the old Ozegahara lake sediments. During the peat sedimentation, volcanic action occurred several times and then layers of volcanic ash and pumice were formed as shown in Fig. 1. The peat is found in two different types of texture in the layers, and the two types are mixed with each other. One is fibrous and maintains the original plant organ; the other is so-called sedimentary peat and the texture has been destroyed by volcanic sediments. The volcanic sediments has 8 layers; among them, No. 2, No. 3 (both Ikaho pumice), No. 6 and No. 7 (Nantai pumice) predominate. The sampling position is shown in Fig. 1. "A" represents the

CHEMISTRY HALL LIBRARY

samples of the first unit, "B" those of the second and "C" those of the third.

Chemical Procedure

Chemical processing was almost the same as Libby's[2], except several points as shown below.

a) Chemical Procedure.—The apparatus, in which the main part of the chemical procedure was conducted, is shown in Fig. 2. The combustion of the sample (40-50 g. dry peat) is carried

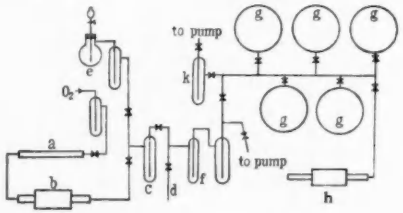

Fig. 2. Chemical preparation apparatus.

out in the quartz tube (a). Oxygen is slowly passed over the sample, which is ignited at its one end. The combustion gas is passed through the copper oxide wire, heated at about 600°C (quartz tube b) to complete the oxidation, is dried in the dry-ice trap (c) and introduced into ammonium hydroxide solution.

In this method, the final product consists only of carbon dioxide, contaminated by oxides of nitrogen and sulfur, resulting from combustion of minor constituents of the peat. It is necessary to carry out a chemical purification before carbon dioxide is submitted to reduction. Therefore the combustion gas is taken out through (d).

A 1 l. flask containing 500 ml. of 6 N ammonium hydroxide is attached to the end of (d). In this vessel, carbon dioxide is absorbed by ammonia and is converted into $(NH_4)_2CO_3$. A rapid absorption of the gas is effected. During this reaction the flask is shaken to insure the absorption until the sample is burnt off. A second solution, containing 180 g. of calcium chloride in 180 ml. of water, is heated nearly to boiling. The flask is removed from the line, and the hot calcium chloride solution is added slowly with stirring. A rapid precipitation of calcium carbonate takes place. The precipitate is filtered and washed with water on a Buechner funnel. At this point, all of the oxides of nitrogen and sulfur have been left behind in the form of soluble salts. After washing, the precipitate is dried in an air bath. This calcium carbonate (about 130 g.) precipitate is transferred to flask (e). Carbon dioxide is now recovered from the precipitate, using the same system employed in the combustion by adding concentrated hydrochloric acid. The stopcock leading to the flask is opened, and acid is added from a separatory funnel (about 200 ml.).

The chemical purification procedure is thus completed. The recovered gas is passed through the dry-ice trap (c) into two successive liquid air traps (f) in which the carbon dioxide is condensed. The Dewars are removed and the solid carbon dioxide is evolved. The gas is passed into the system of reserver (g) (total volume, 25 l.) which has been already evacuated, and then the gas is ready for the reduction step. Reduction is carried out in a seamless stainless steel tube (h) which is filled with 80 g. of magnesium turning together with a little of cadmium turning as a catalyst. An electric furnace, capable of reaching about 800°C, is placed around the tube. One end of the tube is sealed with a rubber stopper and wax, and the reduction system is evacuated and tested for freedom from leaks. Carbon dioxide is now admitted to the tube up to a pressure approaching one atmosphere, and external heat is applied to the magnesium filling. When it gets the melting point of magnesium (660°C), the reaction begins violently and produces sufficient heat to maintain itself, provided that the gas is admitted at a moderate rate from the bulbs. Since the reaction "$2Mg+CO_2=2MgO+C$" yields no gaseous products, no circulation is required. It is the practice to run the gas from the bulb until the pressure is reduced to about 200 mmHg, when the next bulb is cut in. In this way the gas can be reacted smoothly before the other end of the magnesium filling is reached. To complete the reduction, it is necessary to apply external heat using the furnace. The remaining gas is condensed in the trap (k) and may either be expanded into a single bulb or allowed to react directly. After this method, has been used the remaining gas is no more than 50 mmHg. The reduction tube is allowed to cool, and the carbon, magnesium oxide and unreacted magnesium are removed from the tube using an iron rod. These products are transferred to a 5 l. beaker. Concentrated hydrochloric acid is cautiously added (total, of about 800 ml.); violent evolution of gas takes place. The mixture is allowed to stand overnight. It is then brought to boiling point on a large hot plate. One litre of water is added and it is again boiled for about fifteen minutes. The supernatant is then removed by filtration, using a sintered glass filter stick operating directly into a water aspirator; 300 ml. of nitric acid is added to the residue. The nitric acid solution is again nearly boiled for fifteen minutes and filtered. It is recognized that this method eliminates the carbon ash at least down to a fraction of a percent. One and a half litres of water are added; the solution is once again boiled for fifteen minutes and filtered. This cycle is repeated three times more. After the carbon is washed into a small beaker, the water is removed using the filter stick. This beaker is transferred into an air-bath and the carbon is thoroughly dried. The carbon thus obtained weighs about 12–15 g. It is now ready for mounting and measurement. The overall yield of the chemical processing sequence, described above, is in the neighborhood of 80% of the carbon content of the peat. One of the problems in producing a final product free from intrusive radioactivity is, of course, the purity of the reagent used. After burning, the peat ash was analysed by the common plant analytical method. Water content of peat was measured in

a water stop trap. The carbon ash was analysed by the combustion method and the total impurity (mainly Fe, Mg, Ca, etc.) was measured.

b) Mounting Procedure.—At the carbon corrected by the above methods is coarse, it is fully ground by an agate motor. About 8 g. of carbon are weighed into a 150 ml. beaker. Water (total volume, about 50 ml.) is added little by little continuously with stirring, until the well-stirred slurry maintains just the proper consistency. This can be judged by the rate of flow on tipping the beaker. The slimy mass is transferred to the one of the pair of a split cylinder which can be connected together, (for details of counter construction see below), using a long glass rod.

The cylinder is continuously rolled with a moter driven rotator throughout the mounting. A small portion of the slime is placed on the one end of the cylinder and spread with the aid of a long glass rod so that a uniform layer is formed on the inner surface of the cylinder. Care must be taken to make the slurry just slimy enough to keep itself on the surface. Then a hot stream of air is blown over the inside of the rotating cylinder with a hair dryer. After about five minutes, sufficient water will be thus removed and the carbon layer is fixed on the surface so firmly that no appreciable amount falls down during the further procedure. The pair of the cylinders are connected together and inserted into the screen-wall counter through the free end. When the layer is too dry, it may be torn off forming a crack on the surface. Therefore the drying must be given up before it gets too dry. The end cap is put on and attached to a vacuum system and the remaining water is generally pumped off through a dry ice trap. This operations must be carried out rapidly and with special attention not to touch the cylinder or the sample by hand. After two days when no leakage is observed, ethylene (6 mmHg) and argon (100 mmHg) are introduced into the cylinder. After one night the whole is transferred into a shielding box and submitted to measurement.

After each run, the sample is removed from the cylinder with a spatula. The final cleaning of the cylinder (before mounting a new sample) is achieved by carefully wiping it with a powder-paper.

Instrument

The author has used the counter that was made by Yamazaki's group. The instrument is illustrated by Mr. T. Hamada in detail[4].

a) Screen-wall Counter. — The screen-wall counter has the grid wire between the anode and the cathode of an ordinary cylindrical Geiger-Müller tube. The counter, presently in use, is illustrated in Fig. 3. The main part is almost the same as the Libby's counter, but is not so in some material used. The counts of the sample and background can be directly compared by sliding the cylinder from one end to the other.

b) Anticoindence Counter.—It is a common cosmic-ray counter shown in Fig. 4. The necessary reduction in background can be achieved by connecting the screen-wall counter and the eleven shielding counters placed around it in anticointences. These counters are filled with ethylformate (7 mmHg) and argon (100 mmHg).

c) Shiled.—A shiled is constructed of steel plates (1 inch thick; contributed by the Yahata Iron Company); the arrangement is shown in Fig. 5. The total thickness is 7 inches and the total weight amouts to 4.3 tons. The door is made of the same steel plates, and can be moved forward on the rail by hand.

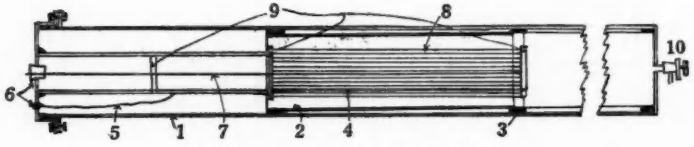

Fig. 3. The screen-wall counter.

1. Screen-wall counter body, brass-made. Inside diameter 75 mm., length 614 mm., thickness 1 mm.
2. Sample tube, copper-made. Inside diameter 67 mm., length 200 mm., two unit.
3. Joinband of above two copper tubes.
4. Grid support 5 drillrod.
5. Lead wire of grid.
6. Stupakoff seal.
7. Center wire. ♯28 Dumet wire.
8. Grid wire ♯30 Dumet wire 33 wires.
9. Methacryl-resin.
10. Bellows value.

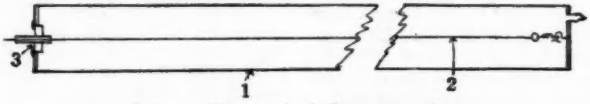

Fig. 4. The anticoindence counter.

1. 2″ Copper tube. thickness 2 mm., length 784 mm.
2. Center wire 0.1 mm. W wire.
3. Stupakoff seal.

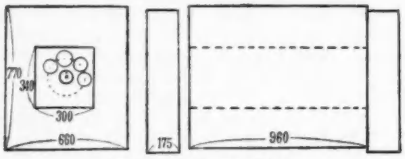

Fig. 5. The shielding.

High voltage and plate supply voltage are stabilized in the usual way.

Result

Sample A represents the upper part, sample B the mean part and sample C the lower part of the peat sediments. Chemical components of these ashes are analysed and shown in Table I.

TABLE I

CHEMICAL COMPONENT

Sample No.	Total Ash (%)	H_2O (%)	HCl (%) Insoluble	Si (%)	Al (%)	Fe (%)	Ca (%)	Mg (%)	Na (%)	K (%)
A	10	40	11.4	—	0.62	0.25	0.75	0.51	0.03	0.07
B	11	36	9.8	tr.	1.09	0.18	0.66	0.28	0.02	0.05
C	10	40	10.4	—	0.36	0.35	1.28	0.47	0.01	0.06

d) Electronic Circuit.—The circuit is shown in Fig. 6 in block diagram. High voltage regulator is shown it Fig. 7; this circuit is an automatic control of high voltage. Univibrator has

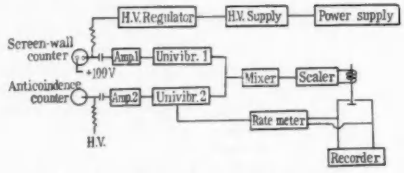

Fig. 6. Blockdiagram of circuits.

The variation of chemical components indicates that sample B has more clay part than the others. It can be explained in two ways: the pumice layer was dispersed into the peat layer or the chemical component migrated into the peat layer.

A chemical study has also been carefully made by Dr Yamagata[5]. Age determination of peat, carried out by the above method, requires about forty hours, for the background measurment twenty hours, and for the sample twenty hours. The two measurement can be carried out by changing the

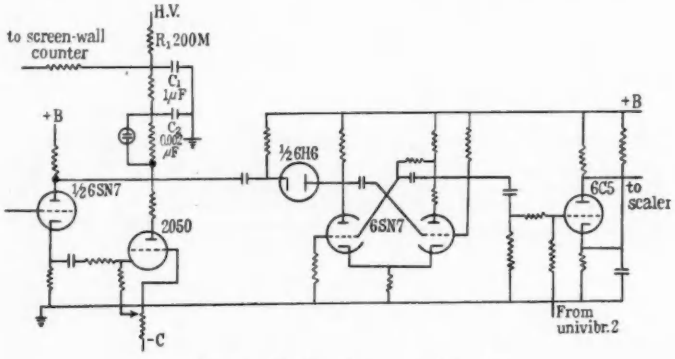

Fig. 7. High voltage regulater.

a dead time of 15 mμ seconds to prevent multiple pulses of the screen-wall counter. The mixer consists of the resistance network. The scaler is a scale of 16 using for 12AU7'S. The output of the scaler is fed to a thyratron. Each 16 counts of the screen-wall counter mark a knick on the recording paper. writing the background counting rate of the anticoindence counters, which is about 1400 cpm. During very long unattended runs which have to be made, there is the possibility of accidents. For this reason the automatic recording device was used.

position of the cylinder. These results are shown in Table II. Background of the instrument used, was about 4.5–5.5 cpm.

Conclusion

Several examples of the counts of the biological substances were shown by Yamazaki's[4] group and found to come between 5.5–6.3 cpm. Then the author considers that

5) N. Yamagata, Read before 1954's Geochemical Meeting of Chem. Soc. of Japan.

sample A can be regarded in the same way as the recent ones.

If so, sample B must be about 1000 years old and sample C 5000 years. The data are shown in Table II.

Dating by means of natural radio-carbon has some problems: constancy of ^{14}C specific activity, contamination by ^{14}C from different sources, constancy of cosmic ray flux, accuracy of measurement etc..

TABLE II

THE COUNTS OF NATURAL RADIO CARBON

Sample No.	Background			Sample counts			C^{14} c. pm.	Dating (y)	Carbon Ash (%)
	Time (min.)	Counts	c. p. m.	Time (min.)	Counts	c. p. m.			
A	1145.5	5856	5.11±0.067	1429.5	15296	10.7 ±0.086	5.59±0.10	0	4.79
B	1350.5	5856	4.34±0.056	1469.0	14584	9.25±0.084	4.91±0.10	1000±250	2.42
C	1161.5	5344	4.61±0.063	1095.5	8320	7.59±0.083	2.98±0.10	5000±400	2.40

The rate of sedimentation of peat is considered to be 1.6 mm. per year for sample A, 1.0 mm. per year for sample B, and 0.25 mm. per year for sample C.

If the rate of sedimentation has been the same as at present, sample C might have decreased its volume to about 1/6. During the 5000 years, sample C could have been pressed on the upper part or have lost some of its components by dissolution to descrease the volume to such an extend.

The volume of sample B has been also slightly decreased during the 1000 years. During the 5000 years, sedimentation of the total depth of this column region as thick as 480 cm. has been accumulated.

In other words the apparent mean rate of sedimentation is 0.7–0.9 mm. per year.

The author is of the opinion, however, that the present study is not interfered with by such factors, so far as the samples obtained from different depths at one position are studied. Further development is expected by fundamental experiments and by geochemical studies.

The author wishes to acknowledge the contributions of Dr. F. Yamazaki and Mr. T. Hamada in the counting equipment, and of Professor Dr. K. Kimura in giving valuable suggestions. The author is also grateful to Mrs. M. Shima (nèe Asada) and to Dr. N. Yamagata, for their kind supply of the samples.

Scientific Research Institute Ltd. Tokyo

Untersuchungen über die photochemischen Additionsreaktionen. III. Die Additionsreaktion von Mercaptanen an Propargylalkohol

Von Kazuo YAMAGISHI, Toyosuke TANAKA[1] und Toshio HOSHINO

(Eingegangen am 17. Januar 1956)

In der vorgehenden Mitteilung[2] konnte über die in besserer Ausbeute erfolgten photochemischen Additionsreaktionen einiger Mercaptane durch Belichtung mit ultravioletten Strahlen von etwa 3660 Å an die Doppelbindung solcher ungesättigten Verbindungen wie Vinylacetat, Vinylchlorid und Allylalkohol berichtet werden. Wir haben nun festgestellt, dass auch Mercaptane unter fast gleichen Bedingungen an die Dreifachbindung des Propargylalkohols addieren können, und dass die gesättigten Verbindungen, anders als bei Anlagerungen an Doppelbindungen, unter Umständen durch die zweifache Addition von Mercaptanen gewonnen werden.

Die Additionsreaktion von Methylmercaptan an Propargylalkohol liess sich herbeiführen beizweistündiger Belichtung mit ultravioletten Strahlen unter Verwendung von Methylmercapto-quecksilber, Merkuriacetaten oder Azo-iso-buttersäurenitril als Katalysatoren in Stickstoffatmosphäre. Es ergab sich ein katalytischer Effekt des Sauerstoffs, wenn die Reaktion in Sauerstoffatmosphäre ausgeführt

1) Institut für Chemie der Saitama Universität, Urawa.

2) T. Hoshino, K. Yamagishi und Y. Ichikawa, *J. Chem. Soc. Japan, (Reiner Chem. Teil)*, **74**, 510 (1953). K. Yamagishi und N. Nakajima, ibid., **75**, 1086 (1954).

wurde. Die Ausbeute unter diesen Bedingungen betrug bis zu 50–60%. Ohne diese Katalysatoren oder Belichtung mit ultravioletten Strahlen kam es zu keiner Additionsreaktion. Die Temperaturerhöhung des Reaktionsgemisches bei der Additionsreaktion sind in Fig. 1 dargestellt.

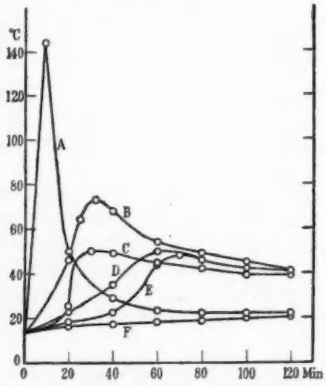

Fig. 1. Schema für die Temperaturerhöhung des Reaktionsgemisches.

A: Azo-iso-buttersäurenitril—N_2
B: Methylmercapto-quecksilber—O_2
C: Methylmercapto-quecksilber—N_2
D: Ohne Katalysator—O_2
E: Merkuriacetaten—N_2
F: Ohne Katalysator—N_2

Bei der Fortsetzung der Belichtung bis zu sechs Stunden steigerte sich die Ausbeute auf etwa 65–80%. Es ergab sich ferner: Die Additionsreaktionen von *n*-Butyl-, Phenyl- und Benzylmercaptan an Propargylalkohol unter Verwendung von Merkuriacetaten als Katalysator bei vierstündiger Belichtung verliefen unter geringer Temperaturerhöhung des Reaktionsgemisches mit langsamer Reaktionsgeschwindigkeit. Die Ausbeute hierbei betrug bis zu 50% beziehungsweise 40% und 30%.

2, 3-Dimethylmercapto-propanol wurde durch Additionsreaktion von Methylmercaptan an Propargylalkohol gewonnen, 2, 3-Di-*n*-butylmecrapto-propanol durch Additionsreaktion von *n*-Butylmercaptan und 2, 3-Dibenzylmercapto-propanol durch Reaktion von Benzylmercaptan. Diese Produkte sind neue Verbindungen ausserhalb 2, 3-Dimethylmercapto-propanol[3,4]. Das Additionsprodukt von Methylmercaptan an Propargylalkohol erwies sich auf Grund der physikalischen Konstanten und der Elementaranalyse als identisch mit dem authentischen Produkt 2, 3-Dimethylmercapto-propanol, das von A. De Barbieri und S. Tricerri[3] aus Natriummethylsulfid und Allylalkoholdibromid dargestellt wurde. Darum darf man von den Konstitutionen anderer Produkte dasselbe annehmen.

3) A. De Barbieri und S. Tricerri, *Boll. soc. ital. biol. sper.*, 25, 522 (1949); *C.A.*, 44, 8862 (1950).
4) R.M. Evans, J.B. Fraser und L.N. Owen, *J. Chem. Soc.*, 1949, 248.

Beschreibung der Versuche

Käuflicher Propargylalkohol wurde einmal fraktioniert, dann mit Kupfersulfat getrocknet, schliesslich innerhalb der Siedegrenzen von 113° rektifiziert und der Additionsreaktion unterworfen. Die Mercaptane wurden auf die übliche Weise dargestellt. Die photochemische Reaktion wurde, wie bei den früher mitgeteilten Versuchen, meist auf die folgenden Weise herbeigeführt:

Eine Mischung von 0.1 Mol Propargylalkohol und 0.22 Mol Mercaptan wurde in einem Reaktionsrohr von 80 ccm Inhalt auf −40° gekühlt. Nach Ersetzung der Rohratmosphäre durch Stickstoff wurde sie mittels einer Quecksilberlampe von 200 Watt (SHL-200, Japan Akkumulator A. G., Kyoto) ultravioletter Belichtung ausgesetzt. Das nach dem Verdampfen des unveränderten Materials zurückgebliebene Produkt wurde im Vakuum destilliert.

Einige Eigenschaften der Additionsprodukte werden im folgenden beschrieben.

1) 2, 3-Dimethylmercapto-propanol: Sdp. 88° (1 mm); $d_4^{19}=1.144$; $n_D^{19}=1.5431$.

Anal. Gef.: C, 39.60; H, 7.82; S, 42.25. Ber. für $C_5H_{12}OS_2$: C, 39.44; H, 7.94; S, 42.11%.

Die farblose und viskose Substanz riecht nach Methionol[5], dem wichtigsten Riechstoff in der japanischen Sojasauce, löst sich leicht in Äther, Methanol, Äthanol, Aceton und Benzol, aber schwer in Petroläther und Wasser. Das aus dieser Substanz und Quecksilberchlorid dargestellte Doppelsalz schmilzt bei 92°.

2) 2, 3-Di-n-butylmercapto-propanol: Sdp. 132–133° (1 mm); $d_4^{15}=0.997$; $n_D^{15}=1.5089$.

Anal. Gef.: C, 55.71; H, 10.03; S, 26.98. Ber. für $C_{11}H_{24}OS_2$: C, 55.88; H, 10.23; S, 27.12%.

3) 2, 3-Diphenylmercapto-propanol: Sdp. 119–122° (10^{-2} mm); $d_4^{21}=1.178$; $n_D^{21}=1.6301$.

Anal. Gef.: C, 64.93; H, 6.05; S, 23.42. Ber. für $C_{15}H_{16}OS_2$: C, 65.18; H, 5.84; S, 23.20%.

4) 2, 3-Dibenzylmercapto-propanol: Sdp. 120–130° (5×10^{-4} mm); $d_4^{24}=1.155$; $n_D^{24}=1.6085$.

Anal. Gef.: C, 66.91; H, 6.61; S, 21.36. Ber. für $C_{17}H_{20}OS_2$: C, 67.06; H, 6.62; S, 21.06%.

Wir möchten hier dem Unterrichtsministrium für die Gewährung einer Unterstützung zur Anregung wissenschaftlicher Forschung Dank sagen, ebenso auch Herrn Asaji Kondoh für die Ausführung der Mikroanalysen.

Das Institut für organische Chemie der Technischen Hochschule Tokyo, Tokyo

5) S. Akabori uud T. Kaneko, *J. Chem. Soc. Japan (Reiner Chem. Teil)*, 57, 832 (1936).

Diphenylcarbazone as an Internal Indicator in Volumetric Analysis. III. Volumetric Determination of Thorium by Ammonium Molybdate

By G. S. Deshmukh and Indumati Bokil

(Received September 19, 1955)

The growing interest in the chemistry of thorium and its compounds has necessitated the development of new and rapid methods of analysis. Of the large number of procedures which have appeared in the literature, practically all are based on the precipitation of thorium in some form from its solution and subsequent gravimetric determination as ThO_2[1,2]. Comparatively few titrimetric methods have been reported for estimating thorium. Among these the iodate method of Chernikhov and Uspenskaya[3] as modified by Moeller and Fritz[4] and the oxidimetric oxalate method of Gooch and Kabayshi[5] are noteworthy. The possibility of precipitating thorium oxinate and titrating the equivalent of iodine as suggested by Berg[6] has been extensively studied. Iodometric titration of selenious acid liberated from a quantitatively precipitated thorium selenite has been reported from these laboratories[7]. The molybdate procedure of Metzger and Zones[8] which has been modified by Banks and Diehl[9] is found to be applicable to pure thorium or the mixed thorium uranium solution.

Amperometric titration of thorium with ammonium molybdate has recently been studied by Gordon[10], and it is claimed that under the specified conditions, this procedure may be adopted for the estimation of thorium in presence of rare earths and other congeners. Recent observations in these laboratories on the use of diphenylcarbazone as an internal indicator in volumetric analysis showed that on treatment with ammonium molybdate this indicator develops an intense pink colour which is destroyed by the addition of a lead salt solution. The colour change was found to be reversible and formed therefore the basis of the titrimetric determination of molybdenum by using Pb $(NO_3)_2$ as the primary standard[11]. Extension of these observations to the estimation of metals forming stable molybdates suggested itself and a series of experiments were carried out to study the possibility of using the above indicator in the titration of ammonium molybdate with a thorium salt solution. A systematic study of the operative conditions led to the development of a simple and rapid titrimetric method for the estimation of thorium. This has now been described in the present communication.

Experimental

Thorium nitrate (or chloride) solution was obtained by dissolving the pure salt in water; the ThO_2 content of an aliquot portion of the solution was determined by the *m*-nitrobenzoic acid method.

To a known volume of the aqueous thorium solution containing 50–60% alcohol, one ml. of saturated alcoholic solution of diphenylcarbazone was added and the yellow or orange yellow solution was titrated slowly with constant swirling against standard ammonium molybdate. The end point was characterised by a sharp pink flush in the precipitated thorium molybdate. At this point the precipitate tended to coagulate rapidly and the supernatent solution also assumed a pink shade. Since the colour change from pale yellow to pink is completely reversible, any error due to overtitration is rectified easily by running in a known volume of thorium solution and continuing the titration as usual. The accuracy and sharpness of the end point was, however, found to enhance by adopting the following modified procedure: To an aliquot of the thorium solution a measured volume of standard aqueous Pb $(NO_3)_2$ was added followed by an equal volume of ethanol and 0.5 ml. of the indicator. The pink coloured solution was titrated slowly against ammonium molybdate. The colour faded during the initial addition of the molybdate with the simultaneous appearance of a white precipitate. The titration was continued till a sharp pink flush was observed in the precipitate. A blank titration of $Pb(NO_3)_2$ against molybdate using the indicator was carried out under identical experimental conditions. This titre value when subtracted from the total volume

1) B. Justel, *Die Chemie.*, **56**, 157 (1943).
2) T. Moeller, G.K. Schweitzer and D.D. Starr, *Chem. Rev.*, **42**, 64 (1948).
3) Y.A. Chernikhov and T.A. Uspenskaya, *Zavodskaya Lab.*, **9**, 276 (1940).
4) T. Moeller and N.D. Fritz, *Anal. Chem.*, **20**, 1055, (1948).
5) F.A. Gooch and M. Kobayashi, *Amer. J. Sci.*, **45**, 227 (1918).
6) R. Berg, *J. Prakt. Chem.*, **115** (ii), 178 (1925).
7) G.S. Deshmukh and L.K. Swamy, *Anal. Chem.*, **24**, 218 (1952).
8) F.J. Metzger and F.W. Zones, *J. Ind. Eng. Chem.*, **4**, 493 (1912).
9) C.V. Banks and H. Diehl, *Anal. Chem.*, **19**, 222 (1947).
10) L. Gordon and C.R. Stine, ibid., **25**, 192 (1953).
11) G.S. Deshmukh, *Bull. Chem Soc. Japan*, **27**, 623 (1954).

of molybdate required for the mixed thorium and lead nitrate solution, gave the quantity of molybdate required for the precipitation of thorium as molybdate. Varying quantities of the thorium solution were thus titrated against standard ammonium molybdate. From a knowledge of the ThO_2 content of the solution taken for titration and the molybdenum content of the titrant, the molar ratio Th: Mo corresponding to the end point was calculated. Series of trial experiments showed that within limits of 100–200 mg. of thorium the molar ratio corresponded on the average to 1 : 1.99. It may therefore be inferred that within the specified limits of the above experimental procedure, the titrimetric estimation of thorium may be carried out with reasonable accuracy. This date are returned in Table I.

It has been observed that the sharpness of the end point depends on the quantity of alcohol added initially to the thorium solution. While in the presence of too large a quantity exceeding 70–80% the end point appears prematurely; an excess of molybdate is consumed if the titration is carried out in a purely aqueous media. The overall alcohol content (50–60%) has been determined by a series of trial experiments. For a permanent and sharp end point it is also not desirable to dilute the contents during and/or towards the end of the titration.

The molar ratio Th: Mo=1: 1.99 as observed in the above series of experiments (cf. Table I) is in close agreement with that reported by Gordon.

The amperometric titration method developed by him offers however, a distinct advantage of being applicable to the determination of thorium in presence of other rare earths. This procedure, however, necessitates a rigid control of operative conditions and a special type of apparatus. On the other hand the titrimetric method of Metzger and Zones involves the use of acetic acid- sodium acetate buffer and diphenyl-carbazide as an *external* indicator. It may therefore be pointed out that the present procedure is more rapid, simple and accurate than other titrimetric methods adopted for the determination of thorium.

TABLE I

10 ml. of $Pb(NO_3)_2 \equiv 0.07550$ gm. Pb

Expt. No.	Vol. of Th Cl_4 in ml. (a)	Vol. of Am. Molybdate required in ml. (b)	Wt. of Th in (a)	Wt. of Mo in (b)	Molar Ratio Th: Mo
1.	10.0	9.40	.06489	.05249	1: 1.955
2.	20.0	19.05	.1297	.1064	1: 1.984
3.	42.5	40.60	.1378	.1133	1: 1.987
4.	22.5	21.50	.1460	.1200	1: 1.987
5.	47.5	45.45	.1541	.1269	1: 1.991
6.	25.0	23.95	.1622	.1338	1: 1.995
7.	52.5	50.55	.1703	.1411	1: 2.004
8.	27.5	26.55	.1784	.1483	1: 2.010
9.	57.5	55.50	.1865	.1550	1: 2.009

Summary

A simple volumetric method for the quantitative estimation of thorium as molybdate is described. This is based on the titration of aqueous thorium nitrate (or chloride) solution against standard ammonium molybdate in presence of ethanol by using diphenylcarbazone as the internal indicator. Under specified operative conditions, normal thorium molybdate is precipitated. The indicator behaves reversibly and the accuracy of the method is comparable with those obtained by classical procedures.

Our grateful thanks are due to Professor S. S. Joshi for kind interest in the work.

Department of Chemistry, Banaras Hindu University

By-products of Acrylonitrile Synthesis from Acetylene and Hydrocyanic Acid. I. Neutral Constituents

By Shiro MORIMOTO

(Received October 10, 1955)

For several years the present author has been studing the vapor phase synthesis of acrylonitrile from acetylene and hydrocyanic acid. It is very likely that many reaction products are produced in this process because the starting materials are very reactive. It seems to be very important from the scientific as well as from the industrial standpoint to detect the byproducts which are produced by this process.

No report seems to have been made on this detection, although some reports have been made on that in the liquid phase synthesis using the so-called Nieuwland's cat-

alyst[1]. According to these reports, what was considered to be a reaction products of acetylene and hydrocyanic acid was only cyanobutadiene: no separation has been carried out between 1- and 2-cyanobutadiene. No report has been made on the formation of higher nitriles. The following substances have been known as the polymerization products of acetylene alone using Nieuwland's catalyst: (Nieuwland[2], Georgieff[3]).

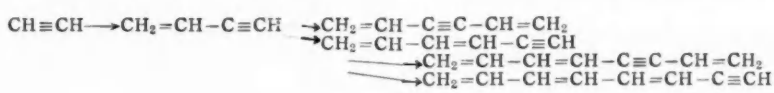

In the case of the reaction between acetylene and hydrocyanic acid, formation of olefinic nitriles is considered possible because hydrocyanic acid may be added to the above mentioned polymerization products of acetylene as follows:

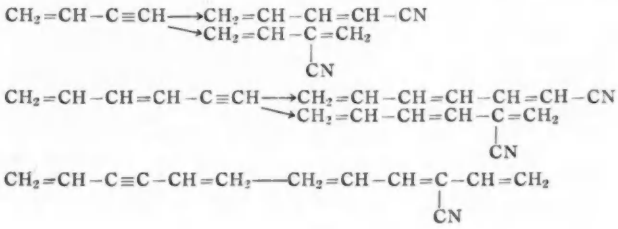

Results and Discussion

A. Reaction Conditions and By-products.—A carrier, reaction temperature, and composition of the feed gas mixture are factors responsible for kinds and amounts of the by-products in the acrylonitrile synthesis from acetylene and hydrocyanic acid using zinc oxide as catalyst.

The author's studies have revealed that the use of some kinds of carrier seems to result in the formation of acetonitrile and basic by-products in a greater amount.

In the present experiment, pumice stone has been used as carrier and the reaction has been carried out at around 400°C[4].

Table I

Boiling points and infrared spectra of constant boiling fractions

Fraction No.	Boiling point °C/mmHg	Distillate cc.	Infrared absorption spectra (μ) C≡N a*	C≡N b*	C=C c*	d*	CH_2 e*	C=O f*	OH g*	**
A-2	95.8–97.0	6.5								(1)
A-4	121.5–120	5.5	++	+	++	±	+	−	+	(2)
B-4	73–75/75	12.5	++	+	++	+	+	−	±	(3)
D-3	80–82/33	5.0	+		+	±	+	+	−	
D-5	85–86/33	4.7	+		+	±	+	++	+	
D-10	93/33	3.3	++		+	+	+	+	−	(4)
E-3	69/7									(5)

* Wave length (μ) a, 4.48–4.51 (conj.); b, 4.44 (nonconj.); c, 6.07–6.11; d, 6.68–6.70, 6.21–6.25; e, 3.4; 6.8; f, 5.8; g, 2.83–2.89.

** The substances which may be expected to exist in the above mentioned fractions are listed below with their literature values of boiling points °C/mmHg.

(1) Propionitrile (identified).
(2) 2-Cyanobutadiene, 24–31/30, 30–40/40; *n*-octane 124.
(3) *p*-Xylene 136; *m*-xylene 139; *o*-xylene 141; ethylbenzene 136; styrene 146; 1-cyanobutadiene 140, 135–8.
(4) Benzonitrile (identified) 190.6, 103.9/50; 1-cyanohexatrine, 56–57/2–3.
(5) Naphthalene (identified).

1) A. Cambron, P.B. 19678; B.L. Hasche and J.G. McNally, P.B. 34813; P.B. 81283; P.B. 47715.
2) J.A. Nieuwland, W.S. Calcott, F.B. Downing and A.C. Carter, *J. Am. Chem. Soc.*, **53**, 4197 (1931); J.A. Nieuwland, U.S. Patent, 1811, 959 (1931).
3) K.K. Georgieff, W.J. Cave and K.G. Blaikie, *J. Am. Chem. Soc.*, **76**, 5494 (1954).
4) Considerable variation of temperature by local heating in the reaction tube was observed.

B. Separation of Neutral Substances.—The intermediate distillation fraction between the two main reaction-products, acrylonitrile and succinodinitrile, was divided into three parts, i. e., neutral, basic and acidic.

The neutral part was fractionally distilled through a Stedmantype column (plate number, 20). And the constant boiling fractions were obtained, i. e., A-2(liq.), A-4(liq.), B-4 (liq.), D-3(liq.), D-5(liq.), D-10(liq.), E-3(sol.) (Table I).

A-2 was treated with thioglycolic acid and hydrogen chloride, resulting in the formation of crystals which melted at 123–124°C (decomp.). The melting point corresponded with that of α-iminopropylmercaptoacetic acid hydrochloride $CH_3 \cdot CH_2 \cdot C(SCH_2COOH) : NH \cdot HCl$ in literature[5].

D-10 was hydrolyzed by a 75% sulfuric acid solution to form benzoic acid with a yield of 50–70%. So it was confirmed that D-10 contained benzonitrile in the above mentioned ratio.

E-3 solidified to crystals melting at 80°C and was identified to be naphthalene by a mixed melting test.

The principal infrared absorption bands of A-4, B-4, D-3, D-5, and D-10 are also shown in Table I.

The most marked and common to all samples has been found to be the characteristic absorption of the nitrile radical (ν-C≡N). The absorption bands are observed at two kinds of wave length, 4.44 μ and 4.48–4.51 μ. According to Kitson et al.[6] nitriles nonconjugated with an olefinic bond give an absorption band at 4.44±0.02 μ; nitriles conjugated with an olefinic bond give an absorption band at 4.49±0.02 μ. Each sample indicates a marked absorption of the conjugated nitrile, but A-4 and B-4 are accompanied by a weak nonconjugated nitrile absorption.

Another common absorption observed is that of the olefinic bond. The absorption bands are observed at 3.24–3.29 μ (ν C-H), 6.07–6.11 μ (ν-C=C-).

D-10 demonstrates the absorption of the benzene nucleus more markedly than that of the olefinic bond.

The absorption bands of the acetylenic bond at 3.0 μ (ν≡C-H) and 4.71–4.78 μ (ν-C≡C-) are absent. (Acetylenic compounds seem to have disappeared in these samples during purification, especially during fractional distillation.)

5) F.E. Condo, E.T. Hinkel, A. Fassero and R.L. Shriner, *J. Am. Chem. Soc.*, **59**, 230 (1937).
6) R.E. Kitson and N.E. Griffith. *Anal. Chem.*, **24**, 334 (1952).

Qualitatively the absorption of D-10 may be regarded as a superposition of absorption of both benzonitrile and 1-cyanohexatriene.

The above mentioned results suggest the existence of 2-cyanobutadiene (cyanoprene) in A-4, 1-cyanobutadiene in B-4, 3-cyanohexatriene in D-3, 2-cyanohexatriene in D-5, and 1-cyanohexatriene besides benzonitrile in D-10.

There also exist absorption bands at 3.4 μ, and 6.8 μ which are considered to be absorption of the methyl or methylene radical. This fact may be explained, considering the existence of nitriles obtained through partial reduction of the above-mentioned unsaturated nitriles, since the existence of propionitrile has been confirmed. Weak absorption of benzene nucleus is somewhat observed in fractions other than D-10. This may be due to the presence of substances having nothing to do with the nitriles.

Formation of benzonitrile seems due to a ring formation of cyanohexatrienes, and especially 1-cyanohexatriene seems easily to aromatize at higher temperature.

$$CH_2=CH-CH=CH-CH=CH-CN \longrightarrow$$

$$[CH_2=CH-CH=CH-CH=\overset{(-)}{C}-CN] \longrightarrow \text{ 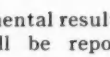 }-CN$$

Other experimental results supporting these suggestions will be reported in following papers.

Experimental

(A) Reaction of Acetylene and Hydrocyanic Acid.—*1) Reaction Tube.*—A stainless steel tube with inner diameter of 6 cm., length of heated part 100 cm. (heated directly without bath), length of part packed with catalyst 60 cm.

2) Catalyst.—A carrier of pumicestone of 8–10 mm. diameter was surmounted with zinc hydroxyde (precipitated) which was burnt in the reaction tube at the reaction temperature to form zinc oxide.

3) Reaction Conditions and Results.—These are shown in Table II.

(B) Chemical Separation of the Intermediate Fraction.—The above-mentioned intermediate fraction (242.5 g.) was dissolved in the same amount of ether and treated with a 25% aq. sodium hydroxide solution and then with a 2% aq. hydrochloric acid solution, resulting in the separation of 5 g. (containing water) of the acidic part, 15 g. (containing water) of the basic part, and 229 g. (containing water) of the neutral part.

(C) Fractional Distillation of the Neutral Part.—The neutral part (liquid, 229 g.) was roughly fractionated into A, B, C, D and E by distillation using a Claeisen-flask under reduced pressure. By further fractionating the respective fractions using a Stedman-Type distillation column (with a brass net, plate number 20) under proper pressure, the results shown in Fig. 1–4 were obtained.

Temperature (°C)

TABLE II

REACTION OF ACETYLENE AND HYDROCYANIC ACID

Expt. No.	Heating temp. °C	Temp. in reaction tube °C	reaction time hrs.	C_2H_2 /HCN	Charg. HCN g.	Consum. HCN g.	Acrylonitrile g.	Intermediate fraction g.	Succinodinitrile g.
1	300–340	330–480	36.5	3.3	716	447	495	30	50
2	300–360	370–510	32	3.2	637	396	376	28.5	53
3	310–390	370–560	32	4.4	529	220	306	103	47
4	350–380	380–560	32	3.9	561	255	294	81	50

Total amounts:
(a) Acrylonitrile 1471 g.
(b) Intermediate fraction 242.5 g.
(c) Succinodinitrile 160 g.

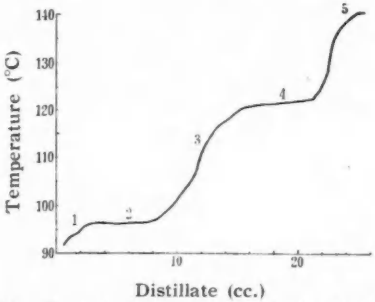

Fig. 1. Distillation curve of fraction A (atm. press.).

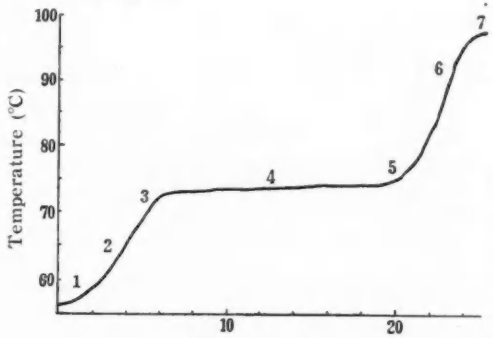

Fig. 2. Distillation curve of fraction B, C (75 mmHg).

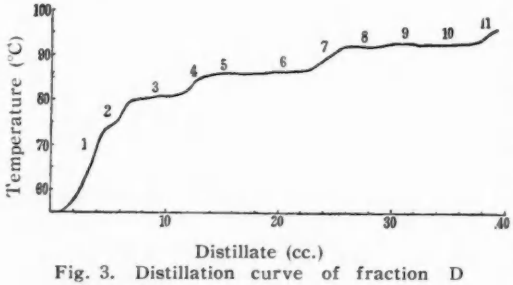

Fig. 3. Distillation curve of fraction D (33 mmHg).

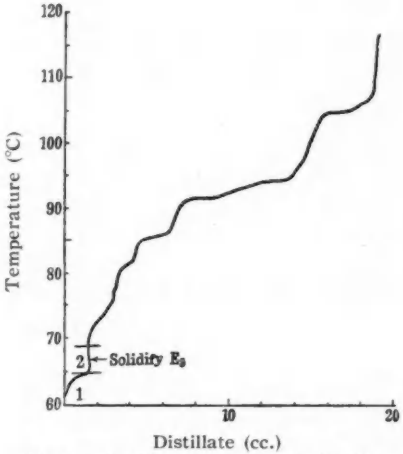

Fig. 4. Distillation curve of fraction E (7 mmHg).

(D) Preparations of Crystalline Derivatives.—*1) Propionitrile.*—A-2 fraction (1 g.) and thioglycolic acid (2 g.) were dissolved in dry ether and tnen treated with dry hydrogen chloride gas under cooling with ice from outside. It was then allowed to stand in a refrigerator for half an hour to form white crystals. It was filtered and dried in a desiccator to form 0.5 g. of crystals melting at 123–124°C (decomp.). The melting point (decomposition) of α-iminopropylmercatoacetic acid hydrochloride so far reported is 124°C.

2) Benzonitrile.—The mixture of D-10 fraction (1.0 g.) and a 75% aq. sulfuric acid solution (5 cc.) together with sodium chloride (0.2 g.) was heated at 160°C and then at 190°C for half an hour. each. After cooling the reaction product was added to 20 g. of ice. The precipitate was filtered. It was dissolved in aq. potassium carbonate solution and the insoluble substances were filtered off. One gram of black insoluble solid was obtained after drying in a disiccator. The filtrate was made acidic with sulfuric acid and then allowed to stand over night. The precipitate was filtered and dried in a desiccator to form 0.85 g. of crystals which melted at 121–121.5°C. The crystals were recrystallized from 20 cc. of water. It was dried in a desiccator to form 0.65 g.

of crystals which melted at 121–121.5°C. These crystals mixed with benzoic acid melted at 121.2–121.7°C, showing no melting point depression.

Anal. Found: C, 68.69; H, 4.97. Calcd. for $C_7H_7O_2$: C, 68.84; H, 4.95%.

3) Naphthalene.—A solid separated in E-3 fraction melted at 80.2°C. It melted at 81.8°C after recrystallization from methanol. It melted at 81.8°C when mixed with naphthalene showing no melting point depression.

Anal. Found: C, 93.63; H, 6.28. Calcd for $C_{10}H_8$: C, 93.71; H, 6.29%.

(E) Infrared Absorption Spectra.—Fig. 5–9 show infrared absorption spectra of A-4, B-4, D-3, D-5, D-10 fractions (Perkin Elmer C12).

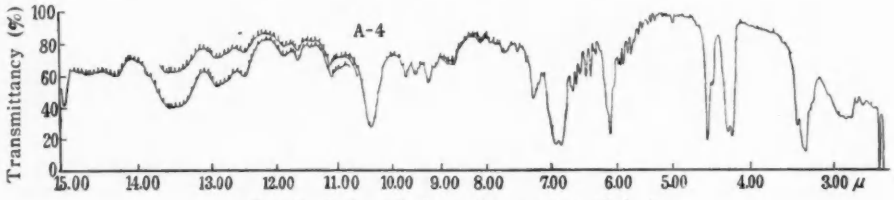

Fig. 5. Infrared absorption spectra of A-4.

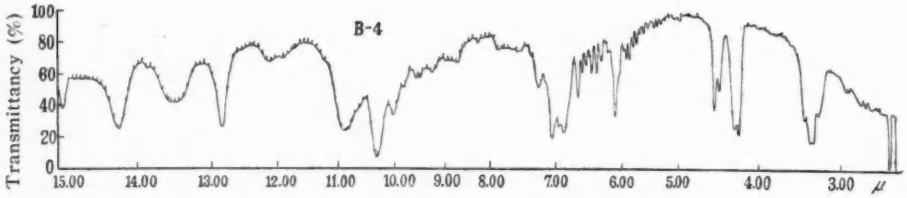

Fig. 6. Infrared absorption spectra of B-4.

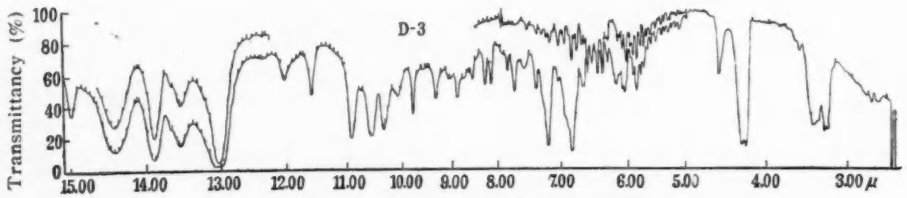

Fig. 7. Infrared absorption spectra of D-3.

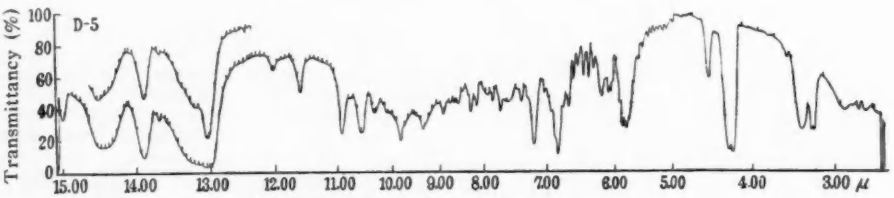

Fig. 8. Infrared absorption spectra of D-5.

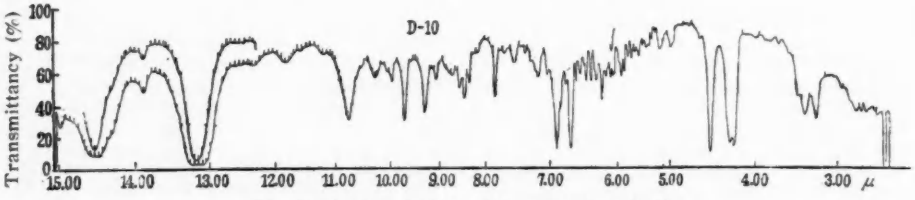

Fig. 9. Infrared absorption spectra of D-10

Summary

By distilling the reaction products of the vapor phase acrylonitrile synthesis from acetylene and hydrocyanic acid an intermediate fraction was obtained between two main fractions, acrylonitrile and succinodinitrile. The neutral portion of the intermediate fraction was carefully distilled through an efficient column and separated into constant boiling fractions. From these fractions propionitrile, benzonitrile naphthalene were isolated and identified as the byproducts. On the basis of the boiling points and the infrared spectra of other fractions, the presence of unsaturated nitriles such as 1-cyanobutadiene, 2-cyanobutadiene, 1-cyanohexatriene, 2-cyanohexatriene, 3-cyanohexatriene as the constituents of the neutral portion was suggested.

Heartfelt thanks are to be returned to Professors Shiro Akabori and Shunsuke Murahashi of Osaka University for their kind instruction and suggestions, to Kazuo Adachi, Masamichi Miura, Tadamichi Fukunaga, Tatsuo Takaya, Yasumasa Kiyokawa, Shinpei Hamada, Sumihiko Mori, Tohoru Okuda and Noriyuki Yamamoto for their helpful technical assistance, and to Yoshiki Matsui for taking infrared absorption spectra.

Part of the expenditure required for this study has been kindly subsidized by the Scientific Fund of the Education Ministry, Textile Research Institute, and Tekkosha, Inc.

Department of Chemistry, Faculty of Science, Osaka University, Osaka

---

Spectrophotometric Determination of Micro Quantities of Titanium with 8-Hydroxyquinaldine

By Kenji MOTOJIMA

(Received November 21, 1955)

Introduction

Titanium forms slightly soluble chelate with oxine and this chelate can be extracted with chloroform, giving a yellow colored solution which has an absorption maximum at 385 mμ. This property can be used for the photometric determination of a small amount of this metal[1]. On the other hand, Gardner[2] has described a method based on a measurement of the color intensity of a chloroform solution of peroxidised titanium oxinate extracted from the solution containing hydrogen peroxide. These two methods are very sensitive, but the reactions are not very selective and, especially, the former method is affected seriously by small amounts of the aluminum and iron which are most likely to accompany titanium. In the method to be described below, 8-hydroxyquinaldine, one of the derivatives of oxine, is used as a reagent, and the method employed by the author for the spectrophotometric determination of beryllium with this reagent[3] is applied to this metal. By this method from 3 to 50 micrograms of titanium in about 35 ml. of solution can be determined without being affected by a few milligrams of aluminum. Moreover, small amounts of iron and titanium can be determined simultaneously in the similar way used for the simultaneous spectrophotometric determination of iron and aluminum with oxine[4].

Apparatus

A Beckman Model DU type spectrophotometer (Shimadzu, QB-50) with 1 cm. glass cell was used for all absorbancy measurements. A glass electrode pH meter (Horiba, Model M) was used for pH measurement. Separatory funnel, automatic measuring pipette and all other glass wares were the same ones used in the previous investigations[3,4].

Reagents

Standard Titanium Solution.—In 30 ml. of hot concentrated sulfuric acid, 3 g. of meta-titanic-acid (about 75% TiO_2) purified by reprecipitation, was dissolved and, after cooling, it was diluted to 1 liter. After suspended insoluble titanium

1) K. Motojima, Unpublished work.
2) K. Gardner, *Analyst*, **76**, 485 (1951).
3) K. Motojima, This Bulletin, **29**, 71 (1956).
4) K. Motojima, *J. Chem. Soc. Japan (Pure Chem. Sect.)*, **76**, 903 (1955).

oxide was filtered off with a fine filter paper, the titanium content was determined gravimetrically as the oxide. Working solutions were prepared by exactly diluting this solution with 0.5 N sulfuric acid. Each 10 ml. of these solutions contained 10.8 and 21.6 micrograms of titanium.

Standard Ferric Iron Solution.—Several ferric iron standard solutions were prepared by dissolving pure ammonium iron alum in 0.1 N sulfuric acid.

8-Hydroxyquinaldine Solution.—1% 8-hydroxyquinaldine acetic acid solution was prepared[3].

Chloroform.—Purified chloroform[3] was used.

Other Reagents.—The other reagents were prepared from reagent grade chemicals.

Experimental

Absorption Spectra.—Absorption spectra of titanium chelate of 8-hydroxyquinaldine extracted with chloroform were studied. The data obtained are shown in Fig. 1. From these curves, it is seen that this chelate in chloroform has an absorption maximum at the wave length of 370 mμ, and at the same time, the reagent alone in this solvent has a considerable absorption at this wave length. Accordingly, the wave length of 380 mμ has been chosen for the analytical purpose.

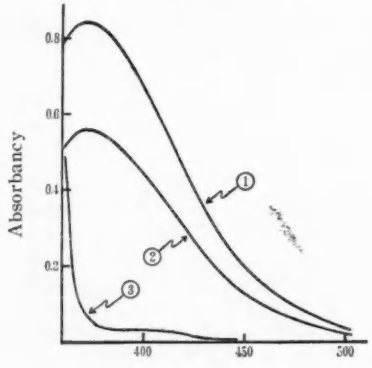

Fig. 1. Absorption spectra of titanium chelate of 8-hydroxyquinaldine in chloroform.
①: 32.4 micrograms of Ti,
②: 21.6 micrograms of Ti,
③: blank.

Effect of pH upon Extraction.—The proper pH for the efficient extraction of titanium was determined. A series of several solutions each containing 21.6 micrograms of titanium in about 35 ml. was treated with 3 ml. of 8-hydroxyquinaldine solution and suitable amount of ammonium acetate or ammonium hydroxide enough to fall within a pH range from 2 to 11. After the volume of the solution was brought to 50 ml., extraction was made with exactly 10 ml. of chloroform. Then, the absorbancy of the extract dried with anhydrous sodium sulfate, was measured at 380 mμ versus chloroform. On the other hand, measurement of pH was made on the aqueous layer after extraction. The results obtained are shown in Fig. 2. Extraction is seen to be almost complete over a pH range from 5.0 to 9.0, and the approximately constant absorbancies are obtained in the pH range from 5.0 to 6.0. A similar experiment was made about the reagent, and it was found that the blanks were reasonably constant in the pH range from 4.0 to 10.0. So that the pH range from 5.0 to 6.0 has been chosen as the optimum range for this method.

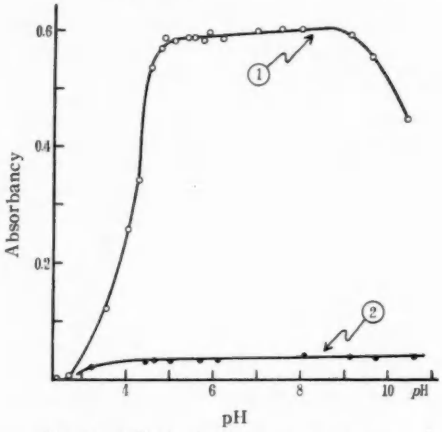

Fig. 2. Effect of pH upon extraction.
①: 21.6 micrograms of Ti,
②: blank.

Amount of Reagent.—Approximately 50 ml. of solutions each containing 43.2 micrograms of titanium and varying amounts of 8-hydroxyquinaldine solution, were extracted with exactly 10 ml. of chloroform respectively, at a pH of 5.3±0.2, and the absorbancies of these dried extracts were measured at 380 mμ, versus chloroform. A similar set but with no titanium present was also done. The results are shown in Table I.

TABLE I

EFFECT OF AMOUNT OF REAGENT

8-Hydroxyquinaldine Added, ml.	Absorbancy Measured		Correct for Blank
	Ti is present	Blank	
0.5	0.404	0.017	0.387
1.0	0.855	0.017	0.838
1.5	0.980	0.015	0.965
2.0	1.100	0.027	1.073
2.5	1.130	0.031	1.099
3.0	1.135	0.033	1.102
3.5	1.150	0.039	1.111
4.0	1.135	0.046	1.089
5.0	1.155	0.047	1.108

When more than 2.5 ml. of reagent solution is added, the absorbancies, after correction for the blank reading are reasonably constant. Therefore, 3 ml. of 8-hydroxyquinaldine solution has been selected as a sufficient amount of reagent.

Effect of Temperature and Digestion.—After five, fifteen, thirty and sixty minutes of digestion

at various temperatures, from 10° to 80°C, extractions were made respectively, in case of high temperature, solution being cooled to room temperature before extraction. And it was found that since the absorbancies of their dried extracts were reasonably constant, no digestion was necessary.

Shaking Period.—The complete extraction of titanium chelate of 8-hydroxyquinadline with chloroform seems to be attained by vigorous shaking for thirty seconds.

Stability.—The absorbancy of the dried chloroform extract of titanium chelate, stored in a glass bottle with a glass stopper and protected from sunlight, was found to remain unchanged for a week.

Spectrophotometric Procedure and Preparation of Calibration Curve

About 35 ml. of acidic solution containing not more than 50 micrograms of titanium, is treated with 3 ml. of 8-hydroxyquinaldine solution and suitable amounts of 2 N ammonium hydroxide and 2 N ammonium acetate solution enough to attain the pH to 5.3±0.2. The solution is transferred to a separatory funnel with a few milliliters of rinsed water and the volume is brought to 50 ml. Then extraction is made with exactly 10 ml. of chloroform by vigorous shaking for a minute. The chloroform layer is drawn off into a small glass bottle with a glass stopper, containing 1 g. of anhydrous sodium sulfate, and is shaken to remove droplets of water. The absorbancy of this extract is measured at 380 mμ using blank as a reference. Titanium is determined by the use of the calibration curve prepared by the same treatment of a series of known amount of this metal.

The calibration curve obtained is shown in Fig. 3. As will be seen from this curve, a close approximation to a linear relationship between titanium concentration and the absorbancy is obtained up to 50 micrograms or more.

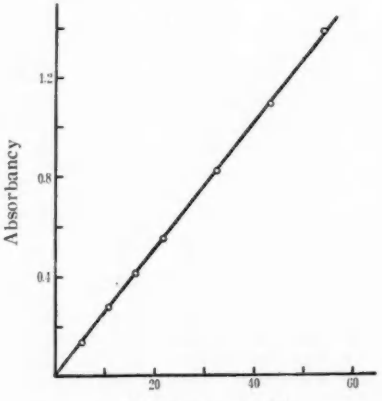

Fig. 3. Calibration curve of titanium (at the wave length of 380 mμ).

Interfering Substances

Relatively large amounts of alkali, ammonium, calcium and magnesium salts of acetate, chloride, nitrate and sulfate, and less than about 10 mg. of aluminum do not interfere with this procedure. Tartrate produces a serious effect and gives a low result. Such metals as bithmus, cobalt, copper, iron, nickel, vanadium and zirconium which form chloroform soluble chelate with 8-hydroxyquinaldine in acetic acid and acetate medium interfere with this method, and these metals, except a small amount of ferric iron, should be absent.

Ferric iron yields a dark blue chloroform solution under the same condition and interferes seriously with this method, but when its amount is less than about 100 micrograms, titanium and iron can be determined simultaneously by a method similar to that presented by the author[3,4].

Simultaneous Spectrophotometric Determination of Titanium and Iron

Ferric chelate of 8-hydroxyquinaldine in chloroform has two absorbancy maxima at 470 and 580 mμ, and Beer's law is obeyed at both 380 and 580 mμ, respectively. On the other hand titanium chelate has no absorption at 580 mμ. Therefore, both titanium and iron can be determined simultaneously, by the very same treatment mentioned above, and by measuring the absorbancies at 380 and 580 mμ and applying the following formulas[5].

$$C_{Fe}=\frac{A_{580}}{a^{Fe}_{580}}$$

$$C_{Ti}=\frac{a^{Fe}_{580}\cdot A_{380}-a^{Fe}_{380}\cdot A_{580}}{a^{Ti}_{380}\cdot a^{Fe}_{580}}$$

Where, C_{Fe}, C_{Ti}: iron and titanium present, in microgram,

A_{380}, A_{580}: absorbancies measured at 380 and 580 mμ,

a^{Ti}_{380}, a^{Fe}_{380}, a^{Fe}_{580}: absorbancy indexes of titanium and iron at 380 and 580 mμ (the absorbancy per microgram of these metals).

In this experiment the values of these absorbancy indexes obtained are as follows:

$$a^{Fe}_{380}=0.0088 \qquad a^{Fe}_{580}=0.0077$$
$$a^{Ti}_{380}=0.0254$$

the values of a^{Fe}_{380} and a^{Fe}_{580} are slightly lower than that when extraction is made in ammoniacal medium[3], because these values slightly increase in proportion to the pH at which extraction is made. Nevertheless, their changes are negligible when extraction is made at the pH range from 5 to 6.

5) E. B. Sandell, "Colorimetric Determination of Traces of Metals", 2nd Ed., Interscience Publisher Inc., New York (1950) p. 70.

Several mixed solutions containing known amounts of titanium and iron in various ratios were prepared and these two metals were determined. Some of the results are shown in Table II, which seem to be quite satisfactory.

TABLE II
SIMULTANEOUS DETERMINATION OF TITANIUM AND IRON

Taken Microgram		Absorbancy Measured		Calculated Microgram	
Ti	Fe	380 mμ	580 mμ	Ti	Fe
5.4	20.0	0.324	0.161	5.5	20.9
5.4	40.0	0.481	0.308	5.1	40.1
5.4	60.0	0.657	0.466	5.3	60.6
5.4	80.0	0.830	0.623	4.6	81.0
5.4	100.0	0.990	0.774	4.2	100.7
10.8	20.0	0.450	0.160	10.6	20.8
10.8	40.0	0.626	0.311	10.7	40.5
10.8	60.0	0.810	0.476	10.5	61.9
10.8	80.0	0.975	0.614	10.9	79.9
10.8	100.0	1.125	0.765	9.9	99.5
21.6	20.0	0.724	0.164	21.1	21.3
21.6	40.0	0.875	0.312	20.5	40.6
21.6	60.0	1.090	0.473	21.8	61.6
21.6	80.0	1.270	0.627	22.0	81.5
32.4	20.0	1.025	0.164	33.1	21.3
32.4	40.0	1.160	0.315	31.5	41.0
32.4	60.0	1.350	0.471	32.0	61.3

Conclusion

The spectrophotometric method for determination of micro quantities of titanium with 8-hydroxyquinaldine was established. By this method from 3 to 50 micrograms of titanium in about 35 ml. of solution can be determined; therefore the sensitivity of this method is almost equal to that of the tiron method established by Yoe and his coworker[6], but is much better than that of the ordinary hydrogen peroxide method[7]. A few milligrams of aluminum do not interferes with this method. Moreover, the method for simultaneous determination of micro quantities of titanium and iron was studied.

The author wishes to express his sincere appreciation to Prof. Dr. M. Ishibashi, Kyoto University, for his encouragement and Mr. H. Hashitani for his frequent assistance throughout the investigation.

Faculty of Science and Engineering
Ritsumeikan University, Kyoto

6) J.H. Yoe and A.R. Armstrong, *Anal. Chem.*, **19**, 100 (1947).
7) E. B. Sandell, "Colorimetric Determination of Traces of Metals", 2nd Ed. (1950), p. 572.

Spectrophotometric Determinatoin of Micro Quantities of Iron, Titanium and Aluminum when They accompany Each Other. Use of 8-Hydroxyquinaldine and Oxine

By Kenji MOTOJIMA and Hiroshi HASHITANI

(Received November 21, 1955)

Introduction

In general, iron, titanium and aluminum accompany each other, and the methods for separation and determination of these three metals are very essential. By the method described below, micro quantities of these three metals can be separated and determined by the use of 8-hydroxyquinaldine and oxine as reagents.

In the previous paper[1] presented by one of the authors, it has been reported that small amounts of iron and titanium can be extracted with chloroform as their chelate of 8-hydroxyquinaldine, and that by measuring the absorbancies of the extract at 380 and 580 mμ, these two metals can be determined simultaneously. At the same time iron and titanium are quantitatively extracted off and aluminum is perfectly left in aqueous phase. Therefore, after the above extraction aluminum can be determined photometrically without being effected by iron and titanium. using oxine as a reagent[2,3].

1) K. Motojima, This Bulletin, **29**, 455 (1956).

Apparatus and Reagents

All the apparatus and the reagents except for the following ones were the same as those had been used in the previous work[1].

Standard Aluminum Solution.—Several stand-

2) E. B. Sandell, "Colorimetric Determination of Metals", 2nd Ed. (1950), p. 152.
3) K. Motojima, *J. Chem. Soc. Japan (Pure Chem. Sect.)* **76**, 903 (1955).

ard aluminum solutions were prepared from pure potassium aluminum alum.

Oxine Solution (1% acetic acid solution).—In 5 ml. of glacial acetic acid 2 grams of pure oxine were dissolved by warming, and the volume was brought to 200 ml. with distilled water.

Procedure

Approximately 50 ml. of acidic solution containing not more than 50 micrograms of iron, titanium and aluminum respectively, 3 ml. of 8-hydroxyquinaldine solution and suitable amounts of ammonium hydroxide and ammonium acetate enough to adjust the pH to 5.3±0.2, is extracted with exactly 10 ml. of chloroform. Then, the measurements of two absorbancies at 380 and 580 mμ of the dry extract are made using blank as a reference, and iron and titanium are determined by the method mentioned in the previous paper[1].

The aqueous layer is washed three times with 10 ml. of chloroform by shaking for about thirty seconds respectively. By this treatment iron, titanium and 8-hydroxyquinaldine will be quantitatively removed from the aqueous phase. Then the aqueous solution is transferred into a 100 ml. beaker with a few milliliters of rinsed water, treated with 3 ml. of 2 N sulfuric acid and heated on water bath to expel the chloroform which comes into the solution, and the volume is brought to about 35 ml. by evaporation.

After cooling, the solution thus resulting is treated with 3 ml. of oxine solution and a suitable amount of 2 N ammonium acetate enough to adjust the pH to 5.0±0.2, and transferred in a separatory funnel with a few milliliters of rinsed water, and the volume is brought to 50 ml. Then the extraction is made by vigorous shaking for a minute with exactly 10 ml. of chloroform. The chloroform layer is dried with a gram of anhydrous sodium sulfate and the absorbancy at 390 mμ is measured using blank as a reference. Aluminum is determined by the use of the calibration curve[2].

Discussion and Results

If 8-hydroxyquinaldine extraction is made with 20 or 30 ml. of chloroform, double or triple amounts of iron and titanium can be determined respectively. When the amount of aluminum is more than 50 micrograms, the acidified solution from which iron and titanium have been removed by 8-hydroxyquinaldine extraction, is exactly diluted to suitable volume with distilled water using a volumetric flask, and an aliquot is taken for determination of aluminum. By this method up to a milligram of aluminum can be determined accurately.

TABLE

DETERMINATION OF IRON, TITANIUM AND ALUMINUM

Taken Microgram			Absorbancy Measured: 8-Hydroxyquinaldine Extraction		Absorbancy Measured: Oxine Extraction		Found Microgram		
Fe	Ti	Al	380 mμ	580 mμ	390 mμ	470 mμ	Fe	Ti	Al
0.0	5.4	25.0	0.124	0.004	0.656	0.011	0.1	4.7	25.4
0.0	10.8	25.0	0.275	0.011	0.678	0.012	0.1	10.3	26.2
0.0	21.6	25.0	0.549	0.000	0.674	0.014	0.0	21.6	26.0
40.0	0.0	25.0	0.338	0.291	0.617	0.014	37.9	0.2	23.8
40.0	5.4	25.0	0.486	0.308	0.612	0.004	40.0	5.3	23.9
40.0	10.8	0.0	0.605	0.303	0.005	0.007	39.4	10.2	0.0
40.0	10.8	10.0	0.633	0.318	0.279	0.008	41.4	10.6	10.7
40.0	10.8	25.0	0.629	0.311	0.640	0.001	40.5	10.8	25.0
40.0	10.8	50.0	0.638	0.319	1.210	0.011	41.5	10.8	47.1
40.0	21.6	0.0	0.905	0.311	0.004	0.006	40.5	21.7	0.0
40.0	21.6	10.0	0.910	0.305	0.284	0.008	39.7	22.2	10.9
40.0	21.6	25.0	0.910	0.302	0.665	0.018	39.3	22.3	25.5
40.0	21.6	50.0	0.900	0.312	1.240	0.021	40.6	21.4	48.0
40.0	32.4	0.0	1.160	0.308	0.010	0.014	40.0	31.8	0.0
40.0	32.4	10.0	1.190	0.306	0.280	0.009	39.8	33.1	10.7
40.0	32.4	25.0	1.190	0.322	0.651	0.005	41.9	32.4	25.4
40.0	32.4	50.0	1.200	0.319	1.210	0.005	41.5	33.0	47.2
0.0	5.4	200.	0.126	0.005	*1.270	0.017	0.1	4.8	197.
0.0	10.8	200.	0.277	0.012	*1.250	0.015	0.2	10.4	194.
0.0	21.6	100.	0.573	0.003	*0.631	0.018	0.0	22.4	97.
0.0	21.6	200.	0.549	0.000	*1.225	0.016	0.0	21.6	190.
40.0	5.4	200.	0.472	0.300	*1.235	0.016	39.0	5.1	190.
40.0	10.8	100.	0.639	0.313	*0.629	0.013	40.7	11.1	97.
40.0	10.8	200.	0.635	0.318	*1.255	0.030	41.4	10.7	194.
40.0	21.6	100.	0.915	0.305	*0.645	0.012	39.7	22.3	100.
40.0	21.6	200.	0.910	0.299	*1.220	0.016	38.9	22.4	189.

* Measurement was made for 25 ml. portion of the solution diluted to 100 ml.

The pH of the solution, after 8-hydroxyquinaldine extraction, is about 5.3 and at this pH aluminum tends to form hydroxide and give low analytical result; for this reason the solution should be acidified with sulfuric or hydrochloric acid before the determination of aluminum is carried out.

When the measurement of absorbancy of aluminum oxinate extract is made, it is desirable to measure the absorbancy of the extract at 470 mμ which is caused by iron oxinate, and, if necessary, make a correction for iron which seems to come accidentally into the solution during the procedure, by the method mentioned by one of the authors[3].

Relatively large amounts of alkali, ammonium, calcium and magnesium salts of acetate, chloride, nitrate and sulfate do not interfere with this procedure. Tartrate, fluoride and metal ions which form chloroform soluble chelate with 8-hydroxyquinaldine and oxine in acetic acid and acetate medium interfere with this method, and they should be absent.

A number of mixed solutions containing known amounts of iron, titanium and aluminum were prepared and these three metals were determined. Some of the results are shown in the following table, which seems to be quite satisfactory.

Conclusion

The method for separation and spectrophotometric determination of micro quantities of iron, titanium and aluminum with 8-hydroxyquinaldine and oxine was established. By this method, from 3 to 50 micrograms of iron, titanium and aluminium mixed in about 35 ml. of solution, are determined, rapidly and accurately.

The authors wish to express their sincere appreciation to Prof. Dr. M. Ishibashi, Kyoto University, for his encouragement and numerous suggestions throughout the investigation.

Faculty of Science and Engineering
Ritsumeikan University, Kyoto

The Electronic Structures of Azine Compounds. I. The Molecular Structures and the Electronic States of Fluoflavine and Fluorubine

By Yûmi AKIMOTO

(Received July 29, 1955)

The recent development of the organic chemistry concerning azine compounds has made it possible to offer us some various theoretically interesting problems. This series includes as its purpose the semi-empirical discussions on such problems, in terms of the simple LCAO molecular orbital theory, which would permit us to take a bird's-eye view of the electronic structures of the azine compounds.

As the first venture, fluoflavine (dihydro-5, 6, 11, 12-tetraaza-naphtacene) and fluorubine (dihydro-5, 6, 7, 12, 13, 14-hexaaza-pentacene) were chosen for consideration here. The electronic absorption spectra were observed and discussed. Attention was also paid to the position of *meso*-H atoms of the molecules.

Experimental

Difficulty arises in the selection of a good solvent of fluoflavine and fluorubine, as none of the non-polar solvents dissolve these compounds or do not dissolve them completely. As a result of the solvent test extended to ten odd solvents and their mixtures*, slight solubility was observed on several alcoholic solvents, where the solubility slightly increased as the size of the alkyl group increased**. Here, considering the absorption ranges of the solvents, *n*-propylalcohol was used. Fluoflavine saturates up to 1/20,000 mol, and fluorubine to 1/150,000 mol. already, so the confidence regarding the absolute intensity of the absorption is slight.

For the observation, a Beckman quartz DU-type spectrophotometer was used. Samples used were synthesized by the members of Kawai Laboratory of Tokyo University of Education. Observed curves were shown in Fig. 1.

* Methyl- to octyl-alcohol, benzene, toluene, $CHCl_3$, CCl_4, dioxane, etc., and their mixtures.

** These samples are slightly soluble in dioxane and in mixtures of CCl_4 and alcohols. But in the former case, the formation of the hydrogen bonds is apprehended, and in the latter, the tendency of deepening of color shows the possibility of the formation of some intermolecular compounds.

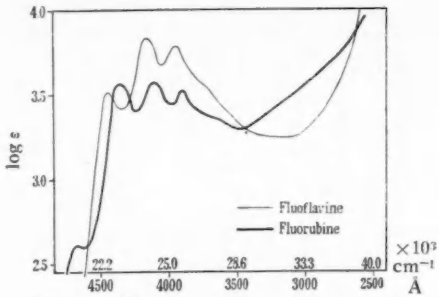

Fig. 1. The absorption curves of fluoflavine and fluorubine.

Interpretation of Spectra

Platt[1] presumed that a weak absorption tail near 24,000 cm^{-1} of phenazine is to be the transition of *n*-type. If we admit his postulate that, with increasing size of the parent conjugated systems, n-π transition moves to the red only about half as far as the longest wave-length π-π transition, we may anticipate that the n-π transition will be hidden when the molecule becomes larger and larger. Moreover, in the case of dihydro-azine as fluoflavine, *n*-electron of the hydrogenated N atoms (N_H atoms) conjugates with the π-electron system increasing the number of the filled orbitals, and so the n-π transition will move farther to the blue side. Because of these aspects, and also from the standpoint of the transition intensity, the longest strong wave-length absorption of fluoflavine may be assumed to be the π-π transition.

In fluorubine, the increase of the number of non-hydrogenated N atoms two to four, will produce some interaction to shift the *n*-band to red, just as the increase of the number of N atom one to two, produced the absorption tail on phenazine which was not present in acridine. Actually, fluorubine has a weak absorption near 21,000 cm^{-1}. If we assume this absorption to be of *n*-type, fluorubine has come to have three absorption maxima in the longest wave-length π-π band just as in the case of fluoflavine.

Such a way of thinking does not conflict with the spectral results of hemofluorindine (dihydro-5, 7, 12, 14-tetraaza pentacene) which was reported by Badger et al.[2] Hemofluorindine has only two nonconjugated *n*-electrons, so n-π transition does not show the independent maximum.

Concerning these dihydro-azine compounds, many isomers are possible in regard to the positions of *meso*-H atoms (N_H atoms). Up to the present, no report has been presented about the isolation of these isomer, and the deduction will be drawn that either there is only the most stable isomer or the tautomerism between these isomers. The resemblance of these spectra to that of the corresponding polyacene compounds, seems to favor the former assumption[3]. But according to Badger et al.[4], the absorption curves of azine compounds generally lack the detailed structures as compared to that of polyacene. The measurement of the oscillator strengths will give the information about this problem, while we simply assume the former hypothesis, namely the presence of only one isomer to each dihydro-azine compound, leaving out further detailed discussion.

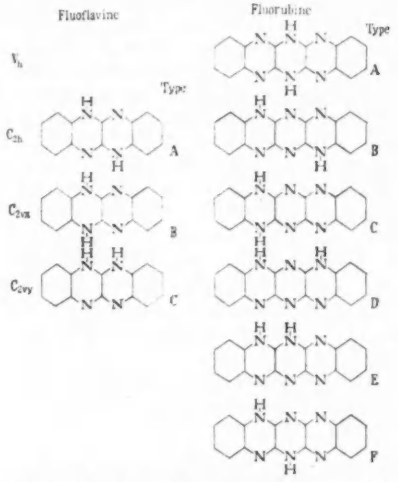

Fig. 2. The quoted isomers of fluoflavine and fluorubine.

MO Calculation

Simple molecular orbital calculations are applied to the various isomers of fluoflavine and fluorbine, as well as to the azine compounds which have the same skeleton with the above dihydro-azine compounds. (see Fig. 2)

The π-orbital energies of the azine compounds: 5, 6, 11, 12-tetraaza-naphtacene and 5, 6, 7, 12, 13, 14-hexaaza-pentacene, are calculated usng the ordinary simple variation method. For each isomer of fluoflavine and fluorubine, the second-order perturbation method is used, taking the changes of Coulomb integral values affected by the introduction of *meso*-H atoms on some N atoms of the former azine molecules, as the pertur-

1) J.R. Platt, *J. Chem. Phys.*, **19**, 101 (1951).
2) G.M. Badger and R. Pettit, *J. Chem. Soc.*, 3211 (1951).
3) A. Buraway, *J. Chem. Soc.*, 1177 (1939).
4) G.M. Badger and R. Pettit., *J. Chem. Soc.*, **1951**, 3211.

bation terms. The adoption of the perturbation method offers us the following advantages:

(1) The labor of calculation is reduced.

(2) The Coulomb integral value of N_H atoms is taken to be changeable easily, as the change of the value of perturbation.

All overlap integrals are neglected.

(1) Variation Method Calculation.—In 1951, P. O. Löwdin discussed the dipole moments of some aza-compounds to determine the most profitable Coulomb integral value α_r, for heterocyclic N atom, which was found to be $\alpha_N=\alpha_C+0.6\beta$[5]. A year later, H. H. Jaffé obtained the same conclusion from facts concerning the reactivity of some aza-compounds[6].

In this calculation we adopt the above value for α_r of every N atom. Inductive effect is assumed on the adjacents of N atoms to be 1/8 of 0.6β. After all concerns about the tolerable changes of the π-electron energies, which may be yielded by the choice of exchange integral values the privation of any reliable data compeles us to take the values as 1β indiscriminately, leaving the detailed discussion hereafter[7]. The results of the calculations are shown in Fig. 3.

(2) Perturbation Method Calculation.—P. O. Löwdin has developed this theory, making it applicable on any changes of Coulomb or exchange integral values of the molecules[8].

In general, when some Coulomb terms are perturbed by V, the π-orbital energy changes as follows:

$$\varepsilon^j=\varepsilon^{j(0)}+\sum_{\mu}{}'V_\mu d_\mu^{jj(0)}+1/2\sum_{\mu\nu}{}'V_\mu V_\nu \pi_{\mu\nu}^{jj(0)}$$

where upper indices $j, \alpha, \ldots\ldots$indicate the molecular orbitals, lower indices $\mu, \nu, \ldots\ldots$the atomic orbitals, and (o) the quantities, belonging to the original system. π is known by the name of mutability, defined as follows:

$$\pi_{\mu\nu}^{jj}=\sum_{\alpha\neq j}\frac{2d_\mu^{j\alpha}d_\nu^{j\alpha}}{(j\alpha)}$$

$$d_\mu^{j\alpha}=C_\mu^j C_\mu^\alpha$$

where C is the orbital coefficient, and $(j\alpha)$ indicates the energy difference between j-th and α-th orbitals.

For the perturbation terms, the differences of the Coulomb integral magnitudes, $\alpha_{NH}-\alpha_N=\Delta\alpha_N$, (conventionally taken to be 0.3, 0.6, and 1.2β) and the induction effects (assumed to be 1/8 for all adjacents of the perturbed atoms) are taken. In Fig. 3, the π-orbital energies of all isomers are shown in regard to the case of 0.6β perturbation. In Table II, the relations between the reduced representations of the π-orbitals and the symmetry properties of the perturbed molecules are shown.

TABLE I

THE ORBITAL ENERGIES OF 5,6,11,12-TETRAAZA-NAPHTACENE (X) AND 5,6,7,12,13,14-HEXAAZA-PENTACENE (Y)

(Calculated by the simple variation method)

$x=(\alpha-\varepsilon)/\beta$

$\beta=1$, $\alpha_N=\alpha_C+0.6\beta$, $S=0$

(X)		(Y)	
B_{3g}	−2.2752	B_{3g}	−2.2706
A_{1u}	−2.1147	A_{1u}	−2.1752
B_{3g}	−1.6657	B_{3g}	−1.8704
B_{1u}	−1.2267	A_{1u}	−1.4739
A_{1u}	−1.2056	B_{1u}	−1.2144
B_{2g}	−1.1037	B_{2g}	−1.1491
B_{3g}	−0.9373	B_{3g}	−1.1266
B_{1u}	−0.5886	A_{1u}	−0.9204
B_{2g}	0.0686	B_{1u}	−0.8050
		B_{2g}	−0.3349
A_{1u}	0.6104	B_{1u}	0.2028
B_{3g}	0.8747		
B_{1u}	1.0581	B_{3g}	0.6086
A_{1u}	1.3849	A_{1u}	0.7969
B_{2g}	1.4018	B_{2g}	1.0721
B_{3g}	1.8285	B_{3g}	1.1902
B_{1u}	1.8609	B_{1u}	1.3382
B_{2g}	2.3082	A_{1u}	1.5972
B_{1u}	2.7212	B_{2g}	1.7437
		B_{3g}	1.8939
		B_{1u}	2.1190
		B_{2g}	2.4935
		B_{1u}	2.7842

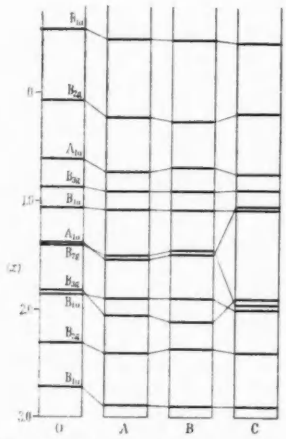

Fig. 3A. The orbital energies of each isomer of fluoflavine. (0 indicates 5, 6, 11, 12-tetraaza-naphtacene (0 was calcalculated by the variation method and the others by the perturbation method)

5) Per-Olov Löwdin, *J. Chem. Phys.*, **19**, 1323 (1951).
6) H.H. Jaffé, *J. Chem. Phys.*, **20**, 1554 (1952).
7) C.A. Coulson and J. der Heer, *J. Chem. Soc.*, **1952**, 482.
8) Per-Olov Löwdin, *J. Chem. Phys.*, **21**, 496 (1953).

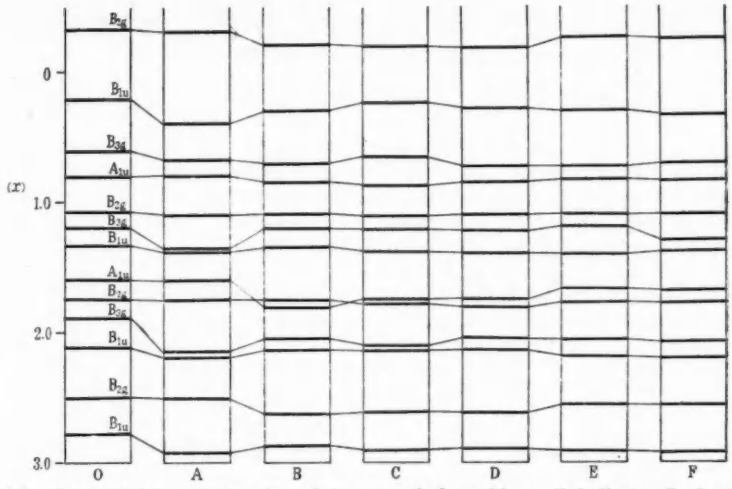

Fig. 3B. The orbtial energies of each isomer of fluorubine. (0 indicates 5: 6: 7: 12: 13: 14-hexaaza-pentacene) 0 was calculated by the variation method, and the others by the perturbation method.

TABLE II

THE RELATION BETWEEN THE REDUCED ORBITAL REPRESENTATION AND THE SYMMETRY PROPERTY OF THE MOLECULE

Symmetry property	V_h	C_{2h}	C_{2vx}	C_{2vy}
Reduced representation	A_{1u}	A_u	A_2	A_2
	B_{1u}	A_u	B_2	B_2
	B_{2g}	B_g	B_2	A_2
	B_{3g}	B_g	A_2	B_2

Discussion

1) Delocalization Energy.—The comparison of the stability are performed between the isomers using the terms of the vertical delocalization energy, defined as follows[9]:

$$\Delta\varepsilon = \varepsilon(L) - \varepsilon(D)$$

In spite of habitual suspicions which are entertained on the propriety of making it the criterion of the molecular stability, the identity of the skeletons such as between the isomers, is observed to offer us the considerable confidence in it. In Fig. 4, the delocalization energies are compared with the changes of $\Delta\alpha_N$.

In the case of fluoflavine, A-type isomer retains invariably the highest stability, but in fluorubine, the stability of A-type isomer is surpassed by B-type isomer over the $\Delta\alpha_N$ of 0.75β.

9) C.A. Coulson and Altmann, *Trans. Faraday Soc.*, **48**, 293 (1952).

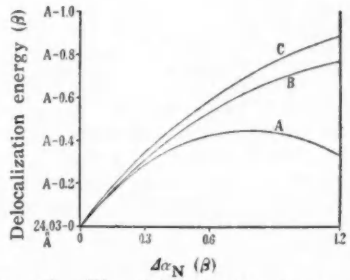

Fig. 4A. The delocalization energy of each isomer of fluoflavine.

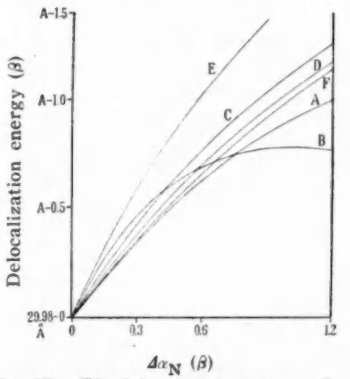

Fig. 4B. The delocalization energy of each isomer of fluorubine.

2) The Correspondency with the Absorption Curve.—The above results are examined from the aspect of correspondency with the

conclusion deduced from the positions of absorptions of absorption maxima. On the conversions of the π-electron transition energies of polyacene molecules (in β unit) into the positions of the longest wave-length absorptions (in wave number unit), good agreements are obtained in taking the exchange rates increasing with the size of molecular skeletons. Here, the rates are taken to agree with the transition energies of naphtacene and pentacene (polyacene molecules which have the same skeletons with fluoflavine and fluorubine respectively) calculated by the simplest MO calculations, with the observed positions of the longest wave-length absorptions: naphtacene 35,500 cm^{-1}/β, and pentacene 39,000 cm^{-1}/β. In Fig. 5, calculated positions of the longest wave-length absorption of each isomer is shown with the magnitude of $\Delta\alpha_N$.

We saw in Fig. 1, the so called blue shift with increase of molecular size: fluoflavine to fluoflavine. In Fig. 4, the curve of the most stable isomer of fluorubine A-type, rises up rapidly with the increase of $\Delta\alpha_N$ to cross to that of fluoflavine A-type about the position of $\Delta\alpha_N=0.4\beta$. Consequently, so long as the $\Delta\alpha_N$ is larger than 0.4β, a satisfactory explanation is obtained on the observed blue shift. (Fluorubine B-type does not explain the blue shift, in removing to further red side with increase of the perturbation.)

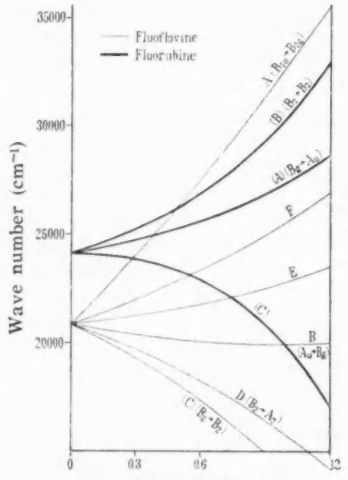

Fig. 5. The calculated longest-wave π-π transition energies of fluoflavine and fluorubine.

3) Conclusion.—As the result of the above discussions, unless we assume the existence of only one isomer, only A-types of both molecules satisfy all the conditions quoted here, and in this case, $\Delta\alpha_N$ must be larger than 0.4β and smaller than 0.75β.

If we set on Fig. 5, the calculated difference between the absorption positions of both molecules, 500 cm^{-1}, the perturbation is concluded by 0.45β. The observed values, 33,500 cm^{-1} for fluoflavine, and 23,000 cm^{-1} for fluorubine, are somewhat smaller than the calculated values corresponding to the perturbation of 0.45β, but within the permissible ranges.

Summary and Conclusion

1) The absorption spectra of fluoflavine and fluorubine were observed in *n*-propyl alcohol solution.

2) The longest wave-length π-π transitions were observed in 22,500 cm^{-1} for fluoflavine, and in 23,000 cm^{-1} for fluorubine.

3) The n-π transition was observed near 21,000 cm^{-1} in fluorubine, while no independent n-π absorption was observed in fluoflavine.

4) The simple MO calculations were applied to 5, 6, 11, 12-tetraaza-naphtacene and 5, 6, 7, 12, 13, 14-hexaaza-pentacene.

5) The π-orbital energies of all isomers of fluoflavine and fluorubine were calculated using the second- order perturbation-method.

6) Supposing that only one isomer exists on each molecule, the blue shift, appearing in fluoflavine to fluorubine, was explained by setting the following structures: 5, 11-dihydro-5, 6, 11, 12-tetraaza-naphtacene for fluoflavine, and 6, 13-dihydro-5, 6, 7, 12, 13, 14-hexaaza-pentacene for fluorubine.

7) The above conclusion was consistant with the conclusion from the comparisons of the vertical delocalization energies.

8) To satisfy the conclusions 6) and 7), the Coulomb integral value of N_H atom must be between $\alpha_C+1.0\beta$ and $\alpha_C+1.35\beta$. Consequently, twice the Coulomb integral value as large as that of N atom will be the most appropriate.

We are deeply indebted to Prof. A. Kotera and Assist. Prof. K. Suzuki for their continued encouragement and valuable advice for this study. The kindness of Prof. S. Kawai who gave us the samples is gratefully acknowledged. Thanks are also due to Mr. S. Noguchi and Mr. K. Ihaya for their helpful discussions.

The cost of this research has been defrayed by the Scientific Research Encouragement Grant from the Ministry of Education to which the author's thanks are due.

Chemical Laboratory, Tokyo Bunrika University, Tokyo
**Hosokura Smelter & Refinery, Mitsubishi Metal Mining Co., Ltd., Miyagi-Prefecture*

* Author's present address.

*Solvent Effects upon Fluorescence Spectra and the Dipolemoments of Excited Molecules**

By Noboru MATAGA, Yozo KAIFU and Masao KOIZUMI

(Received October 19, 1955)

Introduction

Although solvent effects upon the absorption spectra have been studied extensively, there are rather few investigations of the solvent effects upon the fluorescence spectra.

These two are generally different from each other, and from the study of this difference one may expect to derive some information as to the nature of the excited state in contrast to the ground state. To accomplish this program, however, it is necessary to have a general and reliable theory upon the interaction between solute and solvent molecules. Now in 1954 Ooshika[1] published a general theory concerning the solvent effect upon the absorption spectra and the objective of the present communication is to apply his theory to the solvent effect upon the fluorescence spectra, and to compare the two effects.

An important piece of information obtained from this comparison is that one can estimate the dipolemoment of the excited state. An independent and analogous work has already been published by Lippert[2] employing the substances of quite a different type from ours.

Theoretical Consideration

Generally speaking, the difference of the solvent shifts between the absorption and fluorescence spectra is due to the following circumstances.

As to the absorption spectra which correspond to the energy difference between excited state and the ground state, the interaction energies between solute molecule and the solvent molecules sorrounding it are different in the ground and excited state, and this difference produces the solvent shift. Now, according to the Franck-Condon principle, the configuration of the solvent molecules around the the solute molecule does not change during the light absorption, and the above mentioned difference of the interaction energy refers to this Franck-Condon excited state[3] and the equilibrium ground state. But the Franck-Condon excited state is in general not the most stable equilibrium state appropriate to the excited solute molecule. The equilibrium excited configuration is only reached, for example, by reorientation of the solvent molecules, which requires at least a time of the order of 10^{-11} sec., the relaxation time of molecular rotation. The life-time of the excited state, on the other hand, is known to be of the order of 10^{-8} sec., which is ample for the equilibrium configuration to be realized prior to the emission. Hence, for the fluorescence spectrum, the initial state is the equilibrium excited state. During the emission, the solvent configuration does not change, and the momentary ground state in the Franck-Condon ground state which is different from the ground equilibrium state. Thus, when the stabilization energies due to solvent effects are represented as $\langle \Delta E \rangle_e^g$, $\langle \Delta E \rangle_f^g$, $\langle \Delta E \rangle_e^e$ and $\langle \Delta E \rangle_f^e$ for the ground equiribrium and Franck-Condon state and for the excited equilibrium and Franck-Condon state, respectively, the solvent shift of absorption and fluorescence spectrum may be written as follows:

$$hc\Delta\sigma_a = \langle \Delta E \rangle_f^e - \langle \Delta E \rangle_e^g$$

$$hc\Delta\sigma_f = \langle \Delta E \rangle_e^e - \langle \Delta E \rangle_f^g$$

which are different from each other in general.

In the case when these interaction energies are mainly contributed by dipolar interaction, it is expected that a quantitative theory will enable us to estimate the difference of the dipolemoment between the excited state and the ground state, from the data of the two solvent shifts. As such, one may use Ooshika's theory[1] on the light absorption in solution which treats only the long range dipolar interaction between solute and solvent molecules surrounding it without taking into consideration the short range interactions such as higher polar interactions, charge transfer, hydrogen bonding, etc.

Applying the Ooshika's theory to the case where the solvent molecules surrounding the

* A preliminary short communication was published in This Bulletin, 28, 690 (1955).

1) Y. Ooshika, *J. Phys. Soc. Japan*, **9**, 594 (1954).

2) E. Lippert, *Z. Naturforsch.*, **10a**, 541 (1955).

3) N.S. Bayliss and E.G. McRae, *J. Phys. Chem.*, **58**, 1002 (1954).

solute molecule are in the equilibrium configuration appropriate to the dipolemoment $\vec{\mu}_e$ of the excited solute molecule, one obtains the stabilization energy of solute molecule in its m state, $<\Delta E>^m$.

$$<\Delta E>^m = -\left\{\frac{2(D-1)}{2D+1} - \frac{2(n^2-1)}{2n^2+1}\right\}\left\{\frac{\vec{\mu}_e\cdot\vec{\mu}_m}{a^3}\right.$$
$$+\frac{2(D-1)}{2D+1}\frac{2}{a^3}\sum_{m'\neq e}$$
$$\left.\times\frac{\{\vec{\mu}_e(e\,\vec{\mu}_0|m')\}\{\vec{\mu}_m(e\,\vec{\mu}_0|m')\}}{\varepsilon_{m'}-\varepsilon_e}\right\}$$
$$-\frac{1}{2}\frac{2(n^2-1)}{2n^2+1}\frac{\mu_m^2}{a^3}+\frac{2(D+1)(D-n^2)}{3(2D+n^2)D}\frac{kT}{a^3}$$
$$\times\sum_{m'\neq m}\frac{(m\,\vec{\mu}_0|m')^2}{\varepsilon_m-\varepsilon_{m'}}+\left\{\frac{2(D-1)}{2D+1}\right\}^2\frac{1}{a^3}$$
$$\times\sum_{m'\neq m}\frac{\{\vec{\mu}_e(m\,\vec{\mu}_0|m')\}^2}{\varepsilon_m-\varepsilon_{m'}}-\frac{1}{2}\frac{2(n^2-1)}{2n^2+1}\frac{1}{a^3}$$
$$\times\sum_{m'\neq m}(m\,\mu_0|m')^2\left\{1-\frac{\varepsilon_m-\varepsilon_{m'}}{E_g-E_n}\right\} \qquad (1)$$

Where, D, n: dielectric constant and refractive index of the solvent, ε_m: electronic energy of solute molecule in its m state, E_n: electronic energy of solvent molecule in its n state, a: cavity radius in Onsager's theory of reaction field[4], $\vec{\mu}_m$, $\vec{\mu}_0$: dipolemoment in the m state and dipole operator of solute molecule.

The meaning of each term appearing in eq. (1) is as follows: The first term is due to the orientation effect between permanent dipole of solute molecule and those of solvent molecules, the second term represents the interaction of permanent dipole of solute with induced dipoles of solvent molecules (induced by solute permanent dipole), the third term arises from the fact that the average field of the solvent due to interaction between the permanent dipoles and induced dipoles of solvent molecules (induced by solvent permanent dipoles) polarizes the solute molecule, the fourth term is attributable to the interaction between the reaction field due to the mutual orientation of the solvent molecules and the dipole induced on the solute molecule by it, and the fifth term comes from the contribution of dispersion force.

Now the formula for $<\Delta E>_e^e$ and $<\Delta E>_f^g$ can be obtained easily from (1); the solvent shift of fluorescence spectrum $hc\Delta\sigma_f$ is represented as follows:

$$hc\Delta\sigma_f = <\Delta E>_e^e - <\Delta E>_f^g = \frac{2(D-1)}{2D+1}$$
$$\times\frac{\vec{\mu}_e\vec{\mu}_g-\vec{\mu}_e^2}{a^3}+\frac{2(n^2-1)}{2n^2+1}\frac{(\vec{\mu}_e-\vec{\mu}_g)^2}{2a^3}$$
$$+\frac{2(D+1)(D-n^2)}{3(2D+n^2)D}\frac{kT}{a^3}\left\{\sum_{m\neq e}\frac{(e\,\vec{\mu}_0|m)^2}{\varepsilon_e-\varepsilon_m}\right.$$
$$\left.-\sum_{m\neq g}\frac{(g\,\vec{\mu}_0\,m)^2}{\varepsilon_g-\varepsilon_m}\right\}+\left\{\frac{2(D-1)}{2D+1}\right\}^2\frac{1}{a^3}$$
$$\times\left[3\sum_{m\neq e}\frac{\{\vec{\mu}_e(e\,\vec{\mu}_0|m)\}^2}{\varepsilon_e-\varepsilon_m}-\sum_{m\neq g}\frac{\{\vec{\mu}_e(g\,\vec{\mu}_0\,m)^2\}}{\varepsilon_g-\varepsilon_m}\right.$$
$$\left.-2\sum_{m\neq e}\frac{\{\vec{\mu}_e(e\,\vec{\mu}_0\,m)\}\{\vec{\mu}_g(e\,\vec{\mu}_0\,m)\}}{\varepsilon_e-\varepsilon_m}\right]$$
$$+\frac{1}{2}\frac{2(n^2-1)}{2n^2+1}\frac{1}{a^3}\left[\sum_{m\neq g}(g\,\vec{\mu}_0\,m)^2\right.$$
$$\times\left\{1-\frac{\varepsilon_g-\varepsilon_m}{E_g-E_n}\right\}-\sum'(e\,\vec{\mu}_0\,m)^2$$
$$\left.\times\left\{1-\frac{\varepsilon_e-\varepsilon_m}{E_g-E_n}\right\}\right]. \qquad (2)$$

On the other hand, the solvent shift of absorption spectrum is[1].

$$hc\Delta\sigma_a = <\Delta E>_f^e - <\Delta E>_e^g = \frac{2(D-1)}{2D+1}$$
$$\times\frac{\mu_g^2-\vec{\mu}_g\vec{\mu}_e}{a^3}-\frac{2(n^2-1)}{2n^2+1}\frac{(\vec{\mu}_e-\vec{\mu}_g)^2}{a^3}$$
$$+\frac{2(D+1)(D-n^2)}{3(2D+n^2)D}\frac{kT}{a^3}\left\{\sum_{m\neq e}\frac{(e\,\vec{\mu}_0\,m)}{\varepsilon_e-\varepsilon^m}\right.$$
$$\left.-\sum_{m\neq g}\frac{(g\,\vec{\mu}_0|m)^2}{\varepsilon_g-\varepsilon_m}\right\}+\left\{\frac{2(D-1)}{2D+1}\right\}^2\frac{1}{a^3}$$
$$\times\left[3\sum_{m\neq g}\frac{\{\mu_g(g\,\vec{\mu}_0|m)\}^2}{\varepsilon_m-\varepsilon_g}-\sum_{m\neq e}\frac{\{\vec{\mu}_g(e\,\vec{\mu}_0\,m)\}^2}{\varepsilon_m-\varepsilon_e}\right.$$
$$\left.-2\sum_{m\neq g}\frac{\{\vec{\mu}_g(g\,\vec{\mu}_0|m)\}\{\vec{\mu}_e(g\,\vec{\mu}_0|m)\}}{\varepsilon_m-\varepsilon_g}\right]$$
$$+\frac{1}{2}\frac{2(n^2-1)}{2n^2+1}\frac{1}{a^3}\left[\sum_{m\neq g}(g\,\vec{\mu}_0\,m)^2\right.$$
$$\times\left\{1-\frac{\varepsilon_m-\varepsilon_g}{E_n-E_g}\right\}+\sum_{m\neq e}(e\,\vec{\mu}_0\,m)^2$$
$$\left.\times\left\{1-\frac{\varepsilon_m-\varepsilon_e}{E_n-E_g}\right\}\right]. \qquad (3)$$

From (2) and (3) we obtain:

$$hc(\Delta\sigma_f-\Delta\sigma_a) = -\left[\frac{2(D-1)}{2D+1}-\frac{2(n^2-1)}{2n^2+1}\right]$$

4) L. Onsager, *J. Am. Chem. Soc.*, 58, 1486 (1936).

$$\times\frac{(\vec{\mu}_e-\vec{\mu}_g)^2}{a^3}+\left\{\frac{2(D-1)}{2D+1}\right\}^2\frac{1}{a^3}$$

$$\times\Big[3\sum_{m\neq e}\frac{\{\vec{\mu}_e(e|\vec{\mu}_a|m)\}^2}{\varepsilon_e-\varepsilon_m}+3\sum_{m\neq g}\frac{\{\vec{\mu}_g(g|\vec{\mu}_0|m)\}^2}{\varepsilon_g-\varepsilon_m}$$

$$-\sum_{m\neq g}\frac{\{\vec{\mu}_g(g|\vec{\mu}_0|m)\}^2}{\varepsilon_g-\varepsilon_m}-\sum_{m\neq e}\frac{\{\vec{\mu}_g(e|\vec{\mu}_0|m\}^2}{\varepsilon_e-\varepsilon_m}$$

$$-2\sum_{m\neq e}\frac{\{\vec{\mu}_e(e|\vec{\mu}_0|m)\}\{\mu_g(e|\vec{\mu}_0|m)\}}{\varepsilon_g-\varepsilon_m}$$

$$-2\sum_{m\neq g}\frac{\{\vec{\mu}_g(g|\vec{\mu}_0|m)\}\{\vec{\mu}_e(g|\vec{\mu}_0|m)\}}{\varepsilon_g-\varepsilon_m}\Big]. \quad (4)$$

All the discussions given above are on the basis of long range dipolar interaction between solute and solvent molecules. The theory, therefore, is not appropriate to the system with the specific short range interactions. For the consideration of such short range interactions, it may be necessary to compute the quantum mechanical interaction energy for each special pair of solute and solvent molecules, and, in fact, the general treatment as shown above may not be allowed. Even in the limit of the approximation of dipolar interaction, it is practically a very complicated and difficult problem to apply to this case Kirkwood's theory[5] which is a higher approximation than Onsager's[4], taking into consideration the correlation of nearest neighbour dipoles.

Now, consider the case of solutes such as naphtholes in the solvents such as acetic acid esters, where hydrogen bond is formed between solute and solvent molecules but for solvent molecules Onsager's approximation may be fairly well applicable. Put a hydrogen bonded solute molecule in the cavity in dielectric continuum, and apply to this system the Onsager's approximation.

Then one may be able to separate approximately the interaction energy of solute molecule with solvent molecules surrounding it as follows:

$$<\Delta E>^m_{f,e}=<\Delta E(s)>^m_{f,e}+<\Delta E(l)>^m_{f,e} \quad (5)$$

Where, s and l indicate the terms arising from short range interaction due to hydrogen bonding and long range dipolar interaction, respectively. The superscript m represents that $<\Delta E>_m$ is the interaction energy in the m state of solute molecule, and subscript f or e means the Franck-Condon or equilibrium state.

From (5), the solvent shifts of fluorescence and absorption spectra can be written as follows:

$$\left.\begin{aligned} hc\Delta\sigma_f&=(<\Delta E(s)>^e_e+<\Delta E(l)>^e_e)\\ &\quad-(<\Delta E(s)>^g_f+<\Delta E(l)>^g_f)\\ hc\Delta\sigma_a&=(<\Delta E(s)>^e_f+<\Delta E(l)>^e_f)\\ &\quad-(<\Delta E(s)^g_e+<\Delta E(l)>^g_e)\end{aligned}\right\} \quad (6)$$

From (6) we obtain:

$$\begin{aligned} hc(\Delta\sigma_f-\Delta\sigma_a)&=[(<\Delta E(l)>^e_e+<\Delta E(l)>^g_e)\\ &\quad-(<\Delta E(l)>^e_f+<\Delta E(l)>^g_f)]\\ &\quad+[(<\Delta E(s)>^e_e+<\Delta E(s)>^g_e)\\ &\quad-(<\Delta E(s)>^g_f+<\Delta E(s)>^g_f)] \end{aligned} \quad (7)$$

The first term in square bracket in (7) is formally equated to the right hand side of (4), where, however, all the quantities associated with solute molecule must be replaced by those of hydrogen bonded solute. The second term is unknown but we may estimate this experimentally as will be mentioned later.

When the associating liquids such as alcohols are used as solvents, owing to the short range interactions between solvent molecules themselves, applicability of Onsager's theory, becomes much doubtful.

Experimental

According to the idea mentioned above, we have examined the fluorescence and absorption spectra of β-methylnaphthalene, β-naphthyl methyl ether, and α-, β-naphthols in various organic solvents. Fluorescence spectra were photographed with Hilger E_2 type spectrograph and the peaks of fluorescence spectra were visually observed. Absorption spectra were measured with Beckman Quartz spectrophotometer, and also photographed with Hilger E_2 type spectrograph. The solvents used were *n*-hexane, benzene, toluene, acetic acid esters, and alcohols.

α-, β-naphthols and β-naphthyl methyl ethers were the same samples as used before[3], methylnaphthalene was kindly supplied by Shionogi & Co., Ltd. and distilled under the atmosphere of dry nitrogen before use.

n-hexane and acetic acid esters were the same samples as described before[3], benzene, toluene and butanol were extra pure grade and used without further purification. Ethanol was 99% in purity.

Experimental Results and Discussions

The experimental results are shown in Table I, where σ^m_a is the position of the longest wave length peak of absorption spectra which is most prominent in all cases,

5) J.G. Kirkwood, *J. Chem. Phys.*, **7**, 911 (1939).

6) N. Mataga, Y. Kaifu and M. Koizumi, This Bulletin, **29**, 115 (1956).

TABLE I

σ_f^m AND σ_a^m VALUES FOR NAPHTHALENE DERIVATIVES (σ IN cm^{-1})

Solvent	$\left[\frac{2(D-1)}{2D+1}-\frac{2(n^2-1)}{2n^2+1}\right]$	β-Methylnaphthalene			β-Naphthyl methyl ether			α-Naphthol			β-Naphthol		
		σ_f^m	σ_a^m	$(\sigma_a^m-\sigma_f^m)$	σ_f^m	σ_a^m	$(\sigma_a^m-\sigma_f^m)$	σ_f^m	σ_a^m	$(\sigma_a^m-\sigma_f^m)$	σ_f^m	σ_a^m	$(\sigma_a^m-\sigma_f^m)$
n-Hexane	~0	29810	31340	1530	29070	30550	1480	30710	31090	380	29800	30460	660
Benzene	~0	29690	31270	1580	28930	30420	1490	30600	30980	380	29550	30290	740
Toluene	0.026	29670	31280	1610	28910	30430	1520	30540	30990	450	29510	30280	770
Butyl acetate	0.345	29810	31330	1520	28930	30520	1590	30460	30950	490	29220	30130	910
Ethyl acetate	0.398	—	—	—	28930	30540	1610	30460	30980	520	29210	30160	950
Methyl acetate	0.444	—	—	—	28950	30550	1600	30420	30980	560	29200	30180	980
Butanol	0.540	29760	31350	1590	28900	30530	1630	30330	30920	590	29110	30180	1070
Ethanol	0.582	29760	31350	1590	28880	30550	1670	30370	30950	580	29120	30220	1100
Methanol	0.616	—	—	—	28840	30560	1720	30380	30960	580	29110	30270	1160

while σ_f^m is that of the strongest or the most clearly observable peaks of fluorescence spectra, and are shown schematically in Fig. 1.

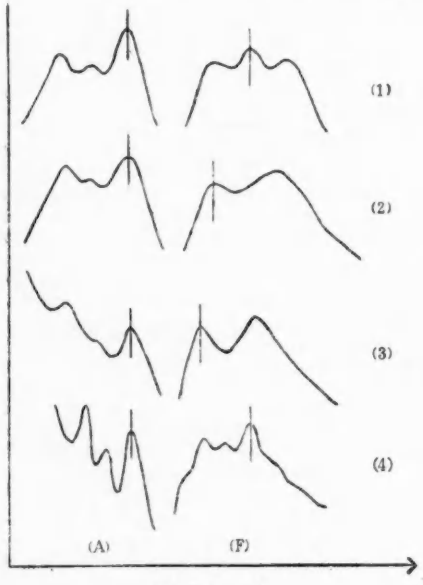

Fig. 1. Schematic diagrams of absorption and fluorescence spectra, the vertical lines showing the chosen peaks. (A), absorption (F), fluorescence; (1), β naphthylmethylether; (2), β naphthol; (3), β naphthol; (4), β methylnaphthalene.

For the comparison of the theory developed in II with the experimental results, the shifts of O–O bands should be employed, but it is very difficult to determine them exactly especially for such large molecules as naphthols. Hence it is necessary at first to consider the difference between O–O band on one hand and σ_a^m, σ_f^m on the other.

When σ_f^m and σ_a^m are used instead of O–O bands, equation (4) can easily be rewritten as follows.

$-hc(\sigma_f^m-\sigma_a^m)=hc(\delta\sigma_f+\delta\sigma_a)+\{$right hand side of (4)$\}$ (8) where $\delta\sigma_f$ and $\delta\sigma_a$ are the wave number differences between O–O bands and the peaks in the fluorescence and absorption spectra, respectively. Now the experimental results show that the solvent shifts of spectra take place as a whole; in other words, both the fluorescence and absorption spectra have respectively the same shape with the same interval between peaks irrespective of the solvents employed. Hence it may be allowed to put $(\delta\sigma_f+\delta\sigma_a)$=const. for one solute molecule.

Next, the theoretical formula (4) can be made much simpler for naphthalene derivatives, because the first term is far greater than the remaining terms in the order of magnitude. Thus a rough estimation for the given solvents mentioned in III, gives,

first term $\lesssim 10^{-13}-10^{-14}$ erg.
second term $\lesssim 10^{-17}-18^{-18}$ erg.

Therefore eq. (8) becomes

$$-hc(\sigma_f^m-\sigma_f^m)\cong\text{Const.}+\left[\frac{2(D-1)}{2D+1}-\frac{2(n^2-1)}{2n^2+1}\right]\times\frac{(\vec{\mu}_e-\vec{\mu}_g)^2}{a^3} \quad (9)$$

Lastly the second term of (7) must be estimated when the hydrogen bond is formed between solute and solvent molecules. As reported already[6], we have compared the

fluorescence and absorption spectra of α-, β-naphthols in pure *n*-hexane on one hand and in *n*-hexane added with acetic acid esters on the other and confirmed that $\Delta\sigma_f$ and $\Delta\sigma_a$ due to hydrogen bonding is nearly equal. Hence second term in (7) in the present case may be neglected in comparison with the first term.

After all, the theory can be tested by (9) using the data tabulated in Table I. The result is that (9) is fairly well satisfied by all the experimental data as shown in Fig. 2.

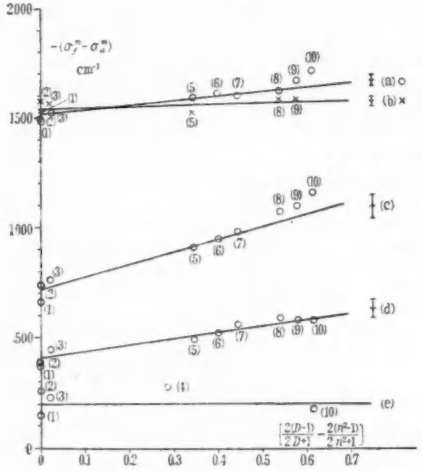

Fig. 2. $(\sigma_f^m - \sigma_a^m) \sim \left[\frac{2(D-1)}{2D+1} - \frac{2(n^2-1)}{2n^2+1}\right]$

relation for naphthalene derivatives and anthracene*.

Solutes: (a), β-naphthylmethylether; (b), β-methylnaphthalene; (c), β-naphthol; α-naphthol; (e) anthracene.

Solvents; (1), *n*-hexane; (2), benzene; (3), toluene; (4) chlorobenzene; (5), butylacetate; (6), ethylacetate; (7), methylacetate; (8), butanol; (9), ethanol; (10), methanol.

The veitical lines in the right hand of figure indicate the ranges of probable errors,

* Data from Ref. (9).

Thus it can be concluded that the orientation polarization is in fact the most prominent factor for the difference of solvent shifts of fluorescence and absorption.

The values for alcohols seem to show some systematic deviations, but the experimental errors are too large for us to say definitely.

From the inclination of these lines, $\frac{(\vec{\mu}_e - \vec{\mu}_g)^2}{a^3}$ can be calculated as follows:

β-naphthol: $\sim 9\times10^{-14}$ erg.
α-naphthol: $\sim 5\times10^{-14}$ erg.
β-naphthyl methyl ether: $\sim 3\times10^{-14}$ erg.
β-methylnaphthalene: $\lesssim 4\times10^{-15}$ erg.

If one puts $\vec{\mu}_e - \vec{\mu}_g \sim 0.5$ and a$\sim$3 Å, then $\frac{(\vec{\mu}_e - \vec{\mu}_g)^2}{a^3}$ becomes ca. 10^{-14} erg, which is near the value for β-naphthyl methyl ether. Thus for this compound the dipolemoment in the excited state is about 0.5 D. larger than in the ground state.

Of course such an evaluation would be valuable only for the estimation of the order of magnitude.

Next some discussions will be given about the value of $\vec{\mu}_e - \vec{\mu}_g$. No doubt this difference originates from π electron systems and most certainly the electron migration from substituent may be predominant in determing this value. Hence it may be reasonable to put in the first approximation,

$$\vec{\mu}_e - \vec{\mu}_g \simeq \vec{\mu}_e^{mig} - \vec{\mu}_g^{mig}$$

The effect of hydrogen bonding in the case of α-, β-naphthols would not alter the relative order,

$$(\vec{\mu}_e - \vec{\mu}_g)^{mig}_{\beta\text{-naphthol}} > (\vec{\mu}_e - \vec{\mu}_g)^{mig}_{\alpha\text{-naphthol}}$$

Thus the increments of dipolemoments in the excited state due to the enhanced electron migration are in the order of magnitude, 0.5–1 D. for β-naphthyl methyl ether and α-, β-naphthols.

It is to be noted here that a theoretical computation of migration dipole in the ground and excited state of phenol was done by Baba[7] using the theory of Sklar[8]. The increment $(\mu_e^{mig} - \mu_g^{mig})$ which he obtained is 0.3 D., which shows that the contribution of electron migration to the dipole increase in the excited state can be fairly large.

The value for β-methylnaphthalene, $\lesssim 4\times10^{-15}$ erg. given above is only provisional as an upper limit, and it is certain that this compound has much smaller dipole increment in the excited state as compared with those of naphthols and β-naphthyl methyl ether.

It may be expected from the present theory, that a nonpolar molecule with high symmetry such as anthracene does not show any effect as shown above.

In fact, the data reported by Sambursky and Wolfsohn[9], as plotted in Fig. 2, do not show any such effect. They interpreted the

7) H. Baba, *Monograph Ser. Research Inst. Applied Electricity Hokkaido Univ.*, No. 4, 61 (1954).
8) A.L. Sklar, *J. Chem. Phys.*, 7, 984 (1939).
9) S. Sambursky and Wolfsohn, *Trans. Far. Soc.*, 36, 427 (1940).

difference of solvent shifts in fluorescence and absorption spectra as due to the dipole-moment produced in the excited anthracene molecule, but it is quite certain from the present analysis that their conclusion is wrong.

As to somewhat larger deviations from the straight line, they may perhaps be due to some short range interaction specific to each solvent molecule. An anthracene molecule is larger than a naphthalene molecule, and for larger molecules even when they have symmetrical structure with a uniform charge distribution for the entire molecule, some short range interaction may arise from the local charge unbalance which may be produced in the excited state.

The results obtained by Lippert[2] for 4-dimethylamino-4′-nitrostilbene, 4-dimethylamino-4′-cyanostilbene and dimethylnaphthenrhodine, show some deviations, rather larger than ours, from the theoretical line. He has recently made a quite different attack on the problem and confirmed that his results are quite reasonable[10].

One of the authors (N. M.) wishes to express his thanks to Mr. T. Yamaguchi of Osaka University for his discussions.

10) E. Lippert, *Z. physiked Chem.*, N. F., **6**, 125, (1956).

Summary

A general formula for the difference of solvent shifts of fluorescence and absorption spectra in the approximation of long range dipolar interaction was derived using Ooshika's theory of light absorption in solution.

Measurements of fluorescence and absorption spectra of some naphthalene derivatives in various organic solvents were undertaken, and the data were analysed by the theoretical formula. The formula reproduces the experimental data satisfactorily, and from this fact it was concluded that the most predominant factor which determines the difference of solvent shifts of fluorescence and absorption spectra of these molecules is the interaction energy between solute and solvent molecules due to orientation polarization. The incremental values of dipolemoments in the excited state were estimated, and those for α-, β-naphthols and β-naphthyl methyl ether were interpreted as due to the increase of electron migration from the substituent in the excited state.

Institute of Polytechnics, Osaka City University, Osaka

The Synthesis of o, o′-Dihydroxydiphenyldiacetylene

By Yoshinobu ODAIRA

(Received October 13, 1955)

The synthesis of *o, o*-dihydroxydiphenyldiacetylene has been carried out along the following schema.

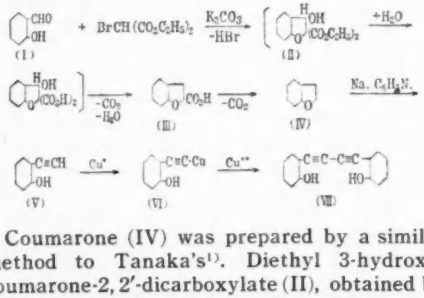

Coumarone (IV) was prepared by a similar method to Tanaka's[1]. Diethyl 3-hydroxycoumarone-2, 2′-dicarboxylate (II), obtained by condensing salicylaldehyde with diethyl bromomalonate in the presence of potassium carbonate, was saponified to coumarylic acid (III). The treatment of this acid (III) with a small amount of copper-chromite in quinoline gave coumarone (IV) with good yield.

Although *o*-hydroxyphenylacetylene (V) was prepared by Reichstein[2] previously from 3-bromocoumarone with Grignard's reagent, the yield was not good. Then Grey's method[3] has been applied to this reaction and the compound (V) has been obtained with good yield. The cleavage of its ether ring with sodium-pyridine under slow current of nitrogen gas gave a compound, having guaiacol-like odour. This has been identified with *o*-hydroxyphenylacetylene by its refractive index and its 3, 5-dinitro-benzoate.

The oxidative condensation of hydroxy-

1) S. Tanaka, *J. Chem. Soc. Japan*, **72**, 307 (1951).

2) Reichstein, *Helv. Chim. Acta.*, **20**, 892 (1951).

3) Grey, *Monatsch.*, **80**, 790 (1949).

phenylacetylene, as described in the experimental part, gave *o, o'*-dihydroxydiphenyldiacetylene (VII), the identity of which was established by elementary analysis and infrared absorption spectra measurement. (see Figs. 1 and 2)

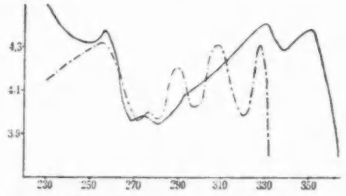

Fig. 1. Ultra-violet absorption spectra of *o, o*-dihydroxydiphenyldiacetylene (—) and diphenyldiacetylene (—·—)[4], all in ethanol solution.

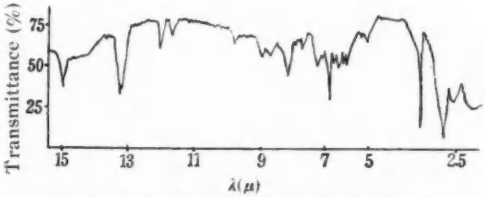

Fig. 2. Infra-red absorption spectrum of *o, o'*-dihydroxydiphenyldiacetylene.

Since the compound (VII) has remained unchanged for several months at room temperature, it seems to be fairly stable.

Experimental

o-Hydroxyphenylacetylene (V).—A mixture of coumarone (5.9 g.), metallic sodium (3.5 g.) and pyridine (5.4 g.) was heated under reflux in an atmosphere of nitrogen gas at 190°C for four hours. After cooling, pyridine (20 cc.) and water (30 cc.) were added slowly with stirring. The reaction mixture was extracted with ether, weakly acidified with dilute hydrochloric acid under cooling with ice, extracted with ether again and then the extract was washed with water. After evaporation, the red residual oil was twice distilled under reduced pressure with a stream of dry nitrogen gas, giving *o*-hydroxyphenylacetylene (V) as a colorless oil (3.2 g, 54.2%), b.p. 82–84°C/20 mm., n_D^{20} 1.5818. The 3,5-dinitrobenzoate had m.p. 169°C. V. Grey[3] cites m.p. 169°C for this compound.

o-Hydroxyphenylacetylene-cuprous salt (VI).—*o*-Hydroxyphenylacetylene (1.8 g.) in ethanol (140 cc.) was added with stirring to a solution of Ilosvay's reagent prepared from hydroxylamine hydrochloride (22.5 g.), copper sulfate (7.5 g.) and aqueous ammonia (28%, 30 cc.). After being allowed to stand overnight, the yellow precipitate was filtered and washed with ethanol (30 cc.).

o, o'-Dihydroxydiphenyldiacetylene (VII).—The cuprous acetylide (VI), prepared from the compound (V) (1.8 g.), was suspended in water (115 cc.), and then cupric chloride (115 cc.) was added gradually to the suspension with stirring for six hours. The reaction mixture was filtered and the filtrate was extracted with ether. The extract was washed with water and finally dried over anhydrous sodium sulfate. After evaporation, a crystalline solid was isolated. By recrystallisation from acetic acid (75%) with charcoal, white needle crystals, which melted at 143°C, were obtained, and weighed 324 mg. (18%).

Anal. Found: C, 81.65; H, 4.41. Calcd. for $C_{16}H_{12}O_2$: C, 82.6; H, 4.43%. Molecular weight Found: 227; Calcd.: 234.

I am greatly indebted to Professor Munio Kotake for his constant attention to my work.

Department of Applied Chemistry, Faculty of Engineering, Osaka University, Osaka

4) M. Nakagawa, *J. Chem. Soc. Japan*, **72**, 561 (1951).

---

*Rheological Properties of Some Polymerized Oils**

By Tsurutaro NAKAGAWA and Manabu SENŌ

(Received December 9, 1955)

Introduction

It has long been known that some colloidal or polymeric solutions exhibit the structural viscosity, the thread-forming property or the Weissenberg effect, and various authors have attributed these properties to some "elastic" nature of the liquid.

Some drying oils, e.g., tung oil or linseed oil get rapidly polymerized when heated to about 250°C and become not only viscous but also elastic; they actually turn back elastically when stirred in a vessel; they show a marked thread-forming ability and the liquid-thread springs back elastically when it snaps. These elasto-viscous liquids are

still more peculiar in that they show obviously the Weissenberg effect; they "climb up" to a rotating rod which is dipped in them to several centimeters or more. When they undergo still more heating, polymerization proceeds to leave a rubber-like brittle solid.

It is intended, in this study, to obtain some relation between these rheological properties by measuring the dynamic visco-elasticity.

Experimental Procedure

Torsional Oscillation.—**(I)**[1,2,3].—If a cylinder (moment of inertia I g.·cm^2) is suspended from a wire coaxially in the other fixed cylinder which is filled with a visco-elastic liquid (whose resistance R, elastance E), and a torsional oscillation of the amplitude Θ_0

$$\Theta=\Theta_0 e^{i\omega t} \tag{1}$$

is applied at the top of the suspension wire whose torsion constant is k dyn.·cm., the complex amplitude ratio $\boldsymbol{m}$ is given by

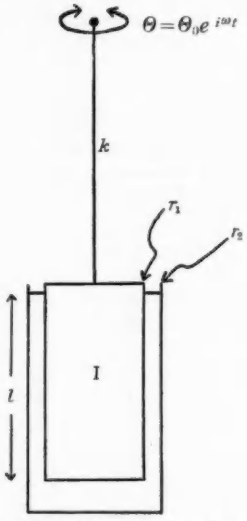

Fig. 1. Top-drive coaxial rheometer.

$$\boldsymbol{m}=\frac{\boldsymbol{A}}{\Theta_0}=\frac{k}{(k+E-\omega^2 I)+i\omega R},$$
$$\theta=Ae^{i\omega t}=Ae^{i(\omega t-\varphi)} \tag{2}$$

where l, r_1, and r_2 are the length of the immersed portion of the internal cylinder, the radii of the

So that if the amplitude ratio $m=\boldsymbol{A}/\Theta_0=A/\Theta_0$ which is the ratio of the amplitude of the motion θ of the inner cylinder to that of the top end of the suspension wire, and the phase angle $\phi=-\mathrm{Arg}(\boldsymbol{A}/\Theta_0)$ by which the inner cylinder lags the top end of the wire are experimentally observed, the complex quantity $\boldsymbol{m}$ is determined as $\boldsymbol{m}=me^{-i\varphi}$, and R and E are known from (2) or from

$$\begin{cases} R=\dfrac{kT\sin\phi}{2\pi m} \\ E=k\left(\dfrac{\cos\phi}{m}-1\right)+\dfrac{4\pi^2 I}{T^2} \end{cases} \tag{3}$$

where T is the period of oscillation ($\omega=2\pi\nu=2\pi/T$). The dynamic viscosity η and the dynamic rigidity G are calculated by the conventional formula

$$\begin{cases} \eta=\dfrac{R}{4\pi l}\left(\dfrac{1}{r_1^2}-\dfrac{1}{r_2^2}\right) \text{ poises} \\ G=\dfrac{E}{4\pi l}\left(\dfrac{1}{r_1^2}-\dfrac{1}{r_2^2}\right) \text{ dyn./cm}^2 \end{cases} \tag{4}$$

internal and the external cylinder respectively.

(II).—The scheme of analysing the visco-elasticity of liquid outlined above is inexact from the theoretical point of view. Recently several authors[4,5,6] have developed the rigorous treatment of this type rheometer. Among them S. Oka[5] proposed a rigorous method of determining the visco-elastic constants by the same top-drive oscillatory device as that described here. According to the theory the complex dynamic rigidity G^* of the liquid studied is obtained as a root of a quadratic equation

$$(B_0+B_1)G^{*2}-\{\mu B_1-(B_2+B_3)\rho\omega^2 r_1^2\}G^* -B_3\mu\rho\omega^2 r_1^2=0 \tag{5}$$

where ρ is the density and μ is a quantity which involves the observable amplitude ratio and the phase difference

$$\mu=\frac{1}{2\pi l r_1^2}\left(I\omega^2-k+\frac{k}{\boldsymbol{m}}\right), \qquad \boldsymbol{m}=me^{-i\varphi} \tag{6}$$

and the coefficients B_0, B_1, B_2,.....are the quantities relating only to the geometry of the vessel, viz. $x=(r_2-r_1)/r_1$ (which must be less than 1)

$$\begin{cases} B_0=\dfrac{1+(1+x)^2}{2(1+x)} \\ B_1=\dfrac{x(2+x)}{2(1+x)} \\ B_2=\dfrac{1}{16}\left\{-4(1+x)\ln(1+x)+4x-6x^2 +2x^3-\dfrac{3x^4}{1+x}\right\} \\ B_3=\dfrac{1}{16}\left\{4(1+x)\ln(1+x)-4x-2x^2 -2x^3+\dfrac{x^4}{1+x}\right\} \end{cases} \tag{7}$$

If G^* is known from Eq. (5), its real and imaginary

* Part of this paper was read before the Third Rheological Meeting at Kyoto, Japan, Nov., 1953.

1) T. Nakagawa, *J. Chem. Soc. Japan* (in Japanese), **72**, 759 (1951).

2) T. Nakagawa, This Bulletin, **24**, 191 (1951).

3) T. Nakagawa, ibid., **25**, 93 (1952).

4) J.G. Oldroyd et al., *Proc. Phys. Soc.* B, **64**, 44 (1951); *Quart. Journ. Mech. and Applied Math.*, **4**, 271 (1951).

5) H. Markovitz et al., *Rev. Sci. Instr.*, **23**, 430 (1952); *J. Appl. Phys.*, **23**, 1070 (1952).

6) S. Oka et al., *Bull. Kobayashi Inst. Phys. Res.*, **3**, 9, 17 (1953) (in Japanese).

* In our unpublished work on the concentrated carbon-black suspensions, a distorted ellipse which had without doubt resulted from the non-linearity of the material itself was obtained (cf. Fig. 6).

parts give the usual dynamic rigidity G and the dynamic viscosity η by the relation

$$G^*=G+i\omega\eta \tag{8}$$

It goes without saying that the rigorous scheme (II) involves the scheme (I) as the limiting case when $\omega\to 0$.

Lissajous' Figure Method for the Determination of m and ϕ.—Whether the approximate analysis (I) or the rigorous treatment (II) is applied, two experimentally determined quantities m and ϕ need to be measured.

When two simple harmonic motions whose directions of oscillation are at right angles to one another are composed, the resulting Lissajous' figure is an ellipse as long as they are of the equal period (cf. Fig. 2). Let the area of the ellipse be

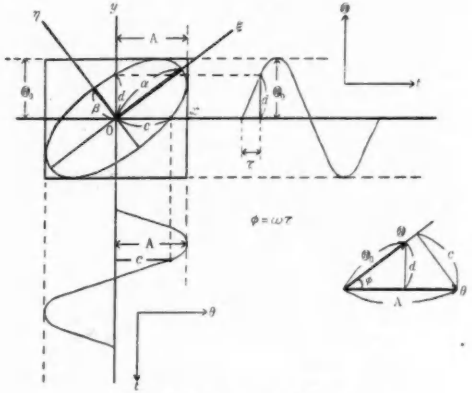

Fig. 2. Lissajous' figure.

(S) and that of the rectangle tangent to the ellipse be $[S]$. Then the next relation is known to hold.

$$\sin\phi=\frac{4}{\pi}\cdot\frac{(S)}{[S]}=1.273\times\frac{(S)}{[S]} \tag{9}$$

Eq. (9) gives a means of computing the phase angle ϕ by the planimetry. Since ϕ is an angle which satisfies

$$0\leqq\phi\leqq\pi,$$

two values of ϕ are generally obtained from Eq. (9), and they are discriminated as follows from the simple consideration.

1°. When the major axis of the ellipse finds itself in the first quadrant of the θ-Θ plane as in Fig. 2, ϕ is an angle of the first quadrant, that is

$$0\leqq\phi\leqq\frac{\pi}{2}$$

2°. When the major axis is in the second quadrant, ϕ is

$$\frac{\pi}{2}\leqq\phi\leqq\pi$$

and if ϕ' satisfying Eq. (9) and being smaller than $\pi/2$ is determined, the true phase angle ϕ is obtained from $\phi=\pi-\phi'$. From 1° and 2° it is possible to determine to what quadrant the angle ϕ belongs by inspecting the direction of the Lissajous' ellipse.

As is known from Fig. 2, it is also possible to determine ϕ from

$$\sin\phi=c/A=d/\Theta_0$$

The apparatus for practising the above-stated is sketched in Fig. 3. The whole apparatus consists of (1) the driving device and (2) the measuring system.

(1) A driving motor (1/16-1/20 HP, 1500 rpm) and a reduction gear train can produce several low speed rotations ranging from 20 rpm to 0.05 rpm by changing the combination of the gears. Use of a friction table and a movable friction wheel makes it possible to change the motion speed continuously. Rotational motion from the

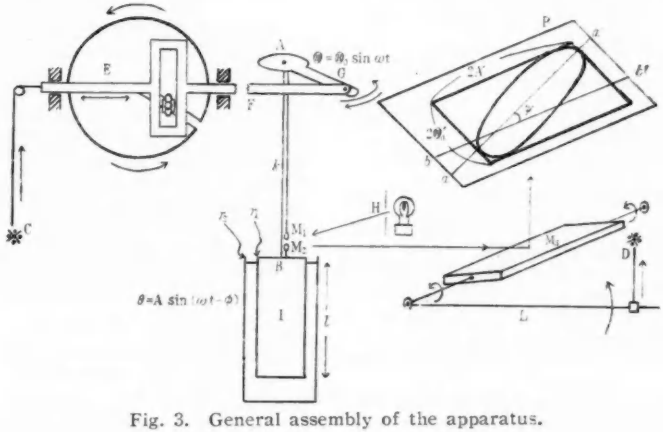

Fig. 3. General assembly of the apparatus.

friction desk is changed into the oscillatory motion at the top A of the suspension wire by the eccentric coupling mechanism E and levers F (33 cm.) and G (28.5 cm.). Eccentricity on E is adjustable along its radius between 0 and 5 cm. It is thus possible to obtain the driving oscillation whose period can be changed continuously from about 0.5 seconds to about thirty minutes and whose

amplitude θ_0 is changeable between 0–10 degrees. It was, of course, confirmed beforehand that the motion is harmonic. The observed θ-t curve is correctly sinusoidal. (The oscillation of the internal cylinder, on the other hand, is not always harmonic. In the case of Fig. 6, it is known from the Fourier analysis that the contribution from the over-tones reaches several per cent.)

(2) The measuring system is constructed as follows. In order to observe the motion of the internal cylinder, a small galvanometer mirror M_2 is attached to a chuck B by which the lower end of the suspension wire is connected to the inner cylinder; and in front of the mirror M_2 a strip mirror M_3 (3 cm.×15 cm.×3 mm.) is placed at the angle 45° to the beam of light from M_2, and is oscillated in phase of the driving motion $\theta=\theta_0 \sin \omega t$ by a lever L (10–40 cm., adjustable) which is connected to the oscillation mechanism E by a cord C-D. A Lissajous' figure is thus traced on a photographic plate or paper P; a proper lens system should be used in order to focus the image of a pin-hole H onto the plate P.

Experimental determination of the amplitude ratio m is a little complicated. It is incorrect to compute m directly as A'/θ_0' from the observed Lissajous' figure, because the transverse deflection A' and the vertical deflection θ_0' on the plate are of different scale by reason of the different paths as is plain from Fig. 3. One way for evaluating m is to use another mirror M_1 which is attached to the lower end of a long rod connected to the upper end of the suspension wire. As M_1 moves in phase of the driving oscillation $\theta_0 \sin \omega t$, the Lissajous' figure obtained from M_1 is an oblique line aa'. If then the strip mirror M_3 is kept in position, a horizontal line bb' is obtained and m is determined as follows

$$m=\frac{A}{\theta_0}=\frac{A'}{\theta_0' \cdot f}=\frac{A'}{\theta_0'} \cdot \tan \psi \tag{11}$$

$$f=\cot \psi \tag{12}$$

where A', θ_0', and ψ are the quantities illustrated in Fig. 3. A' and θ_0' are respectively side lengths of the rectangle in contact with the ellipse which is easily drawn if the base line bb' is obtained.

It goes without saying that the determination of ϕ is not influenced by the difference of the scale unit of the two axes of coordinates as is understood from Eqs. (9) and (10) and Fig. 2. This is the same in the case of the discrimination 1° and 2°.

Torsion constant k and the moment of inertia I are determined from the observation of the period of the free torsional oscillation[1,2,3]. It should of course be kept in mind that k changes with the length of a wire.

The experimental condition is as follows.

Internal cylinder (made of brass): $r_1=2.02$ cm., Height: 15.0 cm., $I=3.28\times10^3$ g.·cm.^{2} (mass: 1608.6 g.)

External cylinder: $r_2=2.51$ cm., Height: 18.14 cm.

Immersion depth l: 14.5–15.0 cm. (to be observed in each run of measurement). End-effect of the internal cylinder was neglected.

Torsion constant k: one wire is properly selected from the piano wires or drill rods tabulated below (Table I) according to the consistency of the liquid being tested. Wire length A-B (about 67 cm. cf. Fig. 3) is measured in each run of the experiment and k is calibrated.

TABLE I

SUSPENSION WIRES USED AND THEIR TORSION CONSTANT

Wire or rod	Length (cm.)	k (dyn.·cm.)
0.30 mm. dia. piano-wire	67.40	9.96×10^2
0.44 mm. dia. piano-wire	67.53	4.44×10^3
0.60 mm. dia. piano-wire	67.29	1.475×10^4
0.80 mm. dia. piano-wire	67.11	4.745×10^4
1.0 mm. dia. drill-rod	67.27	1.258×10^5

θ_0, amplitude of the driving oscillation: 4–6 degrees of angle. A, amplitude of the forced oscillation of the internal cylinder is designed to be less than 2 degrees of angle, so that the maximum angle of shear γ (cf. Fig. 4) of the sample itself at the

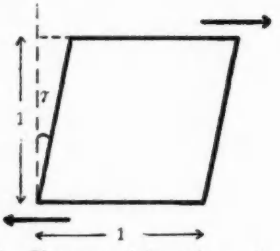

Fig. 4. Shear straining of a unit cube.

wall of the internal cylinder is known to be less than about 11 degrees (cf. Eq. (23)). It may therefore be possible to say that the measurement is done under the condition of small deformation. Temperature control is made by a water thermostat in which the external cup is immersed. For the sake of securing the uniform temperature of the whole measuring vessel, the thermostat is covered by a plate from which only the suspen-

TABLE II

SAMPLES TESTED AND THEIR GENERAL PROPERTIES

Sample	Remark
No. 0	The most highly polymerized, sticky, visco-elastic matter with strong thread-forming ability.
No. 1	Moderately polymerized, thread forming, highly viscous liquid.
No. 2	〃
No. 3	Less thread-forming liquid of lower viscosity without elastic nature

sion wire and the mirror M_2 are led outwards. Measurement was done by changing temperature and frequency as follows.

Temperature: 20°–60°C

Period of oscillation: 10–300 seconds

Samples.—Four sample oils listed below (Table II) were made from the thermal polymerization (above 200°C) of linseed oil, and subjected to test.

Results and Discussion

The rigorous scheme of analysis (II) of the observed results, of which description was made in the previous section, was compared with the simple method (I) which has since been used by the author, and it proved that, in such low frequencies as were used here, the difference between the two methods was negligible. In the present study all the data were therefore analysed along the simple scheme (I).

Amplitude Effect.—Our whole procedure of analysing the observed quantities, including the scheme (I) and (II), is based on the assumption that the shear stress S and the shear strain γ satisfy the generalized Hooke's law

$$S=G^*\gamma \tag{13}$$

in which complex rigidity G^* should not depend upon S and γ, while it is a function of frequency. If the linearity relation (13) does not hold, various non-linear behaviors are expected to be observed; e.g., Lissajous' figure will probably deviate from ellipse, or the amplitude dependence of the dynamic visco-elasticity will be notable.

In all the Lissajous' figures obtained, deviation from ellipticity was not perceptible (cf. Fig. 5)*.

Moreover, it is possible to test experimentally the influence of amplitude on the dynamic properties by keeping the period T constant and by changing the eccentricity at the cam E. As to the amplitude effect the experimental result is summarized in Fig. 7 and Fig. 8, in which $\gamma_{\max.r=r_1}$ is the amplitude of the shear strain at the wall of the internal cylinder[7] (cf. Fig. 4)

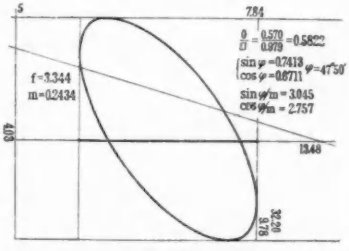

Fig. 5. A sample photograph of the observed Lissajous' figure. (linear visco-elasticity)

7) Th. Schwedoff, *J. de Phys.*, [2], **8**, 341 (1889).

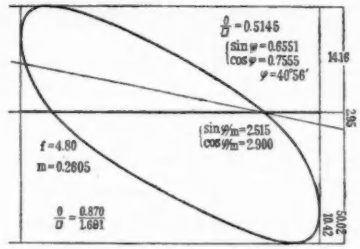

Fig. 6. A sample photograph of the distorted Lissajous' figure. (non-linear visco-elasticity)

$$\gamma_{\max.r=r_1}=\left[\frac{2Ar_1^2r_2^2}{(r_2^2-r_1^2)r^2}\right]_{r=r_1}=\frac{2Ar_2^2}{(r_2^2-r_1^2)}. \tag{14}$$

A is the amplitude of the oscillation of the internal cylinder, and in the present case $\gamma_{\max.r=r_1}=5.67\cdot A$ ($r_1=2.02$ cm., $r_2=2.51$ cm.). $\sin\phi/m$ and $\cos\phi/m$ are the quantities corresponding to viscosity and elasticity respectively, if the period T is kept constant (cf. Eqs. (5), (6)). Three series I, II and III were tested under the following condition using the most sticky varnish No. 0 whose rheological details are shown in Fig 9 (cf. Table III).

TABLE III

EXPERIMENTAL CONDITION ADOPTED FOR THE TEST OF THE AMPLITUDE EFFECT

Oil	Series	Temperature (°C)	Period of oscillation (sec.)
No. 0	I	20	50
	II	30	20
	III	20	20

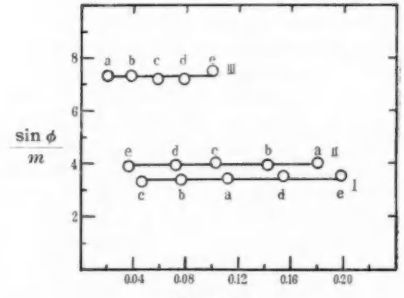

Fig. 7. Amplitude dependence of dynamic viscosity. (No. 0 varnish)

In each series, measurement was done in the order a → b → c → d → e in about six hours, that is, in II the sample first undergoes the largest straining and the other measurements are all carried out within a smaller shear strain; in III, on the other hand, the sample is subjected to a new and larger deformation in each run.

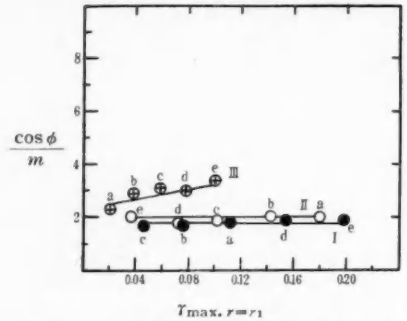

Fig. 8. Amplitude dependence of dynamic elasticity. (No. 0 varnish)

As is known from Figs. 7 and 8, effect of the amplitude on the dynamic viscosity and elasticity is null or slight within the amplitude region tested.

Since the dynamic viscosity is independent on the strain amplitude, it again ought to be independent on the amplitude of the strain velocity from the relations $\theta = Ae^{i\omega t}$, $\dot{\theta} = i\omega A^{i\omega t}$, and

$$\dot{\gamma}_{max.r=r_1} = \frac{2\omega A r_2^2}{(r_2^2 - r_1^2)}. \qquad (15)$$

Visco-elasticity of these varnishes is therefore supposed to be nearly linear.

Series III shows a slight non-linearity, especially in the elastic property. Measurement is, in this series, started from the smallest strain, and the sample suffers a new larger deformation in each run of measurement. No. 0 varnish has, as will be seen later, a viscosity of 10^3 poises and an elastic constant of 10^2 dyn./cm^2 at 20°C of temperature. And such a sticky sol as this generally has a tendency to solidify into a gel-like structure in the course of settling. It will be attributed to this gel-like nature that the elastic constant d(stress)/d(strain) increases with the increase of strain. Since it is expected that this structure breaks down by agitation or straining, the non-linear property will be reduced when the measurement is done in the opposite direction (cf. Series II).

Frequency Dependence.—Frequency dependence of the dynamic viscosity and rigidity was tested under various conditions. The results are summarized in Figs. 9–12. Since it is confirmed in the previous section that no amplitude effect is observed, it will hereafter be possible to consider these data as those of Newtonian and Hookean nature.

Oil No. 0 (Fig. 9) is typically visco-elastic. Dynamic property-frequency curves show a marked dispersion; the dynamic viscosity decreases with the increase of frequency, and the dynamic rigidity increases markedly on the other hand. The lower the temperature, the stronger is the dispersion effect. These materials appear as if they are an elastic mass when handled by a sudden shock; they contract and turn back when freed after being agitated. The external work can, in spite of their fluid nature, be stored up as the elastic potential for a short time. This elastic potential energy gradually dissipates away as a viscous loss; they behave like a viscous fluid when they are treated gently. Varnish No. 0 actually exhibits this property, and Fig. 9 reflects this situation.

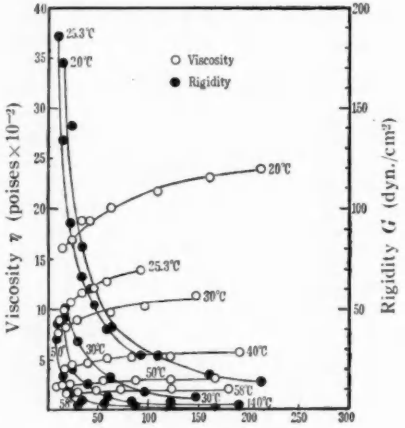

Fig. 9. Dynamic properties of varnish No. 0.

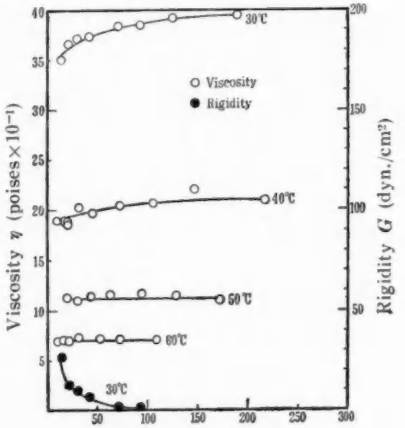

Fig. 10. Dynamic properties of varnish No. 1.

The varnish No. 0 is used as an adding agent in the printing ink manufacturing industry in order to control and improve the "printability" of inks. The peculiar rheological property of the oil No. 0 is supposed to have some influence upon printability.

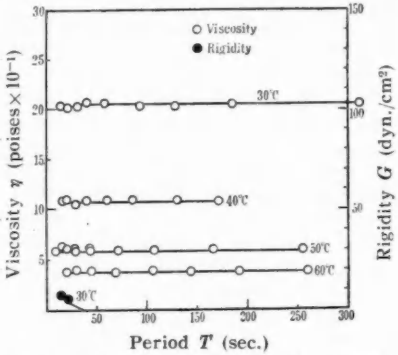

Fig. 11. Dynamic properties of varnish No. 2.

Varnishes No. 1 (Fig. 10) and No. 2 (Fig. 11) are viscous liquids, showing a slight elastic nature at a low temperature and high frequency; towards a very gentle handling they behave as simply viscous liquids. The oil No. 3 (Fig. 12) is a purely viscous liquid and shows no elasticity at any temperature and frequency tested. It is of course possible for this varnish to appear as elastic at a lower temperature and higher frequency than this. In fact, it may occur that these oils act not as simply viscous matter but as a visco-elastic medium between the rollers of a high-speed printing machine when they are used as a vehicle.

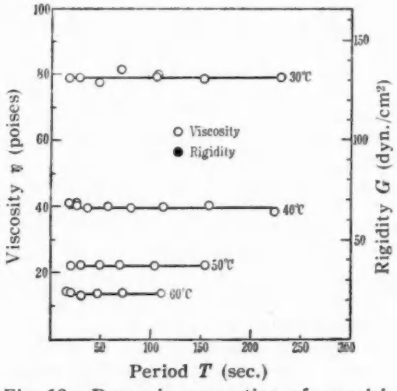

Fig. 12. Dynamic properties of varnish No. 3.

Returning to the varnish No. 0 (Fig. 9), the visco-elastic behavior at 25°C is a little peculiar. The elasticity at 25°C has a value nearly equal to that at 20°C, though the viscosity at 25°C is decreased in an ordinary manner. The fact is that the measurement at 25°C was carried out on the sample which was left and settled in the measuring vessel (between the inner and the external cylinder) for about a month. It is therefore possible for the oil to cause a gel-formation as was stated above, and this gel-formation may be ascribed to a weak network structure of the solute molecules formed in the sol by the secondary forces. On account of the elasticity from this network, the observed dynamic rigidity does not so markedly decrease by raising temperature from 20°C to 25°C. The dynamic viscosity, on the other hand, is supposed to come, in its considerable part, from the flow of the low molecular weight solvent molecules spread in such structure, and therefore it decreases considerably when temperature is raised.

Temperature Dependence.—When the frequency independent viscosities of the varnishes No. 1—No. 3 are plotted against the reciprocal absolute temperature, Fig. 13 is

$$\eta = Ae^{B/T} = Ae^{\Delta E/RT} \qquad (16)$$

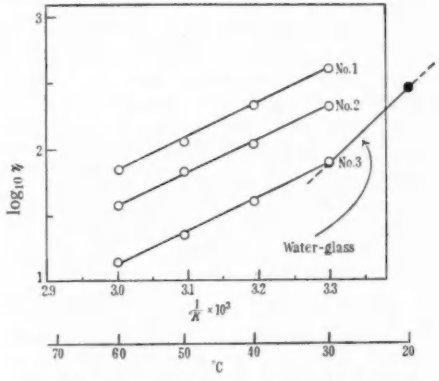

Fig. 13. Temperature dependence of viscosity.

obtained. These curves conform to the Andrade formula T is here the absolute temperature (not the period), and R the gas constant. The constants A and B or the apparent activation energy ΔE are calculated and tabulated in Table IV.

TABLE IV
CONSTANTS OF THE ANDRADE FORMULA
$\eta = Ae^{B/T} = Ae^{\Delta E/RT}$

Oil	A	$B\times10^{-3}$	ΔE (kcal.)
No. 1	2.33×10^{-6}	5.72	11.4
No. 2	1.03×10^{-6}	5.78	11.5
No. 3	2.12×10^{-7}	5.94	11.8

The value of B (or ΔE) is, when compared with those of the other materials[2], larger than those of the low molecular weight liquids (mercury, toluene, water), smaller than those of the highly associated liquids (glass, rosin, tar-pitch, glucose melt), and of the same order as those of asphalts and the glucose-melt at higher temperature. This is possible from the fact that these oils are polymerized to a certain degree.

It is noted that the apparent activation energy ΔE for the viscous flow has almost the same value as that of others in spite of the great difference of the absolute value of viscosity. One of the possible interpretations may be that at a certain stage of the thermal polymerization the growth of the polymer molecule itself does not occur, but the number of polymers simply increases.

Weissenberg Effect

In 1946–1948 K. Weissenberg[8,9,10] noted that some elastic liquids show a peculiar property to climb up to a rotating rod or ascend in a rotating pipe, and the various authors[8–14] have since developed the theoretical and experimental study of this phenomenon.

Our varnishes No. 0–No. 2, as seen in Figs. 9–11, show evidently an elastic property even in the very low frequencies like 0.1 cycles per second. It is therefore expected that the Weissenberg effect may appear even when a rod is slowly rotated in these oils. The result is illustrated in Fig. 14. A rod of 10 mm. dia., sunk to about 3 cm. depth, is rotated at the rate of two and three rotations per second, and the behavior of the liquids was observed. The experiment was made at the room temperature of about 20°C; the visco-elastic constants of the varnishes at 20°C can be estimated from Figs. 9–13.

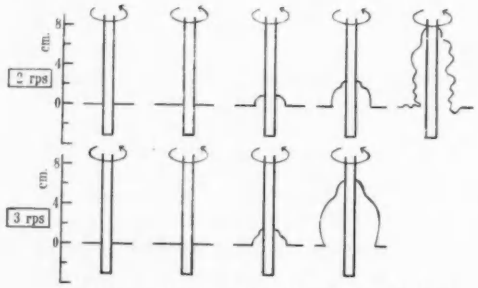

Fig. 14. Weissenberg effect.

In the varnish No. 3 no effect was observed at this temperature and revolution rate, and this situation corresponds to Fig. 12 where no elastic property is shown. The oils No. 2 and No. 1 evidently exhibit the Weissenberg effect, and the varnish No. 1 which is more sticky than No. 2 climbs up higher than No. 2. The effect is stronger when the rotation rate is increased; this is natural from the fact that the Weissenberg effect is concerned with the relaxation phenomena of liquid. In the oil No. 0 which is the most sticky and elastic of all, the effect is so strong that even at 2 rps the oil climbs up to 8 cm. or more in a very irregular manner like a towel which is squeezed.

For the sake of comparison, we tested a water-glass sample, which was previously confirmed to lack an elastic nature in these low frequencies[3]; and no effect was observed. From the falling-sphere method, its viscosity was estimated to be 290 poises at 20°C and it is the similar value to that of No. 3 or No. 2 at 20°C. It is therefore argued that the liquid is too fluid to climb up and that if the viscosity were increased the Weissenberg effect might appear. Water-glass was then cooled to 5°C of temperature in order to make it be more than 1000 poises of viscosity which is the same order of that of No. 1 varnish. The effect was still nothing. As has been discussed above, viscosity alone is not enough to cause the Weissenberg effect however viscous a liquid may be.

Summary

(1) A method for measuring the dynamic visco-elasticity of liquid by the torsional oscillation is described.

(2) The visco-elastic oils produced by the thermal polymerization of linseed oil to various degrees were studied by this rheometer.

(3) The amplitude effect of the dynamic properties was negligible; so that these materials are supposed to be linear in their visco-elastic behavior.

(4) The dynamic visco-elasticity of these oils was measured in the very low frequency region (period: 10 seconds–5 minutes).

(5) The temperature dependence of the dynamic viscosity was discussed.

(6) Weissenberg effect of these oils was tested in a qualitative way.

8) K. Weissenberg, *Nature*, **159**, 310 (1947).
9) S.M. Freeman and K. Weissenberg, *Nature*, **161**, 324 (1948).
10) S.M. Freeman and K. Weissenberg, *Nature*, **162**, 320 (1948).
11) M. Reiner, "Deformation and Flow", H.K. Lewis, London (1949).
12) M. Mooney, *J. Appl. Phys.*, **24**, 675 (1953).
13) F.J. Padden and T.W. DeWitt, *J. Appl. Phys.*, **25**, 1086 (1954).
14) M. Yamamoto, *Busseiron Kenkyu*, No. 78, 51 (1954) (in Japanese).

The authors hereby express their thanks to Prof. H. Akamatu for his interest and leadership in this investigation. All the samples of the polymerized oils used in this program were furnished through the kindness of Mr. T. Enya and Mr. I. Ishizu of the Dainippon Printing Ink Manufacturing Co. It is also a pleasure to acknowledge the assistance of Mr. S. Kojima who built the apparatus. This work was supported in part by the Scientific Research Grant from the Ministry of Education.

Department of Chemistry, Faculty of Science, The University of Tokyo
Hongo, Tokyo

Studies on the Infrared Spectra of Ephedrine and Related Compounds. II. Infrared Spectra of Diastereoisomeric Ephedrines in 3 Micron Region

By Tokunosuke KANZAWA

(Received January 11, 1956)

In the preceding paper[1] the present author showed that the infrared spectra of dilute carbon tetrachloride solutions of ephedrines and related compounds in 3 μ region were useful for the discrimination between diastereoisomers. However, there remain some problems unsolved. For example, the questions why there appear always two bands, sharp and broad, and which of OH and NH groups participates in hydrogen bond formation should be answered. Moreover, the reasons why the frequency difference ($\Delta\nu$) between the sharp band and the broad one (150–238 cm.$^{-1}$) is much larger than that found for 2,3-butanediol[2] (meso-form, 39 cm.$^{-1}$, *d*-form, 45 cm.$^{-1}$) and why $\Delta\nu$'s of pseudo compounds are always larger than those of normal ones also need explanation. In order to obtain information about these problems, the present experiments have been carried out on concentration dependence of ephedrines in carbon tetrachloride solution, solvent effect and the interaction with triethylamine. In connection with these, spectra of ethanolamine and 3-amino-2-butanol and the interaction between benzyl alcohol and triethylamine have been observed.

Experimental

Infrared Measurement.—The spectrophotometer used and its operating conditions were the same as described previously[1]. The spectra were taken with LiF prism at a room temperature adjusted at 25°C±2°. The accuracy of the measurement of wave numbers was ±2 cm^{-1}. Absorption cells of 0.056 cm. (NaCl windows), 0.3, 2.0 cm. (CaF_2 windows), 5 and 10 cm. (silica windows) in length were used. Since the silica cell absorbs 2.75 μ ray by 10–20% in transmission, it is unsuitable for the quantitative measurement of the free OH absorption at 2.76 μ.

Materials and Solvents.—Ephedrine and Ψ-ephedrine were of ther ecemic modification. The spectra of *dl*-ephedrine were quite in agreement with those of *l*-ephedrine. Ethanolamine, diethylamine and triethylamine were carefully distilled through a 40 cm., glass helix-packed column and dried over NaOH. 3-Amino-2-butanol was prepared after the method reported by Vanderbilt et al.[3] The product was liquid and did not crystallize after repeated distillation. Dickey et al.[4] reported that the product obtained by Vanderbilt's method was of erythro series and slightly impure. Benzyl alcohol was washed with sodium hydroxide solution, sodium bisulfite solution and water, dried over potassium carbonate and distilled under a reduced pressure.

Chloroform and carbon tetrachloride were purified as described previously. Benzene was purified by the usual method. Carbon disulfide was shaken with potassium permanganate solution, mercury, mercuric sulfate solution and water, dried over calcium chloride and distilled.

Preparation of Solutions.—On the preparation of solutions care was taken to avoid the contact with atomospheric moisture. It is worth noticing that fine crystallites happen to precipitate gradually in the carbon tetrachloride solution of ephedrines. It was feasible that the precipitation should occur as the concentration increased. Melting points of the precipitates were consistent with hydrochlorides of ephedrines. Although the reason why such precipitation occurred was not clarified, a slow chemical reaction might proceed

1) T. Kanzawa, This Bulletin, **29**, 398.
2) L.P. Kuhn, *J. Am. Chem. Soc.*, **74**, 2492 (1952).
3) B.H. Vanderbilt and H.B. Hans, *Ind. Eng. Chem.*, **32**, 34 (1940).
4) F.H. Dickey, W. Fickett and H.J. Lucas, *J. Am. Chem. Soc.*, **74**, 944 (1952).

in the carbon tetrachloride solution. The similar precipitation occurred in CS_2 solution of ephedrine already at a concentration of 0.03 M, but the precipitates were not identified. The spectra when precipitation occurred were omitted.

Experimental Results

A. Concentration Dependence of the Spectra in 3 μ Region

Ephedrine.—Concentration dependence of the absorption spectrum of ephedrine in 3 μ region is shown in Fig. 1-a. Over a concentration range from 0.001 to 0.01 M, the spectrum of the carbon tetrachloride solution remains almost unchanged in the relative intensities and positions of bands. On raising the concentration of ephedrine up to 0.21 M it is observed that the intensity of the sharp band component at 3619 cm.$^{-1}$ decreases, that of the broad band component at 3451 cm.$^{-1}$ increases, and besides a new band appears at 3321 cm.$^{-1}$. Such behavior of the concentration dependence will be explained as follows. As long as the concentration remains dilute, the bands due to hydrogen bonding are only from the intramolecular origin. It may be added that from the molecular

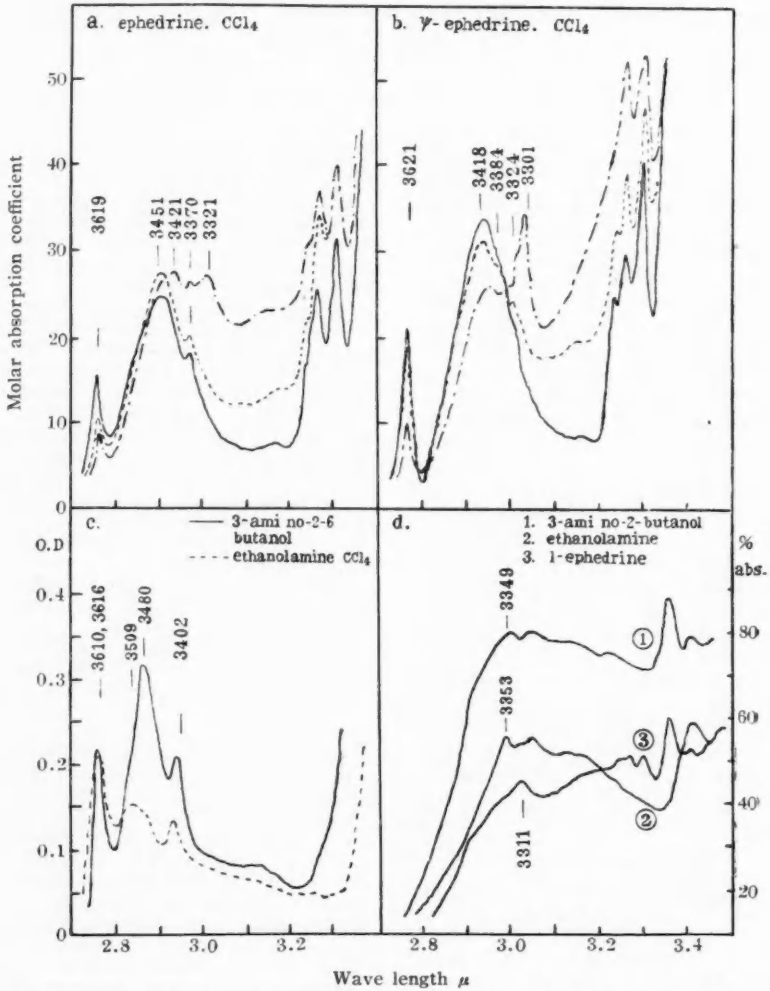

Fig. 1. Spectra of ephedrines, ethanolamine and 3-amino-2-butanol in 3 μ region.
a) —— 0.0054 M/l. ×2 cm., ---- 0.075 M/l. ×0.3 cm., —·— 0.21 M/l. ×0.056 cm.
b) —— 0.003 M/l. ×2 cm., ---- 0.05 M/l. ×0.3 cm., —·— 0.11 M/l. ×0.056 cm.
c) —— ca. 0.005 M/l. d) liquid state. 0.01 mm. thick.

weight determination[5] the formation of ring dimer may be improbable in the dilute solution. However, the change observed at the concentration 0.21 M may be due to the formation of hydrogen bond between molecules.

In the spectra of the solution at lower concentrations the sharp band (3619 cm.$^{-1}$) is clearly due to free OH stretching vibration. The broad band can be ascribed to the intramolecularly hydrogen-bonded OH vibration. Then, a band due to NH vibration may be either covered by the broad band or assigned to a small peak at 3370 cm.$^{-1}$. In this respect the results obtained by Russell and Thompson[6] for carbon tetrachloride solutions of many disubstituted amines will be helpful. According to their results, the absorption of ν (NH) appears in a range 3311–3350 cm.$^{-1}$ for dialkylamines and in 3430–3490 cm.$^{-1}$ for arylalkylamine, diarylamine and heterocyclic compounds. As to the intensity the absorption of dialkylamines is usually very weak compared with that of the other amines. From these results it may be reasonable to assign the band at 3370 cm.$^{-1}$ to free ν (NH), since NH group in ephedrine is very similar in structure to that in dialkylamine. However, whether this ν (NH) band is due to nitrogen atom bridged by a neighboring OH group or not is not certain. Russell and Thompson described that there is some suspicion that the intensity of the NH absorption, so low as almost to disappear, for dialkylamine is connected with a slow chemical reaction of amines with carbon tetrachloride. This description is consistent with the observation in the present experiments that the precipitation of hydrochloride occurs. Therefore the spectra of the alkamine in carbon tetrachloride solution may represent a sort of metastable state of molecule.

At 3.14 μ appears a weak band, which seems to be independent on the change of concentration. The bands at 3.3 μ are due to CH vibration of benzene ring and have no relation with hydrogen bonding.

In connection with the spectra of ephedrines, those of ethanolamine and 3-amino-2-butanol in carbon tetrachloride solution at a concentration of about 0.005 M are recorded and shown in Fig. 1-c., of which the structure is similar to that of ephedrine in 2.7–3.1 μ range. The sharp bands with higher frequency are due to free OH vibration and a band at 3509 or 3490 cm.$^{-1}$ may be due to either free NH vibration or the bonded OH vibration overlapping with free NH vibration. If the bands near 3500 cm^{-1} are due to the intramolecularly hydrogen-bonded OH vibration, the values 101 cm.$^{-1}$ for ethanolamine and 126 cm.$^{-1}$ for 3-amino-2-butanol of the frequency difference between the free and the bonded OH absorption are much less than that for ephedrine (168 cm.$^{-1}$).

The spectrum of the solution at 0.21 M seems to show co-existence of free molecules having intramolecular hydrogen bond and associated molecules. As absorption at a higher concentration than 0.21 M could not be observed because of rapid precipitation of crystallites, a spectrum of *l*-ephedrine in liquid state was taken (Fig. 1-d). It shows a band at 3311 cm.$^{-1}$ with a very weak shoulder near 2.9 μ and continuous absorption over 3.1–3.3 μ. In the previous paper[1], it was reported that in crystalline state *dl*-ephedrine shows only one band at 3300 cm^{-1}, assigned to the perturbed OH vibration. Then, the 3311 cm.$^{-1}$ band for ephedrine in liquid state can be considered to be due to this OH vibration. The weak shoulder near 2.9 μ may be due to the intramolecularly hydrogen-bonded OH absorption still remaining in the liquid state.

From these observations and the assignment of the spectrum at a concentration of 0.0054 M the spectral change accompanied with the changes from dilute solution → concentrated solution → liquid state → solid state may be explained as follows. As the concentration of ephedrine increases from a dilute solution a free molecule having an intramolecular OH···N hydrogen bond (3451 cm.$^{-1}$) gradually associates with a neighboring molecule having free OH group, forming OH···O intermolecular hydrogen bond, which gives rise to a new band at 3321 cm.$^{-1}$*. At the same time the band at 3451 cm.$^{-1}$ shifts to 3421 cm.$^{-1}$ by a reinforcing effect of the intermolecular hydrogen bond formation on the intramolecular one, as is known to occur for the frequency shift during the formation of dimer and polymers of alcohols[2]. In the condensed phase the free OH absorption disappears and only the intense OH absorption (3311 cm.$^{-1}$) relating to the intermolecular hydrogen bond remains.

As to whether NH in the $NHCH_3$ group play a part in hydrogen bond formation, the following fact will be helpful for interpretation; that is, the band at 3370 cm.$^{-1}$ assigned to free NH absorption remains even at a higher concentration (0.21 M), at which the association is appreciable. Thus, it may be concluded that NH group plays almost no rôle in the hydrogen bond formation.

Ψ-Ephedrine.—The spectrum of Ψ-ephedrine in dilute carbon tetrachloride solution is much like that of ephedrine (Fig. 1-b). A sharp band at 3621 cm^{-1} is due to free OH vibration, a broad band at 3418 cm.$^{-1}$ may be due to the intramolecularly hydrogen-bonded OH vibration. However, in this case $\Delta\nu$ (203 cm.$^{-1}$) between the sharp and broad band is larger than that in ephedrine (168 cm.$^{-1}$) and the free NH absorption almost disappears. Although the NH band may be masked by the overlapping of the broad band, a weak band appearing at 3324 cm.$^{-1}$ or a very weak shoulder at 3350 cm.$^{-1}$ may be due to NH vibration.

The spectral change on raising the concentrataion of Ψ-ephedrine proceeds just as in the case of ephedrine; that is, the intensity of the free OH absorption decreases and the broad OH absorption (OH···N) shifts by about 30 cm.$^{-1}$ towarde the lower frequency, accompanied by the appearance of a new band at 3301 cm.$^{-1}$, which is due to intermolecular OH···O hydrogen bonding. As

5) E.D. Bergmann, E. Gil-Av and S. Pincas, *J. Am. Chem. Soc.*, **75**, 68 (1953).

6) R.A. Russell and H.W. Thompson, *J. Chem. Soc.*, **1955**, 483.

* OH absorption for alcohol polymer appears over a range 3338-3384 cm^{-1} [2].

concentration increases, the intensity of the hydrogen-bonded OH absorption (3418 cm.$^{-1}$) rapidly decreases in contrast to the case of ephedrine.

B. Temperature Dependence

In order to observe the temperature dependence of the relative intensities of the free and bonded OH absorption bands, the spectra of ephedrines at about 0.005 M in carbon tetrachloride were taken at about 10° and 55°C. Comparing the spectrum at 10° with that at 25°C, it was found that the intensity of the free OH absorption in the latter increased as usually observed for the intermolecular hydrogen bonding[7]. However, at 55°C the intensities of both free and bonded OH absorptions were lower than those at 25°C for either diastereoisomers. This may be caused by the above-mentioned specific interaction of ephedrines with solvent molecules. A rough estimation of energy of hydrogen bonding for ephedrine and Ψ-ephedrine from the data at 10° and 25°C give the values of about 5 kcal./mol.

C. Solvent Effect

In Fig. 2 are shown the spectra of solutions of ephedrine and Ψ-ephedrine in various solvents, together with that of carbon tetrachloride solutions at a concentration where association is appreciable.

Chloroform.—The free OH absorption shifted slightly towards the lower frequency in chloroform solution (3603 cm.$^{-1}$) more than in carbon tetrachloride solution (3619 cm.$^{-1}$). The bonded OH absorption also shifted by 30–40 cm.$^{-1}$ towards the lower frequency. The band ascribed to ν (NH) in the spectrum of carbon tetrachloride solution appears at almost the same frequency (3360 cm.$^{-1}$) for ephedrine, whereas for Ψ-ephedrine no band corresponding to ν (NH) appears. From the figure it seems that the intermolecular association does not occur at such concentration.

Benzene.—The shift of the free OH absorption towards the lower frequency is large and amounts to 50 cm.$^{-1}$ for both diastereoisomers, compared with that in carbon tetrachloride. The bonded OH absorptions also shift towards the lower frequency. The well-defined band at 3356 cm^{-1} for ephedrine may be due to ν (NH), which remains unchanged on adding triethylamine three times more concentrated as ephedrine, whereas the 3436 cm.$^{-1}$ band shifts to 3401 cm.$^{-1}$. Also a 3311 cm.$^{-1}$ band for Ψ-ephedrine may be due to the NH group. There is no indication that marked association occurs in benzene solution at 0.16 M.

Carbon Disulfide.—The absorption of ephedrines is stronger in carbon disulfide solution, than in other solution. The solution was yellow and unstable, especially for ephedrine.

The free OH absorptions appear at 3597 cm.$^{-1}$ for ephedrine and at 3590 cm.$^{-1}$ for Ψ-ephedrine, which are the frequencies between those in chloroform and benzene solutions. For ephedrine the intensity of the band is greater than for carbon tetrachloride solution of about the same concentration, but for Ψ-ephedrine it is remarkably small and almost zero at 0.16 M.

For ephedrine an intense band appears at 3279 cm.$^{-1}$, which is the lowest value of the bonded

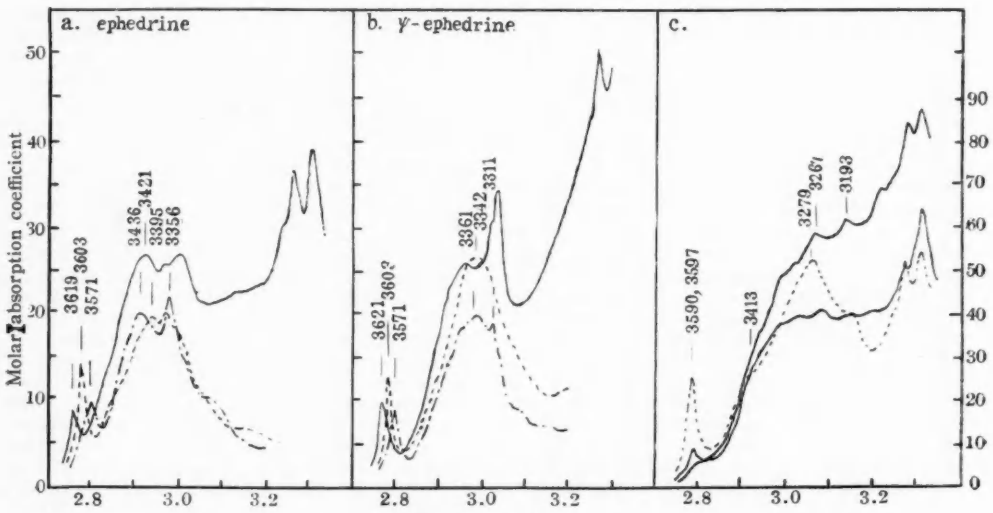

Fig. 2. Solvent effect on spectra of ephedrines. a), b) ——— CCl_4 (ca. 0.1 M/l.), ---- $CHCl_3$ (0.16 M/l.), —·— benzene (0.16 M/l.), cell 0.056 cm. c) CS_2, ---- ephedrine (0.0045 M/l. ×2 cm), ——— ψ-ephedrine, 1) 0.0045 M/l. ×2 cm., 2) 0.16 M/l. ×0.056 cm.

7) e.g. M. Tsuboi, *J. Chem. Soc. Japan (Pure Chem. Sect.)*, **76**, 376 (1955).

OH vibration observed in the present experiments, if this band be ascribed to the bonded OH vibration. A weak shoulder is observed at about 3410 cm.$^{-1}$, corresponding to the band (3451 cm.$^{-1}$) due to the intramolecularly hydrogen-bonded OH vibration in the carbon tetrachloride solution. It is to be added that the spectrum of ephedrine in carbon disulfide solution is very much like that taken in carbon tetrachloride solution with a small amount of crystalline precipitates, both showing a weak shoulder at 3430 cm.$^{-1}$ and an intense peak at 3280 cm.$^{-1}$. Therefore, such spectra may be due to a metastable state of ephedrine molecule.

It is also remarkable that the absorption of Ψ-ephedrine in such a small concentration as 0.0045 M shows a spectrum like that when an intermolecular interaction occurs.

As is well known a relationship exists between dielectric constant of a solvent and the frequency difference in the OH or NH absorption of a substance in vapor state and in the solution[8]. This relationship is satisfied for the free OH absorption in the present experiments. Thus, the dif-

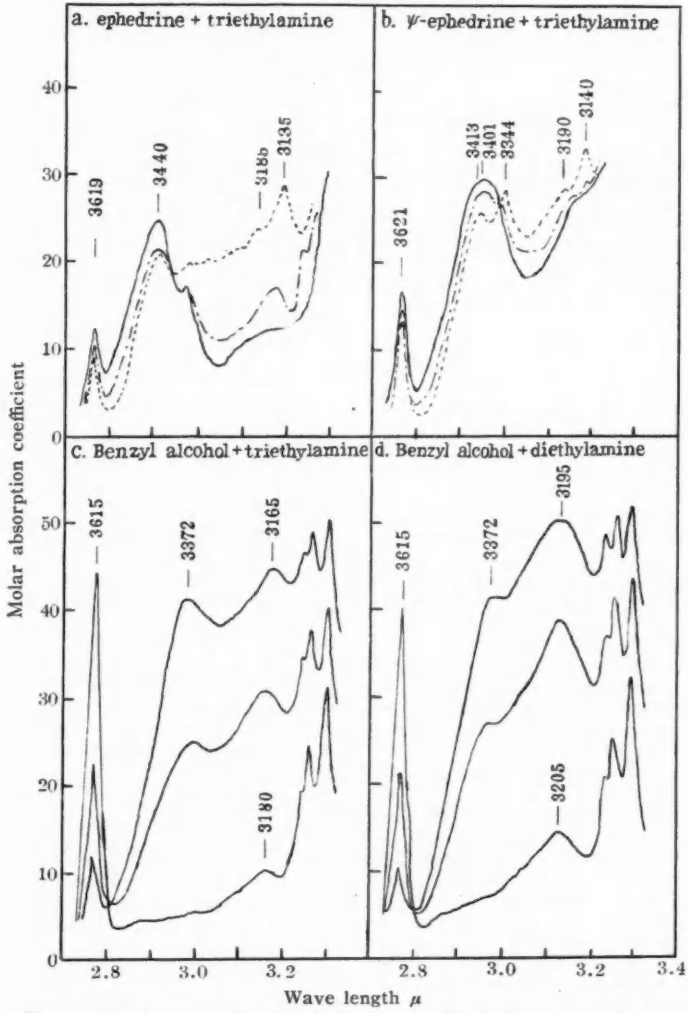

Fig. 3. The interaction of ephedrines and benzyl alcohol with proton acceptor in CCl_4 soln. a), b), ephedrines. 0.03 M/l. + triethylamine, ——— 0.072, — · — 0.27, - - - - 0.50 M/l. c), d) 1 : 1 mixture in mol. 0.51, 0.179, 0.003 M/l.

8) E. Bauer and M. Magat, *J. phys. radium.*, 9, 319 (1938).

ferences in frequency of the free OH absorption in the respective solvents and that of alcohol vapor (3680 cm^{-1}) increases in the order of carbon tetrachloride, chloroform, carbon disulfide and benzene*.

On the other hand, it is also known that the degree of the intermolecular association of phenol in solutions increases in the order of benzene, chloroform and carbon disulfide[9]. From Fig. 2 it will be seen that if the frequency difference in the free and bonded OH absorption means the strength of hydrogen bonding, the above-mentioned relation holds also for the intramolecular hydrogen bonding in the case of ephedrines. In almost the same concentration (about 0.1 M) association seems to occur only in carbon tetrachloride and carbon disulfide solutions, especially strong in the latter.

D. The Interaction with a Proton Acceptor

When a proton acceptor like ethyl ether, ethyl benzoate or pyridine is added to a 0.006 M solution of ephedrine in corbon tetrachloride, no appreciable interaction occurs between ephedrine and the proton acceptor, unless the molar ratio of the latter to the former exceeds 10: 1. In the case of a molar ratio of 40: 1 for pyridine to ephedrine new bands due to the intermolecular interaction appear.

In Fig. 3-a and -b are shown the interaction between ephedrines and triethylamine, which is a strong proton acceptor As seen from the figure the intensity of the free OH band decreases already at the concentration of 0.072 M of triethylamine. As the concentration of triethylamine increases, the intensities of the free and bonded OH vibrations of both isomers decrease, at the same time the bonded OH band shifts towards lower wave number and a new band appears at about 3140 $cm.^{-1}$. Ψ-Ephedrine mixed with higher concentration of triethylamine shows splitting of the band near 3400 $cm.^{-1}$ into two bands at 3413 and 3344 $cm.^{-1}$.

These facts may be explained as follows. At first, a molecule which forms no intramolecular hydrogen bond may interact with triethylamine molecule through either OH or $NHCH_3$ group of the ephedrines. In connection with this assumption, an 1: 1 mixture in mole of benzyl alcohol and triethylamine or diethylamine was examined. The results are shown in Fig. 3-c and -d. A free OH band of benzyl alcohol at 3615 $cm.^{-1}$ increases its intensity with decreasing concentration of the mixture, while a band at 3372 $cm.^{-1}$ disappears, which seems to be due to the interaction between benzyl alcohol molecules themselves, and the intensity of a band at 3165 cm^{-1} (triethylamine) or 3195 $cm.^{-1}$ (diethylamine) decreases. The band at 3165 or 3195 $cm.^{-1}$, which is due to OH···N intermolecular hydrogen bonding, shifts to 3180 or 3205 $cm.^{-1}$ at a lower concentration.

From these results, it will be evident that the band at 3140 $cm.^{-1}$ observed for ephedrines (Figs. 3-a and -b) can be assigned to OH vibration perturbed by OH···N intermolecular hydrogen bond. Although $NHCH_3$ group may also participate in the hydrogen bond formation of the type NH. . .N, this seems to be rather weak because of the weaker proton donating power of $NHCH_3$ group than OH group[10]. However, the appearance of very weak absorption at 3190 $cm.^{-1}$ and the shift of the bonded OH absorption may suggest that the NH group also takes part in the intermolecular hydrogen bond formation. The splitting of the bonded OH absorption into 3413 and 3344 $cm.^{-1}$ in Ψ-ephedrine may be explained as follows. The lower frequency component is due to OH···N intramolecular hydrogen bond strengthened by the increase of proton accepting power of the N atom because of forming an intermolecular hydrogen bond (NH···N) with triethylamine. A band due to NH···N intermolecular hydrogen bond may be assigned to the absorption at 3185 $cm.^{-1}$, but this assignment is not so conclusive because of the lack of data about the interaction between NH group of amine and N atom of another proton acceptor.

As Ψ-ephedrine shows stronger continuous absorption in 3.0–3.2 μ region than ephedrine at the same concentration, it may be suggested that Ψ-ephedrine interacts more easily with the proton acceptors examined than ephedrine.

Discussion

Although the existence of the intramolecular hydrogen bond in the molecules of both diastereoisomers of ephedrine was verified in various solvents, the appearance of the free OH absorption remained unexplained. This may be accounted for as follows. The conformations of ephedrine and ψ-ephedrine capable of forming the intramolecular hydrogen bond may be illustrated as in Fig. 4.

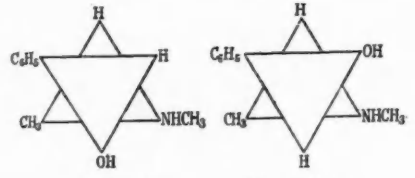

ephedrine Ψ-ephedrine

Fig. 4.

One of them (ephedrine) is different from that hitherto accepted commonly on the chemical ground[11]. However, the present conformation of ephedrine is in agreement with that suggested recently by Murakami and Fukumoto[12] from consideration of reac-

* The results of the same kind have been obtained for pyrrole, phenol and methanol (M. Josien and N. Fuson, *J. Chem. Phys.*, 22, 1169 (1954).

9) R.A. Friedel, *J. Am. Chem. Soc.*, 73, 2881 (1951).

10) S. Mizushima, "Structure of molecules and internal rotation." Academic Press Inc. Publishers, New York (1954), p. 133.

11) e.g. W.J. Close, *J. Org. Chem.*, 15, 1131 (1950).

12) M. Murakami and T. Fukumoto, *J. Chem. Soc. Japan (Pure Chem. Sect.)*, 76, 270 (1955).

tion mechanism and that found by X-ray crystal analysis for ephedrine hydrochloride[13]. The appearance of the free OH absorption suggests that a part of the molecules have a conformation in which OH and $NHCH_3$ groups are trans. Moreover, it is also possible that in a gauche type molecule the OH group may take an orientation not to form hydrogen bond with $NHCH_3$ group. These two possibilities have actually been observed in the case of ethylene chlorhydrine[14].

The above suggestion that the ephedrine and ψ-ephedrine molecules consist of the mixture of the rotational isomers may be supported by the appearance of one or two more bands in the finger print region spectra in $CHCl_3$ solution than those observed in solid state[1] (970–1190 cm^{-1}).

As to whether there are differences in the equilibrium ratio of the rotational isomers between diastereoisomers, only a qualitative discussion may be given. As seen in Fig. 4, it is conceivable that if we assume the repulsion between the phenyl and methyl groups it will give the effects that the OH and $NHCH_3$ groups are more apart for ephedrine than for ψ-ephedrine and thus the hydrogen-bonded conformation of ψ-ephedrine will be relatively more stable, when compared with its trans form, than in the case of ephedrine.

Such a consideration may also explain the difference of $\Delta\nu$ between the present diastereoisomers. In general it is accepted that the magnitude of $\Delta\nu$ is related to the energy of the hydrogen bonding[15] and in solid state related to the distance between a proton donor and an acceptor[15]. Thus, because of the repulsion assumed above, the OH group is to some extent nearer to the $NHCH_3$ group in the gauche type isomer of ψ-ephedrine and the $\Delta\nu$ will be accordingly larger than that for ephedrine. The observed values of $\Delta\nu$ are, as already given, 203 $cm.^{-1}$ for ψ-ephedrine and 168 $cm.^{-1}$ for ephedrine. It is to be remarked that these values are much larger than those found for OH···O intramolecular hydrogen bonds in diols (30–60 cm^{-1})[2]. This may be attributed partly to the difference in the proton affinity of the proton acceptor.

In Table I the values of $\Delta\nu$ of the inter- and intramolecular OH···N hydrogen bonds are summarized. From the Table it is seen that $\Delta\nu$ due to OH···N intermolecular hydrogen bond is very large except that in the case of benzyl alcohol-azobenzene and $\Delta\nu$ due to the intramolecular OH···N hydrogen bond adjucent to a conjugate system like pyridoine is larger than that of intermolecular bond between corresponding pair, phenol-pyridine. It may be said that compared with these $\Delta\nu$ values, those of ephedrines are rather small.

TABLE I

$\Delta\nu$ OF OH. . .N HYDROGEN BOND

Intermolecular	Phenol-pyridine	770*
	Phenol-N-methylpiperidine	820*
	Benzyl alcohol-azobenzene	170**
	〃 -triethylamine	450
	〃 -diethylamine	420
	Acetaldoxime	470***
Intramolecular	α-Pyridoin	880*
	Ephedrine	168
	ψ-Ephedrine	203

* W. Luettke and H. Marsen, *Z. Electrochem.*, 57, 680 (1953).
** M.S.C. Flett, *J. Soc. Dyers and Colourist*, 68, 59 (1952).
*** S. Califano and W. Luettke, *Z. Physik. Chem.*, 5, 240 (1955).

The author wishes to express his sincere thanks to Professor I. Nitta of Osaka University for his kind guidance and to Dr. T. Shimanouchi of Tokyo University for helpful discussions. The author's thanks are also due to Dr. S. Kuwada and Dr. A, Watanabe of this laboratory for their continued encouragement.

Research Laboratory Takeda Pharmaceutical Industries, Ltd. Osaka

13) G.D. Phillips, *Acta Cryst.*, 7, 159 (1954).
14) S. Mizushima, loc. cit, p. 86.
15) R.M. Badger, *J. Chem. Phys.*, 8, 288 (1940).
16) R.C. Lord and R.E. Merrifield, *J. Chem. Phys.*, 21, 166 (1953).

Studies on Serine Peptides. I. Optical Resolution of O-Benzyl-DL-serine and Synthesis of DL-Serine Peptides

By Kenzi OKAWA

(Received January 1, 1956)

The serine peptides are important in organic and biological chemistry. For example, these peptides readily undergo hydrolysis with dilute acids or alkalis and acyl migration occurs in the acidic condition. Some of these peptides have been considered to have growth-promoting effect or enzymatic activity. However, there have been few papers available concerning the synthesis of the serine peptides[1], mainly because this amino acid has a free hydroxyl group which induces side reaction in the peptide synthesis.

The author tried in the present work to synthesize the serine peptide from the O-benzyl-serine[2] in which the hydroxyl group was protected with a benzyl rest. An optically active O-benzyl-L-serine was prepared by the enzymatic resolution of the N-acetyl derivative with the takadiastase. The O-benzyl-L-serine was easily obtained in 78% yield from the reaction mixture, since this amino acid was slightly soluble in water.

Price reported in his paper that the optical active L-serine was obtained from the N-acetyl-DL-serine in 40% yield[3].

The O-benzyl-L-serine showed a specific rotation of +5.86 in 1 N-hydrochloric acid solution at 15°C, and the L-serine which was prepared quantitatively by the acid hydrolysis of the benzyl derivative, showed a rotation of +14.6 in 1N-hydrochloric acid solution at the same temperature.

At the preliminary experiment, the O-benzyl-L-serine peptides have been synthesized by the N-carboxylic acid anhydride method (N. C. A. method) of Bailey[4], but satisfactory results were not obtained except in the case of a seryl-glycine peptide.

With O-benzyl-DL-seryl-L-glutamic acid, O-benzyl-DL-seryl-L-leucine, and O-benzyl-DL-seryl-L-phenylalanine, so many by-products were formed during the reaction period that the purification of the products was very difficult.

O-Benzyl-DL-seryl-L-leucine ethyl ester and DL-seryl-L-leucine have been synthesized by the Fischer's acid chloride method.

It has been found from the above experiments that the O-benzyl-serine can be utilized as the starting material in the peptide synthesis.

Experimental

Enzymatic Resolution of O-benzyl-DL-serine. —O-Benzyl-N-acethyl-DL-serine.—Into a mixture of 33 g. of O-benzyl-DL-serine and 83 cc. of 2N-sodium hydroxide solution were added separately 25 cc. of acetic anhydride and 163 cc. of 2N-sodium hydroxide solution under cooling. The reaction mixture was neutralized with 1 N-hydrochloric acid solution, when white crystals precipitated. Recrystallization from hot water gave 37 g. of the crystals in 80% yield, m.p. 139–140°C.

Anal. Found: C, 60.59; H, 6.67. Calcd. for $C_{12}H_{15}O_4N$: C, 60.76; H, 6.38%.

Carboxypeptidase Preparation.—Twenty six grams of Takadiastase were extracted with distilled water at 0°C. The mixture was filtered using Celite. This extracted solution was used directly in the enzymatic resolution. The acetyl derivative (33 g.) was dissolved in 24 cc. of 6N-sodium hydroxide solution. To this solution were added the above enzymatic extract and 60 cc. of phosphate buffer which brought the total mixture to pH 6.8. In order to insure complete hydrolysis, the digests were usually set up in the late afternoon and allowed to stand at 37°C. until early next morning. The L-amino acid crystallized in high yield and usually filled the digestion flask. The mixture is brought to pH 5.0 by the addition of glacial acetic acid. The L-amino acid was filtered by suction, and washed with cold water. The mother liquor was combined with washings and concentrated in vacuo to a low bulk. A small amount of the L-amino acid appeared during this concentration. The crystals were combined with the main product and recrystallized from hot water with the aid of Celite. Optically active 11 g. of crystals were obtained in 78% yield, $[\alpha]_D^{15} = +5.86$. (in 1N-hydrochloric acid) The residual concentrated solution was brought to pH 2.0 with conc. hydrochloric acid. The acetyl derivative was extracted several times into ethylacetate. The extracts were combined, dried for a few minute over anhydrous sodium sulfate, and finally filtered. The ethylacetate was removed in vacuo. To the oily residue was added twice their volume of petroleum ether and it was allowed

1) A. Miekely and J. Fruton, *J. Biol. Chem.*, **146**, 463 (1942); D. Wooley, *J. Biol. Chem.*, **159**, 753 (1948); R.F. Fischer and R.R. Whetson, *J. Am. Chem. Soc.*, **76**, 5076 (1954); M. Botunik, *Zhur. Obschchiei. Khim*, **23**, 1716-19 (1953).

2) K. Okawa and H. Tani, *J. Chem. Soc. Japan*, **75**, 1199 (1954).

3) V. Price, *J. Biol. Chem.*, **179**, 1169 (1949).

4) J. Bailey, *J. Chem. Soc.*, **1950**, 3461.

to stand over night in an ice bath, then white precipitate was obatined. After recrystallization from hot water, 13.6 g. of N-acetyl-D-derivative was prepared in fine crystals. in 80% yield, m.p. 103°C.

D- and L-Serine.—D- and L-Serine were obtained by acid hydrolysis of benzyl derivatives with 5N-hydrochloric acid for half an hour. The D- and L-form exhibit $[\alpha]_D^{15}$ of −14.6 and +14.6 in 1N-hydrochloric acid solution, respectively.

O-Benzyl-DL-serine N.C.A.—This was prepared by the reaction of carbonylchloride with O-benzyl-DL-serine in dioxane at 40°-50°C by the method of Leuchs[5,6]. Several times recrystallization from ethylacetate-petroleum ether gave white crystals, m.p. 76°-77°C, in 82% yield.

Preparation of Serine Peptides.—The peptide coupling experiments were carried out under anhydrous conditions. All solvents were stored over suitable dry reagents.

O-Benzyl-DL-seryl-glycine.—Glycine ethylester hydrochloride (0.7 g.) was treated with 3.3 cc. of 1.66N-ammonium-chloroform solution and the reaction mixture filtered from the precipitated ammonium-chloride. After removal of a slight excess of ammonia by the concentration of the solvent in vacuo, 6.6 cc. of ethylacetate were added and the solution was cooled to 65°C in solid carbondioxide-aceton bath. After addition of triethylamine (0.5 cc.) to the ester solution, a solution of DL-serine N.C.A. (0.9 g.) in 6.6 cc. of ethylacetate was precooled to 65°C and slowly run into the mixture. The reaction mixture was allowed to stand at this temperature for six hours, the mixture was then warmed to room temperature and the solvent removed in vacuo. The O-benzyl-DL-seryl-glycine ethylester was hydrolized with 11.1 cc. of 0.37 N-barium hydroxide, neutralized with 11.1 cc. of 0.37 N-sulfuric acid and concentrated in vacuo. White crystals were obtained. Recrystallization gave 0.15 g. of O-benzyl-DL-seryl-glycine, m.p. 202°C, in 65% yield.

Anal. Found: N, 10.95. Calcld. for $C_{12}H_{15}O_4N_2$: N, 11.10%.

DL-Seryl-glycine.—O-Benzyl-DL-seryl-glycine (0.3 g.) was suspended in 30 cc. of methyl alcohol. After addition of palladium oxide (0.3 g.) and 0.2 cc. of hydrochloric acid, the mixture was reduced for six hours. Then palladium oxide was removed and the reaction mixture was concentrated in vacuo. Recrystallization of residual precipitate gave 0.23 g. of seryl-glycine hydrochloride, m.p. 195°C, with decomposition, in 95% yield.

Anal. Found: N, 14.24. Calcd. for $C_5H_{11}O_4N_2Cl$: N, 14.16%.

O-Benzyl-DL-seryl-L-glutamic acid.—Glutamic acid ethylester was prepared from 1.5 g. of the hydrochloride. The free ester was treated with 1.1 g. of O-benzyl-DL-serine N.C.A. and 0.1 cc. of triethylamine under the same conditions. White precipitate was obtained in 50% yield.

Anal. Found: N, 8.36. Calcld. for $C_{15}H_{20}O_5N_2$: N, 8.60%.

O-Benzyl-DL-seryl-L-leucine.—Under the same conditions, 0.37 g. of crystals were obtained in 10% yield from 2.5 g. of leucine ethylester hydrochloride and 2.2 g. of O-benzyl-DL-serine N.C.A.

Anal. Found: N, 9.48. Calcd. for $C_{15}H_{24}O_4N_2$: N, 9.10%.

O-Benzyl-DL-seryl-L-phenylalanine.—Under the same conditions, 0.17 g. of crystals were obtained in 10% yield, from 1.4 g. of phenylalanine ethylester and 1.1 g. of O-benzyl-DL-serine N.C.A.

Anal. Found: N, 8.19. Calcld. for $C_{19}H_{22}O_4N_2$: N, 8.18%.

O-Benzyl-N-carbobenzyloxy-DL-serine.—O-Benzyl-N-carbobenzyloxy-DL-serine was prepared in the previous experiments by the author[7]. The carbobenzyloxy derivative (2.8 g.) was synthesized in 80% yield from 2 g. of O-benzyl-DL-serine and 2.68 g. carbobenzyloxychloride.

O-Benzyl-O-carbobenzyloxy-DL-seryl-L-leucine ethylester.—N-Carbobenzyloxy derivative was treated with 2.5 g. of phosphorus pentachloride in 30 cc. of absolute ether. After dissolution of N-carbobenzyloxy derivative, excessive phosphorus pentachloride was filtered off and the filtrate was concentrated in vacuo at 0°C. The concentrated syrup was extracted twice with petroleum ether in order to remove phosphate oxychloride, and the residual syrup was dissolved in 20 cc. of ethylacetate. To the 20 cc. of ethylacetate solution of L-leucine ethylester which was prepared from 3.3 g. of the hydrochloride, was added the acid chloride solution. After removal of the leucine ethylester hydrochloride, the reaction mixture was washed twice with petroleum ether, and then allowed to stand over night in an ice box. White precipitate was obtained. Recrystallization from ethylacetate-petroleum ether gave 2.7 g. of peptide, in 70% yield, m.p. 78°C.

Anal. Found: N, 5.80. Calcld. for $C_{21}H_{34}O_5N_2$: N, 5.95%.

O-Benzyl-N-carbobenzyloxy-DL-seryl-L-leucine.—The peptide ester (2.6 g.) was hydrolized with mixed reagent (4 cc. of 1N-sodium hydroxide and 5 cc. of aceton). The reaction mixture was neutralized with 1N-hydrochloric acid being obtained in white crystals. Recrystallization from ethylacetate-petroleum ether gave 1.0 g. of peptide, m.p. 92°C, in 72% yield.

DL-Seryl-L-leucine.—N-Carbobenzyloxy peptide was suspended in 30 cc. of methyl alcohol. Into the methyl alcohol solution were added 0.1 cc. of acetic acid and 0.3 g. of palladium oxide. The mixture was reduced under the ordinary pressure in the hydrogen atmosphere at room temperature. After removal of palladium oxide, the reaction mixture was concentrated in vacuo; then white crystals were obtained. Recrystallization gave 0.12 g. of seryl-L-leucine, m.p. 189°C., in 71% yield.

Anal. Found: N, 12.63. Calcld. for $C_9H_{18}O_4N_2$: N, 12.80%.

5) H. Leuchs, *Ber.*, **39**, 857 (1906).
6) K. Okawa and H. Tani, *J. Chem. Soc. Japan*, **75**, 1199 (1950).
7) K. Okawa and H. Tani, *J. Chem. Soc. Japan*, **75**, 1199 (1954).

Summary

The optically active O-Benzyl-L-serine was prepared in 78% yield by the enzymatic resolution of the N-acetyl derivative with Takadiastase.

DL-Seryl-glycine was prepared by the N. C. A. method of Bailey and DL-seryl-L-leucine was synthesized by the Fischer's acid chloride method respectively.

As was expected, it was found that O-benzyl-serine can be utilized as the starting material in the peptide syntheses.

The author wishes to express his appreciation to Prof. S. Akabori for his kind guidance during the course of this work and also to thank Asst. Prof. H. Tani for his frequent advice.

Department of Chemistry, Faculty of Science, Osaka University, Osaka

---

Studies on Serine Peptides. II. Synthesis of Optically Active Serine Peptide Derivatives

By Kenzi OKAWA

(Received January 1, 1956)

Although a number of peptides containing several kinds of the simpler amino acids have been prepared, little is known about the preparation of peptides which include more than one of trifunctional amino acids. This is especially true for peptides of L-serine and L-histidine.

In the previous paper[1], the author reported on the DL-serine peptides which include monofunctional amino acids.

In the present work, some derivatives of optically active peptides containing L-serine have been synthesized by means of the Sheehan's dicyclohexylcarbodiimide method[2], with O-benzyl-L-serine as starting material.

O-Benzyl-N-carbobenzyloxy-L-seryl-L-histidine methyl ester, O-benzyl-N-carbobenzyloxy-L-seryl-L-tyrosine methyl ester and bis-(O-benzyl-N-carbobenzyloxy-L-seryl)-L-cystine dimethyl ester have been synthesized in good yield.

Sheehan reported in his paper that the hydroxyl group of the serine was not affected by this coupling reagent, and L-seryl peptide was synthesized in 59% yield. But the relatively lower yield of the peptide shows that some side reactions may take place in the coupling procedure.

In the present experiments, a tyrosine peptide has been prepared in 76% yield. It seems that the free hydroxyl group of tyrosine is less reactive than that of serine.

It has been found from the above experiments that this coupling reagent is useful for peptide syntheses.

Experimental

N-N'-Dicyclohexyl Thiourea[3].—Into the solution of 100 g. of cyclohexylamine and 250 cc. of ethylalcohol was added 100 g. of carbondisulfide through the reflux condenser at the presence of

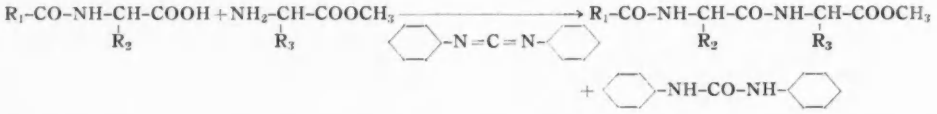

two or three pieces of sodium hydroxide, and the mixture was refluxed for twenty-four hours on a waterbath. After cooling the reaction mixture, precipitated yellowish crystals were filtered. Recrystallization of the crystals from hot alcohol gave 100 g. of the pure material, m. p. 180–181°C.

Dicyclohexylcarbodiimide[4].—The intimate mixture of 100 g. of freshly pulverized mercuric oxide and 40 g. of dicyclohexylthiourea were placed in a suitable bottle of 500 cc. After adding 200 cc. of freshly distilled carbondisulfide, the mixture was shaken on a shuttle machine for 1.25 hrs. The precipitate was filtered and the

1) K. Okawa, Part I. This Balletin, **29**, 486.
2) J.C. Sheehan and G.P. Hess, *J. Am. Chem. Soc.*, **77**, 1067 (1955).
3) A. Skita und H. Rolfes, *Ber.*, **53**, 1242 (1955).
4) R. Herbeck and M. Pezzati, *Ber.*, **71**, 1933 (1938).

solvent was removed. The residual syrup was dissolved in petroleum ether and an insoluble precipitate was filtered. After removal of petroleum ether the residual gelatinous mass was distilled under reduced pressure. Colourless crystals (b. p. 132°C/4 mmHg) were obtained in 80% yield. Dicyclohexylcarbodiimide was stored in a sealed tube at 5°C.

O-Benzyl-N-carbobenzyloxy-L-serine[5].—Five grams of O-benzyl-N-carbobenzyloxy-L-serine were prepared from the 3.5 g. of O-benzyl-L-serine and 3.8 g. of carbobenzyloxychloride by the method as with O-benzyl-N-carbobengyloy-DL-serine, m. p. 98°C.

Syntheses of L-serine peptide derivatives.—All the condensation reactions carried out under anhydrous conditions.

O-Benzyl-N-carbobenzyloxy-L-seryl-L-tyrosine Methyl ester.—L-Tyrosine methyl ester hydrochloride (1.51 g.) was treated with 0.9 cc. of triethylamine in 10 cc. of tetrahydrofuran. After removal of triethylamine hydrochloride, the filtrate was mixed with 1.34 g. of carbodiimide and 1.65 g. of carbobenzyloxy derivative in 10 cc. of tetrahydrofuran at room temperature. Immediately, N-N'-dicyclohexylurea was precipitated from the above reaction mixture; then the coupling solution was kept for four hours in room temperature. To remove unchanged carbodiimide 0.15 cc. of acetic acid was added and the mixture was allowed to stand at this temperature for one hour, and filtered from the precipitate. Then, tetrahydrdofuran as the solvent was replaced with ethylacetate. Since a small amount of precipitate was formed in the ethylacetate solution, the precipitate was filtered off and petroleum ether was added to the solution until crystals of the peptide ester appeared. Recrystallization from ethylacetate-petroleum ether gave 1.8 g. of peptide, m. p. 111-112°C, in 72% yield. $[\alpha]_D^{15}=+15.5$ (28.4 mg./cc. in 99% EtOH).

Anal. Found: N, 5.74. Calcd. for $C_{28}H_{30}O_7N_2$: N, 5.53%.

O-Benzyl-N-carbobenzyloxy-L-seryl-L-histidine Methyl ester.—The free ester of histidine was obtained by the Fischer's method[6]. A methyl alcohol solution of histidine methyl ester dihydrochloride was treated with 13 cc. of 2 N-CH_3ONa solution and the reaction mixture filtered from the precipitated sodium hydrochloride. After removal of methyl alcohol, the free ester was dissolved in 15 cc. of tetrahydrofuran. The tetrahydrofuran solution was coupled with 3.3 g. of carbobenzyloxy derivative and 2.1 g. of carbodiimide in tetrahydrofuran. Under the same conditions as those of the above experiments, 4.2 g. of peptide ester were prepared in 87% yield, m. p. 110°C. $[\alpha]_D^{15}=+7.21$ (49.2 mg./cc. in 99% EtOH).

Anal. Found: N, 12.04. Calcd. for $C_{25}H_{33}O_6N_4$: N, 11.7%.

Bis-(O-benzyl-N-carbobenzyloxy-L-seryl)-L-cystine Dimethyl ester.—Into 20 cc. of the solution of cystine dimethyl ester in the tetrahydrofuran which was prepared from 2.2 g. of the dimethyl ester dihydrochloride and 1.8 cc. of triethylamine, were added 3.3 of carbobenzyloxy derivative and 2.6 g. of carbodiimide in 20 cc. of tetrahydrofuran. From the coupling mixture, 2.5 g. of crystals were obtained, m. p. 101-102°C, in 57% yield. $[\alpha]_D^5=+22.17$ (26.6 mg./cc. in ethylacetate.

Anal. Found: N, 6.33. Calcd. for $C_{44}H_{50}O_{12}N_4S_2$: N, 6.29%.

Summary

The derivatives of optically active L-seryl peptides containing trifunctional amino acids have been synthesized by the Sheehan's method in good yield.

In this method, the free hydroxyl group of the serine must have been substituted by a suitable protecting group, fx. benzyl rest, in order to obtain good results.

The present author wishes to express his appreciation to Prof. S. Akabori for his kind guidance throughout this work.

Department of Chemistry, Faculty of Science, Osaka University, Osaka

5) K. Okawa and H. Tani, *J. Chem. Soc. Japan*, **75**, 1197 (1950).

6) E. Fischer and L.H. Cone, *Ann.*, **363**, 107 (1908).

Rheology of Surface Films. V. Mechanical Behaviours and Structures of 6-Nylon at Air Water Interface

By Kiyoshi INOKUCHI*1

(Received January 24, 1956)

Introduction

In the preceding paper[1], detailed description was made on the rheological characteristics of 6-nylon at air/water interface. It is desirable to investigate the film structure, which is responsible for the development of the rheological properties of the film. For this purpose, electron microscopic examination was carried out at various areas, together with the simultaneous determination of surface pressure and potential. Microfibrillar structures were thus revealed, and the change of the mechanical properties of the film, accompanied by the compression process, was discussed in terms of such structures.

Experimental

Materials and the experimental conditions were just the same as described in the preceding paper[1]. Unless otherwise stated, the sample was spread on distilled water from the mixed solution of benzene/phenol (3: 1 in volume) at the initial spreading area of about 90 A^2/residue. About twenty minutes were allowed to stand before the determination of the isotherms under the compression of constant speed 9.6 cm²/min. For the determination of surface pressure-area curve (π-A curve), the surface balance of a float type was used, which was constructed by the present author[2]. Surface potential was measured by means of a vibrating electrode apparatus. For the electron microscopic examination, the films were transferred onto the collodion support with use of the following technique. The collodion supports were held and touched parallel to the surface film on the substrate water and then immersed into the water. After the film was swept off, these supports were picked up through the clean surface of water, and dried. In order to avoid heterogeneity of the film near the enclosing barriers, all the film specimens were taken from the middle part of the enclosing area of the surface films. Hitachi HS-II type electron microscope was used.

Results

(I) Surface Pressure

(1) Force-Area Curve. — The general trend of the form of the π-A curve was shown in Fig. 1. Surface pressure at large

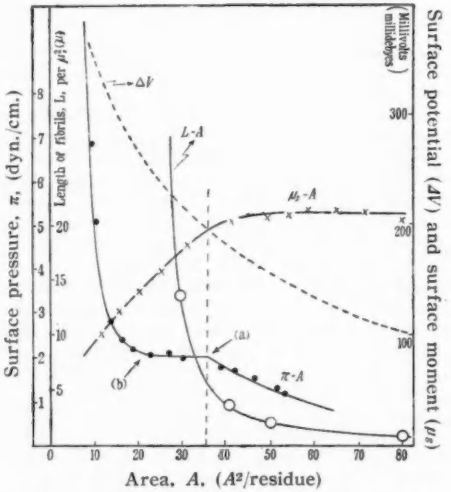

Fig. 1. Relationships of surface pressure versus area (π-A, full circles), surface electric moment versus area (μ_s-A, crosses), and amounts of fibrils versus area L-A, open circles). Broken line represents the surface potential versus area curve.

areas gradually increased as the film was compressed until a distinct kink point (a) appeared at the area of about 37 A^2/residue. Below the area of the kink point, however, the pressure ceased to increase upon compression forming a high compressibility region— a plateau—, whereas the pressure again rose, on further reducing area below about 20 A^2/residue, more steeply up to the pressure of 40 dyn./cm. The end of the plateau is denoted as point (b) hereafter. The pressure relaxation after compression was sudden and pronounced below the kink point, and hence, the more the plateau became distinct, the slower the compression rate was.

In view of our experience, it was likely that the Wilhelmy dipping slide method registered a more distinct kink point (a) than the case in which the float balance was used. This may be due to the considerable change

*1 Present adress: The 2nd Surgical clinic, Medical School, Kyushu University, Fukuoka, Japan.

1) K. Inokuchi, This Bulletin, 28, 453 (1955).
2) K. Inokuchi, This Bulletin, 26, 471 (1953).

of the wetting condition of the slide. In any case, it is evident that there occurred a sudden change in the film structure at the point (a).

(2) **Effect of the Composition of the Substrate Water.**—It has been emphasized that coherent films generally badly spread at air/water interface. So, it seemed necessary to examine the extent of the spreading under various conditions. The results were summarized in Table I, in which the areas of

TABLE I

EFFECT OF THE SUBSTRATE WATER UPON THE π-A CURVE

Substrate water	a	b	c	Pressure at point (a)	Temperature
	A^2/residue			dyn./cm.	C°
Distilled water	37	20	7.5	2.2	21.5
3 N H_2SO_4	37	21	7.5	5.4	21.3
3% Urea	38	24	7.6	2.1	21.2
20% Urea	—	—	7.6	—	20.0

point (a), (b), and the limiting area (c), obtained by extrapolating the straight portion of the high pressure region*2 (15 to 40 dyn./cm.) to zero pressure, were tabulated together with the pressure at the kink point. It was found that these characteristic areas were not appreciably influenced by the composition of the substrate solution, yielding identical values of (a)=37 A^2/residue, (b)=20 A^2/residue, and (c)=8.5 A^2/residue, respectively. On the other hand, the pressure was appreciably raised when spreading was made on the acidic solution (3 N sulfuric acid solution). That is, the film became expanded, as reported by Crisp[3] with nylon $[\text{-}(CH_2)_4\text{-}CO\text{-}NH\text{-}]_n$.

(3) **Effect of the Composition of the Dropping Solution.**—Spreading was also tested in relation to the composition of the dropping solution. Mixtures of benzene-phenol as a solvent, whose proportions vary from 2.5/7.5 to 9.2/0.8 (in volume), gave practically identical values of the characteristic area (a, b, and c), whereas the solution, whose benzene/phenol proportions exceeded 9.5/0.5, yielded far smaller areas than that above (Table II). The solvent of too large proportions of phenol made the experiment impossible, since the solvent was solidified at room temperature. Since 6-nylon does not dissolve, either in pure benzene or in pure phenol, this fact may indicate that the poor solvent caused bad spreading. when the sample was spread from the mixed solution of sulfuric

TABLE II

EFFECT OF THE SOLVENT OF THE DROPPING SOLUTION UPON THE π-A CURVE

Solvent proportion in volume	a	b	c	Pressure at point (a)	Temperature
Benzene/Phenol	Area in A^2/residue			dyn./cm.	°C
2.5/7.5	—	—	8.5	—	19.4
7.5/2.5	37	20	8.5	2.4	19.5
9.2/0.8	36	20	8.4	2.4	19.4
9.5/0.5	20	11	5.7	2.4	20.3
9.8/0.2	—	—	—	—	21.6
H_2SO_4/Isopropanol 1/10	28	19	7.0	1.6	19.4

acid and isopropyl alcohol (1/10 in volume), somewhat smaller characteristic areas were obtained than that from benzene-phenol solution. Since partial hydrolysis of the sample cannot be denied in strong sulfuric acid solution, reduced values of the characteristic points may partly be attributed to this. From the facts that the spreading areas were not appreciably influenced by the hydrogen bond breaking agents, and that the change of the composition of the dropping solution does not practically affect the extent of spreading except for the extreme case, it may be considered that spreading attains to saturation even on the distilled water.

(4) **Molecular Weight Variations.**—As shown in Table III, it was found that the

TABLE III

EFFECT OF MOLECULAR WEIGHT OF 6-NYLON UPON THE π-A CURVE

Molecula weight	a	b	c	Present at point (a)	Temperature
	Area in A^2/residue			dyn./cm.	°C
17,300	37	20	8.5	2.2	21.5
4,600	37	—	7.8	2.5	30.0
2,800	38	—	7.5	2.5	20.0
1,000	31	18	4.8	2.4	20.5
Caplolactam	—	—	4.8	—	20.5

form of the π-A curve was not affected by the molecular weight of the sample so far as the molecular weight changed from 2800 to 17300. This phenomenon is similar to the case with the surface films of cellulose acetates reported by Borgin[4]. With the fraction of extremely low molecular weight 1000, however, a slightly small value of the point (a) was produced, and the plateau in the π-A curve was less distinct. When caprolactum, a monomer of 6-nylon, was spread on a sat-

*2 The high pressure region used for obtaining the point (c) did not appear in Fig. 1.

3. D.J. Crisp, *J. Colloid Sci.*, **1**, 161 (1946).

4) K. Borgin, *Trans. Far. Soc.*, **49**, 956 (1953).

urated ammonium sulfate solution, a comparatively stable surface film was produced, having no plateau and showing less value of point (c) in the π-A curve, and exhibiting no elasticity covering the whole range of compression.

(5) **Compression-Expansion Hysteresis.**—Hysteresis of the π-A curve was also tested at various areas by exercising the compression and re-expansion at constant speed. Fig. 2 shows an example of the results thus obtained, in which the arrows represented a

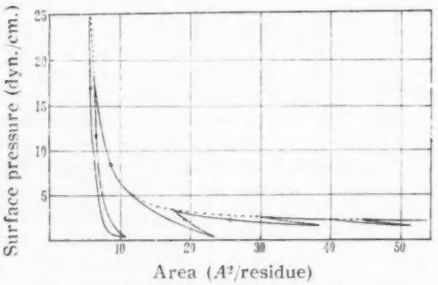

Fig. 2. Compression-expansion hysteresis curve. Temperature, 16°C. rate of expansion, 9.6 cm²/min.

series of the hysteresis loop. In general, the pressure, when the film was re-expanded, became lower than that of the foregoing compression, such a trend was found to be slight at larger areas than the point (a), whereas it became appreciable at the areas below the plateau region. Marked hysteresis occurred below the areas of about 20 A^2/residue, where the steep increase in pressure took place. In this region, the pressure dropped down to almost zero only when the film was slightly re-expanded. Such a phenomenon may reasonably be related to the coherent nature of the film.

(6) **Anisotropy of Surface Pressure.**—It was observed that one drop of castor oil, the form of which was perfectly circular when dropped down onto the surface film of 6-nylon, became deformed to an ellipsoid as the film was compressed, the longer axis being at right angles to the direction of compression. This is schematically illustrated in Fig. 3. It was also observed that the deformation of the oil drop which thus occurred became relaxed as the time elapsed after compression. It was also found that two blades of the Wilhelmy dipping slide for measuring the surface pressure, which were so hung that one was parallel to the direction of compression, the other at right angles to it, respectively, registered different pressures

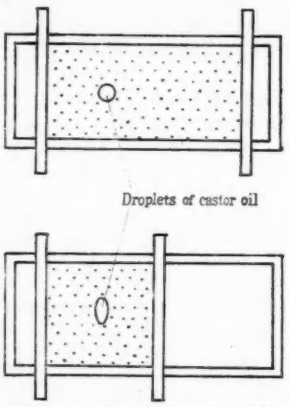

Fig. 3. Schematic illustrations of the anisotropy of surface pressure set up after compression of the films.

below the area of about 40 A^2/residue, somewhat larger values being obtained with the latter slide. These facts readily show that the surface pressure became anisotropic under compression.

(7) **Effect of Temperature on Surface Pressure.**—Temperature dependence of the surface pressure at a fixed area was examined at various areas. Temperature change was performed at a rate of 10 minutes/temperature degree, and the results were listed in Fig. 4. The pressure decreased with the

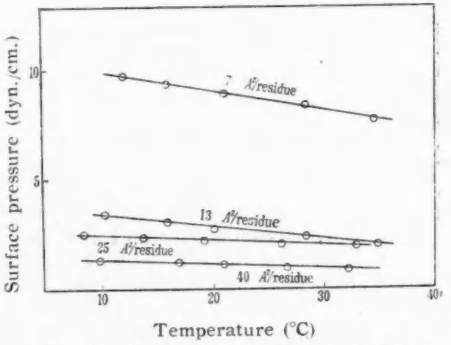

Fig. 4. Temperature dependence of surface pressures at various areas.

rise of temperature at all areas. Such a temperature effect is similar to that on the films of synthetic polypeptides[5], Buna-N[6], and of the long chain Ureas[7].

5) T. Isemura and K. Hamaguchi, This Bulletin, **25**, 40 (1952).
6) K. Suzuki, *Kōshitsugaku-ronso* (Discussions of Colloid Science), **1**, 63 (1947).
7) J. Glazer and A.E. Alexander, *Trans. Far. Soc.*, **47**, 401 (1951).

(II) Surface Potential-Area Curve

The surface potential versus area curve was shown together with the π-A curve in Fig. 1. The surface moment (μ_s), which persisted almost constant value about 230 millidebyes at large areas, began to decrease below the area of about 40 A^2/residue which was fairly consistent with the point (a) in the π-A curve.

(III) Electron Microscopic Examinations

It is of importance to inquire what structural change of the film corresponds to the

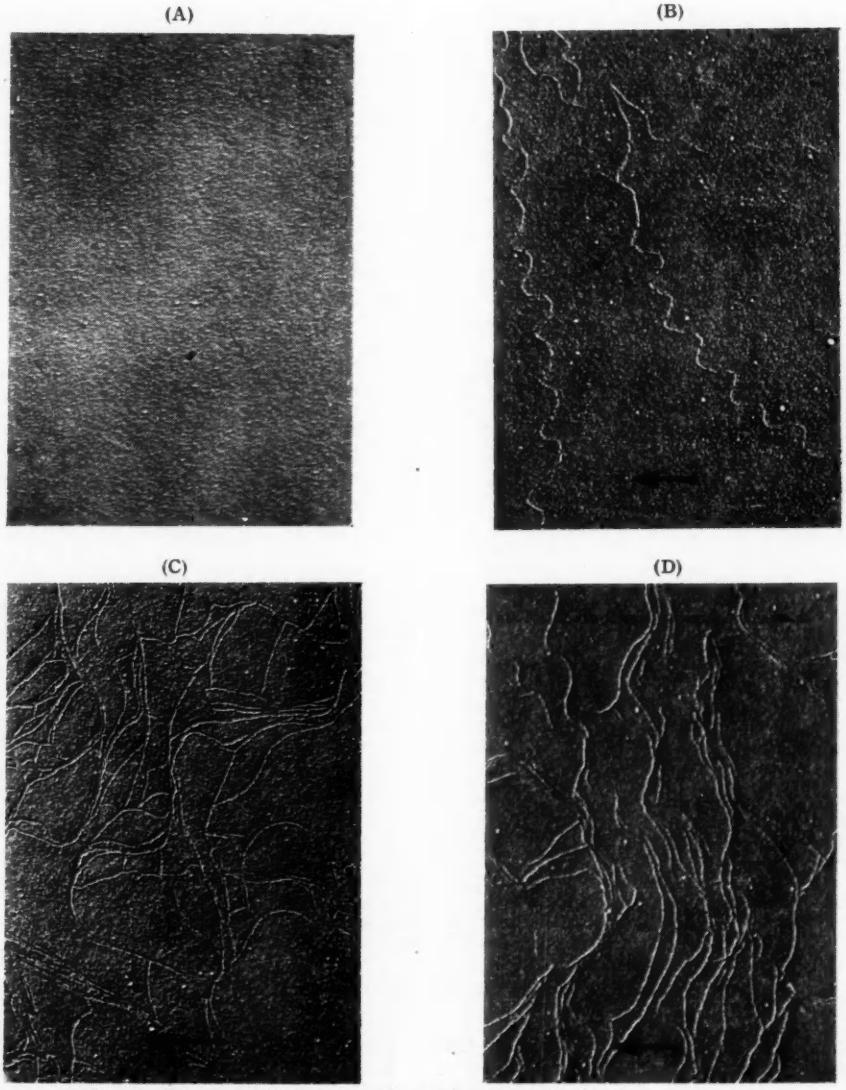

Fig. 5. Electron micrographs of monolayers of 6-nylon;
A, Blank, no film, magnification 13500;
B, Uncompressed films at 80 A²/residue, magnification, 13500
C, Compressed films at 50 A²/residue, magnification 13500
D, Compressed films at 40 A²/residue, magnification 13500

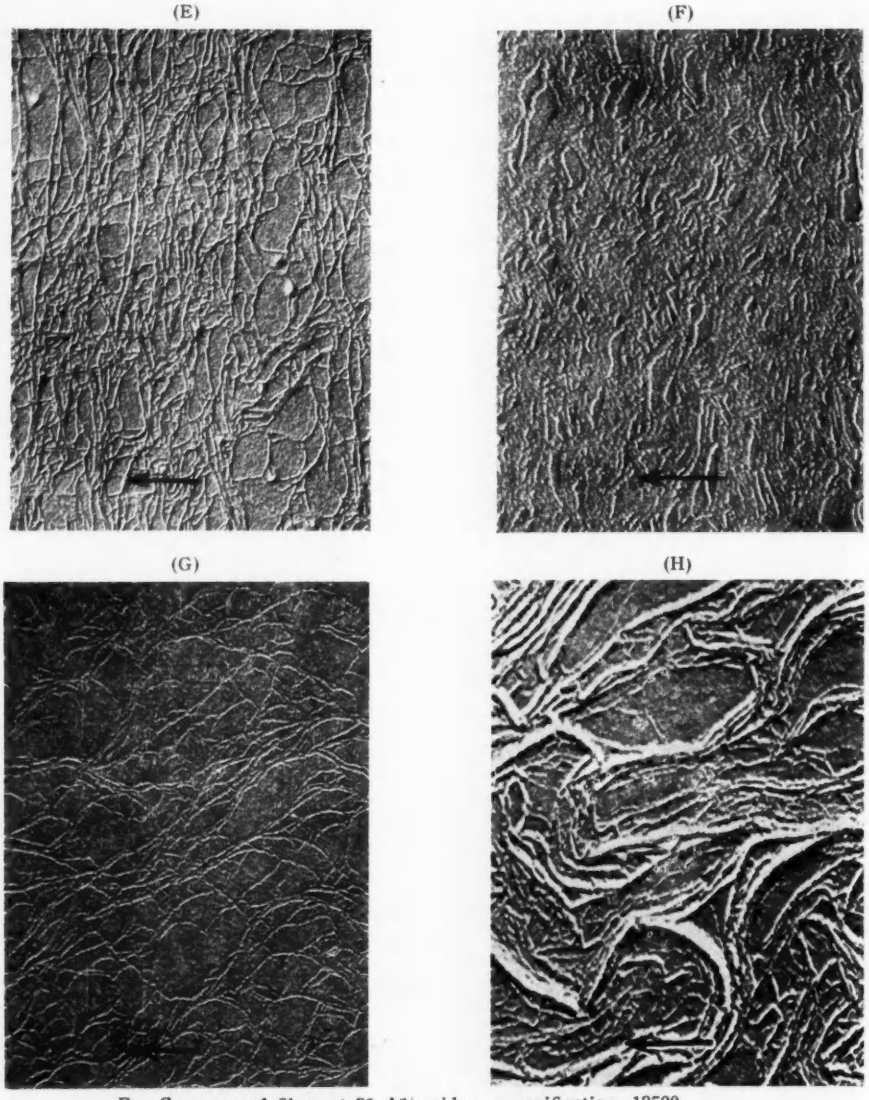

E, Compressed films at 30 A²/residue, magnification, 13500
F, Compressed films at 18 A²/residue, magnification, 13500
G, Uncompressed films at 18 A²/residue, magnification, 13500
H, Uncompressed films of low molecular fraction at 18 A²/residue, magnification, 135000
Arrows indicate the direction of compression.

characteristic areas (a) and (b). For this purpose, electron microscopic examination of the film[8], developed in our laboratory, have proved considerable merits.

A blank water sample is shown in Fig. 5A. Fig. 5B shows the film, taken at 80 A^2/residue at which the film was initially spread. There exist unspread materials which appeared as several fibrils running windingly. This film was compressed to various areas, at which the film specimens for electron microscopy were taken. Figs. 5C, 5D and 5E

8) T. Tachibana, K. Inokuchi and T. Inokuchi, *Nature* **176**, 1117 (1955).

are the films compressed to 50 A^2/residue, 40 A^2/residue, and 30 A^2/residue, respectively. It is shown that as the reducing area, more fibrils appeared than those which were expected to increase by the compression of the films, and came to link together forming a network structure. It is to be noted that at 30 A^2/residue, fibrils oriented normal to the direction of compression. Such an orientation, which could hardly be seen above 40 A^2/residue, was more and more pronounced as the compression advanced. Fig. 5F is an appearance of the film, which was compressed to 18 A^2/residue. Bare portions inside the network of fibrils disappeared, the whole area of the film being covered by the skinlike texture. Fig. 5G shows the uncompressed film which was initially spread at 18 A^2/residue. In contrast with the compressed film, it was noted that uncompressed films have fewer fibrils, and showed no sign of orientation of microfibrils. The effect of the degree of polymerisation on the structure of surface films has also been revealed by electron microscope. In Fig. 5H is shown the structure of uncompressed films (M. W. 1000) spread at 18 A^2/residue. Comparison of Fig. 5G, and Fig. 5H shows that the low molecular weight fraction produced thicker microfibrils than the high molecular one.

The relationship between amounts of microfibrils and area were roughly evaluated from the micrographs at various areas. In Fig. 1, the avarage total sum of the length of the microfibrils per sq. micron was plotted against the area together with the π-A curve and the potential curves. It is seen in this figure that increase in microfibrils, which was relatively slight at large areas, became pronounced below about 40 A^2/residue. It is suggestive that this area is fairly consistent with the point (a) in the π-A curve as well as with the point of the levelling off in the surface moment-area curve.

Discussion

Microfibrillar Structure of Surface Films. —It is first noticed that electron micrographs exhibit microfibrils, the size of which is almost constant at all compression, being estimated close to 40 Å from the width of the shadow. Although it is not clear at the present stage why the molecular association is stable with this size, it is very interesting to refer the Ribbi's experiment[9] that demonstrated the submicroscopic fibrils of forming the structural unit in the fibre of 6-nylon. Since, as the film was compressed, more fibrils appeared than the increase which is to occur as the result of the compression alone, it is clear that the bare portions of the micrographs, at which the microfibrils are absent, also possess film molecules. Although it is difficult to inquire in detail the film structure of this bare portion, it is readily known from the simple calculation*3 that the fraction of the molecules participating to form the microfibrils against the total amount of the spreading molecules is comparatively small at large areas, being about 10% at the point (a), and the remainder forms the bare portions of the films. Moreover, the co-area of the molecular residue at the bare portions of the area of point (a) is roughly estimated by counting the increase of about 10% to the value of the mean co-area of the point (a) (37 A^2/residue), and it is noticed that this value obtained is approximately consistent with the co-area of a residue of flat configuration calculated from the molecular model (40 A^2/residue). Hence, it may be assumed that the bare portions of the surface film at the point (a) possess close-packed molecules with their chains flat on water surface.

It was found from the rheological measurement that the film manifested a distinct elasticity below the areas of about 80 A^2/residue (gelation-area), which is about twice the area of the close-packed area. From the molecular weight dependence of the gelation-area, it was shown in the preceding paper that the film molecules took configuration which was considerably stretched and of less flexibility. Such a molecular configuration may be favorable for the alignment of adjacent molecular chains to form two-dimensional micellar structure. Such film molecules may come into contact with each other under compression to form a two-dimensional network at the gelation-area, at which a distinct elasticity begins to manifest itself. Thus, there must be a two-dimensional network covering the bare portion of the electron micrograph at 80 A^2/residue. Further compression would make

9) Cf. E. Ribbi, *Nature*, **168**, 1082 (1951).

*3 Percentage of molecules of forming the microfibrils against the total molecules (P) at the area of point (a) (mean co-area, 37 A^2/residure) is given as

$$\left\{\left(\frac{L}{m}\right)\times n \Big/ \frac{1}{37\times10^{-8}}\right\}\times 100,$$

where L is the mean total sum of the length of the microfibrils per μ^2, expressed in μ, the value of which at the point (a) is obtained as about 5 μ from Fig. 1, and m, the length of the residue which is 8.5 A with 6-nylon, and n, the number of molecules within the cross section of the microfibril. Assuming that a microfibril is made of the molecular chains, closely packed against each other and running parallel to the length of it, it follows that the cross section of the fibrils consists of about 64 molecules, since the cross sectional area of a molecular chain is calculated as about 20 A^2 from the molecular model. Hence, P is obtained as about 10%.

the network denser until a monomolecular layer of the close-packed molecules is formed at the point (a), though a few of the molecules happen to associate with each other to form microfibrils. Below the area of point (a), all the molecules at the monolayer portions are no longer allowed to stand flat on water surface, and the film may fall into collapse. This is indicated by the surface moment-area curve, which shows sudden decrease in electric moment below about 40 A^2/residue. It is likely that this collapsing process actually involves fibril formation of molecules in the monolayer, since it is visualized from Fig. 1 that a steep increase in the amount of microfibrils appears below the areas 35 to 40 A^2/residue, fairly coincident with the point (a). Thus, the onset of the plateau in the π-A curve is accounted for by the sudden increase in association of molecules to the three-dimensional direction (formation of microfibrils), in which the lateral pressure might relax on further compression. As visualized in Fig. 5 E and F, with the advancing compression, the microfibrils become denser and denser until they cover the whole area at about 20 A^2/residue, below which the pressure again rises steeply, and the micrographs fail to exhibit any fibrillar structure, showing. a skinlike texture. At 18 A^2/residue (Fig. 5F), there exsist a number of islands of about 50 A thick upon the back texture. From these findings, it may be considered that the plateau region in the π-A curve corresponds to the stage of formation of monofibrillar layer, and that the compression below the plateau region results in bifibrillar layer which transforms to polyfibrillar layer on further compression. In brief, it was evidently proved that the surface film of 6-nylon possesses microfibrillar structures, which presumably develop from monomolecular network, and transform to polyfibrillar layer under compression process.

Rheological Characteristics of Surface Films.—As shown in the electron micrographs, surface concentration of microfibrils at larger areas than the point (a) is so small that they fail to link together. So it is considered that the microfibrils are not primarily concerned with the film elasticity, but the portions of the monolayer network (bare portions of the micrographs) are chiefly responsible for the development of the elasticity. On the contrary, it was found that the microfibrils link together at areas below about 40 A^2/residue, forming a network of microfibrils. This time, it is easily understood that the microfibrils play an important role in the development of the film elasticity. This trend may be pronounced as the film is compressed, since the network of the microfibrils become more and more dense. In short, two types of surface films are presented; a monomolecular network at larger areas, and a network of the microfibrils at smaller areas.

In the preceding paper[1], it was reported in detail that the film at areas larger than about 40 A^2/residue behaves as a purely elastic body which is hardly seen in the ordinary materials at bulk, whereas it became viscoelastic as is often the case with the ordinary materials at bulk when the film was compressed to small areas. It is readily noticed that the ideal elastic film corresponds to the monomolecular network, and the viscoelastic film, to the network structure of microfibrils. Fibrillar structure is essentially the same as that of the bulk materials, and it is rather natural that the film of fibrillar structure shows viscoelasticity.

It is also suggested that, with the films of ideal elasticity, the cross-linkings of the molecular chains are necessarily homogeneous. As is indicated from Fig. 2, showing that the expansion hysteresis of the π-A curve is only slight at areas larger than the point (a) (the portion of the monomolecular network), it is easy to accept the thought that orientation and alignment of molecules at the monomolecular network may be relatively easy compared with the films at smaller areas, and the relatively homogeneous network may result. Ideal elasticity of the monomolecular film of 6-nylon may thus be explained.

Correspondence between Surface Pressure and Surface Elasticity.—There are many evidences which support the view that the apparent surface pressure exerted here is intimately related to the surface elasticity. It has been observed that the characteristic form of the force-area curve, involving the plateau, bears considerable resemblance to that of the rigidity-area curve. The sign of the temperature dependence on the surface pressure was found to be negative, being just the same with the case of surface rigidity as reported in the preceding paper[1]. Moreover, surface compressibility $\left(-\frac{1}{A}\frac{dA}{d\pi}\right)$ was obtained from the π-A curve, and according to Bateman[10], the surface modulus of rigidity was calculated under the assumption that the film is isotropic and the poisson ratio 0.4. The calculated values were compared with the observed ones obtained with our direct measurement of the surface rigidity. The result is given in Fig. 6, in which

10) J. B. Bateman and J. A. Chambers, *J. Phys. Chem.*, 45, 209 (1941).

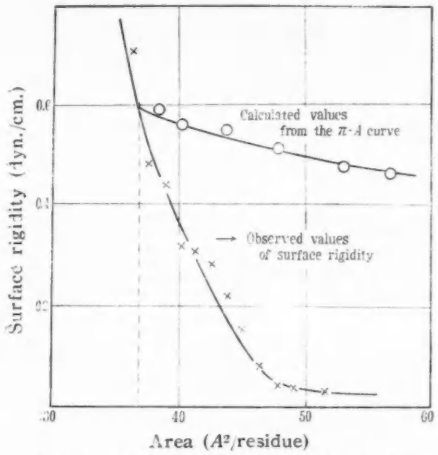

Fig. 6. Correspondence between surface pressure and surface rigidity.

considerable departure between the observed values and the calculated ones at larger areas became less serious as the reducing areas, and finally coincide with each other at the vicinity of 37 A^2/residue. Discrepancy of these values at larger areas may be plausible, since, at larger areas than the point (a), the observed pressures involve osmotic natures of the film molecules which do not participate in the formation of network. Coincidence of these values at the close-packed monolayer may possibly indicate that the surface pressure from the close-packed monolayer is wholly due to the internal stress of the solid film. These facts strongly suggest that the pressure exerted from the compressed films is not likely to have osmotic pressure of entropy nature as commonly considered, but is intimately related to the elasticity of solids.

Orientation of Microfibrils during Compression.—It is worth noticing that below about 40 A^2/residue, the microfibrils came to orient at right angles to the direction of compression. Extremely high compression of surface film gave rise to tiny visible striations running across the width of the through and finally produced fibrous threads which can be picked up from the water surface. It was observed that the structure of such films exhibited an array of microfibrils developed in straight lines orienting in a parallel manner to the striation or to the fibre. On the other hand, as shown in Fig. 5G, the uncompressed film initially spread at small area, e. g., 18 A^2/residue, gave winding microfibrils which had no sign of orientation.

It was demonstrated above that the compression process makes the surface pressure anisotropic, the pressure against the right angles to the direction of compression being larger than that parallel to it. This is not surprising, because it is considered that the film under investigation is not fluid, but probably solid. It is easily surmised that the orientation effect of the film molecules is brought about from this anisotropic nature of the surface pressure, which may probably orient the molecules with their long axis to the right angles to the direction of compression, in order to relax the pressure difference set up readily after compression.

The author believes that these interesting results provide a new line of evidence for the information of surface films of crystalline polymers.

Summary

(1) Surface films of 6-nylon at air/water interface were investigated by means of electron microscopic observation together with the study of the surface pressure and potential.

(2) An unique structure involving the microfibrils of about 40 A thick were revealed which are formed from the monomolecular network at large areas, and are transformed to polyfibrillar layer during the compression process.

(3) Network structures of the film were divided into two types: a monomolecular network at large areas, and a network of the microfibrillar structure at small areas. Rheological characteristics of 6-nylon film were explained in terms of such structures.

(4) Many evidences were provided which support the view that the surface pressure measured with this film is not likely to have the osmotic pressure as commonly considered, but is intimately related to the surface elasticity of the film.

(5) It was observed that the compression process orients the microfibrils at right angles to the direction of compression. This phenomenon was explained by the anisotropy of surface pressure set up by the compression of the film.

The present author wishes to express his hearty thanks to Prof. T. Tachibana for his helpful advice and encouragement throughout this study, and to Mrs. T. Inokuchi for her elaborate technique of the electron micrography.

Department of Chemistry, Faculty of Science, Ochanomizu University
Tokyo

*Effect of Surface Active Reagents on Electrode Process in Oscillographic Polarography**

By Hideo IMAI and Shokichi CHAKI

(Received February 7, 1956)

The effect of a surface active reagent on a polarographic reduction has been investigated from two points of view, one of which is the suppression of a maximum wave and the other is the retardation of an electron transfer process. Delahay[1], Randles[2], Gierst and Juliard[3], Heyrovský[4], and others studied the latter phenomenon, and from their experimental results Frumkin[5] proposed the "sieve" theory and Heyrovský suggested a mechanism with respect to the dismutation or disproportionation process of polyvalent cations. On the other hand, Loshkarev and Kryukova[6] observed that in solutions of 6 N-H_2SO_4 containing Ag^+ or Tl^+ ions their electrodeposition was hindered by surface active materials. More recently, Tamamushi[7] pointed out the similar effect on monovalent Tl^+.

An investigation of the same phenomenon has been carried out by one of the present authors[8]. The result of the more detailed investigation is presented in this report.

Experimental

A Ševčik type oscillographic polarograph was employed. The apparatus and the method of measurement were described in the previous report[9]. The details of the experimental conditions are as follows: the rate of variation of the applied voltage (v)=40 V./s. (in the case of gelatine solution), 50 V./s. (in the case of methyl cellulose solution); sweep frequency=20 c. p. s.; mercury head =40 cm.; the rate of mercury flow=1.94 mg./s.; the life time of the dropping mercury electrode (D. M. E.)=3.1-3.8±0.02 sec.; the current measuring resistor (Rm)=30-70 Ω; temp.=30±0.1°C.

From reagent grade chemicals was prepared the test solution of a constant concentration of 0.5 mol./l. Tl^+, Cd^{++} or Zn^{++}, and each test solution contained 1 mol./l. KBr, KCl, KNO_3 or Na_2SO_4 as the supporting electrolyte and 0.002-0.01% gelatine (G.) or methyl cellulose (M.C.), respectively.

Purified nitrogen was used to remove the dissolved oxigen of the test solution prior to taking a polarogram.

Results and Discussion

The current-potential oscillograms are exemplified in Figs. 1 and 2 in the cases of Tl^+ in mol./l. KCl and Na_2SO_4 containing 0-0.01% M. C., respectively. From these polarograms the maximal peak current, i. e. the current at the maximum life time of the D. M. E., is plotted against the concentration of G. or M. C. as illustrated in Figs. 3, 4 and 5.

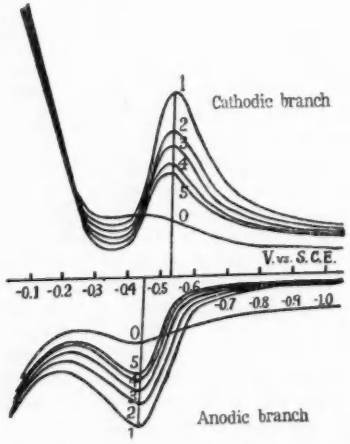

Fig. 1. Maximal peak current-potential oscillogram of 0.5 mM/l. Tl^+ in M KCl: Curve 1; 0% M.C., Curve 2; 0.002%, Curve 3; 0.005%, Curve 4; 0.008%, Curve 5; 0.01%. Curve 0; charging current. R_m=40 Ω, t=3.1$_4$ sec.

* Presented at the discussion on polarography held by the Chemical Society of Japan, the Electrochemical Society or Japan and the Japan Society for Analytical Chemistry in November, 1955.

1) P. Delahay, *J. Phys. Colloid Chem.*, **53**, 1279 (1949).

2) J. E. B. Randles, *Discs. Faraday Soc.*, **1**, 11 (1947).

3) R. Gierst and A. L. Juliard, *J. Phys. Chem.*, **57**, 70 (1953).

4) J. Heyrovský, *Collection Czechoslov. Chem. Communs.*, **19**, S. 58 (1954).

5) A. H. Frumkin, *Discs. Faraday Soc.*, **1**, 224 (1947), *Dokl. Akad. Nauk S.S.S.R.*, **85**, 373 (1952).

6) M. A. Loshkarev and A. A. Kryukova, *Dokl. Akad. Nauk S.S.S.R.*, **62**, 97 (1948).

7) R. Tamamushi, *Polarography*, **3**, 56 (1955); R. Tamamushi and T. Yamanaka, This Bulletin, **28**, 673 (1955).

8) M. Shinagawa and H. Imai, *J. Electrochem. Soc. Japan*, **23**, 187 (1955). Presented at the discussion on analytical chemistry held by the Chemical Society of Japan in November, 1953.

9) H. Imai, This Bulletin, **29**, 276 (1956).

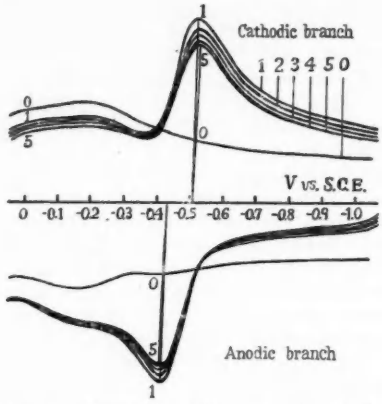

Fig. 2. Maximal peak current-potential oscillogram of 0.5 mM/l. Tl^+ in M Na_2SO_4: The curve numbers correspond to those of Fig. 1. $R_m = 70\,\Omega$, $t = 3.3_0$ sec.

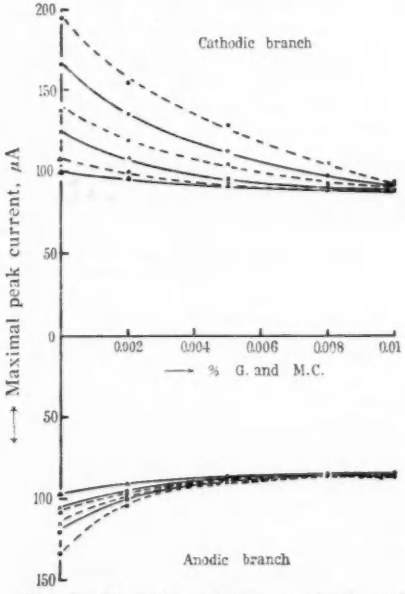

Fig. 3. Variation of the maximal peak current of 0.5 mM/l. Tl^+ with the concentration of G. or M.C.: G.; full curve, M.C.; interrupted curve. G: full curve, M.C: interrupted curve, -●- Cl^-, -×- NO_3^- -▲- SO_4^{--}.

In Fig. 4 it is evident that the cathodic peak current of the solution containing no surface active reagent increases in the solution of SO_4^{--}, NO_3^-, Cl^-, Br^- in the order given. This trend is emphasized in the case of Tl^+ (Fig. 3) and is weakened in the case of Zn^{++} (Fig. 5). Since the peak potential of Tl^+ is more positive than that of Cd^{++} and the

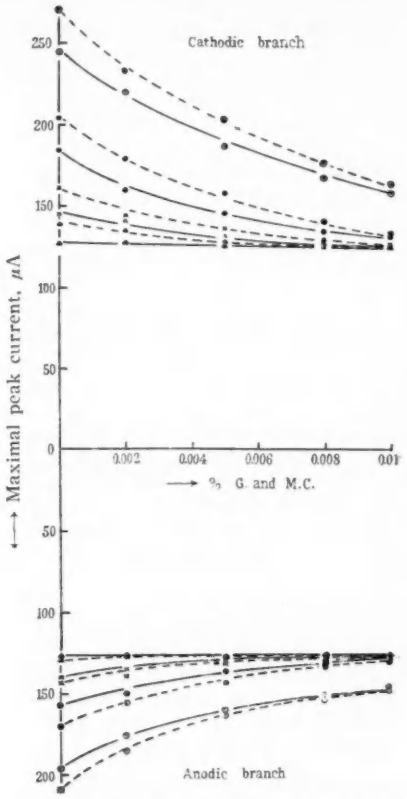

Fig. 4. Variation of the maximal peak current of 0.5 mM/l. Cd^{++} with the concentration of G. or M. C.: G: full curve, M. C.: interrupted curve, -⊙- Br^-, -●- Cl^-, -×-NO_3^-, -▲- SO_4^{--}.

peak potential of Zn^{++} is more negative than that of Cd^{++}, it is assumed that the above mentioned trend becomes weaker as the reduction potential shifts toward more negative potentials. In the anodic branch the same trend is also observed, although the net variation of the peak current is in any case less than the cathodic one.

The above mentioned effect of anions has already been reported by Heyrovský[10], Randles[2], Doss and Agarwal[11], and others[5,12]. One of the present authors[13] has pointed out the parallelism between the catalytic

10) J. Heyrovský, *Discs. Faraday Soc.*, **1**, 212 (1947).
11) K.S.G. Doss and H.P. Agarwal, *J. Phys. Colloid Chem.*, **54**, 804 (1950).
12) P. Lukovtsev, S. Levina and A.H. Frumkin, *Acta Physicochim. U.R.S.S.*, **11**, 21 (1939). J'OM. Bockris, *Chem. Revs.*, **43**, 525 (1948). R. Pointelli, Int. Comm. Electrochem. Therm. Kin., Proc. 2nd meeting, Tamburini, Milan, 1950, p. 185.
13) H. Imai, Presented at the discussion on polarography held by the Chemical Society of Japan etc. in November, 1955.

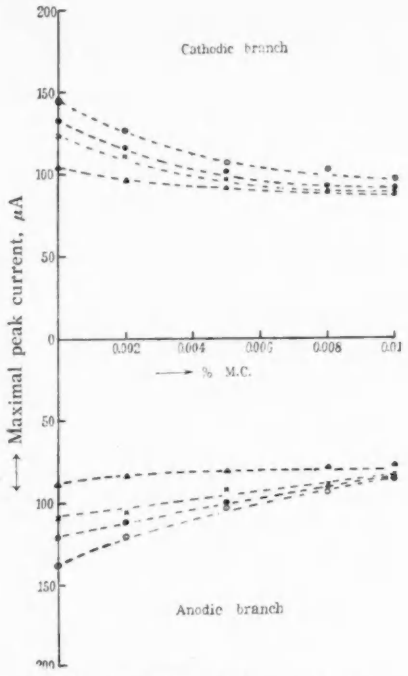

Fig. 5. Variation of the maximal peak current of 0.5 mM/l. Zn^{++} with the concentration of M.C.: -(⊙)- Br^-, -●- Cl^-, -×- NO_3^-, -△- SO_4^{--}.

effect of an anion and the charging current[14] resulting from anions adsorbed on the surface of the D. M. E.; namely, the charging current becomes more pronounced in the solution containing SO_4^{--}, NO_3^-, Cl^-, Br^-, I^- in the order given and it decreases as the applied potential shifts toward more nagative potentials in the cathodic branch. In the anodic branch a less charging current than the cathodic current is observed in every supporting electrolyte solution. Assuming that the adsorptive density of an anion is proportional to the charging current, one can conclude that the catalytic effect originates from the establishment of the combination such as Hg (electrode)—Adsorbed Anion—Depolarizer Ion, through which the electrone transfer is facilitated.

In the presence of G. or M. C. the catalytic process of an anion is retarded as is illustrated in Figs. 3, 4 and 5. Namely, the effect of G. or M. C. becomes more pronounced in the test solution of the same depolarizer (Tl^+, Cd^{++} or Zn^{++}) containing SO_4^{--}, NO_3^-, Cl^-, Br^- in the order given, and also in the solution of the same supporting electrolyte containing Zn^{++}, Cd^{++}, Tl^+ in the order given. In the anodic process the effect is less than the cathodic one. The parallelism between the catalytic effect and the retarding effect is best realized in the solution containing 0.01% G. or M. C.; that is, in this solution the catalytic effect of an anion is almost perfectly reduced, and accordingly, the cathodic current is nearly equal to the anodic current regardless of the anion constituent.

In the test solution containing Tl^+ no appreciable shifts of the peak potential owing to the presence of G. or M. C. was observed either in the cathodic branch or in the anodic branch. $E_p - E_{p1/2}$ (E_p; the peak potential, $E_{p1/2}$; the half peak potential), however, slightly increases within a few millivolts as the concentration of G. or M. C. increases. The increase of $E_p - E_{p1/2}$ results from the retardation of the rate of the electrode process as is indicated theoretically by Matsuda and Ayabe[15].

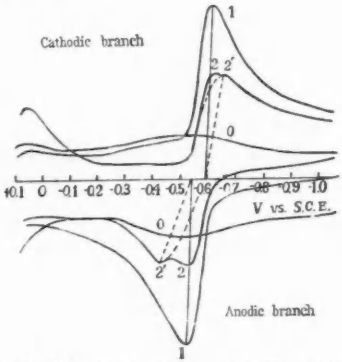

Fig. 6. Maximal peak current-potential oscillogram of 0.5 mM/l. Cd^{++} in M KNO_3: Curve 1; no M.C., Curve 2; 3/4 life time of D.M.E. (0.008% M.C.), Curve 2'; just before the drop falls. (0.008% M.C.)

In the case of Cd^{++} in KNO_3 solution containing more than 0.008% M. C. the peak remarkably shifts toward more negative or more positive potentials in the cathodic or the anodic branch, respectively, as the mercury drop grows ripe. The current-potential oscillogram is illustrated in Fig. 6. Zn^{++} behaves likewise. It is assumed that the phenomenon results from the steric hindrance by the film formation of surface active molecules.

Finally the molecules of a surface active reagent, the concentration of which is as low as 0.002–0.01%, exchange with the anions

14) H. Imai, This Bulletin, 29, 281 (1956).

15) H. Matsuda and Y. Ayabe, *Z. Elektrochem.*, 59, 494 (1955).

existing in the electrode surface (Helmholtz layer) and result in the retardation of the catalytic process displayed by the anions. Hereupon, not only a polyvalent cation but also a monovalent cation (Tl^+) suffer from the catalytic effect of the anion and the retarding effect of the surface active reagent. In this conncetion Heyrovský[4] observed that the electrodeposition of Tl^+ is reversible and is not hindered by the presence of gelatine. From Matsuda and Ayabe's theory[15] it is reasoned that the electrode process of Tl^+ is quasi-reversible and is controlled not only by the diffusion of Tl but also by the rate of the electrode process as far as the rate constant, k_G, of the electrode process does not exceed 2 cm./sec. This value is estimated by substituting the numerical values of n and v in $0.3\sqrt{nv}$, where n is the number of electrons transferred per ion and v is the rate of variation of the applied voltage. By the way, the value of k_G of Tl^+ in mol./l. KNO_3 solution is given as great as >1 cm./sec. by Randles and Somerton[16]. Since the electrode process of Tl^+ suffered from the catalytic action of anions in this experiment, it seems that the value of k_G will not be greater than 2.

The phenomenon occurring in the concentration region greater than 0.008% of the surface active reagent is mentioned above, and in the region from 0.008% to 0.04% the diffusion controlled current of an ordinary polarograph is scarcelly retarded, but the peak potential in the oscillographic polarograph shifts remarkably. This effect can be assigned to the film formation of the surface active reagent. The retardation of the diffusion controlled current of an ordinary polarograph in the concentration region of the surface active reagent more than 0.04% is probably explicable on the basis of the "sieve" effect.

Randles[2] observed that the rate constant of the electrode process of Cd^{++} in mol./l. KCl solution is reduced in two steps as the concentration of gelatine increases, and the first step appears in the concentration region from 0 to 0.01% of gelatine and the second step appears in the concentration region of more than 0.04% gelatine. Since these results coincide with those of the present authors, the mechanisms of Randles's results are reasonably explicable by adopting the above mentioned conclusion.

The authors wish to express their hearty gratitude to Dr. Takeshi Taketa and Dr. Mutsuaki Shinagawa for their encouragement throughout this study.

Laboratory of Chemistry, Minami College
Hiroshima University, Hiroshima

16) C.W. Conway, "Electrochemical Data", Elsevier Publ. Co., Amsterdam (1952), p. 356.

Ionization Potentials of Some Organic Molecules. I. Apparatus

By Itiro Omura, Keniti Higasi and Hiroaki Baba

(Received February 7, 1956)

With the rapid progress in the theories of molecular orbitals the study of ionization potentials of molecules has gained much theoretical importance. Besides being used to determine which electron is the most loosely bound[1], they can provide data for the calculation of electronic wave functions[2]. And recently these data have been employed even in interpreting the mechanism of organic reactivity[3]. In spite of these facts there are available comparatively few data for only a small number of molecules. In the series of the present reports some results of our measurement will be given which have recently been carried out by the use of a mass spectrometer constructed in the laboratory of the present writers.

Instrumental Details and Experimental Method

The apparatus constructed and employed by the present writers belongs to a Hagstrum type mass spectrometer[4]. Its main part of the electron and ion gun circuits is shown schematically in Fig. 1. Electrons emitted from the hot tungsten

1) R.S. Mulliken, *Phys. Rev.*, **46**, 549 (1934); *J. Chem. Phys.*, **3**, 514 (1935).
2) G.G. Hall and J.E. Lennard-Jones, *Proc. Roy. Soc.* (London), **A 202**, 155 (1950); **A 205**, 541 (1951).
3) S. Nagakura and J. Tanaka, *J. Chem. Phys.*, **22**, 563 (1954).

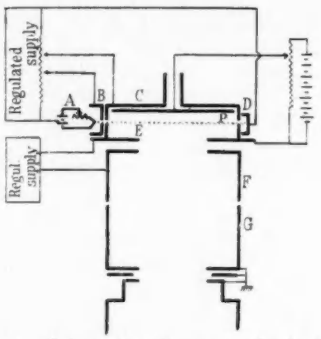

Fig. 1. Schematic diagram of electron and ion gun circuits of a mass spectrometer. A filament, B, C electron accelerating plates, C ionization chamber, D electron trap, P pusher electrode, E electron beam, F, G ion accelerating plates.

filament A are collimated into a beam by the systems of electrodes, B, C, enter the ionization chamber and finally are collected into the trap, D. The energy of the electrons causing ionization is largely determined by the potential difference between C and A, which can be varied. Ions formed in this chamber are acted on by a cross-field of up to one volt, which is applied between the pusher electrode P and the ionization chamber, and then they pass into the F—G lens in which they focus upon the input slit of the magnetic analyzer[4]. In order to make the collimation of the electron beam easier, a magnetic field of 200 oersted is applied, the lines of force of which are parallel to the axis of the electron beam.

Finally, ion currents to the collector plate are measured and their dependence on the potential difference between C and A is recorded. The

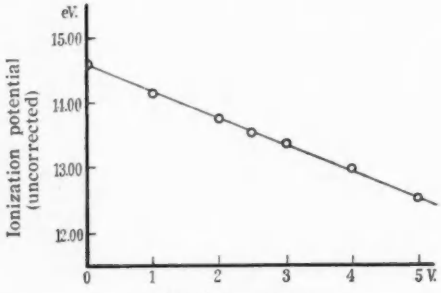

Fig. 2. Variation of the uncorrected ionization potential of argon with the potential of the cross field.

4) H. D. Hagstrum, *Revs. Modern Phys.*, **23**, 185 (1951).

5) See, for example, G.P. Barnard, "Modern Mass Spectrometry", London (1953).

6) E.B. Jordan and N.D. Coggeshall, *J. Appl. Phys.*, **13**, 539 (1942).

latter quantity is not to be simply put as equal to the energy of the ionizing electron beam. That is, there are many complicating factors which influence the energy of the ionizing electron[5]. From among the factors examined in the present work, two will be mentioned; viz., the effects of the pusher voltage and the intensity of ion current. First, the effect arising from the pusher voltage is shown in Fig. 2. The linear relationship exists between the ionization potential and the pusher voltage which is in accord with the calculation of Jordan et al[5]. Second, Fig. 3 shows

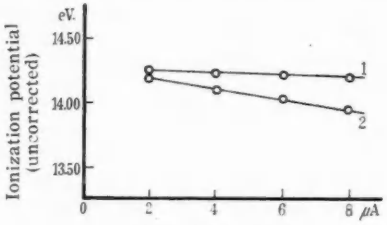

Fig. 3. Variation of the uncorrected ionization potential of argon with the intensity of the electron current.
1 critical slope method; 2 extrapolation method.

the effect due to the intensity of the electron current. The variation of the ionization potential is less pronounced in the critical slope method[7] than in the usual extrapolation method.

The ionization potentials recorded in the present work were determined in comparison with the spectroscopic value of argon, 15.76 eV. This standard gas is introduced and measured, immediately before and after the ion being studied. The fluctuations in this correction in a day were usually less than ± 0.02 eV.

Measurements of the ionization potentials were made with the following conditions;

i) Electron currents trapped at D 5 μA,
ii) Electron accelerating voltage $0 \sim +20$ V.,
iii) Trap potential at D+100 V.,
iv) Potential at the pusher electrode $0 \sim +1$ V.,

The slits employed in the ion lenses are wider than usual, the slit in ionization chamber 4×10 mm., and the final slit 0.25×10 mm.

Accuracy of the Experimental Results

Two methods have been frequently employed in determining the ionization potentials[5]: (1) the method of linear extrapolation and (2) Honig's[7] critical slope method. Both of them were examined in the present work (see Table I). Values obtained by critical slope method were in better agreement with spectroscopic values. Generally the critical slope method gave reproduceable values. Therefore, this method was employed throughout in the present work.

In Table II representative values of ionization

7) R.E. Honig, *J. Chem. Phys.*, **16**, 105 (1948).

TABLE I

APPEARANCE POTENTIALS MEASURED BY VARIOUS METHODS, eV.

Substance	Linear extrapolation	Critical slope	Spectroscopic
Argon	(15.76)	(15.76)	15.76[a]
Neon	21.68	21.62	21.58[5]
Nitrogen	15.67	15.56	15.58[5]
Hydrogen disulfide	10.62	10.54	10.47[b]

a) Moore's value cited by D.P. Stevenson (*Trans. Faraday Soc.* **49,** 867 (1953)).
b) W.C. Price, *Chem. Rev.*, **41,** 257 (1947).

TABLE II

FIRST IONIZATION POTENTIALS OF MOLECULES, eV.

Substance	Present work (Electron impact)	Values in literature (Electron impact)		(Spectroscopic)	
Argon	15.76[a]	15.76[a]	(15.77)[5]	15.76[a]	(15.77)[5]
Neon	21.62±0.05	21.53[b]	(21.61; 21.24; 21.42; 21.57)[5]	21.58[5]	
Hydrogen	15.51±0.10	15.40[c]		15.42[d]	
Nitrogen	15.56±0.10	15.66[b]	(15.60; 15.57)[5]	15.50[e]	
Oxygen	12.45±0.10	12.50[b]	(12.20; 12.39)[5]	12.26[5]	
Methyl alcohol	10.97±0.05	10.95[b]		10.80[f]	
Ethyl alcohol	10.65±0.05	10.60[b]		10.70[f]	
Methyl amine	9.41±0.02	9.41[b]		9.80[f]	
Benzene	9.52±0.10	9.52[b]		9.24[f]	
Toluene	9.20±0.05	9.23[b]		8.82[f]	
Pyridine	9.76±0.05	9.8[h]			
Furan	9.00±0.10	9.05[b]		9.01[g]	

a) Moore, loc. cit.
b) J.D. Morrison and A.J.C. Nicholson, *J. Chem. Phys*, **20,** 1021 (1952).
c) W. Bleakney, *Phys. Rev.*, **35,** 1180 (1930).
d) H. Beutler und H.-O. Jünger, *Z. Physik.*, **100,** 80 (1936).
e) R.E. Worley and F.A. Jenkins, *Phys. Rev.*, **54,** 305 (1938).
f) W.C. Price, *Chem. Rev.*, **41,** 257 (1947).
g) W.C. Price and A.D. Walsh, *Proc. Roy. Soc.* (London), **A179,** 210 (1941).
h) A. Hastrulid, P. Kusch and J.T. Tate, *Phys. Rev.*, **54,** 1037 (1938).

potentials determined in the present studies are compared with those of previous workers. They include five inorganic gases and seven organic vapours. Observed potentials lie in the range between 9 and 22 eV. In all these examples there is general agreement with the values of the previous workers obtained by electron impact method.

On the comparison with spectroscopic values there exists some divergence in values. But there is no need of perfect agreement among the values of the two methods[8], if the impact value of argon is taken from its spectroscopic value.

In conclusion, it may be said that the use of a single standard gas is justfied and also that ionization potentials of molecules are satisfactorily obtained by the apparatus of this experiment for the samples treated so far.

8) J.D. Morrison and A.J.C. Nicholson, *J. Chem. Phys.*, **20,** 1021 (1952).

Summary

Instrumental details of electron impact method for determining ionization potentials are recorded. Further, it is shown that the potential values obtained by the present method are in good agreement with the data reported by the previous workers.

The authors wish to express their gratitude to Prof. K. Hirota for initiating the present work, and also to the Ministry of Education for a Grant in Aid.

Research Institute of Applied Electricity
Hokkaido University, Sapporo

Ionization Potentials of Some Organic Molecules. II. Aliphatic Compounds

By Itiro OMURA, Keniti HIGASI and Hiroaki BABA

(Received February 7, 1956)

Introduction

There are numbers of molecules the ionization potentials of which are largely determined by non-bonding electrons. When dealing with these molecules it was often assumed that there is some relation between the dipole moment and the ionization potential[1]. First, in the present article, the appearance potentials obtained for seven aliphatic alcohols and three aliphatic amines will be reported. Contrary to the majority of the homologous series the polarity of homologous alcohols remains constant or even decreases with the increase in the carbon number[2,3].

Second, the appearance potentials of two unsaturated aldehydes and two ketones will be treated. From the studies on the dipole moment[4] it is known that there are two factors which affect the electron migration in these molecules, viz., hyperconjugation and inductive effect. For instance, it was inferred that the molecule of acrolein facilitates the transmission of charge to the negative oxygen by means of contribution from structures such as

$$^{+}CH_2-CH=CH-O:^{-} \qquad H^{+}\ddot{C}H-CH=CH-O:^{-}$$

If the ionization potential of acrolein is determined by the lone pair of electrons on the oxygen atom, the effect of hyperconjugation will appear in the observed values of potentials.

Lastly, discussion will be presented on the ionization potentials of the molecules, $CH_3CO\cdot X$ (X=OH, NH_2, H and CH_3).

Experimental Materials

Alcohols (Kanto Chem. Co., Inc.) were distilled and their purity was checked by measuring the refractive index for D-line at room temperature. Methyl alcohol b. p. 64.5°C, $n^{20}=1.3310$; ethyl alcohol b. p. 78°C, $n^{20}=1.3623$; *n*-propyl alcohol b. p. 97°C, $n^{20}=1.3846$; isopropyl alcohol b. p. 82.4°C, $n^{25}=1.3764$; *n*-butyl alcohol b.p. 117.0°C, $n^{20}=1.3962$; isobutyl alcohol b. p. 107.0°C, $n^{15}=1.3975$; *tert*-butyl alcohol b. p. 82.4°C, $n^{25}=1.3847$.

Amines (Kanto Chem. Co., Inc.) were prepared by distilling off their 25% water; and the degree of purity was examined by a mass spectrometer.

The sample of mesityl oxide in the pure form was very kindly provided by Dr. Nagakura of Tokyo University. Crotonaldehyde was kindly provided by Mr. Maekawa; b. p. 95–110°C, $n^{20}=1.4394$. The remaining samples were obtained from Kanto Chem. Co., Inc. Acrolein b. p. 52–53°C, $n^{20}=1.4005$; acetone b. p. 56.2–56.5°C, $n^{20}=1.3592$; acetic acid b. p. 117–118°C, $n^{20}=1.3723$; ethyl mercaptan b. p. 36–37°C, $n^{20}=1.4307$; acetamide m. p. 79.5°C.

Experimental Method and Result

The measurement of the first appearance potentials was made by the use of an apparatus described in a previous report[5]. Honig's critical slope method was employed throughout, and examples of this application to butyl alcohols are shown in Fig. 1. It is to be noted in this connection that Morrison and Nicholson[3] reported that

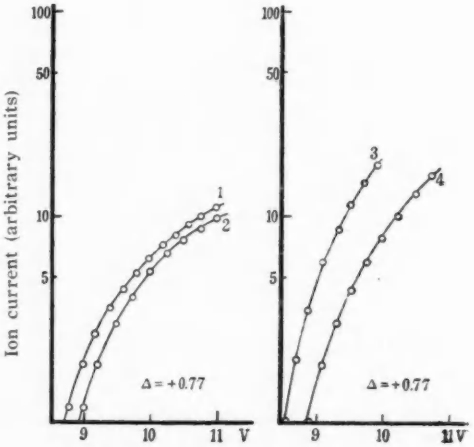

Fig. 1. Relative ionization efficiency curves for alcohols. 1 *tert*-butyl alcohol; 2 isopropyl alcohol; 3 isobutyl alcohol; 4 *n*-butyl alcohol.

1) C.A. Coulson, "Valence", Oxford (1952), p. 186.
2) M. Kubo, *Sci. Pap. Inst. Phys. Chem. Res.* (Tokyo), **26**, 242 (1953); **27**, 65 (1935).
3) K. Higasi, ibid., **31**, 311 (1937).
4) C.P. Smyth, "Dielectric Behavior and Structure", McGraw-Hill Book Co., New York (1955).
5) I. Omura, K. Higasi and H. Baba, This Bulletin, **29**, 501 (1956).
6) J. D. Morrison and A. J. C. Nicholson, *J. Chem. Phys.*, **20**, 1021 (1952).

no measurement on *n*-butyl alcohol was possible for them on account of the small quantity of molecular ion. Further, Franklin[7] appears to have also failed in measuring the appearance potential of *tert*-butyl alcohol. The reason why such difficulty could be overcome in the present work is probably due to the use of the cylindrical ion lenses[5].

In Table I the results of the present work are collected and compared with the data available. It will be seen that the agreement is satisfactory throughout.

TABLE I

FIRST IONIZATION POTENTIALS, eV.

Substance	Present work	Previous workers	
Methyl alcohol	10.97±0.05	10.95[3]	(10.80[9])
Ethyl alcohol	10.65±0.05	10.60[3]	(10.70[9])
n-Propyl alcohol	10.42±0.10	10.46[3]	(10.70[9])
Isopropyl alcohol	10.27±0.10		
n-Butyl alcohol	10.30±0.10		
Isobutyl alcohol	10.17±0.10		
tert-Butyl alcohol	9.92±0.10		
Methyl amine	9.41±0.02	9.41[3]	(9.80[9])
Dimethyl amine	9.21±0.05		(9.60[9])
Trimethyl amine	9.02±0.05		(9.40[9])
Ethyl mercaptan	9.21±0.05		(9.70[9])
Acetone	9.89±0.05	9.92[6]	
Acetic acid	10.66±0.05	10.70[4]	
Acetamide	10.39±0.05		
Acrolein	10.25±0.05	10.34[5]	
Crotonaldehyde	9.81±0.05		
Mesityl oxide	8.89±0.05		

Values in parentheses refer to spectroscopic potentials.

Discussion

As reported in a previous note[8] the general lowering of the ionization potential with the increase in carbon number is found in the observed values of aliphatic alcohols. When one hydrogen atom is replaced by one methyl radical at α carbon atom, the decrease 0.3–0.4 eV. is found, while such decrease amounts to only 0.2 eV., if the same occurs at β carbon atom (see Table II).

Three kinds of explanation can be offered for the observed change of the potential. The first may result from the following assumptions; (1) the ionization potentials of alcohols are solely determined by the nonbonding electrons on the oxygen atom[9]; and (2) alkyl radicals have the property of electron repulsion, the latter being increased along the series[10]

$$-CH_3 < -CH_2(CH_3) < -CH(CH_3)_2 < -C(CH_3)_3.$$

By the so-called inductive effect electrons tend to move from the alkyl group to the oxygen atom, thus reducing the electronegativity of the oxygen atom. Consequently, it would result in the lowering of potentials which is in qualitative agreement with the results shown in Table II.

TABLE II

BRANCH EFFECT OF ALIPHATIC ALCOHOLS ON POTENTIALS (eV.) and MOMENTS (DEBYE)

Substance	Potential (obs.)	Potential (calcd.)	Moment[3] (gas)	Moment[3] (solution)
CH_3OH	10.97	[10.95]	1.69	1.62
	(0.32)			
$CH_2(CH_3)OH$	10.65	10.54	1.69	1.66
	(0.38)			
$CH(CH_3)_2OH$	10.27	10.07	1.63	1.66
	(0.35)			
$C(CH_3)_3OH$	9.92	9.69	——	1.66
CH_3CH_2OH	10.65	10.54	1.69	1.66
	(0.23)			
$CH_2(CH_3)\cdot CH_2OH$	10.42	10.36	1.66	1.66
	(0.25)			
$CH(CH_3)_2\cdot CH_2OH$	10.17	9.97	1.63	1.65

Potential value in brackets was taken as the standard in calculations.

To argue against the above view, one may point out the fact that the electric moment of alcohols does not increase with the increase in the carbon number[2,4]. But this evidence may not be convincing. There are two dipoles in the molecule: one along the O–H linkage, the other along the C–O linkage and they make an angle with each other. Although the C–O bond moment may increase with the electron transmission toward the oxygen atom, the larger O–H moment will not increase but possibly decrease. Consequently, it is likely that no appreciable increase in the whole moment would result, if such electron displacement actually occurs. One is to note instead that the above series of the electron repelling property have been derived from chemical reactivities and they rest on no sound physical evidence*. If this mechanism of the electron displacement be true, it is highly doubtful whether it is significant enough to produce the observed effect.

The second explanation comes from the application of group orbitals[11]. As is well known this method requires the solution of the secular equation

$$e_{ij} - E\delta_{ij} = 0$$

7) J.L. Franklin, Private communications.

8) I. Omura, H. Baba and K. Higasi, This Bulletin, 28, 147 (1955).

9) W.C. Price, *Chem. Rev.*, 41, 257 (1947).

10) C. K. Ingold, "Structure and Mechanism in Organic Chemistry", Cornell Univ. Press (1951); Table 7-2, p. 71.

* One of the present writers discussed this problem in other place (cf. K. Higasi and K. Hirota, "Theory of Organic Chemistry", Asakura Book Co., Tokyo (1951), Chap. V).

11) J.L. Franklin, *J. Chem. Phys.*, 22, 1304 (1954).

where i and j refer to various groups in the molecule. The roots of secular equation represent the ionization potentials of the molecule, the lowest root being the first ionization potential measured.

Calculation of ionization potentials according to this method has been done by Franklin[11] for methyl, ethyl and *n*-propyl alcohols. In the present work, further calculations are carried out for remaining alcohols, assuming the same values for the constants, e, b, g, and c with those of Franklin. Calculated results are given in the third column of Table II. In view of the fact that this calculation is based on many bold assumptions, it is surprising that the calculated values are in fair accord with those observed.

Both of the views stated above are based on the assumption that the ionization potential is concerned solely with the normal state of neutral molecule before electron impact. Therefore, the third explanation comes from the view that this assumption is not always valid. For instance, Price[9] argues that the effect of alkyl substitution on the ionization potential is due mainly to preferential stabilization of the ionic or excited state. Indeed, his explanation for the ionization potential of RX is in good accord with our results on alcohols. The only regret in regard to this view is that no estimation is possible as to the effect of such a mechanism.

In Table III the measured potentials of

TABLE III

POTENTIALS IN eV. AND MOMENTS IN DEBYE OF ALIPHATIC AMINES

Substance	Potential (obs.)	Potential[11] (calcd.)	Moment[2,3] (gas)
Methyl amine	9.41	[9.41]	1.28
Dimethyl amine	9.21	8.67	1.02
Trimethyl amine	9.02	8.06	0.8

aliphatic amines are recorded. The calculated values based on group orbital method by Franklin[11] are shown in the same table together with the dipole moment values. It will be seen that both potentials and moments decrease with the increase in the number of methyl groups. Agreement with the calculated values is not good. Possibly, this is a case when the effect of molecular ion stabilization is important.

Before discussing the ionization potentials of unsaturated aldehydes and ketones, attention will be drawn to those of saturated compounds in which the lone-pair electrons of the O-atom play a dominant role in the ionization potential[1] (Table IV). Upon the alkyl substitution the decrease in the potential which is accompanied by the increase

TABLE IV

IONIZATION POTENTIALS (eV.) AND DIPOLE MOMENTS (DEBYE) OF KETONES AND ALDEHYDES

Substance	Potential (obs.)	Potential (calcd.)	Moment[3] (gas)
HCHO	10.88[9]	[10.88]	2.27
CH_3CHO	10.28[5]	[10.28]	2.72
CH_3COCH_3	9.89	9.84	2.85
$CH_2{=}CHCHO$	10.25	——	3.04
$CH_3{\cdot}CH{=}CHCHO$	9.81	9.74	3.67
$(CH_3)_2C{=}CHCOCH_3$	8.89	8.75	2.84*

* Moment obtained in solution.

in moment occurs in these molecules. This is in accord with the simple view that the effect of hyperconjugation as well as the inductive effect of the alkyl group cooperate to concentrate the electrons more towards the oxygen atom, thus resulting in a higher CO bond moment and a lower ionization potential.

The situation in acrolein and crotonaldehyde is somewhat complicated, since there are π-electrons in the C=C bond. The potential decrease on the introduction of one methyl group into the β carbon atom of acrolein amounts to 0.44 eV. If this large decrease be attributable to the change in the electron concentration on the oxygen atom*, this would indicate that the electron transfer is greatly facilitated along the π-bonds. The potential value of mesityl oxide $(CH_3)_2C{=}C{\cdot}COCH_3$ is of special interest. It shows a further decrease of 0.92 eV. over the value of crotonaldehyde $CH_3{\cdot}CH{=}CHCHO$. For comparison's sake, the results of calculation based on the group orbital method are included in Table IV. The calculated values are in accord with the observed.

Lastly, the potential values of $CH_3CO{\cdot}X$ will be considered. According to the present measurement (Tables I and IV), $CH_3CO{\cdot}OH$ 10.66, $CH_3CO{\cdot}NH_2$ 10.39, CH_3CHO 10.28 and $CH_3CO{\cdot}CH_3$ 9.89 eV. If the ionization potential is largely determined by the non-bonding electrons at the O-atom, the sequence of $OH > NH_2 > H > CH_3$ would indicate that the groups attract electrons more strongly along this series from the oxygen atom. Indeed, this expectation may be fulfilled, if only the inductive mechanism[10] be taken into consideration. But this is a problem which needs further investigation, because there are complicating factors including another mechanism of the electron displacement.

* A support for this view may be found in McMurry's work (*J. Chem. Phys.*, 9, 231, 241 (1941)). According to him, in ketones and aldehydes including acrolein and croton aldehyde, one of the non-bonding electrons corresponds to the most loosely bound electron.

Summary

Ionization potentials of seven alcohols, three amines and nine other aliphatic compounds were determined by a mass spectrometer of Hagstrum type. In view of the fact that no reliable explanation of the ionization potentials of molecules has been given an examination of the possible interpretations of the results was presented. The relation of ionization potentials to the dipole moments, non-bonding electrons and the group orbital method are briefly discussed.

The authors wish to express their gratitude to Dr. S. Nagakura for valuable criticisms and suggestions, and also to the Ministry of Education for a Grant in Aid.

Research Institute of Applied Electricity
Hokkaido University, Sapporo

*Hydrazinolysis of Peptides and Proteins. II. Fundamental Studies on the Determination of the Carboxyl-ends of Proteins**

By Shiro AKABORI, Ko OHNO, Tokuji IKENAKA, Yoshimi OKADA, Hidesaburo HANAFUSA, Ichiro HARUNA, Akira TSUGITA, Kin-ichi SUGAE and Taijiro MATSUSHIMA

(Received January 17, 1956)

Since it was first proposed by Akabori, Ohno and Narita in 1952[1] the hydrazinolysis method has been applied by the same authors and others for the characterization of carboxyl-terminal amino acids in various proteins. On heating the protein in anhydrous hydrazine, peptide bonds are split with the formation of amino acid hydrazides, while the C-terminal residues only are liberated as free amino acids. In earlier works[1,2] hydrazides were removed by condensing with benzaldehyde to give insoluble dibenzal derivatives and the remaining amino acids were identified by paper chromatography. Although it has been applied to several proteins and peptides[1-6], this procedure was rather troublesome, and some less soluble amino acids might be lost in the treatment. Later we have improved the method in the following way: dinitrophenylating the hydrazinolysates and separating the C-terminal DNP-amino acids from di-DNP-amino acid hydrazides, the former thus extracted were characterized and estimated quantitatively by silica gel chromatography[7,8]. Further a method of pre-treatment with isovaleraldehyde followed by dinitrophenylation was also reported briefly[7]. These improved methods were applied to lysozyme[7,8], Taka-amylase A[7], ovalbumin[7], α-chymotrypsinogen[9], α-chymotrypsin[9], tobacco mosaic virus[10,11], and protease hydrolysates of lysozyme[12]. Another application of this method to characterize the mode of linkage of acidic amino acids in the protein was also reported[13].

Another technique to separate C-terminal amino acids from hydrazides using ion-exchangers was also proposed[14].

On the other hand, criticism on the hydrazinolysis method (chiefly on the hydrazinolysis-benzaldehyde method) was proposed in which it was said that the results obtained

* The present paper was written before the Symposium on Protein Structure held on November 15, 1954 at Osaka University.

1) S. Akabori, K. Ohno and K. Narita, This Bulletin, 25, 214 (1952).

2) S. Akabori and K. Ohno, II^{e} Congres Internationale de Biochimie, Paris, 1952, Resume des communications, p. 47.

3) K. Schlögl and E. Wawersich, *Naturwiss.*, 41, 38 (1954).

4) R.H. Locker, *Biochim. Biophys. Acta*, 14, 533 (1954).

5) K. Satake, K. Kusama and H. Ozawa, Symposium on Protein Structure, Osaka, 1954.

5a) N. Ohta and M. Yamasaki, Symposium on Protein Structure, Osaka, 1954.

6) K. Narita, *J. Chem. Soc. Japan*, 75, 487 (1954).

7) S. Akabori, K. Ohno, T. Ikenaka, A. Nagata and I. Haruna, *Proc. Japan Acad.*, 29, 561 (1953).

8) K. Ohno, *J. Biochem.*, 40, 621 (1953).

9) N. Sakota, S. Kubo, Y. Okada and S. Akabori, *Symposia on Enzyme Chemistry*, 10, 155 (1954).

10) G. Braunitzer, *Z. Naturforsch.*, 9b, 675 (1954).

11) C.I. Niu and H. Fraenkel-Conrat, *Biochim. Biophys. Acta*, 16, 597 (1955).

12) K. Okunuki, B. Hagihara and H. Matsubara, Symposium on Protein Structure, Osaka, 1954.

13) K. Ohno, *J. Biochem.*, 41, 345 (1954).

14) A.J. Ultee, Personal communication.

by this procedure were not in line with those obtained by carboxypeptidase method[15,16] and that the hydrazine is not an entirely satisfactory reagent for this purpose[16].

The present investigation was designed to reinspect this method according to the results obtained by various fundamental experiments, to establish the best method applicable to various proteins, and to consider the scope of it. Experiments reported in this paper include those on (a) the decomposition of free amino acids, (b) the hydrolysis of amino acid hydrazides to amino acids during the treatment, (c) the separation procedure of amino acids from hydrazides, and (d) the rate of hydrazinolysis of peptide bonds. From the results obtained here it can be concluded that the hydrazinolysis-DNP method gives mostly correct results with the exception of the case where tyrosine, cystine, histidine and tryptophan are situated at the C-terminal. These amino acids can be characterized by adopting the modified method described below.

Materials

Anhydrous hydrazine.—Anhydrous hydrazine was prepared by the method of Stähler[17]. Fifty grams of 80 per cent hydrazine hydrate and 175 g. of calcium oxide were mixed in a copper flask and gently heated in an oil bath. The distillate was led through a glass tube and a cooler and collected into a flask, which was attached by a calcium chloride tube. All cork fittings were covered with tin foil. After a few ml. of forerun were discarded, the main distillate was run at a bath-temperature range of 130–160°C. This was immediately kept in sealed tubes, each containing a 1 ml. portion. Yield 15–18 g. Purity was more than 99 per cent.

Amino acid hydrazides.—Leucine hydrazide dihydrochloride is the same one as reported previously[1]. Glycine-, alanine- and serine-hydrazides were prepared as follows: amino acids were esterified as usual, and hydrochlorides of amino acid esters were treated with computed amounts of dry chloroform saturated with dry ammonia. After filteration, the solution was concentrated under diminished pressure to give a syrup. The computed amount of anhydrous hydrazine was added to the syrup under cooling, and after standing overnight at room temperature, the reaction mixture was concentrated in vacuo. In all the treatments care was taken to avoid moisture. Thus glycine- and serine-hydrazides were obtained as crystals, but alanine hydrazide was crystallized as hydrochloride by adding dry alcohol saturated with HCl gas to the syrup of hydrazide until the pH of the solution reached to pH 6 and was concentrated in vacuo. The former two hydrazides were recrystallized three to five times from ethanol-ether, and the latter hydrazide hydrochloride from hot methanol.

Glycine hydrazide. m.p. 84–85°C (Found: N, 47.16. Calcd: 46.91%)

Serine hydrazide. m.p. 99–100°C (Found: N, 35.28. Calcd: 35.25%)

Alanine hydrazide dihydrochloride. m.p. 222–223°C (Found: N, 23.84. Calcd.: 23.87%)

Experiments and Results

(1) Decomposition of Amino Acids during Hydrazinolysis

It has been observed that C-terminal amino acids liberated during hydrazinolysis are partly decomposed. Locker[4] reported that common amino acids were recoverable in amounts exceeding 85 per cent with the exception of glutamic and aspartic acids, tryptaphan, arginine, cystine, cysteine and asparagine after heating them for eight hours at 100°C in a sealed tube. We have, therefore, estimated recoveries of about fifteen amino acids during hydrazinolysis, and we have studied briefly the decomposition products.

(a) Recoveries.—About 1 mg. of each amino acid was heated at 100°C with 0.5 ml. anhydrous hydrazine for five and ten hours. After excess hydrazine was evaporated in vacuo over sulphuric acid, the residue was dinitrophenylated, extracted, chromatographed and the recoveries of DNP-amino acids were estimated in the same way as in the case of proteins[7]. The procedure is similar to that shown in Table VIc. On the other hand, free amino acids were treated, without heating with hydrazine, in the same way to find control values of this procedure. The control values were mostly found to be more than 85 per cent. The recoveries cited in Table I are corrected by these control values. Histidine is dinitrophenylated not quantitatively—to an extent of only 30 per cent of theory—and was estimated, therefore, as the free amino acid by column chromatography using Dowex-50. Cystine and proline were also not fully dinitrophenylated. As DNP-derivatives of tyrosine and tryptophan are extracted by sodium bicarbonate solution not completely from ethyl acetate solution but completely from ether solution.

Table I indicates that the recoveries of amino acids during the hydrazinolysis of ten hours range from 90 per cent (leucine) to 27 per cent (cystine) and most of them are 50 to 70 per cent. Arginine decomposes completely in ten hours' hydrazinolysis, but is recoverable as ornithine. Contrary to the report of Locker[4], methionine does not change to sulfoxide, but remains about 80 per cent unchanged in ten hours. The reason of discrepancies between the results of Locker and ours is not clear. Some experiments were done in a dark room, but the effect of light was not remarkable.

It is not known whether C-terminal amino acid residues in protein decompose or not in the same way as free amino acids in the course of hydrazi-

15) A.C. Chibnall, "Les protéines", (1953) p. 126.
16) A. C. Chibnall and J.L. Bailey, "CIBA Symposium" (1952) p. 148, 149.
17) A. Stähler, *Ber.*, **42**, 3018 (1909).

TABLE I
RECOVERY OF AMINO ACIDS

Amino acid	Blank	After heating with anhydrous hydrazine for 5 hr.	10 hr.	Locker[4]
Glycine	87%	85%	52, 53**%	85
Alanine	84	81	48, 55**	85
Valine	100*		85**	85
Leucine	100*		90	85
Serine	86	75	57	85
Proline	71		65	
Tyrosine	100	92	74	85
Tryptophan	94**	57**	47**	40
Histidine	89	73	62	85
Arginine	83	36	0	0
(Ornithine)	85*	39	45	
Aspartic acid	85*		50**	20
Glutamic acid	85*		46**	40
Cystine	60	38	27	—
Methionine	91		80	sulphoxide

* Assumed values.
** Treated under shutting from direct light.

nolysis, but, being recovered 80 to 90 per cent of theory in the case of protein[7,13], C-terminal amino acid seems to be recoverable not less than free amino acids (Table I) as discussed later.

(b) Decomposition Product.—It is not yet known how amino acids decompose by the treatment with hydrazine. They did not change to hydrazides principally. Decomposition products gave no DNP-compounds which might be apprehensive for confusion with DNP-amino acids with the exception of cystine. Cystine changes partially to three sorts of by-products, two of which, on dinitrophenylating, changes to DNP-compounds which have nearly the same R values of DNP-glycine and -alanine, respectively, but on treating with isovaleraldehyde before dinitrophenylation, these compounds disappear almost completely.

In the case of arginine, a trace of DNP-compounds other than DNP-ornithine was detectable on silica gel columns, but on dissolving in acetic acid the yellow colour disappeared.

The degree of decomposition of amino acids in hot hydrazine seems to depend on the purity of anhydrous hydrazine. Anhydrous hydrazine of lower concentration (about 95 per cent) might cause more decomposition and undersirable by-products as reported previously[8].

(2) Hydrolysis of Hydrazides

Amino acid hydrazides which are produced in the course of hydrazinolysis might partially change to other substances by side-reactions. If free amino acids were produced during hydrazinolysis and/or after-treatment, they might be mistaken for C-terminals. Therefore the degrees of hydrolysis of hydrazides in aqueous solution and in hot hydrazine were determined.

(a) Estimation Method of Hydrolysis.—(i) Estimation as DNP-derivatives of Amino Acids produced by Hydrolysis.—The mixture of amino acid hydrazides and free amino acids, the latter resulting from the former by treating with hydrazine, were together dinitrophenylated, and DNP-amino acids were extracted fractionally by the same procedure as in the case of C-terminal, chromatographed on silica gel and estimated colorimetrically.

(ii) Estimation of Hydrazine liberated by Hydrolysis.—Preliminary experiments indicated that the hydrazine reacted with piperonal quantitatively to give a condensation product and that the product in acidic solutions showed a specific absorption curve which is distinctly different from those of amino acid hydrazides with the aldehyde in the range of the wave lengths of 365–380 mμ as shown in Fig. 1. The optical density

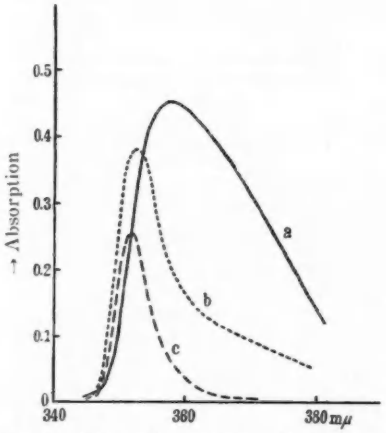

Fig. 1. Absorption spectra of condensation products of piperonal with hydrazine and amino acid hydrazides.
(a) Condensation product of piperonal with hydrazine (0.08 μM).
(b) Condensation product of piperonal with leucine hydrazide (4.36 μM).
(c) Condensation product of piperonal with serine hydrazide (4.87 μM).

reached a constant value within thirty minutes and was stable at least one to two hours. The colour intensity obeyed Beer's law. Basing on the results the following standard method to estimate microgram quantities of hydrazine was devised: to one ml. of sample solution containing about 5 to 10 μg. of hydrazine 2 ml. of propanol containing 34 mg. piperonal and 1 ml. of glacial acetic acid were added. After standing one hour at room temperature, the reaction mixture was subjected to colorimetric estimation by Beckman's spectrophotometer at the wave lengths of 363–375 mμ.

(b) Hydrolysis of Hydrazides in Aqueous Solution.—Serine hydrazide was kept at room temperature for various times in aqueous solution, in dilute acetic acid (pH 4) and in 1% sodium bicarbonate solution. The degrees of hydrolysis under these conditions were estimated by the method **(ii)**. As shown in Fig. 2 serine hydrazide

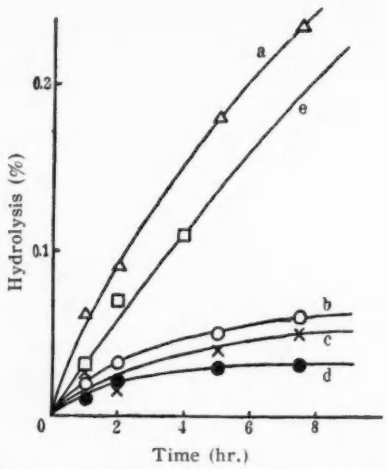

Fig. 2. Hydrolysis of amino acid hydrazides in aqueous solutions at room temperature

(a) Serine hydrazide in 1% sodium bicarbonate solution.

(b) Serine hydrazide in 66% alcoholic solution of sodium bicarbonate (medium for dinitrophenylation).

(c) Serine hydrazide in water.

(d) Serine hydrazide in dilute acetic acid (pH 4).

(e) Leucine hydrazide in 1% sodium bicarbonate solution.

is hydrolysed 0.05% in 7.5 hours in aqueous solution, 0.03% in acetic acid solution of pH 4, and 0.25% in 1% sodium bicarbonate solution. Further results obtained by the method (i) with glycine-, alanine- and leucine-hydrazides (Table II) indicate that the extent of hydrolysis of these hydrazides in neutral solution is less than 0.1 per cent in eighteen hours at room temperature.

From these results it is concluded that the amino acid hydrazides are stable in neutral and slight acidic media but somewhat unstable in alkaline medium. Therefore, one must avoid standing the hydrazides in solutions, especially in alkaline, for a long time. Consequently, it might be better to avoid treating the hydrazinolysates with strong basic and acidic ion-exchange resins.

The extent of hydrolysis of hydrazides by dinitrophenylation are shown in Table II, that is, 0.1 to 0.5 per cent of hydrazides are hydrolysed by the dinitrophenylation for two hours. The longer the time of dinitrophenylation, the greater the extent of hydrolysis.

To examine the hydrolysis during the extraction of C-terminal amino acids according to the above-mentioned procedure ethyl acetate solution of di-DNP-serine hydrazide was shaken with 2% sodium bicarbonate solution for three and five hours and the extent of hydrolysis of the DNP-hydrazide was estimated, the results of which are shown in Table II.

From these results, it can be concluded that the hydrazinolysates must be given a preliminary treatment with aldehyde to remove the bulk of the hydrazides, and all the treatment must be carried out as rapidly as possible.

(c) Hydrolysis of Hydrazides during Hydrazinolysis.—Amino acid hydrazides, such as serine-, glycine-, alanine- and leucine-hydrazides were heated with anhydrous hydrazine in the same conditions as in the case of proteins, and free amino acids liberated by this treatment were estimated. The results shown in Table II indicate that serine-, glycine-, alanine- and leucine-hydrazides are hydrolysed by 1.2, 1.7, 0.4 and 0.5 per cent, respectively, which are considerably higher than in aqueous solutions. Of course, these data do not indicate directly the percentage of free amino acids of non-C-terminal liberated during hydrazinolyses of proteins, as discussed later, and it might be preferable to compare results of hydrazinolysis of various reaction time, when C-terminal amino acids of proteins are intended to be characterized.

(3) Hydrazinolyses of Peptides

It is desirable to know the rates of hydrazinolysis of various peptides and to have some informations about the extent of hydrolysis of non-C-terminal peptide bonds during the hydrazinolysis. Experiments have been carried out on three peptides, L-leucyl-L-alanine, glycyl-L-alanine and glycyl-L-leucine. The results are cited in Table III, in which it is remarkable that as much as 30 percent of leucyl-alanine remains intact by hydrazinolysis for ten hours.

TABLE II

HYDROLYSIS OF AMINO ACID HYDRAZIDES IN VARIOUS CONDITIONS

	Serine hydrazide	Glycine hydrazide	Alanine hydrazide	Leucine hydrazide
Dinitrophenylation in 2 hr.	0.1%	0.5%	0.1%	0.2%
Dinitrophenylation in 7 hr.	0.7			
Shaking for 3 hr.*	0.15			
Shaking for 5 hr.*	0.3			
Heating with N_2H_4 for 5 hr.	0.5	0.7	0.2	0.2
Heating with N_2H_4 for 10 hr.	1.1	1.2	0.3	0.3
Standing in solution (pH 7.2) for 18 hr. at room temp.	0.06	0.02	0.04	0.08

* Hydrazides were dissolved in ethyl acetate and shaken with 2% sodium bicarbonate solution (to test the hydrolysis in extractive process).

TABLE III

HYDRAZINOLYSIS OF PEPTIDES

Peptide	Time of hydrazinolysis	Residual peptide	C-terminal liberated	Free amino acid non-C-terminal
L-Leucyl-L-alanine	5 hr.	60%	33%	
	10	30	45	
Glycyl-L-alanine	10	0	60	
Glycyl-L-leucine	3	10	83	
	5	Trace	87	Trace
	10	0	90	Trace

(4) Separation between Amino Acids and their Hydrazides

(a) Treatment with Aldehydes.—From the data cited in Table III, it is preferable to treat hydrazinolysates with aldehyde prior to the dinitrophenylation in order to remove the bulk of the hydrazides. We in our earlier works[1,2] and other investigators[3,4] used benzaldehyde, but it must be used as a freshly distilled preparation because it is apt to produce peroxide, which might oxidize hydrazides to form free amino acids. Thus we used piperonal and isovaleraldehyde in place of benzaldehyde. As the former did not give very good results, the latter was employed throughout this investigation. The procedure, which is nearly the same as reported before[7], is shown in Table VIa. Care was taken to avoid the hydrolysis of hydrazides by treating in shorter time under mild conditions.

(b) Fractional Extraction of C-terminal Amino Acids as DNP-derivatives.—The solution obtained by the above treatment contains C-terminal amino acids and residual hydrazides which could not be removed. After dinitrophenylation, the C-terminal DNP-amino acids must be separated from di-DNP-amino acid hydrazides. To separate the DNP-amino acids we have used the procedure cited in Table VIa, in which ethyl acetate was employed as organic solvent. Although nearly all sorts of DNP-amino acids were extracted quantitatively by dilute sodium bicarbonate solution from ethyl acetate solution while di-DNP-hydrazides remained in the latter, all of the di-DNP-tyrosine, and a part of the di-DNP-histidine and DNP-tryptophan were found to remain in the organic phase. Accordingly, if these amino acids are situated at C-terminal, they are fully or partly lost and cannot be characterized as DNP-derivatives.

This is the reason why contrary to the result by carboxypeptidase method, tyrosine has not been found as C-terminal of chymotrypsin by our earlier method.

To take measures on this problem, ethyl acetate was replaced by ethyl ether or isopropyl ether, or using ethyl acetate as organic solvent a special treatment for the three amino acids was established. These procedures are shown in Table VIb.

Of these procedures the ethyl acetate method gives the most clear-cut separation between DNP-amino acids and di-DNP-hydrazides. By the other methods, di-DNP-hydrazides contaminate the C-terminal fraction, so that it is necessary to treat hydrazinolysate with aldehyde prior to the dinitrophenylation. Applying these methods to lysozyme hydrazinolysates plus tyrosine, results shown in Table IV were obtained, i.e. about 90 per cent of leucine (C-terminal of lysozyme) and tyrosine added were recovered.

TABLE IV

RESULTS OBTAINED BY STANDARD METHODS WITH LYSOZYME PLUS TYROSINE

Sample	Method	Results
Lysozyme* tyrosine**	I	Leucine, 88%; tyrosine 90%
Lysozyme* tyrosine**	II (ether)	Leucine, 94%; tyrosine 88%
Lysozyme* tyrosine**	II (isopropyl ether)	Leucine, 90%; tyrosine 86%
Lysozyme*	III	Leucine, 90%

* Lysozyme was hydrazinolysed for ten hours at 100°C.
** Tyrosine was added to the hydrazinolysate of lysozyme.

Being not dinitrophenylated quantitatively histidine might be better estimated by other methods, such as ion-exchanger chromatography etc., after treating the hydrazinolysates with aldehyde.

(5) Characterization of Aspartyl and Glutamyl Residues in Chain and C-terminal Asparagine and Glutamine

Contrary to the case of determination of N-terminal by DNP method, in which lysine residue in chain is also detected as DNP-derivative, by the hydrazinolysis method aspartic and glutamic acid residues bearing free carboxyl group in the chain and C-terminal asparagine and glutamine are extracted into acidic fraction together with other C-terminals. The possible products throughout this method are shown in Table V.

TABLE V

POSSIBLE PRODUCTS OF HYDRAZINOLYSIS AND DINITROPHENYLATION DERIVED FROM ASPARTIC AND GLUTAMIC RESIDUES

Dicarboxylic acid residue	Products of hydrazinolysis	Corresponding DNP-derivatives
—NH—CH—COOH | $(CH_2)_n$ | COOH (Ia)	NH_2—CH—COOH | $(CH_2)_n$ | COOH (Ib)	DNP—NH—CH—COOH | $(CH_2)_n$ | COOH (Ic)
—NH—CH—CO | $(CH_2)_n$ | COOH (IIa)	NH_2—CH—$CONHNH_2$ | $(CH_2)_n$ | COOH (IIb)	DNP—NH—CH—CONHNH—DNP | $(CH_2)_n$ | COOH (IIc)
—NH—CH—COOH | $(CH_2)_n$ | CO—NH— (IIIa)	NH_2—CH—COOH | $(CH_2)_n$ | $CONHNH_2$ (IIIb)	DNP—NH—CH—COOH | $(CH_2)_n$ | CONHNH—DNP (IIIc)
—NH—CH—CO | $(CH_2)_n$ | $CONH_2$ (IVa)	NH_2—CH—$CONHNH_2$ | $(CH_2)_n$ | $CONHNH_2$ (IVb)	DNP—NH—CH—CONHNH—DNP | $(CH_2)_n$ | CONHNH—DNP (IVc)

By the treatment with isovaleraldehyde followed by dinitrophenylation, other derivative such as (V) and/or (VI) might be formed from dicarboxylic acids bearing one free carboxyl group.

DNP—NH—CH—CONHN=CH—CH_2—CH(CH_3)(CH_3)
\|
$(CH_2)_n$
\|
COOH
(V)

DNP—NH—CH—$CONHNH_2$
\|
$(CH_2)_n$
\|
COOH
(VI)

In the fractional extractions by the procedure of Table VIa, (I) and (IV) are distributed as sharply as other DNP-amino acids and di-DNP-hydrazides, respectively, and (II) and (III) are distributed less sharply but finaly all extracted to alkaline solution from ethyl acetate, but (V) and (VI) behave somewhat irregularly and are distributed to all the fractions by the procedure. These facts seem to disturb the characterization of C-terminal amino acids of proteins, although no appreciable difficulties were experienced in the case of the proteins which we have investigated. For the quantitative estimation of C-terminal amino acids, however, it is convenient to estimate DNP-aspartic and/or DNP-glutamic acids, if they exist, and then to estimate other DNP-amino acids after hydrolysing the C-terminal fraction with 6 N hydrochloric acid at 100°C for several hours, whereby (II), (III) or (V), (VI) are hydrolysed to DNP-aspartic and glutamic acids. Thus a clear-cut estimation of all the C-terminal amino acids and aspartyl and glutamyl residues in chain are attained.

In spite of the complexity of these dicarboxylic acid derivatives, we can make use of the fact described above, to characterize the mode of linkage of these acidic amino acids in peptide chain and also to determine the C-terminal glutamine and asparagine. This advantage can not be achieved by the original benzaldehyde method. Thus lysozyme was proved to have one aspartyl, 12 asparaginyl and 4 glutaminyl residues in the molecule[13]. The characterization of a free carboxyl group in peptide chain have been reported by Jollès and Fromageot[18] and the characterization of the amide group was reported by Chibnall and Rees[19].

Preliminary experiments to distinguish four types of derivatives of dicarboxylic acids were done as described hereinafter.

Di-DNP-aspartic acid-α-hydrazide was prepared as follows: Hydantoin acetic acid was hydrazinolysed for ten hours at 100°C, whereby it converted partly to aspartic acid-α-hydrazide, which was purified as di-DNP-derivative through silica gel chromatography. Di-DNP-glutamic acid-α-hydrazide was prepared in the same manner from hydantoin propionic acid, which was identical with that obtained by the hydrazinolysis of poly-α-glutamic acid*. The syntheses through hydantoin

18) T. Jollès and C. Fromageot, *Biochim. Biophys. Acta*, 9, 287, 416 (1952).

19) A.C. Chibnall and M.W. Rees, *Biochem. J.*, 48, xlvii 1951); ibid., 52, iii (1952).

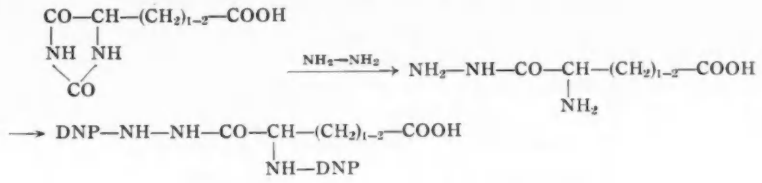

derivatives were rather poor in yields and many other by-products were also detected as DNP-derivatives. Di-DNP-glutamic acid-γ-hydrazide was obtained by dinitrophenylating the hydrazide*.

These four DNP-derivatives can be detected together with other DNP-amino acids, on suitable silica gel columns. Fig. 3 is an example indicating that all the DNP-derivatives can be separated distinctly. Moreover, di-DNP-aspartic and glutamic acid monohydrazides can be distinguished easily from DNP-amino acids as they develop brown red colour on dissolving in dilute bicarbonate solution.

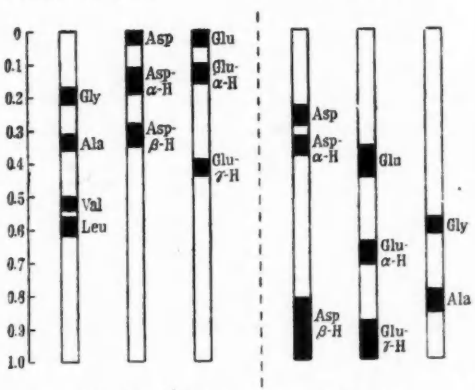

Fig. 3. Chromatograms of DNP-derivatives of aspartic and glutamic acid monohydrazides and DNP-amino acids on silica gel chromatograms.
Solvent: 3B-C-2A: n-BuOH: $CHCl_3$: 2% acetic acid=3: 97: 100
10B-C-2A: n-BuOH: $CHCl_3$: 2% acetic acid=10: 90: 100

Standard Methods

Considering the results mentioned above, three standard methods shown in Table VIa, VIb and VIc are established to characterize C-terminal amino acids and aspartyl and glutamyl residues in chain. In most cases all methods are available to give correct results, but differ in some points described below, so that the suitable method(s) may be chosen for the protein investigated.

The methods described here were applied succesfully to the proteins, but the volumes or weights of reagents described in Table VI may be modified according to the proteins investigated. As the C-terminal fraction is contaminated with DNP-derivatives of acidic amino acid monohydrazides and some C-terminal peptides, each component separated on chromatograms is better to be identified after hydrolysis with hydrochloric acid. Hydrazinolysis must be done twice or more varying the time of hydrazinolysis to estimate the amount of C-terminals, where the time of hydrazinolysis must not be longer than fifteen hours, as non-C-terminal amino acids appear and C-terminal amino acids decompose considerably for the longer hydrazinolysis.

By the three methods described below almost all amino acids can be characterized almost entirely quantitatively, but care must be taken when tyrosine, tryptophan, arginine, histidine, cystine, glutamine and asparagine are at the C-ends, among which histidine, cystine and amides may be characterized less quantitatively. The mode of linkage of acidic amino acids in peptide chain may be characterized, too, but less quantitatively.

Standard Method I.—This is a slightly modified method reported previously[7] and may be applied for general protein except the case where histidine and tryptophan are at C-ends and when one desires to seek terminal glutamine and asparagine or glutamyl and aspartyl residues in chain. If tyrosine is situated at C-terminal, the ethyl acetate fraction asterisked of Table VIa must be treated further, where all DNP-tyrosine and a part of DNP-histidine and DNP-tryptophan which are not included in the C-terminal fraction are detected.

Standard Method II.—While method I gives very clear-cut separation of DNP-amino acids from di-DNP-amino acid hydrazides, method II, in which ethyl ether or isopropyl ether is used in place of ethyl acetate, has more advantages than the method I in the case where tyrosine, histidine and tryptophan are at C-terminals. However, separation of DNP-amino acids from di-DNP-hydrazides is rather dull, so that the pretreatment of the hydrazinolysates with isovaleraldehyde is necessary.

Standard Method III.—This method which is nearly the same as reported previously[7,8] is established for the purpose of determining C-terminal glutamine and asparagine or glutamyl or aspartyl residues in chain. Of course other C-terminal amino acids can be characterized as in the case of method I, but small amounts of non-C-terminal amino acids would also be detected, though they would be almost negligible. Ethyl-

* Poly-α-glutamic acid was available through the kindness of Mr. H. Yuki, Laboratory of Fibre Research of this University, to whom the authors' thanks are due.
* Glutamic acid-γ and α-hydrazides and aspartic acid-β-hydrazide were also supplied by Mr. K. Narita, to whom we are grateful.

TABLE VIa

STANDARD METHOD I

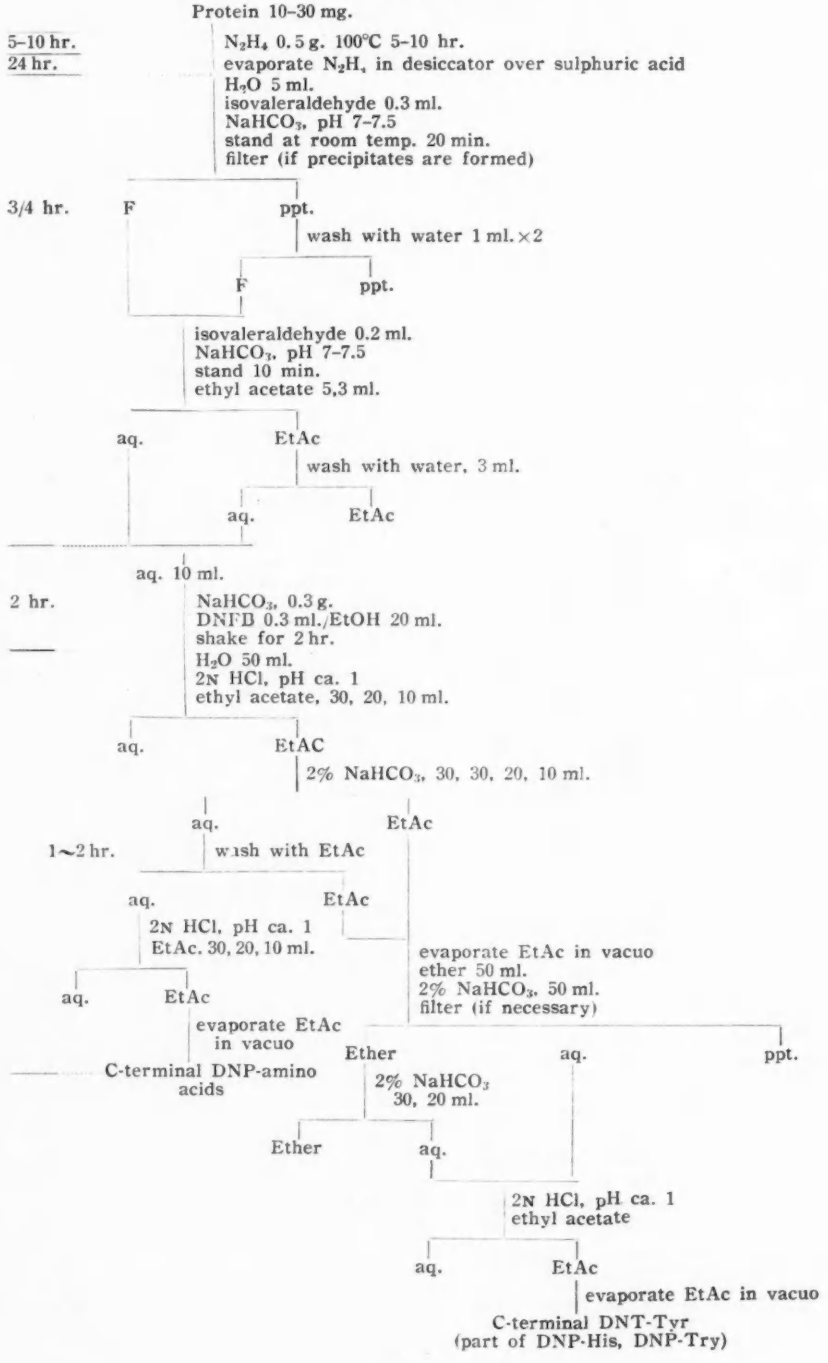

TABLE VIb

STANDARD METHOD II

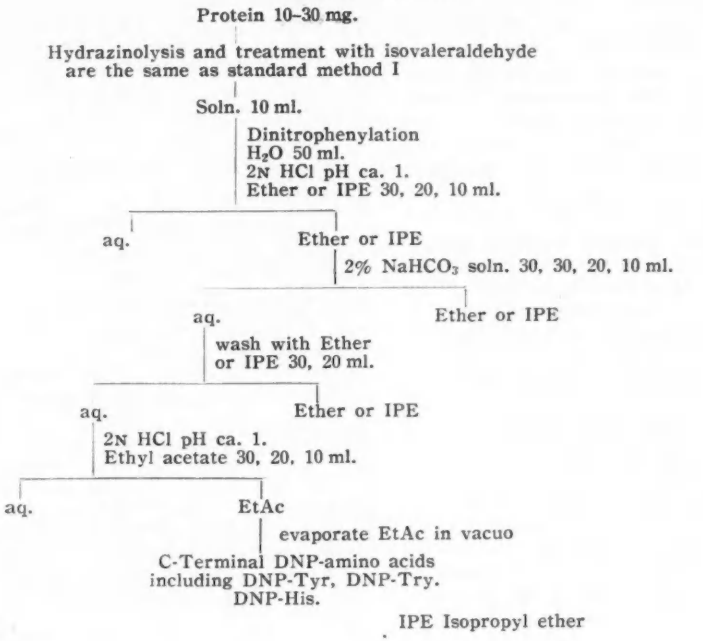
Protein 10–30 mg.
Hydrazinolysis and treatment with isovaleraldehyde are the same as standard method I
Soln. 10 ml.
Dinitrophenylation
H_2O 50 ml.
2N HCl pH ca. 1.
Ether or IPE 30, 20, 10 ml.
aq.
Ether or IPE
2% $NaHCO_3$ soln. 30, 30, 20, 10 ml.
aq.
Ether or IPE
wash with Ether or IPE 30, 20 ml.
aq.
Ether or IPE
2N HCl pH ca. 1.
Ethyl acetate 30, 20, 10 ml.
aq.
EtAc
evaporate EtAc in vacuo
C-Terminal DNP-amino acids including DNP-Tyr, DNP-Try. DNP-His.
IPE Isopropyl ether

TABLE VIc

STANDARD METHOD III

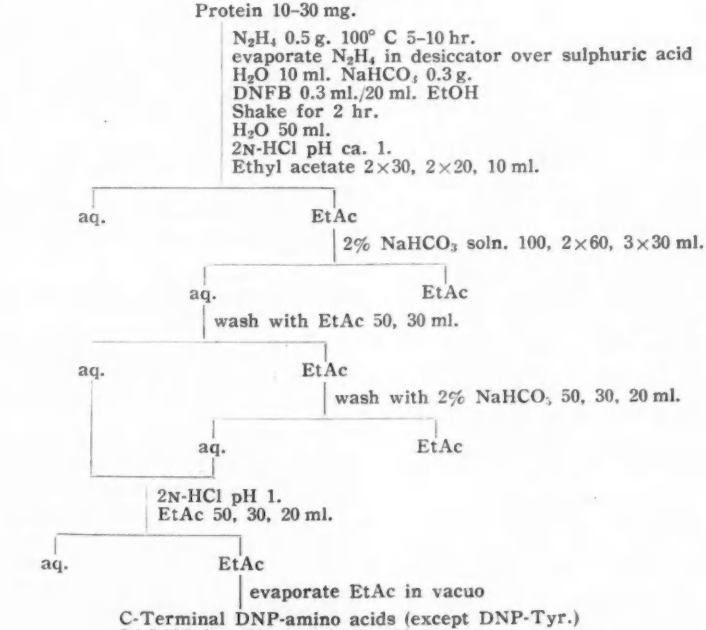

acetate cannot be replaced by ethyl ether or isopropyl ether in this case.

Discussion

As a matter of course, various data obtained by the present fundamental experiments cannot be applicable directly in the case of proteins; for example, it was really confirmed that about one per cent of amino acids were liberated during the ten hours' "hydrazinolysis" of amino acid hydrazides, but in the case of proteins, it takes several hours to produce amino acid hydrazides which, in turn, were subjected to hydrolysis partially, thus the percentages obtained in fundamental experiments indicate only the maximum values. About the decomposition of amino acids during the "hydrazinolysis", too, it is uncertain whether the amino acids bound at the C-end decompose similarly to the results cited in Table II. Therefore, we shall discuss below how to interpret the results obtained in the hydrazinolysis of real proteins.

First of all, let us consider all possible reactions involved in the hydrazinolysis. These may be expressed by the following scheme. The principal reaction is, of course,

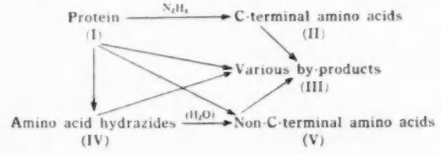

the splitting of the peptide bonds with formation of amino acid hydrazides (I → IV) and the liberation of C-terminal residues as free amino acids (I → II). Yet the hydrazides thus formed liberate, though very slightly, free amino acids (IV → V), and free amino acids are also partly decomposed to unknown by-products (II → III, V → III). Being not yet comfirmed directly, following other side reactions might be possible: splitting of peptide bond under formation of free amino acids (I → V); decomposition of amino acid residues in peptide and at C-terminal before their liberation by hydrazinolysis (I → III); and decomposition of amino acid hydrazides directly to some by-products (IV → III).

On applying the hydrazinolysis to a protein, participations of all side reactions depend on the sorts of C-terminal amino acids and compositions and sequences of amino acids in the protein, so that it cannot be decided summarily which is predominant among these reactions. However, we have estimated almost one mole of each C-terminal, but no appreciable other amino acids applying this method to two proteins (lysozyme, and Taka-amylase A). If we are allowed to generalize the results from these few examples, we might be able to consider that results really obtained on proteins are mainly due to the desired principal reaction, no matter how many side reactions are possible theoretically. It can be admitted, at least, to speak generally, that if more than 0.5 mol. of free amino acids are obtained by the hydrazinolysis of ten hours, they can be regarded as C-terminals, but if only less than 0.2 mol. of them are detected they may be artifact, and it needs further study if 0.2 to 0.5 mol. appears.

The supposition described above was justified also by some calculations from the fundamental data obtained. We shall calculate for example, the amount of non-C-terminal amino acid formed through the reactions $I \xrightarrow{k_1} IV \xrightarrow{k_2} V$.

Assuming that the each step of the reactions is the first order reaction and the step of V → III is negligible, the concentration of V at time t is given by equation (1).

$$[V]_t=[I]_0+\frac{[I]_0}{k_1-k_2}(k_2e^{-k_1t}-k_1e^{-k_2t}) \qquad (1)$$

where $[I]_0$ and $[V]_t$ are the concentration of I and V at time 0 and t respectively, k_1 and k_2 are the rate constants of each step.

If the conversion of I → IV is 90 per cent in eight hours' hydrazinolysis and IV → V is one per cent in ten hours, the amount of V at ten hours is calculated as only 0.67 per cent.

The similar calculation can be applied to the reactions $I \xrightarrow{k_3} II \xrightarrow{k_4} III$. Assuming that, here again, each step of the reactions is the first order, the concentration of II at time t is

$$[II]_t=\frac{k_3[I]_0}{k_3-k_4}(e^{-k_4t}-e^{-k_3t}) \qquad (2)$$

where $[I]_0$ is the initial concentration of I and $[II]_t$ is the concentrations of II at time t, k_3 and k_4 are the rate constants of each step.

If the conversion I → II is 90 per cent in ten hours and II → III is 10 per cent in ten hours the following result is obtained.

Time (hr.)	2	5	10	14
Mol. of II from 1 mol. of I	0.37	0.74	0.84	0.87 (max.)

This value is rather coincident with the observed value in the case of liberation of leucine from lysozyme[7].

Further if the conversion of I → II is 90 per cent in twenty hours and II → III is 45 per cent in ten hours (decomposition of alanine, Table I), the calculated value of II is as follows:

Time (hr.)	5	10	12
Mol. of II from 1 mol. of I	0.37	0.49	0.50 (max.)
Mol. of alanine from 1 mol. of leucyl-alanine (observed)	0.33	0.45	

Since these calculations involve some assumption and simplification of complex reactions, one must avoid attaching too much importance to the result derived from these calculations. However, it is obvious from these considerations that liberation of C-terminal is a function of time, which has one maximum value, so that it may be necessary to determine C-terminal at various time intervals.

On Taka-amylase A, we have other data not mentioned before. Even if the amylase solution in hydrazine was brought to dryness in vacuo at room temperature directly after the addition of hydrazine 0.3 mol. of serine and 0.1 mol. of glycine were detected as C-terminals. On the other hand, 8.955 mg. (47.7 μM.) of glycyl-L-leucine, the content of glycine of which is about the same as that of Taka-amylase[20], were added to 51.5 mg. (1.1 μM,) of Taka-amylase A followed by hydrazinolysis, whereby 0.068 mg. (0.9 μM.) and 0.082 mg. (1.1 μM.) of glycine were found, respectively, by the hydrazinolysis of five and ten hours. These results indicate that only 0.4 per cent of glycyl residue was liberated as free amino acid from added glycyl-leucine in ten hours' hydrazinolysis. From these two facts it can be concluded that glycine and serine are really C-terminals of this protein. On another terminal, alanine, there might be some doubt because of its slow liberation by hydrazinolysis[7], but on considering that the rate of hydrazinolysis of L-leucyl-L-alanine is slow as in case of this protein (see Table IV), it is more probable that alanine is bound at a C-terminal by some hard-hydrazinolysable bond.

On the C-terminal of ovalbumin, Steinberg[21] reported the liberation of alanine by carboxypeptidase but later[22] found this due to a DFP-sensitive, contaminated enzyme. Locker[4] also reported that the protein was not attacked by DFP-treated carboxypeptidase. Turner and Schmerzler[23], however, have found alanine to be a C-terminal by the thiohydantoin method. Although some of us[7] also reported the presence of one alanine at the C-terminal, Dr. Fraenkel-Conrat[24] informed us recently that the C-terminal of this protein is valyl-seryl-proline. Thus we reinvestigated on the protein and found that we had taken proline for alanine. The DNP-derivative of the C-terminal amino acid was proved to be proline and not alanine by variety of chromatography and its absorption curve. The detail of this account shall be published later by one of the authors.

Although carboxypeptidase method has been applied successfully to many proteins, it has several distinct restrictions by nature. For example, it is not applicable to insoluble proteins such as wool keratin[14] and silk fibroin[7]; its action depends not only on the nature of the C-terminal but also on the adjacent amino acid residues; when a protein has more than two C-terminals, it is difficult to characterize it distinctly; and so on. The hydrazinolysis method has, at least, the advantages in these cases. The result on ovalbumin might be the best example of the success of the hydrazinolysis method, becauce proline situated at C-terminal is liberated neither by carboxypeptidase nor by the thiohydantoin method.

Summary

1. Fundamental experiments on the hydrazinolysis method, a method for characterization of C-terminal amino acids of proteins, were carried out.

2. Amino acids were found to decompose to various extents by heating with anhydrous hydrazine.

3. Amino acid hydrazides were hydrolysed about 1% or less by heating with anhydrous hydrazine (ca. 99%) for ten hours. Hydrolyses of them in neutral and slightly acidic solutions at room temperature are negligible, but in alkaline solution the extent of hydrolyses are somewhat greater though less than 0.2% in five hours in 1% bicarbonate solution.

4. Procedures for separating free amino acids from amino acid hydrazides as DNP-derivatives with or without treatment of iso-valeraldehyde prior to dinitrophenylation were reinvestigated thoroughly.

5. Some experiments on the hydrazinolyses of peptides were done.

6. Fundamental investigations of the characterization of the mode of linkage

20) S. Akabori, T. Ikenaka, H. Hanafusa and Y. Okada, *J. Biochem.*, **41**, 803 (1954).
21) D. Steinberg, *J. Am. Chem. Soc.*, **74**, 4217 (1952).
22) D. Steinberg, *J. Am. Chem. Soc.*, **75**, 4875 (1953).
23) R.A. Turner and G. Schmerzler, *Biochim. Biophys. Acta*, **11**, 586 (1953).
24) H. Fraenkel-Conrat, Personal communication. The authors are grateful to him for his information prior to his publication. *J. Am. Chem. Soc.*, **77**, 5882 (1955).

of monoaminodicarboxylic acids in peptide chains by the hydrazinolysis method indicate its availability.

7. Standard methods for quantitative estimation of C-terminal amino acids or proteins are established based upon the results obtained by the present investigation.

8. Brief consideration on the mechanism of the hydrazinolysis was described and the scope of this method was discussed in connection with that of the carboxypeptidase method.

Laboratory of Biochemistry, Faculty of Science, Osaka University. Osaka

---

Dielectric Polarization of Some Aliphatic Amines in the Liquid State

By Michio SHIRAI

(Received February 14, 1956)

Introduction

The relation between the dielectric constant of a liquid and the properties of its individual molecule is a complicated problem. Debye[1] derived the well-known formula,

$$\frac{M}{d}\frac{\varepsilon-1}{\varepsilon+2}=\frac{4\pi N}{3}\left(\alpha+\frac{\mu^2}{3kT}\right),$$

based on Mosotti's hypothesis, where M is the molecular weight, d the density, ε the dielectric constant, N Avogadro's number, α the polarizability, μ the dipole moment, k Boltzmann's constant, and T the absolute temperature. Debye's formula was found to be in agreement with the experimental results for gases and dilute solutions in non-polar solvents. In this formula the intermolecular interactions are neglected. But, when any effect of interactions between polar molecules exists, some modifications of this theory are required.

Onsager[2] worked out this problem by taking into account the so-called reaction field as well as the cavity field. The formula derived by him is as follows:

$$\frac{M}{d}\frac{(\varepsilon-n)^2(2\varepsilon+n^2)}{\varepsilon(n^2+2)^2}=\frac{4\pi N}{3}\frac{\mu^2}{3kT}$$

where n is the refractive index for optical region. Onsager's formula accounts for the dielectric constants of all substances except a few highly associated liquids, and can be used to calculate dipole moments from the dielectric constants of several polar liquids.

Previously, Estermann[3] found that in pure liquids of diethyl ether, diphenyl ether, and ethylamyl ether, the molecular polarization calculated from the dielectric constant of the pure liquid by means of Debye's formula was in good agreement with that measured with the dilute solution in non-polar solvent, in spite of the considerable polarity of its molecule. Recently, the author has found that the same rule also holds for some aliphatic amines.

Experimental

Method of Measurement.—The measurement of dielectric constant was carried out at a frequency of 2 Mc./sec. by means of resonance method, the details of which were described elsewhere[4]. The density was measured with a pycnometer.

Materials.—Diethylamine was purified from a commercial sample by drying over caustic soda and distillation. b. p. 55.5°C.

Triethylamine was purified from a commercial sample by the method given for diethylamine. b. p. 88.8°C.

i-Propylamine was purified from a commercial sample by distillation. b. p. 33.0–33.5°C.

n-Heptane was purified from a commercial sample by shaking with sulfuric acid, washing with water, drying over metallic sodium, and fractional distillation. b. p. 97.5°C.

Cyclohexane was purified from a commercial sample by the method given for *n*-heptane. b. p. 81.0°C.

Results and Discussion

Dipole Moment.—The mole fraction of the solute x, the dielectric constant ε, and the density d are indicated in Table I, together with the molecular polarization P_2, calculated from them. The molecular polarization was calculated by the following formula;

1) P. Debye, "Polare Molekeln", S. Hirzel Press, Leipzig (1929), p. 33.
2) L. Onsager, *J. Am. Chem. Soc.*, 58, 1486 (1936).
3) I. Estermann, *Z. physik. Chem.* B 1, 134 (1928).
4) M. Yasumi and M. Shirai, This Bulletin, 28, 193 (1955).

$$P_2 = P_1 + \frac{P_{12} - P_1}{x}$$

where P_1, P_2, P_{12} are the molecular polarization of the solvent, solute, and solution, respectively.

The molecular polarization at infinite dilution $P_{2\infty}$ and the dipole moment μ calculated from it are also shown in Table I. The dipole moment is given by

$$\mu = 0.0128\sqrt{(P_2 - P_E - P_A)T} = 0.0128\sqrt{P_0 T}$$

where P_E, P_A, and P_0 are the electronic, atomic, and orientation polarization, respectively. $P_E + P_A$ for diethylamine and that for triethylamine were taken to be 25.7 cc. and 33.0 cc., respectively. These were determined by the temperature dependence of their molecular polarization in the gaseous state[5]. For *i*-propylamine, P_E was taken to be equal to the molar refraction for sodium D line, and P_A was assumed to be 5% of the electronic polarization.

The dipole moment of diethylamine and that of triethylamine measured in different solvents are nearly the same, but they are a little greater than those in the gaseous state. This fact is interpreted in terms of solvent effect[6].

TABLE I

DIELECTRIC CONSTANT, DENSITY, MOLECULAR POLARIZATION, AND DIPOLE MOMENT

Diethylamine ($P_E + P_A = 25.7$ cc.)

n-Heptane Solution (−25°C)

x	ε	d	P_2 (cc.)
0.00000	2.0167	0.7229	(58.0)
0.03235	2.0590	0.7233	58.0
0.05199	2.0855	0.7235	57.9
0.07101	2.1123	0.7238	58.2
0.09068	2.1399	0.7241	58.0

$P_{2\infty} = 58.0$ cc. $P_0 = 32.3$ cc. $\mu = 1.14$ D

(25°C)

0.00000	1.9529	0.6824	(50.0)
0.03235	1.9816	0.6826	49.9
0.05199	1.9997	0.6827	50.1
0.07101	2.0178	0.6828	50.3
0.09068	2.0361	0.6829	50.2

$P_{2\infty} = 50.0$ cc. $P_0 = 24.3$ cc. $\mu = 1.09$ D

Cyclohexane Solution (25°C)

0.00000	2.0309	0.7735	(50.6)
0.03079	2.0672	0.7710	50.6
0.05106	2.0905	0.7691	50.4
0.07069	2.1153	0.7675	50.6
0.09052	2.1391	0.7655	50.7

$P_{2\infty} = 50.6$ cc. $P_0 = 24.9$ cc. $\mu = 1.10$ D

i-Propylamine ($P_E + P_A = 20.6$ cc.)

n-Heptane Solution (−25°C)

x	ε	d	P_2 (cc.)
0.00000	2.0167	0.7229	(56.3)
0.03214	2.0624	0.7229	56.3
0.05110	2.0907	0.7229	56.5
0.07577	2.1292	0.7230	56.5
0.09341	2.1564	0.7220	56.4

$P_{2\infty} = 56.3$ cc. $P_0 = 35.7$ cc. $\mu = 1.20$ D

(25°C)

0.00000	1.9529	0.6824	(50.0)
0.03214	1.9863	0.6820	50.1
0.05110	2.0067	0.6818	50.0
0.07577	2.0337	0.6815	50.1
0.09341	2.0531	0.6813	49.8

$P_{2\infty} = 50.0$ cc. $P_0 = 29.4$ cc. $\mu = 1.20$ D

Triethylamine ($P_E + P_A = 33.0$ cc.)

n-Heptane Solution (−25°C)

x	ε	d	P_2 (cc.)
0.00000	2.0167	0.7229	(47.8)
0.03179	2.0344	0.7240	48.0
0.05113	2.0459	0.7247	48.3
0.07319	2.0584	0.7252	48.4
0.09115	2.0690	0.7258	48.4

$P_{2\infty} = 47.8$ cc. $P_0 = 14.8$ cc. $\mu = 0.78$ D

(25°C)

0.00000	1.9529	0.6824	(45.8)
0.03179	1.9665	0.6836	45.9
0.05113	1.9745	0.6840	46.0
0.07319	1.9852	0.6849	46.2
0.09115	1.9921	0.6853	46.0

$P_{2\infty} = 45.8$ cc. $P_0 = 12.8$ cc. $\mu = 0.79$ D

Cyclohexane Solution (25°C)

0.00000	2.0309	0.7735	(46.5)
0.03090	2.0473	0.7716	46.5
0.05119	2.0578	0.7700	46.6
0.07103	2.0676	0.7687	46.5
0.09195	2.0778	0.7672	46.4

$P_{2\infty} = 46.5$ cc. $P_0 = 13.5$ cc. $\mu = 0.81$ D

Dielectric Polarization in Pure Liquid State.—Dielectric constant and density measured at different temperatures are shown in Table II. The molecular polarization and the dipole moment calculated from them according to Debye's formula and Onsager's formula, respectively, are also listed there. The refractive index which is to be inserted into Onsager's formula should contain the atomic polarization, so that it was calculated by the following formula:

$$\frac{M}{d}\frac{n^2-1}{n^2-2} = P_E + P_A$$

assuming that Lorentz field is valid for the electronic and atomic polarization.

5) G.A. Barcley, R.J.W. Le Fèvre and B.M. Smyth, *Trans. Faraday Soc.*, **46**, 812 (1950).
6) K. Higashi, *Sci. Pap. I.P.C.R.*, **31**, 311 (1937).

TABLE II

DIELECTRIC CONSTANT, DENSITY, MOLECULAR POLARIZATION, AND DIPOLE MOMENT IN THE LIQUID STATE

Diethylamine ($P_E+P_A=25.7$ cc.)

Temp. (°C)	ε	d	Debye P_0 (cc.)	Debye μ (D)	Onsager P_0 (cc.)	Onsager μ (D)
−45	7.2301	0.7684	38.5	1.20	66.0	1.57
−40	6.8079	0.7665	37.2	1.19	61.5	1.53
−30	6.1119	0.7534	35.5	1.19	55.0	1.48
−25	5.8220	0.7508	34.3	1.18	51.8	1.45
−20	5.5797	0.7484	33.3	1.18	49.1	1.43
−10	5.1246	0.7382	31.6	1.17	44.5	1.38
0	4.7734	0.7286	30.2	1.16	41.0	1.36
10	4.4575	0.7183	28.8	1.16	37.9	1.34
20	4.1823	0.7070	27.5	1.15	35.2	1.30
25	4.0656	0.7016	27.0	1.15	32.8	1.28
30	3.9639	0.6964	26.5	1.15	33.1	1.27
40	3.7615	0.6856	25.4	1.14	31.0	1.25
50	3.6063	0.6754	24.6	1.14	29.7	1.25

i-Propylamine ($P_E+P_A=20.6$ cc.)

Temp. (°C)	ε	d	Debye P_0 (cc.)	Debye μ (D)	Onsager P_0 (cc.)	Onsager μ (D)
−60	9.5531	0.7732	37.0	1.14	75.0	1.61
−50	8.8388	0.7630	36.4	1.15	70.1	1.60
−40	8.1835	0.7497	36.0	1.17	65.9	1.58
−30	7.5819	0.7401	35.2	1.18	61.5	1.56
−25	7.2929	0.7354	34.8	1.19	59.2	1.55
−20	7.0448	0.7308	34.4	1.19	57.4	1.54
−10	6.5882	0.7216	33.7	1.20	53.9	1.52
0	6.2176	0.7098	33.3	1.22	51.5	1.52
10	5.9490	0.7012	32.9	1.23	49.6	1.51
20	5.6268	0.6900	32.4	1.24	47.4	1.51
25	5.4656	0.6843	32.1	1.25	46.2	1.50

Triethylamine ($P_E+P_A=33.0$ cc.)

Temp. (°C)	ε	d	Debye P_0 (cc.)	Debye μ (D)	Onsager P_0 (cc.)	Onsager μ (D)
−60	3.0238	0.7923	18.4	0.80	21.7	0.87
−50	2.9387	0.7812	17.8	0.80	19.0	0.83
−40	2.8552	0.7739	16.9	0.80	18.1	0.83
−30	2.7795	0.7678	16.0	0.80	17.4	0.83
−25	2.7470	0.7651	15.6	0.80	16.9	0.82
−20	2.7161	0.7626	15.3	0.80	15.9	0.82
−10	2.6550	0.7549	14.6	0.79	15.7	0.82
0	2.5922	0.7472	13.9	0.79	14.9	0.82
10	2.5348	0.7379	13.4	0.79	14.2	0.82
20	2.4886	0.7280	13.1	0.79	13.8	0.82
25	2.4651	0.7229	13.0	0.80	13.6	0.82
30	2.4492	0.7181	12.9	0.80	13.6	0.82
40	2.3910	0.7097	12.1	0.79	12.7	0.81
50	2.3161	0.7007	11.0	0.76	11.5	0.78

As shown in Tables I and II, both for diethylamine and for *i*-propylamine the dielectric polarization calculated from the dielectric constant and the density of a pure liquid by Debye's formula is in fairly good agreement with that measured in solution at 25°C and −25°C. And, the dipole moment measured by the solution method agrees well with that calculated from the dielectric constant and the density of a pure liquid by Debye's formula throughout the range of temperature −50°C–50°C at which the measurement was performed. On the other hand, the molecular polarization and the dipole moment calculated by Onsager's formula are considerably greater than those in dilute solutions both for diethylamine and *i*-propylamine. Of course, ambiguity about the estimation of the atomic polarization exists, but the contribution of the atomic polarization to the dielectric constant is so small that it has little effect on the value of molecular polarization or dipole moment. For triethylamine, it is impossible to determine whether Debye's formula or any other formula holds, on account of its low dielectric constant. Dielectric polarizations of some other aliphatic amines such as ethylamine, *n*-propylamine, *n*-butylamine, etc. have been measured both in dilute solutions and in pure liquids by Barcley et al[5]. All of them show a considerable departure from Debye's formula and are rather consistent with Onsager's formula.

The difference between the derivation of Debye's formula and that of Onsager's formula may be described as follows: in deriving the former formula, the polarizing effect of the molecule on the surrounding medium is assumed to have average rather than its instantaneous value whereas the latter formula is derived for the instantaneous orientation of each molecule. In other words, in Onsager's field it is taken into account that the field due to the permanent moment polarizes the surrounding medium and produces a reaction field to the dipole. Accordingly, whether Debye's formula or Onsager's formula is valid, depends upon the existence of dipolar interaction.

In this way, it is reasonable to say that the reason why Debye's formula is valid in these pure liquids is the absence of a dipolar interaction. In fact, for these molecules the permanent dipole is screened by non-polar groups and has little effect on the surrounding medium. The result obtained in this work will be useful for the discussion of dipolar interaction in the liquid state, such as micelle formation in organic solvent. The latter problem will be discussed later.

Summary

For diethylamine, *i*-propylamine, and triethylamine, Debye's formula holds as the relation between dielectric constant and dipole moment over a wide range of temperature. This fact can be attributed to the absence of the dipolar interaction on account of the screening of the permanent dipole by non-polar alkyl groups.

The author wishes to express his sincere thanks to Prof. B. Tamamushi for his guidance and encouragement.

College of General Education
The University of Tokyo
Tokyo

Ionization Potentials of Some Organic Molecules. III. Aromatic and Conjugated Compounds

By Hiroaki BABA, Itiro OMURA and Keniti HIGASI

(Received February 7, 1956)

Introduction

There are available considerable numbers of reports dealing with the characteristic properties of aromatic and conjugated molecules. Resonance energy, bond length, dipole moment, absorption spectrum and directive power in substitution reactions have been extensively investigated. But unfortunately little information exists in the literature about the ionization potentials.

In the present article some results of the measurement on the appearance potentials of conjugated molecules will be reported. And an interpretation of the results will be given with special reference to its relation to the ultraviolet data of the same compounds.

Experimental Materials

The samples with a few exceptions were obtained from Kanto Chem. Co., Inc. and purified by distillation whenever possible. The refractive index was measured by D-line at 20°C if not recorded.

Benzene b.p. 80°C, $n^{25}=1.4974$; toluene b.p. 109.2°C; thiophenol $n^{23.5}=1.5882$; aniline b.p. 182.8°C, $n=1.5867$; *o*-xylene b.p. 143°C, $n^{21.5}=1.5031$; *m*-xylene b.p. 138°C, $n^{15.7}=1.4994$; *p*-xylene b.p. 137°C, $n^{16}=1.4970$; pyridine b.p. 115.9°C, $n^{21}=1.5087$; α-picoline b.p. 128–9°C, $n^{16.7}=1.5023$; β-picoline b.p. 142.8–143.0°C, $n^{24}=1.5038$; γ-picoline b.p. 144–144.5°C, $n^{17}=1.5057$; pyrrole b.p. 130.7°C, $n=1.5098$; furan b.p. 32.5°C, $n=1.4212$ and thiophene b.p. 83.8°C, $n^{19.7}=1.5267$.

The samples of phenol, anisole and mesitylene were kindly provided by Dr. S. Nagakura of Tokyo University in the pure form. For the pure sample of cyclo-octatetraene we are indebted to Dr. I. Tanaka, Tokyo Institute of Technology.

TABLE I

FIRST IONIZATION POTENTIALS, eV.

Substance	Present work	Previous workers	
Benzene	9.52±0.10	9.52[a]	(9.24)[b]
Toluene	9.20±0.05	9.23[a]	(8.82)[c]
Phenol	9.01±0.05	9.03[a]	
Thiophenol	8.56±0.02		
Aniline	8.23±0.02		
Anisole	8.56±0.05		
o-Xylene	8.96±0.02	8.97[d]	(8.58)[c]
m-Xylene	9.01±0.02	9.02[d]	(8.58)[c]
p-Xylene	8.86±0.02	8.88[d]	(8.48)[c]
Mesitylene	8.76±0.05	8.79[d]	
Pyridine	9.76±0.05	9.80[e]	
α-Picoline	9.66±0.05		
β-Picoline	9.71±0.05		
γ-Picoline	9.56±0.05		
Pyrrole	8.97±0.05		(8.90)[f]
Furan	9.00±0.10	9.05[g]	(9.01)[f]
Thiophene	9.10±0.20		(8.91)[f]
Cyclo-octatetraene	8.63±0.15		

Values in parentheses refer to spectroscopic potentials.

a) J.D. Morrison and A.J.C. Nicholson, *J. Chem. Phys.*, 20, 1021 (1952).
b) W.C. Price and R.W. Wood, *J. Chem. Phys.*, 3, 439 (1935); W.C. Price, *Chem. Rev.*, 41, 257 (1947).
c) V.J. Hammond, W.C. Price, J.P. Teegan and A.D. Walsh, *Discuss. Faraday Soc.*, 9, 53 (1940).
d) F.H. Field and J.L. Franklin, *J. Chem. Phys.* 22, 1895 (1954).
e) A. Hustrulid, P. Kusch and J.T. Tate, *Phys. Rev.* 54, 1037 (1938).
f) W.C. Price and A.D. Walsh, *Proc. Roc. Soc.* (London), A179, 201 (1941).
g) J.D. Morrison, *J. Chem. Phys.*, 19, 1395 1951).

Experimental Method and Results

The measurement of the appearance potential was made by an apparatus described in a previous report[1]. The evaluation of the ionization potentials was made by Honig's critical slope method. Argon was employed as the reference standard.

The results of this experiment are recorded in Table I. Agreement with the data by previous workers is seen to be satisfactory.

Discussion

With the progress in the molecular orbital theory, various calculations of electronic properties have been made for a wide range of molecules. It appears not possible, however, for accurate prediction to be made as to the exact values of ionization potentials when dealing with such complicated molecules as are treated in the present work. In the following, only qualitative discussion will be undertaken in regard to some experimental results of this work.

As mentioned in the previous paper[2], the first ionization potential is related to the most loosely bound electron, which, in the majority of conjugated molecules, will be an electron belonging to the highest occupied π-orbital. However, in a heterocyclic molecule containing a nitrogen atom, which has a pair of non-bonding electrons, the ionizing electron may possibly be due to one of the non-bonding electrons. This point is important when discussing the potentials of pyridine and picolines.

Substituted Benzenes.—The effect of substitution on the absorption spectrum of benzene has been investigated by Sklar[3], Herzfeld[4], Nagakura and Baba[5] from the viewpoint of electron migration; and the red shift of the near ultraviolet absorption, caused by an ortho-para directing substituent, has been interpreted as due to the following facts. (1) The migration of electrons from the substituent into the unoccupied ring π-orbitals gives rise to an extra stabilization energy. (2) This extra stabilization energy is greater in the excited state than in the ground state. Later, it was shown by Matsen[6] that the electron migration theory is equivalent to the usual perturbation treatment.

The method of electron migration may be used to explain the ionization potentials of substituted benzenes. When one π-electron belonging to the aromatic ring is ionized, a substituent electron will be allowed to migrate into the previously filled π-orbital. As a result of this migration, the extra stabilization energy of the molecular ion will become great compared with that of the neutral molecule. Then the energy difference between the ionized and neutral states will be less for the substituted molecule than for the unsubstituted one. Thus we can expect that the ionization potential will decrease by the introduction of a substituent into the benzene ring. Actually, the potentials of all the substituted benzenes listed in Table I are lower than that of benzene.

The degree of electron migration, hence, the amount of the extra stabilization energy is dependent on the sort of substituent. It is largely determined by ionization energy of the substituent X: the smaller the ionization energy, the greater is the stabilization energy. However, it depends also upon the magnitude of overlapping between X and the neighbouring carbon atom in the ring. Thus, as Robertson and Matsen[7] concluded from ultraviolet absorption data, the stabilization energy will increase in the sequence

$$CH_3 < OH < SH < NH_2;$$

while the ionization energies of the groups X, estimated from those for HX or CH_3X molecules, are in the order $CH_3 > OH > NH_2 > SH$[3]. We may then expect that the ionization potentials of the substituted benzenes will be in the order

benzene > toluene > phenol > thiophenol > aniline.

This expectation is fulfilled by our experimental results shown in Table I.

Next, we shall turn to the ionization potentials of polymethyl benzenes. Herzfeld[4] showed for polysubstituted benzenes that the red shift of absorption spectrum is nearly additive. In fact, it is seen from Table II that this rule of additivity holds for polymethyl benzenes. Taking into account the electron migration theory, a similar additivity rule may be expected for the change in ionization potential with methyl substitution. The ionizatioh potential data given in Table II and also the plot of potential values versus the number of methyl substituents in Fig. 1 are all in fair accord with the above view.

1) I. Omura, K. Higasi and H. Baba, This Bulletin, 29, 501 (1956).

2) I. Omura, K. Higasi and H. Baba, This Bulletin, 29, 504 (1956).

3) A.L. Sklar, *J. Chem. Phys.*, 7, 984 (1939); *Revs. Modern Phys.*, 14, 232 (1942).

4) K.F. Herzfeld, *Chem Rev.*, 41, 233 (1947).

5) H. Baba and S. Nagakura, *J. Chem. Soc. Japan*, 72, 72 (1951); S. Nagakura and H. Baba, *J. Am. Chem. Soc.*, 74, 5693 (1952).

6) F.A. Matsen, *J. Am. Chem. Soc.*, 72, 5243 (1950).

7) W.W. Robertson and F.A. Matsen, *J. Am. Chem. Soc.*, 72, 5248 (1950).

TABLE II

ULTRAVIOLET ABSORPTIONS[a] and IONIZATION POTENTIALS OF POLYMETHYL BENZENES

Substance	$\nu(0\text{-}0)$[b] (cm^{-1})	$\Delta\nu$ (cm^{-1})	I[c] (eV.)	ΔI (eV.)	
Benzene	38089		9.52		
Toluene	37484	−605	9.20	−0.32	
o-Xylene			8.96	−0.56	Average −0.58
m-Xylene			9.01	−0.51	
p-Xylene			8.86	−0.66	
Mesitylene	36488	−1601	8.76	−0.76	

a) The data on the ultraviolet absorptions were taken from Table III (in ref. 4).

b) $\nu(0\text{-}0)$ represents the wave-number of the 0–0 transition in the vapor state.

c) I represents the first ionization potential.

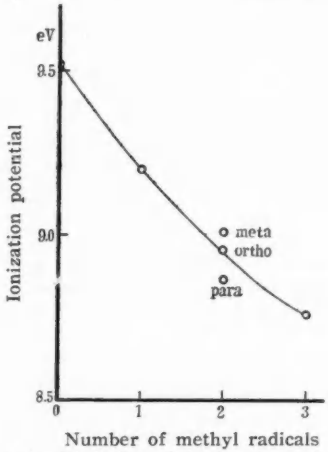

Fig. 1. Variation of ionization potential with the number of methyl radicals in polymethyl benzenes.

Pyridine and Picolines.—According to Table I, the differences of the potential values between pyridine and three isomeric monomethyl pyridines, viz., α-, β-, γ-picolines, are −0.10 eV., −0.05 eV., −0.20 eV., respectively. That is, the lowering of ionization potential caused by the methyl substitution is seen to be less pronounced in pyridine than in benzene (cf. Table II). On the contrary, the red shift of the $\pi\rightarrow\pi^*$ transitions in picolines appears to be not very different from that in toluene[8,9], so that the perturbation effect of methyl radical on the ring π-orbitals will be almost the same for pyridine and benzene rings. Therefore, if the ionizing electron in question were the one belonging to the π-orbital, the lowering in the ionization potential would not be so small as observed in this experiment. Consequently, it seems very likely that the first ionization potentials of pyridine and its methyl derivatives are primarily determined by the nonbonding $sp^2\sigma$-electron of the N atom.

Indeed, the above view seems to have support from the studies of ultraviolet absorption spectra[8,9,10,11]. Both in pyridine and picolines, there appear two absorptions of markedly different intensities. The weaker one has been assigned to the transition from the non-bonding orbital of the N atom to the lowest vacant π-orbital ($n\rightarrow\pi^*$ transition), and the stronger one to the transition from the highest occupied π-orbital to the lowest vacant π-orbital ($\pi\rightarrow\pi^*$ transition). The $n\rightarrow\pi^*$ transitions of all these substance occur at the longer wave-lengths, indicating that there is a non-bonding level of the N atom situated above the highest occupied π-level. Therefore, one electron in this non-bonding orbital must be inferred to be responsible for the first ionization*.

Lastly, we shall try to explain the slight decrease in ionization potential upon the methyl substitution. As a result of the resonance among various structures including those of Fig. 2 the methyl group in toluene

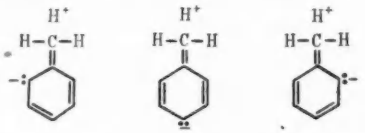

Fig. 2.

sends partial negative charge to the carbon atoms of the ortho and para positions. The situation in isomeric picolines may be deduced from this. That is, extra negative charges will appear at the N atoms of α- and γ-picolines, but not at the N atom of β-picoline. Therefore the ionization potentials of the former two substances will become smaller on account of the increased electron density at the N atom, while the potential of β-picoline will remain almost the same as pyridine (cf. Table I).

Summary

First ionization potentials of 18 aromatic and conjugated compounds were measured by the electron impact method. Seven out of

8) J.H. Rush and H. Sponer, *J. Chem. Phys.*, 20, 1847 (1952).

9) H.P. Stephenson, *J. Chem. Phys.*, 22, 1077 (1954).

10) M. Kasha, *Discuss. Faraday Soc.*, 9, 14 (1950).

11) F. Halverson and R.C. Hirt, *J. Chem. Phys.*, 19, 711 (1951).

* There is still some uncertainty about the above assignment. Next, we are intending to measure the ionization potentials of the isomers of diazines and triazines. And then we shall be able fo present more complete and fuller discussion on this problem.

these were newly determined in the present work. Discussion of the results was given with special reference to their relation to the ultraviolet data.

It was suggested that the ionization potentials in benzene derivatives are primarily determined by π-electrons, while those in pyridine and picolines are largely by one of the non-bonding electrons belonging to the N atom in the ring.

The authors with to express their gratitude to Dr. S. Nagakura for valuable criticisms and suggestions, and also to the Ministry of Education for a Grant in Aid.

Research Institute of Applied Electricity
Hokkaido University, Sapporo

Studies on the Intramolecular Hydrogen Bond in Conjugated Systems by the Measurements of Dipole Moments. I. o-Nitrophenol

By Bunzo EDA and Kazuo ITO

(Received February 9, 1956)

Introduction

When a molecule having conjugated double bonds forms an intramolecular hydrogen bond, it is expected that the charge migration is caused by the bonding in the molecule. But the magnitude and direction of the migration have not been determined experimentally as yet. For the purpose of obtaining these, we measured the dipole moments of several compounds. In this paper we report the results obtained on *o*-nitrophenol.

From the infrared absorption spectrum it has been found that *o*-nitrophenol has no free hydroxyl group and consequently all the molecules form the intramolecular hydrogen bond[1]. In order to get information on the charge migration caused by the hydrogen bond in the molecule, it is necessary to compare the dipole moment of *o*-nitrophenol with the moment of a hypothetical *o*-nitrophenol molecule having no intramolecular hydrogen bond in regard to the directions of moments as well as their absolute values. The components of the dipole moment of *o*-nitrophenol can be obtained from the measurements of the dipole moments of *o*-nitrophenol, 4-chloro-2-nitrophenol and 4-methyl-2-nitrophenol, while the components of the dipole moment of the hypothetical *o*-nitrophenol having no hydrogen bond can be obtained from the sum of the respective components of the dipole moments of phenol and nitrobenzene. The order of magnitude of errors due to the assumption that the dipole moment of a molecule can be expressed by the vector sum of bond moments was estimated with the aid of the dipole moments of anisole and its derivatives.

1) L. Pauling, "The Nature of the Chemical Bond", Cornell University Press, Ithaca, New York (1940), p. 318.

Experimental

Materials.—All the materials were prepared in our laboratory except *o*-nitrophenol and 4-chloro-2-nitroanisole which were purchased and purified by recrystallization. 4-Chloro-2-nitrophenol and 4-methyl-2-nitrophenol were purified by steam distillation followed by recrystallization, while *o*-nitroanisole was purified by vacuum distillation.

Measurements.—All the measurements were made in benzene solutions at 25°C. The dielectric constants were measured by heterodyne beat method. A modified Hedestrand method was employed for obtaining the specific polarization at infinite dilution. The method was similar to that introduced by Halverstadt and Kumler[2], differing in that densities were used rather than the specific volumes. The sum of electronic polarization and atomic polarization was assumed to be equal to the molecular refraction for D-line calculated additively from the atomic refractions of the constituent atoms.

Results.—The results are shown in Table I and II, where μ is the dipole moment in Debye unit. All the notations have the same significances as those used by Kurita et al.[3]. The data found in literatures to be compared with the present results are those of Jenkins on *o*-nitrophenol[4] and of Cowley and Partington on *o*-nitroanisole[5].

2) I.F. Halverstadt and W.D. Kumler, *J. Am. Chem. Soc.*, **64**, 2988 (1942).
3) Y. Kurita, T. Nozoe and M. Kubo, This Bulletin, **26**, 242 (1953).
4) H.O. Jenkins, *J. Chem. Soc.*, **1936**, 1049.
5) E.G. Cowley and J.R. Partington, *J. Chem. Soc.*, **1933**, 1257.

TABLE I

DIELECTRIC CONSTANTS AND DENSITIES IN BENZENE SOLUTIONS OF *o*-NITROPHENOL, *o*-NITROANISOLE AND THEIR DERIVATIVES AT 25°C

Compounds	$w\times10^5$	ε	d
o-Nitrophenol	138	2.2825	0.87169
(m. p. 45°)	777	2.3328	0.87372
	1681	2.4050	0.87642
	3019	2.5110	0.88040
4-Chloro-2-nitrophenol	295	2.2836	0.87211
(m. p. 86°)	594	2.2943	0.87331
	1172	2.3144	0.87516
	2741	2.3717	0.88096
4-Methyl-2-nitrophenol	214	2.2928	0.87192
(m. p. 32°)	778	2.3401	0.87329
	1664	2.4183	0.87565
	2913	2.5272	0.87904
o-Nitroanisole	152	2.2971	0.87130
(b. p. 165° at 39 mmHg)	331	2.3271	0.87182
	520	2.3598	0.87239
	765	2.3991	0.87307
4-Chloro-2-nitroanisole	302	2.3117	0.87344
(m. p. 98°)	496	2.3360	0.87413
	824	2.3761	0.87503

Let it be assumed that the methoxy group is in the plane of an anisole molecule as illustrated in Fig. 1 (a). The components of dipole moment in x- and y-directions are

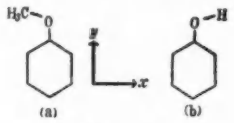

Fig. 1.

denoted by μ_x and μ_y, respectively. Since the observed moment of anisole in benzene solution is 1.28 D[8] we have

$$\mu_x^2+\mu_y^2=1.28^2 \qquad (1)$$

The mesomeric moment from the methoxy group to benzene ring is, of course, included in these two components. The dipole moment of hydroquinone dimethylether $C_6H_4(OCH_3)_2$ would have the same value[9], which is equal to $\sqrt{2}\mu_x$, whether (i) the methoxy groups rotate freely, (ii) they are fixed in equally probable *cis*- and *trans*-forms, (iii) the groups in these *cis*- and *trans*-forms rotate freely within certain limits of angle, or (iv) the oscillation, not being free, is such that the probability of any angle, of swing is some function of that angle, the same function applying to each group. The observed moment in benzene solution is 1.73 D[8], hence μ_x is $\pm$1.2 D. As it is most probable that the direction is $H_3{}^+C\text{–}O^-$, we prefer $\mu_x=+1.2$ D. Putting it in (1), we get $\mu_y=\pm0.4$ D. If we use the components $\mu_x=+1.2$ D and $\mu_y=-0.4$ D, the calculated moments of anisole, its *ortho*- and *para*-derivatives and 4-chloro-2-nitroanisole agree with the observed ones to within less than 0.1 D as shown in Table III. Therefore, the moments of anisole, its *ortho*- and *para*-derivatives and the *para*-derivative of *o*-nitroanisole can be expressed by the vector sum to within less than 0.1 D including the difference in mesomeric effect and solvent effect unless they are compelled to be in the other particular configuration by

TABLE II

MOLECULAR POLARIZATIONS AND DIPOLE MOMENTS OF *o*-NITROPHENOL, *o*-NITROANISOLE AND THEIR DERIVATIVES IN BENZENE SOLUTIONS AT 25°C

Compounds	ε_1	d_1	α	β	$P_{2\infty}$	MR_D	μ
o-Nitrophenol	2.2714	0.87132	7.94	0.301	239.4	34.4	3.16
4-Chloro-2-nitrophenol	2.2727	0.87106	3.60	0.360	152.8	39.3	2.35
4-Methyl-2-nitrophenol	2.2734	0.87129	8.71	0.265	287.8	39.2	3.49
o-Nitroanisole	2.2720	0.87086	16.68	0.290	517.2	39.2	4.83
4-Chloro-2-nitroanisole	2.2746	0.87248	12.33	0.314	476.3	44.0	4.60

Their values of 3.11 D and 4.83 D respectively are in good agreement with ours.

Discussion

The near-ultraviolet absorption spectra of phenol and anisole in cyclohexane solutions[6] agree with each other to a high degree of precision both in the wavelengths of maximum absorption and in intensities. Moreover, the resonance energy of phenol is almost the same as that of anisole[7]. Accordingly, if the observed moments of anisole, its *ortho*- and *para*-derivatives and the *para*-derivative of *o*-nitroanisole are fairly consistent with those calculated by vector addition, it will be reasonable to suppose that the method of vector sum of bond moments can also be used with nearly the same accuracy in the corresponding phenol derivatives.

6) R.A. Friedel and M. Orchin, "Ultraviolet Spectra of Aromatic Compounds", John Wiley & Sons, Inc., New York (1951); Fig. 31 and Fig. 55.

7) G.W. Wheland, "The Theory of Resonance", John Wiley and Sons, Inc., New York (1944), p. 69.

8) K.B. Everard and L.E. Sutton, *J. Chem. Soc.*, 1949, 2312.

9) K.B. Everard and L.E. Sutton, *J. Chem. Soc.*, 1951, 19.

TABLE III
DIPOLE MOMENTS OF ANISOLE DERIVATIVES IN BENZENE SOLUTIONS

Substituents	$\mu_{calcd.}$ (D)[a,b]	$\mu_{obs.}$(D)[c]
p-CH_3	1.20	1.20
p-Br	2.31	2.23
p-Cl	2.33	2.24
o-F	2.50*	2.31
o-Cl	2.60	2.50
o-Br	2.58	2.47
o-CH_3	1.05	1.0
o-NO_2	4.92	4.83
4-Cl-2-NO_2	4.66	4.60

a) The bond moments of the substituents are based on the following data[10], bromobenzene 1.57 D, chlorobenzene 1.60 D, fluorobenzene 1.48 D, toluene 0.4 D and nitrobenzene 4.0 D in benzene solutions.

b) In *ortho*-derivatives it is assumed that the methoxy group is fixed in the molecular plane and the methyl carbon is in the side opposite to *ortho*-substituent.

c) The observed values were taken from "Tables of Electric Dipole Moments"[11] except those of *o*-nitroanisole and 4-chloro-2-nitroanisole.

* The difference for *o*-fluoroanisole is greater because the small size of the fluorine atom makes the *cis*-configuration less improbable for this compound than for the other *ortho*-substituted anisoles.

steric hindrance, etc. Likewise, were it not for the hydrogen bond or a remarkable change of configuration, it should be possible to express the dipole moments of phenol, its *para*-derivatives and *ortho, para*-disubstituted derivatives by the vector sum to within less than 0.1 D.

The x- and y-components of dipole moment of phenol, Fig. 1 (b), can be obtained from the moment of phenol and its *para*-derivatives. If it is assumed that $\mu_x=1.55$ D and $\mu_y=0.0$ D, the observed moments agree with the calculated ones as shown in Table IV. On the contrary, the calculated moments of *o*-nitrophenol, 4-chloro-2-nitrophenol and 4-methyl-2-nitrophenol do not agree with the observed ones by the order of 0.4 D as shown in Table V. These discrepancies are definitely greater than those in Table III and IV. Since all the compounds given in Table V

TABLE IV
DIPOLE MOMENTS OF PHENOL AND ITS *para*-DERIVATIVES IN BENZENE SOLUTIONS

Compounds	$\mu_{calcd.}$(D)	$\mu_{obs.}$(D)[a]	$\Delta\mu$(D)[b]
Phenol	1.55	1.56	+0.01
p-Bromophenol	2.21	2.13	−0.08
p-Chlorophenol	2.23	2.22	−0.01
p-Methylphenol	1.59	1.57	−0.02
p-Fluorophenol	2.14	2.10	−0.04

a) The observed values for all compounds were taken from "Tables of Electric Dipole Moments[11]" except *p*-fluorophenol, the value of which is due to Leonard and Sutton[12].

b) $\Delta\mu$ denotes the difference between $\mu_{obs.}$ and $\mu_{calc.}$.

TABLE V
DIPOLE MOMENTS OF *o*-NITROPHENOL AND ITS DERIVATIVES IN BENZENE SOLUTIONS

Compounds	$\mu_{calcd.}$(D)	$\mu_{obs.}$(D)	$\Delta\mu$(D)
o-Nitrophenol	2.77	3.16	0.39
4-Chloro-2-nitrophenol	1.95	2.35	0.40
4-Methyl-2-nitrophenol	3.07	3.49	0.42

are supposed to have an intramolecular hydrogen bond between the hydroxyl group and the nitro group, this abnormality may be due mainly to the hydrogen bond. The components of *o*-nitrophenol that satisfy the observed moments of *o*-nitrophenol, 4-chloro-2-nitrophenol and 4-methyl-2-nitrophenol are $\mu_x=$ 2.2–2.3 D and $\mu_y=2.2$–2.35 D, respectively. The calculated components based on the aforementioned components of phenol and the dipole moment of nitrobenzene are $\mu_{x\,calcd.}=$ 1.9 D and $\mu_{y\,calcd.}=2.0$ D, respectively. Hence we have $\Delta\mu_x=0.3$–0.4 D and $\Delta\mu_y=0.2$–0.35 D as the abnormal values.

In *o*-nitrophenol, therefore, the formation of intramolecular hydrogen bond causes the charge migration of the order of 0.3–0.4 D in x-direction and 0.2–0.35 D in y-direction. Such charge migration may be explained, for instance, by two main charge migrations illustrated in Fig. 2. Further studies are required, however, of other compounds similar to *o*-nitrophenol in order to see whether or not such charge migrations are common in the molecule having an intramolecular hydrogen bond.

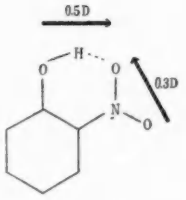

Fig. 2.

Summary

Dipole moments of *o*-nitrophenol, 4-chloro-2-nitrophenol, 4-methyl-2-nitrophenol, *o*-nitroanisole and 4-chloro-2-nitroanisole were meas-

10) K.B. Everard, L. Kumar and L.E. Sutton, *J. Chem. Soc.*, **1951**, 2814.
11) L.G. Wesson, "Tables of Electric Dipole Moments", The Technology Press, M.I.T. (1948).
12) N.J. Leonard and L.E. Sutton, *J. Am. Chem. Soc.*, **70**, 1566 (1948).

ured in benzene solutions. Their values are 3.16, 2.35, 3.49, 4.83 and 4.60 D respectively. Instead of obtaining the directions of the dipole moments of phenol and anisole, μ_x and μ_y, the two components in x- and y-directions in the molecular plane, were evaluated from the moments of their derivatives. When the dipole moments of *o*-nitrophenol, *o*-nitroanisole and their derivatives were calculated according to the vector addition using these components, the calculated moments for *o*-nitrophenol and its derivatives do not agree with the observed ones whereas fairly good agreement was found between the observed and calculated ones for *o*-nitroanisole and its derivative. The order of the discrepancy is 0.3–0.4 D in x-direction and 0.2–0.35 D in y-direction. The authors suggest that the cause of this discrepancy is due mainly to the formation of an intramolecular hydrogen bond.

The authors wish to express their sincere thanks to Prof. M. Kubo and Dr. Y. Kurita for their kind discussions. A part of the expense for the experiment has been defrayed from a grant given by the Ministry of Education, to which the authors' thanks are due.

Department of Chemistry, Faculty of Science, Nagoya University
Nagoya

A Theoretical Treatment of Activity Coefficients in Resin Phase

By Hiroshi SOBUE and Yoneho TABATA

(Received July 25, 1955)

Introduction

The phenomena of ionic exchange have been studied from the statistical point of view by several investigators. Hamada[1] and Davis[2] independently applied a statistical model to the ion exchange equilibria. Hamada derived the equation of the simple mass action type by assuming a lattice model as ion exchange equilibria, while Davis dealt with ion exchange equilibria, assuming a regular model for ionic exchange, by a modification of a statistical theory of a localized monolayers derived from Fowler and Guggenheim[3]. The latter author first applied the theory to an uni-uni-valent exchange and showed that the resultant equation is of the simple mass action type, ignoring the interaction energy between ion pairs in the exchanger phase. Afterwards he studied two types of irregular models of ionic exchange systems. Seiyama, Sakaki and Nagamatsu[4] developed the statistical theory of Hamada and Davis, by applying "a quasi-chemical method" of Guggenheim[5], and they discussed in detail the ion exchange equilibria involving uni-uni-valent and uni-di-valent exchange.

According to the experimental results of Argersinger, Davidson[6] as well as the present authors[7], it can be expected that the activity coefficients in any exchange ratio will be affected markedly by the interaction energy of each ion pair in the solid phase. Generally the interaction of each pair presumably involves the following forces: ion-dipole, van der Waals and covalent bond forces as short range forces, and electrostatic forces (Coulomb force) as long range forces.

Accordingly ion exchange phenomena should be investigated under consideration of all these forces. Above all, the anomaly in the activity coefficients in the resin phase will principally depend on the interaction forces described above.

Davis[2] and Hamada[1] ignored the interaction energy between ion pairs in the exchanger phase, while Seiyama, Sakai and Nagamatsu[4] gave a statistical explanation of the ion exchange equilibrium constants under consideration of the interaction energy between ion pairs in the resin phase. But they did not treat the activities in the exchanger phase extensively. The authors

1) H. Hamada, *The Journal of Japanese Chemistry (Kagaku-no-ryoiki)*, **1**, 83 (1946).
2) L.E. Davis, *J. Colloid Sci.*, **5**, 71, 107 (1959).
3) R.H. Fowler and E.A. Guggenheim, "Statistical Thermodynamics" (1938).
4) T. Seiyama, M. Nagamatsu and W. Sakai *Electro. Chem.*, **21**, 218, 393 (1953).
5) E.A. Guggenheim, *Trans. Faraday Soc.*, **44**, 1007 (1948).
6) W.J. Argersinger, Jr. and A.W. Davidson, *J. Phys. Chem.* **56**, 92 (1952).
7) H. Sobue and Y. Tabata *J. Chem. Soc. Japan (Ind. Chem. Sect.)* **56**, 938 (1653); ibid. **57**, 469 (1954).

present here a theoretical treatment under several assumptions, in which it will be shown that the energy of mutual ionic-interaction has an important significance in the activity determination in the solid phase.

Theoretical

The following discussions are based on Guggenheim's theory which deals with "A Generalization of the Quasi-Chemical Method". In this treatment, the following conditions are assumed.

1) Ionic exchange systems have no empty sites.

2) A polyvalent ion will occupy a set of r adjacent sites, r being the number of sites occupied by an ion.

3) We may neglect interaction between pairs of ions that are not nearest neighbours, so that the total interaction energy of the ions can be expressed as the sum of contributions from each pair of nearest neighbours.

4) We treat ion exchange resins as slightly swollen gels so that the volume change of the system due to the exchange process is small.

5) It is assumed that the electrolyte solution involving the exchangeable ions is able to diffuse freely through the network of the exchange resin, so that there is no mechanical resistance associated with ionic size in the exchange process.

6) We also considered the case where the ionic concentration of the electrolyte solution in the exchange system is comparatively small, so that the effect of the presence of the free electrolytes (non-fixed electrolytes at the exchanging lattice points) in the resin phase at equilibrium will be small.

Let us consider a lattice model which has regular N sites as the ion exchange resin phase and in which one site has one negative charge.

Let N_A: Number of ions of any type of A.
r_A: Number of sites occupied by one ion of type A.
z: Number of sites which are nearest neighbours of any given site in regular array.
q_A: A function of z and r_A which determines the frequency with which a valence element of an ion of type A will occupy a site adjacent to another occupied site.

In a specific state having any exchange ratio, we have

$$N=r_AN_A+r_BN_B$$

Parameters q_A, q_B are defined by

$$z(r_A-q_A)=2(r_A-1)$$

$$z(r_B-q_B)=2(r_B-1)$$

zq_A is the so-called corrected co-ordination number, i.e., the number of sites, neighbours of the r_A sites occupied by an ion A, excluding those neighbours of each site occupied by the next element of the same ion. The physical meaning of q_B is similar to q_A. It is assumed that in any given configurations of the system, inter-ionic (inter-ionic of hydrogen ion and metallic ions) potential energy consists of a sum of the following terms ϕ_{AA}, ϕ_{BB} and ϕ_{AB}. ϕ_{AA}, ϕ_{BB} and ϕ_{AB} denote the contribution to the internal energy by a pair of sites occupied both by A ions, botn by B ions, and one occupied by A and the other occupied by B respectively.

Let the number of pairs of neighbouring sites in which one site is occupied by an ion A and the other by an ion B be denoted by zX. The partition function Q of the system is written in the form

$$Q=\sum_X g(N_A, N_B, X) \exp(zX\phi/2kT),$$

where $\phi=\phi_{AA}+\phi_{BB}-2\phi_{AB}$ and $g(N_A, N_B, X)$ denotes the number of distinguishable configurations of all the N_A ions of A and N_B ions of B for a given value of X. This combinatory factor $g(N_A, N_B, X)$ is expressible as an explicit function of N_A, N_B, X, involving z, r_A, r_B, q_A, q_B as parameters. In a real exchange system, each ion in an exchangeable point (lattice point) will exist in a hydrated state according to the size of the framework and the kinds of the exchangeable ions.

The total free energy F' can be represented by the following equation,

$$F'=N_A\mu_A^{0'}+N_B\mu_B^{0'}+\Delta F_1+\Delta F_2,$$

where ΔF_1 and ΔF_2 are the free energies of mixing, which contain the configurational term and the term due to the interaction energy respectively.

The terms of $\mu_A^{0'}$ and $\mu_B^{0'}$ in the total free energy F' should be expressed by the following equations.

$$\mu_A^{0'}=-\frac{q_Az}{2}\phi_{AA}+u_A^0-kT\log v_{f_A}-kT\times\log\left(\frac{2\pi m_AkT}{h^2}\right)^{3/2}$$

$$\mu_B^{0'}=-\frac{q_Bz}{2}\phi_{BB}+u_B^0-kT\log v_{f_B}-kT\times\log\left(\frac{2\pi m_BkT}{h^2}\right)^{3/2}$$

In these expressions, u_A^0 and u_B^0 are the potential energies of ions A and B in an equilibrium state respectively. v_{f_A}, v_{f_B} are the free volumes and m_A, m_B the masses of

the respective ions in the exchangeable point at constant temperature. If we consider free energy due to configuration only, the free energy F can be expressed by the following equation,

$$F=N_A\mu_A^0+N_B\mu_B^0+\Delta F_1+\Delta F_2=kT\log Q.$$

In this expression, μ_A^0 and μ_B^0 are respectively the chemical potentials of each pure resin. The quantity which has the most important meaning in the problem treated here is free energy of mixing $\Delta F=\Delta F_1+\Delta F_2$. If we use Flory's approximation for ΔF_1,

$$\Delta F_1/kT=\left(1-\frac{1}{2}z\right)r_AN_A\log r_AN_A$$
$$+\left(1-\frac{1}{2}z\right)r_BN_B\log r_BN_B-\left(1-\frac{1}{2}z\right)$$
$$\times(r_AN_A+r_BN_B)\log(r_AN_A+r_BN_B)$$
$$+\frac{1}{2}z\{q_AN_A\log q_AN_A+q_BN_B\log q_BN_B$$
$$-(q_AN_A+q_BN_B)\log(q_AN_A+q_BN_B)\}.$$

ΔF_2 which contains the term of the interaction energy can be expressed as,

$$\Delta F_2/kT=\frac{1}{2}z(q_AN_A+q_BN_B)\left\{\theta\log\frac{\beta-1+2\theta}{\theta(\beta+1)}\right.$$
$$\left.+(1-\theta)\log\frac{\beta+1-2\theta}{(1-\theta)(\beta+1)}\right\}.$$

In this expression β and θ are represented as follows,

$$\beta=\left\{(1-2\theta)^2+4\theta(1-\theta)e^{\frac{\phi}{kT}}\right\}^{1/2}$$

$$\theta=\frac{q_AN_A}{q_AN_A+q_BN_B},\quad 1-\theta=\frac{q_BN_B}{q_AN_A+q_BN_B}.$$

Therefore by using the above equations the chemical potentials of ions A and B are given as the differential forms of the corresponding free energies:

$$\mu_A=\frac{\delta F}{\delta N_A}=\mu_A^0+kT\left\{(1-\frac{1}{2}z)r_A\right.$$
$$\log\frac{r_AN_A}{r_AN_A+r_BN_B}+\frac{1}{2}zq_A\log\frac{q_AN_A}{q_AN_A+q_AN_B}$$
$$\left.+\frac{1}{2}zq_A\log\frac{\beta-1+2\theta}{(\beta+1)\theta}\right\}$$

$$\mu_B=\frac{\delta F}{\delta N_B}=\mu_B^0+kT\left\{(1-\frac{1}{2}z)r_B\log\right.$$
$$\times\frac{r_BN_B}{r_AN_A+q_BN_B}+\frac{1}{2}zq_B\log\frac{q_BN_B}{q_AN_A+q_BN_B}$$
$$\left.+\frac{1}{2}zq_B\log\frac{\beta+1-2\theta}{(\beta+1)(1-\theta)}\right\}$$

The relation between the activity and the chemical potential is expressed by the following equations,

$$\mu_A=\mu_A^0+kT\log a_A$$
$$\mu_B=\mu_B^0+kT\log a_B$$

where a_A, a_B are activities of A and B ions in the resin phase respectively, therefore the activity coefficients are given by the following expressions,

$$\frac{N_A}{N_A+N_B}f_A=e^{\frac{\mu_A-\mu_A^0}{kT}}$$

$$\frac{N_B}{N_A+N_B}f_B=e^{\frac{\mu_B-\mu_B^0}{kT}}.$$

Then we can calculate the activity coefficients in the ion exchange resin phase from the above equations. The results obtained by calculation using the above equations are shown in Figs. 1, 2 and 3.

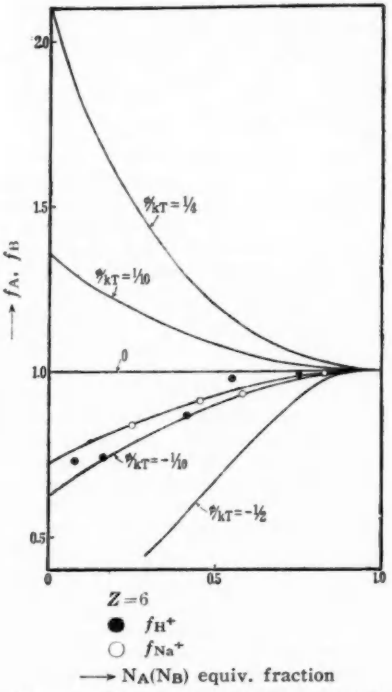

Fig. 1. Relationship between activity coefficients and exchange ratios in the resin phase of uni-uni-valent exchange system. (The dots show the experimental values).

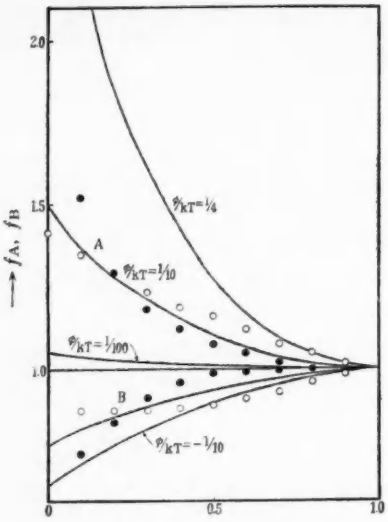

$Z=8$
● f_{H^+}
○ f_{Na^+}, f_{Ag^+}
⟶ $N_A(N_B)$ equiv. fraction

Fig. 2. Relationship between activity coefficients and exchange ratios in the resin phase of uni-uni-valent exchange system. (The dots show the experimental values of Argersinger and Davidson).

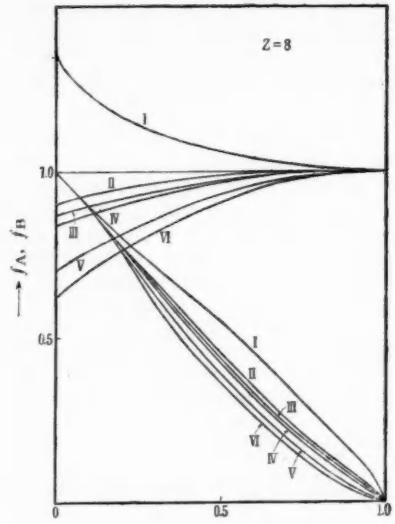

⟶ N_A equiv. fraction

Fig. 3. Relationship between activity coefficients and exchange ratios in the resin phase of uni-di-valent system.

I. ..... $\frac{\phi}{kT}=1/10$
II. I/100
III. 0
IV. ..... -1/100
V. ..... -2/100
VI. ..... -1/10

Experimental

A film of carboxymethylcellulose (ion exchange capacity 3.29 meq./g. for dry sample) was used as the cation exchanger. The film (acid form), which was about $2.5\times2.5\,cm^2$ and about10 μ thick, was used as the sample. Equilibrium studies of the H–Na, H–NH_4 and H–Ca exchanges were made while maintaining Na, NH_4 and Ca concentrations constant at various hydrogen ion concentrations in the solution phase.

In each exchange experiment, the sample was placed in a ground glass stopperd flask in contact with an aqueous solution of the appropiate salts of the cations. The volume of the electrolyte solution was 100 ml. Initial and equilibrium concentrations of hydrogen ions were determined by the glass electrode in the solution phase. The films, which reached equilibrium, were washed with sufficient 70% alcoholic solution in the uni-uni-valent case (H–Na exchange), and with distilled water in the uni-di-valent case (H–Ca exchange). The equilibrium temperature was maintained at 15±1°C. The infrared spectra of the exchanger film were measured with a double beam system spectrometer of Baird Co. with a rock salt prism*.

As described in the previous paper[7], several precautions were necessary to minimize errer in measurements of the infrared spectra. The apparent equilibrium constants were calculated by the following equation, using the spectrophotometric method,

$$pKa=r_B\log\varepsilon_a-r_A\log k\varepsilon_b-(r_B-r_A)\log(\varepsilon_a+k\varepsilon_b)+r_A\log B^{+r_B}-r_B\log A^{+r_A}+\log\frac{\gamma_B{}^{r_A}}{\gamma_A{}^{r_B}}$$

where A and B are the concentrations of the two exchangeable ions respectively, r_A is the valence of the A ion, γ_A is the activity coefficient of the A ion in the electrolyte solution, ε_a is the absorption intensity of carbonyl band (5.6 μ or 6.3 μ) of carboxyradical fixing the A ion in an exchanger, when the C–H stretching vibration in 3.4 μ was selected as the reference band, and k is a constant. In the calculation of pKa, the mean activity coefficients of the electrolyte from "Lewis, Table" were used.

Evaluation of the Activity Coefficients

For an ion exchange system we could consider the true equilibrium constant K as

$$K=Ka\frac{f_B{}^{r_A}}{f_A{}^{r_B}}$$

In the above equation, f expresses the activity coefficient of resin component on mole fraction basis, with pure resin as the standard state. The following equation is given from the Gibbs-Duhem relation,

$$m_A d\mu_A+m_B d\mu_B=(n_A/r_A)d\mu_A+(n_B/r_B)d\mu_B=0,$$

where m and n represent a mole fraction and an equivalent fraction of the respective ion in the solid exchanger phase respectively, and μ the chemical potential of the exchangeable ions in the resin phase. We can obtain the differential form of the logarithmic relation between K and Ka from the Gibbs-Duhem equation at constant temperature and pressure for the solid solution phase.

$$\left(\frac{n_A}{r_A}\right) d \log f_A + \left(\frac{n_B}{r_B}\right) d \log f_B = 0$$

On the other hand, the following equation is obtained from the above equation.

$$r_A d \log f_B - r_B d \log f_A = -d \log Ka$$

Now, we calculate the activity coefficient f from these equations. We carried out the calculation of the activity coefficients of salts in the three exchange systems of Na-H, NH_4-H and Ca-H at 0.02 N ionic concentration. The results are shown in Fig. 1. and Table I.

TABLE I

ACTIVITY COEFFICIENTS IN RESIN PHASE

Activity coefficients of Na^+ and H^+ in Na-H exchange system

n Equivalent fraction of Na^+	pKa Apparent equil. const.	f_A Activity coeff. of Na^+	f_B Activity coeff. of H^+
1.0	2.72*	1.000	0.79*
0.9	2.71	0.998	0.790
0.8	2.70	0.995	0.795
0.7	2.69	0.990	0.800
0.6	2.66	0.987	0.818
0.5	2.62	0.948	0.860
0.4	2.57	0.860	0.926
0.3	2.53	0.796	0.968
0.2	2.48	0.757	0.988
0.1	2.46	0.737	0.933
0	2.44*	0.72*	1.000

Activity coefficients of Ca^{++} and H^+ in Ca-H exchange system

n Equivalent fraction of Ca^{++}	pKa Apparent equil. const.	f_A Activity coeff. of Na^+	f_B Activity coeff. of H^+
1.0	2.97*	1.000	0.69*
0.9	2.96	1.000	0.697
0.8	2.95	0.988	0.705
0.7	2.93		0.719
0.6	2.88	0.953	0.747
0.5	2.80	0.871	0.783
0.4	2.66	0.731	0.842
0.3	2.50	0.582	0.904
0.2	2.30	0.412	0.957
0.1	2.10	0.278	0.990
0	1.88*	0.13*	1.000

* After the samples were dried at 70-80°C for ten hours under reduced pressure, the measurements of the infrared spectra were carried out in the room of approximately constant relative humidity (35-40%) and constant temperature (20°C) during twenty minutes. Under such experimental circumstances, the authors confirmed that the quantity of water contained in the film was quite small and the relative optical density of ν(CO) was affected to an extremely small extent by the contained water.

Extrapolated Values

These experimental results obtained by the authors and the results obtained by Argersinger and Davidson have been compared with the theoretical values.

Discussion

Activity coefficients vary with the exchange ratio (fraction n in the resin phase) for constant co-ordination number z and inter-ionic interaction energy ϕ. In case of an uni-uni-valent system, both activity coefficients vary symmetrically, but in the case of an uni-di-valent system the activity coefficient of the di-valent ion varies more intensively than the uni-valent ion, with the increase of the exchange ratio.

In this derivation, the authors wish to emphasize that the activity coefficients are predominantly affected by the interaction energy.

In the uni-uni-valent case, corresponding to $\phi<0$, $\phi=0$, or $\phi<0$, the activity ceofficients are found to be smaller than unity, equal to unity, or greater than unity, respectively. According to the experimental results obtained by the authors and Argersinger and Davidson, the resin activity coefficients in Na-H and NH_4-H systems were found to be smaller than unity, therefore $\phi<0$. But in the Ag-H exchange system, both activity coefficients were found to be larger than unity.

Argersinger and Davidson[5] have explained that the difference in both cases may be due to the greater dissimilarity between the silver and hydrogen resins, as compared with the sodium and hydrogen resins. According to the theory derived here, this difference may be explained as due to the inter-ionic interaction in the resin phase, which plays an extremely important role.

From the above statements, it is evident that an activity coefficient larger than unity corresponds to one case only, that is $\phi>0$. Accordingly the activity coefficients generally may be explained as a function of the ionic interaction energy between each ion pair. In Na-H and NH_4-H exchange systems of carboxymethylcellulose the interaction energies ϕ/kT of each system are about -0.1 and -0.7-0.8 respectively.

In the case of the uni-di-valent exchange, when $\phi=0$, the activity coefficients are not unity owing to the contribution due to the configurational term. The activity coefficients of the di-valent ion, as compared with those of the uni-valent ion, vary extremely depending on the exchange ratio, but are always

smaller than unity. On the other hand, the coefficients of the uni-valent ion in the uni-di-valent system have a trend similar to the uni-uni-valent case.

According to the experimental results by Argersinger and Davidson, the activity coefficients in the solid phase are affected only to an extremely small extent by the concentration of the electrolyt solutions. On the other hand, the activity coefficients are shown to be independent of the concentration of the electrolyte solutions and are denoted only as a function of n (equivalent fraction) in the resin phase. Thus the results obtained by the theoretical consideration coincide with experimental ones.

In real exchange phenomena, the experimental results would deviate more of less from the theory due to the following reasons:

1) The effect of the free ions which exist in the resin phase.

2) The swelling of the ion exchange resin actually does vary the exchange ratio, although it was assumed that the resin maintained a constant structure, independent of the exchange ratio.

3) The hydrated ions of Na and Ca have approximately the same volume under the same conditions. The ions of Na and Ca exist in the hydrated state in the resin phase. Therefore the size of each hydrated ion will also be nearly equal in the resin phase. Then the di-valent ion such as Ca would not be able to occupy the two ajacent sites completely, as was assumed in this theory.

In future work, it will be possible to predict and analyse the phenomena of both the "relative selectivity" of the ions in the exchanger and the separation efficiency, from the concept of the inter-ionic interraction involving ϕ. Of course, the size of the ions and the degree of hydration must be taken into consideration.

Conclusion

A theoretical treatment of activity coefficients in the resin phase of cation exchangers is given by using Guggenheim's theory which deals with "A Generalization of the Quasi-Chemical Method".

The results indicate that the activities in the resin phase are markedly affected by the interaction energy ϕ between ion pairs and they are expressed as a function of ϕ, z, r and n.

Experimental evidence indicates that this conclusion is useful in several cases to explain the activity behavior of ions in the resin phase.

As a result, it is pointed out that the activity behavior in the resin phase of cation exchanger would be generally explained fairly well by considerations of the concept of the interaction energy.

Department of Applied Chemistry
Faculty of Engineering
The University of Tokyo
Hongo, Tokyo

Distribution of Boron in Natural Waters

By Satoru MUTO

(Received November 2, 1955)

Introduction

The distribution of boron in natural waters was reported on some mineral springs[1], thermal springs[2], and irrigation waters[3]. The amounts of boron in the ground waters[4], rains and snows[5] were also reported by several authors. But the discussion on the distribution of boron in these waters has never been made in detail.

The author has reported on the boron content of mineral springs[6], thermal springs[7], river waters[8,9], rains[10], snows[11] and plant

1) T. Tagaya, et al., *Bull. Inst. Phys. Chem. Research* (Tokyo), **21**, 165 (1942).
2) T. Tagaya, et al., *Bull. Inst. Phys. Chem. Research* (Tokyo), **21**, 188 (1942).
3) L.V. Wilcox, *U.S. Dept. Agr. Tech. Bull.* No. 962, 40 (1948).
4) K. Sugihara, *J. Chem. Soc. Japan (Pure Chem. Sect.)*, **73**, 359 (1952).
5) K. Sugawara, *Science* (in Japanese), **18**, 485 (1948).
6) S. Muto, *J. Chem. Soc. Japan (Pure Chem. Sect.)*, **73**, 108 (1952).
7) S. Muto, ibid. **75**, 407 (1954).
8) S. Muto, ibid. **74**, 576 (1953).
9) S. Muto, ibid. **74**, 640 (1953).
10) S. Muto, ibid. **73**, 446 (1952).
11) S. Muto, ibid. **74**, 420 (1953).

ashes[12]. Although, the analyses were performed mainly with the samples from Kantô District, the author is of the opinion that the following discussion could be extended to the samples from various districts.

As an average content of boron in rains and snows, a value of 0.1 mg. B/l. was obtained. The Watarase River and the Kiriu River in Kantô District are supposed to have no supply of boron from mineral or thermal springs in the upper stream region, and the element seems to be supplied only by rains and snows. The average content of boron in these river waters is as much as 0.20 mg. B/l. Therefore, it is likely that rain and snow play an important role as the supplying source of boron to the rivers. Biological matters and soils are considered to be another supplying source of boron. The present author made the analyses of some plant ashes and obtained a value of 10–1000 p. p. m. B as the average content of the element, while some authors obtained the values of 0.1–1.2 p. p. m. B as the content of boron which exists in water-soluble form in soils[13]. In the main stream of the Tone River, the average content is 0.36 mg. B/l. This value is higher than those of the Watarase River and the Kiriu River. This high value may be due to the supply of boron by mineral and thermal springs, rich in boron, which issue in the upper stream region. The higher boron content is obtained among the mineral springs. For example, Isobe Mineral Spring has an average value of 123.3 mg. B/l. The thermal springs in Gunma Prefecture have an average value of about 10 mg. B/l.; they are supplying a large quantity of water in the upper stream region of the Agatsuma River. The Agatsuma River, which originates from the thermal spring region contains more than 1 mg. B/l. of the element. Numerous springs such as Kawarayu, Shima and Manza Springs etc. are located along the stream of this river.

Boron in Rain and Snow Waters

On the basis of chemical analyses of rain and snow waters which were reported by K. Sugawara and I. Iwasaki, the former author explained that boron was condensed remarkably in rain waters and the gravimetric ratios of boron to chlorine are 4000 times that of sea water[5]. Similar phenomena are for the ratios Ca/Cl and SO_4/Cl in rains and snows. K. Sugawara pointed out that the inorganic constituent of rain water originates from sea water and the rain of the hinterland has the greater value on the ratios Ca/Cl and SO_4/Cl. And he explained that this fact is based on the selective dissolution of the element to the rain.

In this study the present author collected 5 kinds of rain at Kiriu City. The boron content of the samples analysed by L. V. Wilcox's electrometric titration method[14] is summarised in Table I.

TABLE I

BORON CONTENT OF RAIN WATER

No.	Sampling station	Date	Cl mg./l.	B mg./l.	B/Cl
RKM-1	Kiriu	IX '51	2.9	0.03	0.011
RKM-2	Kiriu	VI '52	5.9	0.13	0.020
RKM-3	Kiriu	VI '52	1.3	0.11	0.084
RKM-4	Kiriu	VI '52	1.8	0.11	0.060
RKM-5	Kiriu	VI '52	0.3	0.11	0.367
Average value			2.44	0.098	0.0403
RAM-1*	8°34′ S 156°53′ E	II '52	176.7	0.13	0.001
Sea water (Western Pacific Ocean)[15]			18760.	4.73	0.00025

The gravimetric ratio of boron to chlorine in rain water is about 200 times that of sea water, but it is not clear whether or not the fact is due to the selective dissolution of boron in rain water. The average value of the element in rain water in Table I is about 0.1 mg. B/l. However, there is a possibility that the value tends to fluctuate according to the sampling station. Still more, the boron content of fresh snow is shown in Table II.

TABLE II

BORON CONTENT OF FRESH SNOW

No.	Sampling station	Date	Cl mg./l.	B mg./l.	B/Cl
SKM-1	Kiriu	II '52	2.7	0.04	0.015
SKM-2	Kiriu	II '52	2.2	0.13	0.059
SKM-3	Kiriu	III '52	2.7	0.15	0.056
Average value			2.53	0.107	0.0436
SNY-1	Norikura	VII '52	—	0.002	—
SSM-1	Sennokura	I '55	0.43	0.002	0.004
SAM-1*	64°18′ S 163°16′ E	XI '51	351.9	0.36	0.001

Although there were only a few samples, the boron content in fresh snow was found to be about 0.1 mg. B/l. The gravimetric ratio of boron to chlorine is approximately 0.04. In

12) S. Muto, *J. Chem. Soc. Japan (Pure Chem. Sect.)*, **75**, 1028 (1954).

13) J. A. Naftel, *Ind. Eng. Chem. Anal. Ed.*, **11**, 407 (1939).

14) L. V. Wilcox, *Ind. Eng. Chem. Anal. Ed.*, **4**, 38 (1932).

15) Y. Miyake, This Bulletin, **14**, 56 (1939).

* RAM-1 and SAM-1 were given for the reference of boron content of falling waters at the heart of the ocean. They were collected through the kindness of Taiyô Fisheries Co. while on duty, and the author offers his thanks for it.

other words, the boron content in fresh snow is almost equal to the rain water. It is notable that such lower values were obtained for the snow in a mountainous area (SNY–1, SSM–1).

Table III shows the boron content of a series of rains which were collected at different times from the begining of a rainfall.

TABLE III

BORON CONTENT OF RAIN PARTITIONS

Sample No.	Part	pH	Cl mg./l.	B mg./l.	B/Cl
KR-2	1	5.6	2.91	0.03	0.011
	2	—	—	0.03	—
	3	—	0.38	0.02	0.063
KR-5	1	6.7	5.86	0.13	0.022
	2	6.7	4.85	0.12	0.026
	3	6.7	0.50	0.11	0.210
KR-9	1	6.6	6.41	0.06	0.010
	2	6.6	1.95	0.08	0.041

The inorganic constituents of rain water are condensed in the initial stage of rain fall and as was shown in Table III. But when the table is more carefully observed, it is discovered that the rate of decrease in boron content is lower than that of chlorine. Consequently, the ratio of boron to chlorine in the later stage of rain fall is larger than in the initial stage.

Boron in River Waters

According to the above experiments, the water of rain and snow contains about 0.1 mg. B/l. Rains and snows are considered to be the main supplying source of water to the rivers and their tributaries. The boron content of the main stream of the Tone River in Kantô District is shown in Table IV.

TABLE IV

BORON CONTENT OF THE TONE RIVER

Sampling station No.	pH	Cl mg./l.	B mg./l.	B/Cl
St-1	—	6.48	0.38	0.059
St-2	—	6.89	0.40	0.058
St-3	6.9	7.16	0.40	0.056
St-4	6.8	6.89	0.36	0.052
St-5	6.9	6.21	0.40	0.066
St-6	6.9	5.54	0.45	0.081
St-7	6.8	5.27	0.45	0.081
St-8	6.9	5.67	0.28	0.049
St-9	6.8	5.67	0.16	0.028
St-10	6.9	5.94	0.13	0.022
Average		6.162	0.345	0.0560

According to Table IV, the boron content of the Tone River is approximately 3 times those of rain and snow, while the chlorine content is approximately 2.5 times larger than those of rain and snow. Therefore the gravimetric ratio of boron to chlorine is larger than those of rain and snow. As for the chlorine content of river water, for example, about 4 mg. Cl/l. is given by J. Kobayashi, et al.[16] for the Kôryô River at Hiroshima Prefecture, and 5.67 mg. Cl/l. by Clarke[17] as the average content of river waters. Compared to those values, the chlorine content of the Tone River gives rather high value. The social effect of human beings could be considered as one of the important supplying sources of chlorine, but the thermal and mineral springs in the upper stream region seem to be a more important source. The Watarase River and the Kiriu River, the tributaries of the Tone River have no springs in their upper stream region. The composition of those river waters is given in Table V, while the composition of the Agatsuma River and the Okuresawa River to which the spring waters are supplied in the upper stream are given in Table VI.

TABLE V

BORON CONTENT OF THE WATARASE RIVER AND THE KIRIU RIVER

(a) Watarase

Sample no.	pH	Cl mg./l.	B mg./l.	B/Cl
1	7.0	10.1	0.24	0.024
2	7.1	9.4	0.14	0.015
3	7.0	11.7	0.21	0.018
Average value		10.40	0.197	0.0190

(b) Kiriu

Sample no.	pH	Cl mg./l.	B mg./l.	B/Cl
1	6.6	0.16	0.30	1.879
2	6.9	0.17	0.15	0.879
3	7.2	0.11	0.20	1.818
4	7.2	0.14	0.25	1.799
5	7.2	0.16	0.17	1.063
6	7.1	0.21	0.17	0.810
Average value		0.158	0.207	1.310

TABLE VI

BORON CONTENT OF THE AGATSUMA AND THE OKURESAWA

(a) Agatsuma

Sample no.	pH	Cl mg./l.	B mg./l.	B/Cl
1	2.3	167.5	2.25	0.013
2	2.3	140.4	2.25	0.016
3	5.5	18.0	1.88	0.105
4	5.7	10.8	1.50	0.139
Average value		84.2	1.97	0.0234

16) J. Kobayashi, et al., *J. Chem. Soc. Japan (Pure Chem. Sect.)*, **72**, 567 (1951).

17) F.W. Clarke, "Data of Geochemistry", **63**, 119 (1924).

(b) Okuresawa

Sample no.	pH	Cl mg./l.	B mg./l.	B/Cl
1	2.4	3.5	0.75	0.214
2	2.9	0.7	1.88	2.689
3	2.9	1.4	1.23	0.985
4	3.0	3.5	1.25	0.357
Average value		2.28	1.305	0.5724

High boron content is observed for the Agatsuma River and the Okuresawa River which run through the thermal spring region, and have a minimum value of boron content for such rivers are about 1 mg. B/l. But as much as 0.2 mg./l. of boron content is observed for the Watarase River and the Kiriu River which have no supplying source of boron, like thermal springs. This value is almost equal to those of rain and snow. As the result of the social effect on its drainage, the Watarase River has high value of chlorine content, whereas the Kiriu River has no such drainage and the chlorine content is found to be very much lower than that of the former river. Therefore, the gravimetric ratio of boron to chlorine for the former is low, but the corresponding value for the latter is approximately 1. The Agatsuma River contains the larger amounts of boron and chlorine as the water of many thermal springs flows into the river directly. The values of boron and chlorine content of this river are about 2 mg. B/l., and 10–170 mg. Cl/l. respectively. Accordingly the ratio of lower value is observed for the upper stream and the value decreases for the lower stream which has no supplying source of boron, like springs. However, the value for the lower stream is higher than that of the main stream of the Tone River. The Okuresawa River contains no spring in its drainage so that the chlorine content of the river is almost 1–3 mg. Cl/l. It is slightly higher than those of rain and snow. But the boron content of the Okuresawa River is high and some supplying source of boron might be considered beside the spring.

Boron in Spring Waters

In the foregoing chapter, the author discussed one of the supplying sources of boron in river water. However, before we draw a definite conclusion about the source which supplies boron to river waters, the following three facts should be considered. Mineral and thermal springs, geological erosion and communities of human beings will have some effects on the boron content of river waters. And the effect of mineral and thermal springs will be discussed in this chapter.

The author has stated that the water of the Tone River has higher value of boron content owing to the existence of springs in its upper stream region. The springs which have highest boron content are among the alkaline common salt springs such as Isobe and Yashio Mineral Springs, etc. In Table VII some data on the boron content of the mineral springs are shown.

TABLE VII

BORON CONTENT OF ALKALINE COMMON SALT SPRINGS

Name	pH	Cl mg./l.	B mg./l.	B/Cl
Isobe No. 1	8.2	11926.	124.7	0.0105
Isobe No. 2	8.6	12658.	136.9	0.0108
Isobe No. 3	8.4	13642.	156.7	0.0115
Yashio No. 1	7.3	11004.	105.8	0.0096
Yashio No. 2	7.5	8262.	92.8	0.0112
Yashio No. 3	7.6	12989.	122.7	0.0084
Average Value		11747.3	123.33	0.01052

The gravimetric ratio of boron to chlorine for the samples in Table VII is about 0.01, which is lower than that of the Tone River, although the spring water shows the high value of boron and chlorine content. These spring waters are considered to be the petrified marine water similarly to the petroleum salt water. In these springs, the amount of flowings is not very large.

The neutral springs in Table VIII and acid springs in Table IX have large flowing amounts, but these give low boron and chlorine content.

TABLE VIII

BORON CONTENT OF NEUTRAL SPRINGS

Name	pH	Cl mg./l.	B mg./l.	B/Cl
Yunohana	7.3	361.3	5.98	0.0166
Yunokoya	7.5	122.6	4.35	0.0355
Kawarayu	5.8	322.3	8.75	0.0371
Kirizumi	7.1	48.9	0.59	0.0121
Hatonoyu	7.9	683.4	7.01	0.0103
Takaragawa	7.6	246.3	4.44	0.0180
Minakami	7.6	145.9	4.94	0.0340
Sarugakyo	7.4	342.5	14.81	0.0433

TABLE IX

BORON CONTENT OF ACID SPRINGS

Name	pH	Cl mg./l.	B mg./l.	B/Cl
Kusatsu No. 1	2.0	470.5	9.84	0.0210
Kusatsu No. 2	2.0	645.4	3.92	0.0069
Manza No. 1	—	501.8	9.97	0.0199
Manza No. 2	—	123.9	3.98	0.0321
Average value of neutral and acid sprins.		334.61	6.547	0.01964

Generally, the boron and chlorine content of the neutral and acid springs are almost the same and considerably lower than that of the alkaline common salt springs. The

gravimetric ratio of boron to chlorine of the former springs has the higher value than the latter springs. But the average ratio for all springs is lower than that of the main stream of the Tone River.

Summary

On the basis of the data and discussions in the preceding chapters, the distribution and migration of boron in natural waters are summarized in Figure 1. And the data in the figure were confirmed mainly with the samples from Kanto District, whereas the author is of the opinion that the distribution of boron and chlorine in natural waters is generally illustrated as here shown.

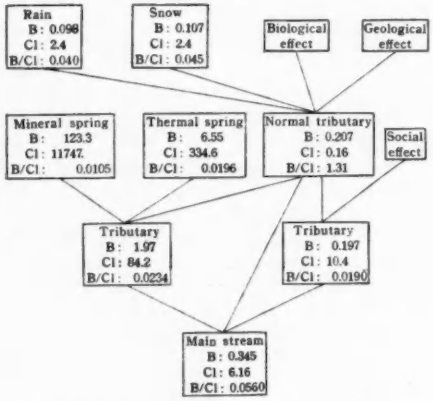

Fig. 1. Boron in natural waters (mg./l.).

The water of rain and snow at Kiriu District contain 0.1 mg. B/l., and 2.4 mg. Cl/l., and the ratio of boron to chlorine is 0.04. (these values might be lower at high mountainous area) Being affected by the biological and geological influences of the drainage, the original water becomes to contain 0.2 mg. B/l. and 0.16 mg. Cl/l. The ratio of boron to chlorine amounts to 1.31 as in the Kiriu River. At this stage, the increase of boron content or decrease of chlorine content are remarkable. When these branches of tributaries are affected by the mineral springs (123.3 mg. B/l., 11747 mg. Cl/l. and 0.0105 of B/Cl) and the thermal springs (6.55 mg. B/l., 334.6 mg. Cl/l. and 0.0196 of B/Cl) the boron and chlorine contont change their value to 1.97 mg. B/l., 84.2 mg. Cl/l. as well as the ratio of boron to chlorine 0.0234 as respectively in the Okuresawa River and the Agatsuma River. And the values of 0.197 mg. B/l., 10.4 mg. Cl/l. and boron to chlorine 0.0190 are obtained for the Watarase River which is affected by communities. Of course the actual condition will not be so simple and many complicated factors may exist before they join the river water. The main stream collects various kinds of tributaries and comes to have the value of 0.345 mg. B/l., 6.16 mg. Cl/l. and the ratio of boron to chlorine 0.0560. Then the stream flows down to the ocean while it is affected by many kinds of things during the way.

The auther's best thanks are due to Dr. S. Matsuura and Dr. N. Yamagata for their continued interest and advice.

Kiriu College of Technology
Gunma University
Kiriu

Study on the Electric Conductivity of Sodium Silicate Aqueous Solution. I.

By Hiroshi UKIHASHI

(Received November 14, 1955)

Introduction

The electric conductivity of sodium silicate solution has been only rarely reported, since Harman[1] measured it in 1925 in one of his consecutive experiments attempted for the electrochemical investigation of this solution. Though his experiment exceeds far beyond that previously reported by Kohlrausch[2], with repect to the range of molar ratio and concentration of solutions measured, it still lacks satisfactory abundance of data, especially for higher concentration. In the present study the measurement was made for the solution of molar ratio (SiO_2/Na_2O) 1.00, 1.52, 2.15, 3.02. and 3.95 at the concentration ranging from 0.001 N up to that, over which the solution hardly flows due to high viscosity, with reasonable numbers of measured points between both extreme concentrations. Where the ratio and concentration of the hereby measured silicate solutions corresponds to those measured by Harman, the two values were in good accordance.

The equivalent conductivity was derived from the specific conductivity, using the molecular weight as indicated by a formula. Thus far no theoretical treatment has been given for the conductivity of sodium silicate solution. Herein theoretical calculation was attempted for the equivalent conductivity of the molar ratio 3.95 silicate solution, and the results were found to be in good agreement with experimental data, if some supposition was admitted. In lower ratio solution, as hydrolysis takes place considerably, the results could not be dealt with theoretically, due to the complicated state of ions in solution.

Experimental

Materials.—Two methods were used for the preparation of pure sodium silicate solution. (1) First, sodium metasilicate crystal $Na_2(H_2SiO_4)\cdot 8H_2O$ was prepared by the following method from the original solution of molar ratio 3.0 and Na_2O concentration of 9%, then it was electrolyzed with mercury cathode to obtain the desired molar ratio. The original solution, of commerical grade produced by Asahi Glass Co., was diluted by the same volume of water, adding 2 volumes of NaOH solution of sp. gr. 1.26 and 2 volumes of ethyl alcohol. A small number of crystals were used as nuclei in order to hasten the crystallization which otherwise would have taken several days. After the crystals developed, they were filtered off by Buchner funnel, washed by 50% alcohol, drained off thoroughly, then resolved again into pure water. To the solution, containing about 20% sodium metasilicate, was added one tenth volume of NaOH solution (sp. gr.=1.26), ethyl alcohol and a bit of nuclei. The solution was kept cool in ice water under stirring. Then sodium metasilicate recrystallized out in a few hours. This was filtered off, washed, drained and dried completely in a vacuum desiccator. The stock solution was prepared by dissolving these crystals. In order to make higher molar ratio silicate solution, this stock solution, usually containing 20% metasilicates was electrolyzed with mercury cathode and rotating platinum plate anode. An electrolytic cell is shown in Fig. 1.

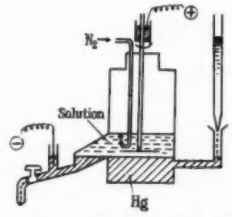

Fig. 1. Electrolytic cell.

The anode, a disk of 5 cm. diameter, was rotated with a velocity of 200 r. p. m. keeping 5 mm. away from the surface of mercury. The Na-amalgam produced was pushed out towards the outlet owing to the increased surface level caused by constantly supplied fresh mercury. During the electrolysis CO_2-free nitrogen gas was bubbled through the solution. In a run 150 cc. of solution was treated. The current density was kept at 0.8 amp. per sq. cm. Electrolysis was conducted for the time necessary for removing the definite amount of Na_2O to reach the degired molar ratio. (2) As it was time-consuming to make a concentrated solution of high molar ratio by the foregoing method, the following method of purification was substituted for it. The original various solutions, of commercial grade, were diluted to the concentration of about 3% Na_2O. After being filtered twice through hardened, alkali-proof filter paper, they were concentrated by vacuum evaporation. The

1) R.W. Harman, *J. Phys. Chem.*, **29**, 1155 (1925).
2) F.W. Kohlrausch, *Z. Physik. Chem.*, **12**, 773 (1893).

products were quite transparent, though retaining their original yellowish colour. The silicate solutions of ratio 2 prepared by the two methods were compared with each other as to their conductivity. The results showed no significant differences between the two series of data. The stock solutions thus prepared were analysed respecting their SiO_2 and Na_2O content and the molar ratio was decided strictly. Besides, the CO_2 content was analysed for check because of its deleterious effects. The more dilute solutions were prepared by diluting the stock solution with pure water which was distilled twice using quartz apparatus. It has the conductivity of $1\sim2\times10^{-6}$ $\Omega^{-1}\,cm^{-1}$. Every solution was stored in a polyethylene bottle free from the atmosphere. All chemicals used were of reagent grade.

Apparatus for the Conductivity Measurement.—Conductivity was measured by Wheatstone bridge, using cathode ray oscillograph as detector. The bridge consisted of shielded variable resistance boxes, of which two had 10,000 Ω, and one 100,000 Ω. A variable condenser was set up parallel with the latter one. The measurement was made at 1000 cycles. A variable audio-frequency oscillator served as current source. The constants of four conductivity cells used were 1.242, 1.380, 0.4850 and 0.6568. The former two had platinized electrodes and they were used for the concentrated silicate solutions, the latter two, used for the dilute solution had non-platinized electrodes. The inner surface of the cell was coated with epoxy resin film to protect the glass wall from corrosion by the alkaline solution. The temperature was controlled to ±0.01° at 25°C, employing a double thermostat with sensitive regulator operated by electronics circuit.

Measurement.—Measurement was made at twenty-four hours after new dilute solution had been prepared, except for a very dilute solution, where it was made at thirty minutes after the preparation. The variation of conductivity with time was small enough to allow the later theoretical consideration without correction, even with very dilute solutions. The data were reproduced within ±0.2% except for a very dilute solution. The cell constant was checked frequently with 0.01 N or 0.1 N KCl standard solution. Even after the most concentrated silicate solution was measured, the constant did not change appreciably, if washed carefully.

Results

The specific conductivity λ for various molar ratio sodium silicate solutions is shown in Fig. 2 and Fig. 3. The concentration is indicated by Na_2O weight percent. The conductivity increases with increasing concentration until it attains its maximum, then begins to decrease. This tendency of conductivity curve is not very different from what is seen with common low molecular electrolyte solution. As shown here, all the curves seem to have much the same form regardless of molar ratio of sodium silicate solution, although the change of conductivity becomes greater as the molar ratio of solution decreases. It is noteworthy that the form of conductivity curves, having similarity among different molar solutions, appears to have little dependence on

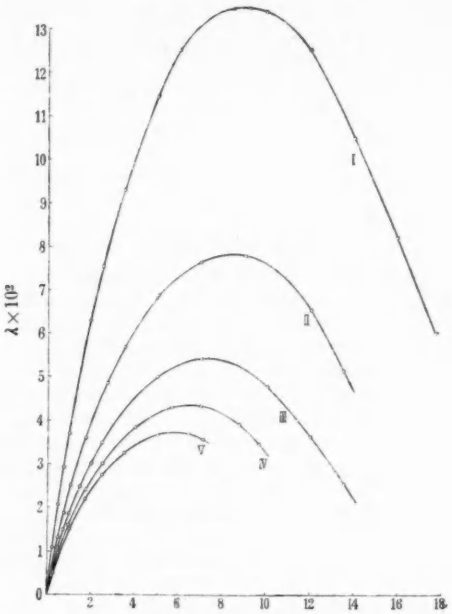

Fig. 2. Variation of specific conductivity of sodium silicate solutions with concentration at 25°C.

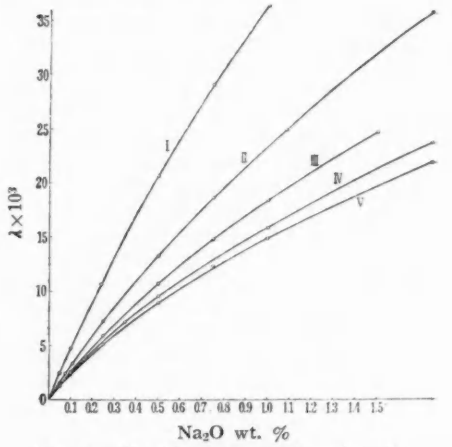

Fig. 3. Specific conductivity of sodium silicate solutions for lower concentration range at 25°C. Molar ratio, I 1.00; II 1.52; III 2.15; IV 3.02; V 3.95.

their viscosity. For instance the solution of molar ratio 3.95 has the maximum specific conductivity at the concentration of 6%, and at 7% it has a slightly lower, but still high conductivity. However, viscosity increases surprisingly between the two concentrations (0.25 poise at 6%, more than 1000 poise at 7%). On the other hand, for the solution of molar ratio 2.15, viscosity changes slowly from 0.032 poise at the concentration where maximum conductivity is shown, to 1.03 poise at as high as 13%. Also there is only a little increase of viscosity for the metasilicate solution over the measured concentration range, though specific conductivity varies very widely.

Fig. 4 shows the change of specific conductivity with molar ratio of silicate solution

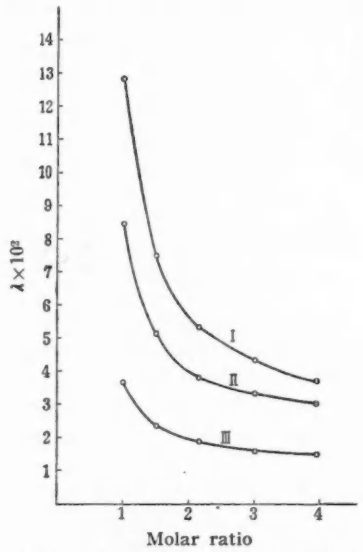

Fig. 4. Relationship between specific conductivity and molar ratio. Na_2O wt. %. I 6.50; II 3.00; III 1.00.

of the definite Na_2O content. The variation of conductivity with the ratio appears to be sharp around molar ratio 2. This would be explained by the fact that hydrolysis increases rapidly as the molar ratio of solution falls below 2, and OH ion with exceptionally high mobility comes to contribute to the conductivity.

Equivalent conductivity Λ was calculated from the following equation.

$$\Lambda = 1000\,\lambda \cdot N/A \cdot d = 1000\,\lambda/C$$

A represents the solid content (g.) per 1000 g. solution, d, the density of solution, N, normal weight, and C, normality. For the estimation of normality, expressed with regard to Na gram equivalent per 1000 cc. of solution, molecular composition such as Na_2SiO_3, $Na_2O \cdot 2SiO_2$, $Na_2O \cdot 3SiO_2$, etc. was employed. Thus, for example, 1 N solution of 2.15 molar solution contains 1/2 ($Na_2O \cdot 2.15\,SiO_2$) expressed in grams, in 1000 cc. solution. Fig. 5 shows Λ vs. C curves for various

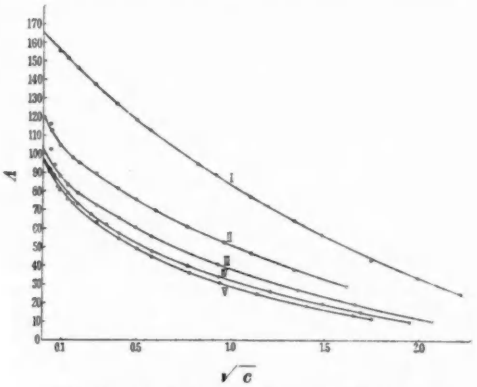

Fig. 5. Variation of the equivalent conductivity of various sodium silicate solutions with square root of concentration. Molar ratio, I 1.00; II 1.52; III 2.15; IV 3.02; V 3.95.

silicate solutions. The fact that curves in Fig. 5 show no breaking point would evict any idea of discontinuous change of molecular constitution, e. g. micelle formation, over the whole range of concentration. At the extreme dilution it appear that equivalent conductivity tends to go up irregularly high, so that it is difficult to extrapolate them to zero concentration. It may have been caused partly by hydrolysis effect[3].

Nevertheless, limiting equivalent conductivity was estimated by the extrapolation of curves on Fig. 5. The extrapolation would have eliminated the effect of hydrolysis which increased rapidly below the concentration of 0.005 N. Thus obtained values for silicate solution of molar ratio 1.00, 1.52, 2.15, 3.02 and 3.95 were 165, 120, 103, 98, and 96 respectively. Since the limiting equivalent conductivity of sodium ion is 50.1, that of silicate ion seems to be fairly high, almost comparable with that of sodium ion, taking into consideration the fact that the contribution of OH ion is very small for the higher molar ratio solution[4].

3) Harman[5] calculated hydrolysis percentage for various molar ratio solutions from the pH values, showing that it increases rapidly in the extreme dilution for the lower ratio solution.

4) According to Harman's data hydrolysis % of $Na_2O \cdot 4SiO_2$ solution at 0.01N is 1.5% which contributes only 2 to its limiting equivalent conductivity.

Discussion

It is well accepted that a molecule of sodium metasilicate[6,7] consists of $Na_2(H_2SiO_4)$ which dissociates in solution into four kinds of ion, i.e. Na^+, $H_3SiO_4^-$, $H_2SiO_4^{--}$ and OH^-. Here OH^- ion is brought about by hydrolysis which takes place in two steps,

$$H_2SiO_4^{--} + H_2O \rightleftarrows H_3SiO_4^- + OH^-$$
$$H_3SiO_4^- + H_2O \rightleftarrows H_4SiO_4 + OH^-$$

As for the silicate solutions having other molar ratio than 1, there is not yet a definite theory as to the kinds and behaviors of ions present in solution. However, the light scattering experiments[8] revealed that in these solutions molecules were still not of large size as with organic high molecular compound, but at most, of several hundreds in molecular weight. This fact was also well explained by viscometric study[8,9]. Furthermore there are other indications[7,10] showing that the existence of molecular-type compounds such as expressed by $Na_2O \cdot 2SiO_2$, $Na_2O \cdot 3SiO_2$, etc.[11] in solution may not be highly inadequate. First of all, assuming this is the case, it was attempted to see whether the equivalent conductance could be explained by theory. For this purpose the silicate solution of molar ratio 3.95 was sampled, because its negligible hydrolysis made it possible to consider the existence of only two kinds of ion, i.e. two sodium ions and one silicate ion. Secondly it was assumed that the silicate ion possessed two minus charges as a result of dissociation of two sodium ion. The theoretical treatment was based on Falkenhagen's equation which was the recent theoretical extension of the theory of Onsager to include the effect of definite ionic size and has been proved to show excellent agreement with experimental data for 1:1 type electrolyte solution[12].

Wishow and Stokes[13] showed furthermore, that Falkenhagen's equation stands good for 1:1 electrolyte solution up to surprisingly high concentration if applied with the correction for bulk viscosity. For unsymmetrical electrolytes, the apparent defect of the theory, caused by the unsatisfactory convergence of electrophoretic terms may be eliminated, if a large effective ionic diameter can be assigned to them. With these facts, it would be interesting to attempt here the comparison of the experimental data with those derived from the theory, though electrolyte was assumed hereby to be 1:2 type instead of 1:1.

Falkenhagen's expression for the equivalent conductivity of single electrolyte solution is written as follows:

$$\Lambda = \left\{ \Lambda^0 - \frac{1.546 \times 10^{-7}}{6\pi\eta} (|z_1| + |z_2|) \frac{\kappa}{1+\kappa a} \right\} \times \left(1 + \frac{\Delta X}{X} \right)$$

$$\kappa = \left(\frac{8\pi N e^2}{1000 \varepsilon K T} \right)^{1/2} \sqrt{I}$$

e: electronic charge
N: Avogadro's number
η: viscosity of solvent
z_1, z_2: valencies of cations and anions respectively
I: ionic strength
K: Boltzmann's constant
T: absolute temperature
ε: dielectric constant of solvent
a: mean ionic diameter

The second term on the right hand expresses the electrophoretic effect on conductivity. The last term $\Delta X/X$ expresses the relaxation field and is shown as[14]

$$\frac{\Delta X}{X} = \frac{z_1 z_2 e^2}{3\varepsilon K T} \cdot \frac{q}{1-q} \cdot \frac{\kappa}{\kappa a (1+\kappa a)} [e^{\kappa a (1-\sqrt{q})} - 1]$$

q is defined by

$$q = \frac{z_1 z_2}{|z_1 + z_2|} \cdot \frac{\lambda_1^0 + \lambda_2^0}{z_2 \lambda_1^0 + z_1 \lambda_2^0}$$
$$= \frac{|z_1 z_2|}{(z_1 + z_2)(z_2 t_1^0 + |z_1| t_2^0)}$$

t_1, t_2 and λ_1^0, λ_2^0 denote transport number and equivalent conductivity of cation and anion respectively at infinite dilution. Here the Eigen and Wicke distribution function was replaced by the Boltzmann distribution function.

Inserting the values of constants the equation reduces to

$$\Lambda = \left(\Lambda^0 - \frac{156.5}{1+0.568\mathring{a}\sqrt{c}} \right) \times \left(1 - \frac{0.721\sqrt{c}}{1+0.568\mathring{a}\sqrt{c}} \cdot F \right)$$

5) R.W. Harman, *J. Phys. Chem.*, **30**, 1100 (1926).
6) E. Thilo and W. Miedreich, *Z. anorg. allgem. Chem.*, **267**, 76 (1951).
7) P.P. Roller and G. Erwin, *J. Am. Chem. Soc.*, **62**, 461 (1940).
8) P. Debye and P.V. Nauman, *J. Phys. Chem.*, **55**, 1 (1951).
9) H. Ukihashi, *Reports of the Research Laboratory, Asahi Glass Co.*, Vol. II. No. 1, 48 (1952).
10) R.W. Harman, *J. Phys. Chem.*, **30**, 359 (1926).
11) The foregoing molecular formulae are stoichiometrically satisfied by writing as $Na_2O \cdot 2SiO_2 \cdot 2H_2O$, $Na_2O \cdot 3SiO_2 \cdot 3H_2O$, etc.
12) R.A. Robinson and R.H. Stokes, *J. Am. Chem. Soc.*, **76**, 1991 (1954).
13) B.F. Wishaw and R.H. Stokes, *J. Am. Chem. Soc.*, **76**, 2065 (1954).
14) R.H. Stokes, *J. Am. Chem. Soc.*, **76**, 1988 (1954).

$$F=(e^{\kappa a(1-\sqrt{q})}-1)/\kappa a(1-\sqrt{q}),$$
$$\kappa a=0.568\mathring{a}\sqrt{c}$$

$\mathring{a}$: mean ionic diameter expressed in Ångstrom

In order to calculate the equivalent conductivity of sodium silicate solution according to this equation it is important to assign the most probable value to $\mathring{a}$ and q. Here, t_1 was assumed to be equal to t_2, thus $t_1=t_2=0.5$. This assumption would not be so far away from the truth, as judged from the value of limiting equivalent conductivity and also the result obtained by Harman[10] regarding the transport number of sodium silicate solution[15]. For evaluating $\mathring{a}$, calculations were made on the equation by inserting to it various values of $\mathring{a}$, and the results were plotted on Fig. 6. It seems that the use of the value 7 Å. of $\mathring{a}$ on the calculation fits best for the agreement between experimental and theoretical curve. This value appears rather small. However, if attention is turned to the fact that at the concentration where the viscosity of sodium silicate solution abruptly increases to a remarkable degree, the distance between solute molecules was approximately 10 Å.[8,9], it would be allowable value, considering the hydration effect in the above case, along with such a discrepancy between the value of $\mathring{a}$ required theoretically and estimated from ionic radii, as usually encountered in the case of unsymmetrical electrolyte solution.

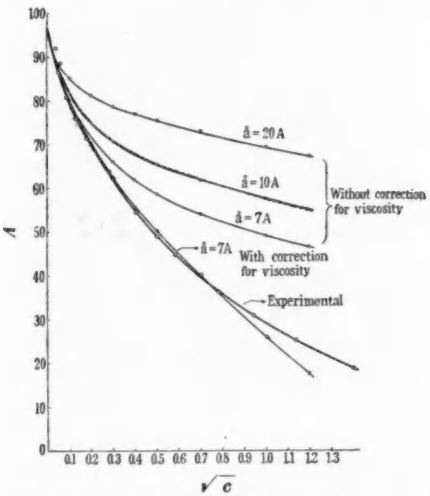

Fig. 6. Comparison of the equivalent conductivity of sodium silicate solution of molar ratio 3.95 with those calculated from the theoretical equation.

Since sodium silicate solution bears high viscosity owing to its hydration as with lithium chloride solution[13], the correction for the bulk viscosity would be necessary. For this purpose, Falkenhagen's equation has to be divided by relative viscosity of solution. After this was done, the agreement was further improved up to the higher concentration, about 0.8 N (2% of Na_2O concentration). Above that, the viscosity correction increases rapidly so that the theoretical line fall increasingly below the experimental values.

Thus, it is possible to explain the conductivity of sodium silicate solution, within the moderate concentration range, on the basis that its molecule essentially be small, and silica ion be polymerized to such an extent as expressed by its formula, even if it might be supposed to contain some aggregated molecules in the higher concentration. This fact is well consistent with the results obtained by both viscometric and light-scattering investigation.

The author wishes to express his sincere thanks to Dr. Tadashi Yawataya for his inspiring support and kind interest in this work.

Research Laboratory, Asahi Glass Co., Ltd., Bentencho, Tsurumi-ku Yokohama

15) A little difference in this value does not affect sensitively on the result of calculation. In Fig. 6 a curve is drawn which was obtained by using the values $t_1=0.6$, $t_2=0.4$ as a comparison.

SHORT COMMUNICATIONS

Ion Dissociation in a Parabola Mass-spectrogram

By Yosaburo Yoshikawa and Kozo Hirota

If we ionize some molecules by the electron-impact method, instead of the usual glow-discharge method, in a Thomson's parabola mass-spectrograph, several spots will appear, all of which correspond to the ions deflected to the same degree by the electric field. However, Henglein and Ewald[1] found that secondary spots also appear lying on parabolas and taking the positions of the lower energy side, i.e., on the right side of the vertical line x_0 formed by the primary spots, as shown in Fig. 1. They ascribed the secondary spots to the ion fragments which cracked, flinging themselves between the ionizing and analyzing field, and

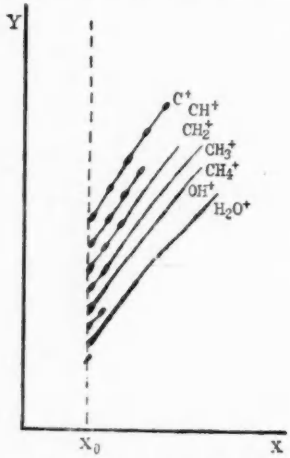

Fig. 1. Ion dissociation; mass-spectrogram of illuminating gas taken by Henglein and Ewald[1].

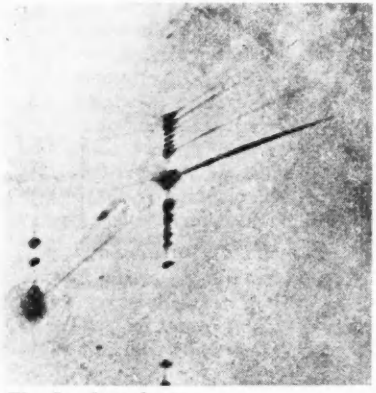

Fig. 3. Acetylene:
Impact electron voltage 200 V,
Ion accelating valtage 7500 V.

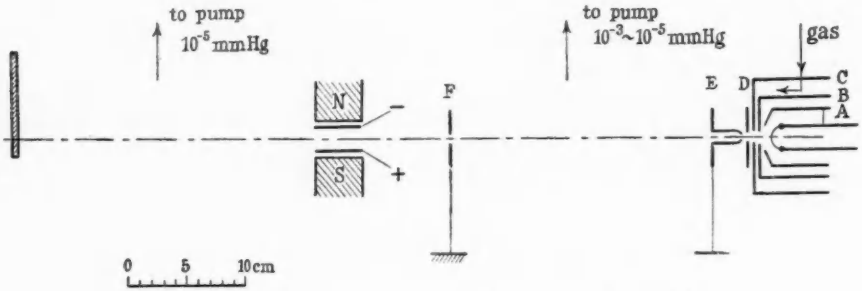

S_A	4 mmφ	A ~ B (+)	50 ~ 200 V
S_B	2 〃	B ~ C (−)	4.5 V
S_C	3 〃		
S_D	1 〃	C ~ D (−)	4.5 V
S_E	0.3 〃		
S_F	0.1 〃	D ~ E (−)	0.5 ~ 20 KV

Fig. 2. Scheme of the apparatus.

their energy thus became smaller than that of the primary ions, while their velocity was kept constant.

The authors repeated their experiment, but found slightly different results as will be described.

The ionizing chamber and scheme of the apparatus are shown in Fig. 2, while two examples of the mass-spectrograms taken are shown in Fig. 3 (acetylene) and Fig. 4

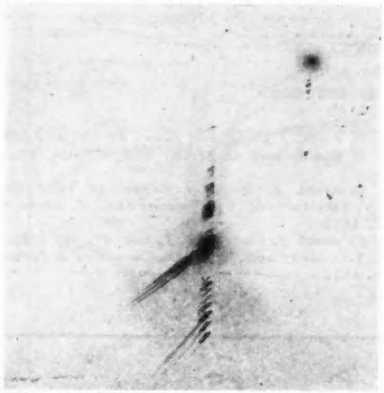

Fig. 4. Ethylene:
Impact electron voltage 100 V,
Ion accelating voltage 7500 V.

ethylene). It will be seen clearly that several spots of secondary ions really appear together with some secondary lines, and that the secondary spots have more prolonged tails than those of Henglein and Ewald. Moreover, our secondary "spots" do not appear in the parabolas whose m/e is 12-15, but the intense ones correspond to m/e=26 ($C_2H_2^+$) in Fig. 3 and to m/e=28 ($C_2H_4^+$) in Fig. 4; they are calculated to be the dissociation fragments of the polymerized acetylene and ethylene ($(C_2H_2)_3^{++} \rightarrow C_2H_2^+$ and $(C_2H_4)_3^{++} \rightarrow C_2H_4^+$, etc.), respectively. Such a result may be due to the difference of the apparatus and, even more, of the experimental conditions. To our regret, owing to the brief description given by Henglein and Ewald, we cannot discuss the real cause of the present discrepancy in detail.

The time of the ions flinging themselves between the ionizing and analyzing field is calculated to be the order of 10^{-7} second, the secondary "spots" being thus produced by the ions cracked within that time. It is smaller by one order of magnitude than the mean life of the metastable ions found by Hipple and others[2].

Detailed studies are going on.

The authors are greatly indebted to Dr. K. Ogata and his laboratory members for affording various kinds of conveniences to their work, and express their thanks to Mr. T. Nakatsuka for preparing Schumann plates.

Chemical Department, Science Faculty
Osaka University, Osaka

1) A. Henglein and H. Ewald, "Mass Spectroscopy in Physics Research" (1953), p. 205.
2) J.A. Hipple and E.U. Condon, *Phys. Rev.*, **68**, 54 (1945).

Structure of the Agarose Constituent of Agar-agar

By Choji Araki

(Received February 7, 1956)

The latest communication[1] together with the previous ones contributed from this laboratory has enabled me to come to the following conclusion concerning the composition and the structure of agar.

Agar is composed of two polysaccharides, agarose and agaropectin, a composition similar to starch, which is composed of amylose and amylopectin. Agarose, a main constituent of agar, exhibits a composition $[C_{12}H_{14}O_5(OH)_4]_n$; whereas agaropectin is a more complicated polysaccharide with sulfuric and uronic acid residues. This view is supported by the actual separation of the acetylated agar into two different constituents; agarose acetate and agaropectin acetate, most of the sulfuric acid and uronic acid present in agar being accumulated in the latter constituent[2]. The former constituent, having the formula $[C_{12}H_{14}O_5(OCOCH_3)_4]_n$, is converted into the corresponding methyl ether $[C_{12}H_{14}O_5(OCH_3)_4]_n$ being treated with dimethylsulfate and sodium hydroxide[3].

Now, it is possible to propose that agarose consists of alternatively repeated residues of 1,3-linked β-D-galactopyranose and 1,4-linked 3,6-anhydro-α-L-galactopyranose as shown in Fig. 1, the chain being terminated by D-galactose and 3,6-anhydro-L-galactose residues at the reducing and non-reducing ends, respectively.

The above structure, which is in agreement with the composition $[C_{12}H_{14}O_5(OH)_4]_n$, accounts for all the experimental facts reported previously. Since the 3,6-anhydro-L-galactoside linkages appearing every second unit in the molecule are extremely susceptible to acid-cleavage, even very mild methano

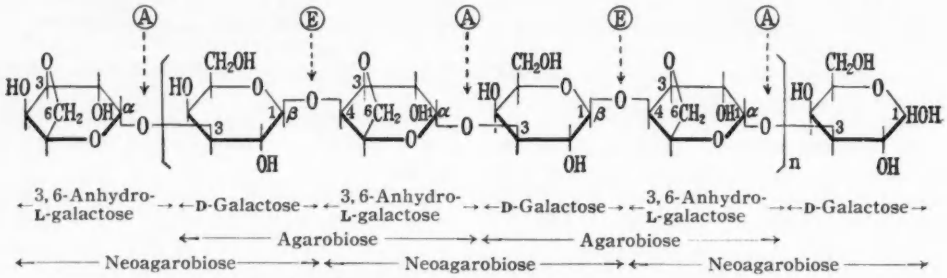

Fig. 1. Possible structure of agarose.
Ⓐ: the position cleaved by acid.
Ⓔ: the position cleaved by enzymes.

lysis led to the isolation of agarobiose dimethylacetal in an excellent yield, together with small amounts of methyl D-galactoside and 3, 6-anhydro-L-galactose dimethylacetal[4]. The last two products are inferred to have arisen chiefly from the reducing and non-reducing ends of the molecule, respectively. The partial acid-hydrolysis[5] and mercaptolysis[6] also afforded agarobiose (4-*O*-β-D-galactopyranosyl-3, 6-anhydro-L-galactose) and its diethylmercaptal, respectively, supporting the structure proposed. On the other hand, when agar was subjected to the enzymatic hydrolysis[1], neither D-galactose nor 3, 6-anhydro-L-galactose was detected in the hydrolysate, but neoagarobiose (3-*O*-3, 6-anhydro-α-L-galactopyranosyl-D-galactose) was isolated as the lowest cleavage fragment. This fact is also explained by the structure, if the enzymes are capable of splitting only the β-D-galactoside linkages. Moreover, the structure is in accordance with the fact that scission of the methylated agarose yielded 2, 4, 6-tri-*O*-methyl-D-galactose[7], 2-*O*-methyl-3, 6-anhydro-L-galactose[8], and none of tetra-*O*-methyl-D-galactose. In addition, the absence of adjacent hydroxyl groups in the molecule of the polysaccharide is corroborated by the observation of Barry and Dillon[9] that agar consumed no periodate at all.

In conclusion, all the experimental results are compatible with only one structure (Fig. 1) for agarose, which constitutes the greatest part of agar. The sole problem to be solved is whether it is a linear polysaccharide or a branched one.

Faculty of Industrial Arts
Kyoto Technical University
Matsugasaki, Kyoto

1) C. Araki and K. Arai, This Bulletin, **29**, 339 (1956).
2) C. Araki, *J. Chem. Soc. Japan*, **58**, 1338 (1937).
3) C. Araki, *J. Chem. Soc. Japan*, **58**, 1351 (1937).
4) C. Araki and S. Hirase, This Bulletin, **27**, 109 (1954).
5) C. Araki, *J. Chem. Soc. Japan*, **65**, 533, 627 (1944).
6) S. Hirase and C. Araki, This Bulletin, **27**, 105 (1954).
7) C. Araki, *J. Chem. Soc. Japan*, **58**, 1362 (1937); E.G.V. Percival and J.C. Sommerville, *J. Chem. Soc.*, **1937**, 1615.
8) C. Araki, *J. Chem. Soc. Japan*, **61**, 775 (1940).
9) V.C. Barry and T. Dillon, *Chemistry & Industry*, **1944**, 167.

*On the Dismutation Process of Zinc Ion**

By Hideo IMAI and Hiroshi SUNAHARA

(Received February 7, 1956)

In the current-potential curve of the Ševčik type oscillographic polarograph a quantitative relation between the cathodic and anodic currents of zinc ion was found.

Under the high rate of variation of the applied voltage (20 c. p. s., 50 v./s) the cathodic branch of zinc ion consists of two peaks in the solution containing iodide ions or bromide ions. On the contrary, a single peak can be observed in the anodic branch, as is illustrated in Figs. 1 and 2. Since the first cathodic peak is symmetrical with the anodic one, the first reduction is assumed to be reversible, and the second reduction to be irreversible. In this case the cathodic currents superposed on each other were estimated by the modified method developed by the present authors[1] (cf. Breyer et al.[2]).

The cathodic currents and the anodic currents thus estimated are plotted against the concentration of KI and KBr in Fig. 3 or 4, respectively. In this case the ionic strength of the supporting electrolyte is maintained at a constant value as much as 4 mol./l. by adding KNO_3 solution. In Fig. 3 it is easy to see that the value of $R_1+1/2\ R_2$ is, in any case, equal to the anodic current. This rela-

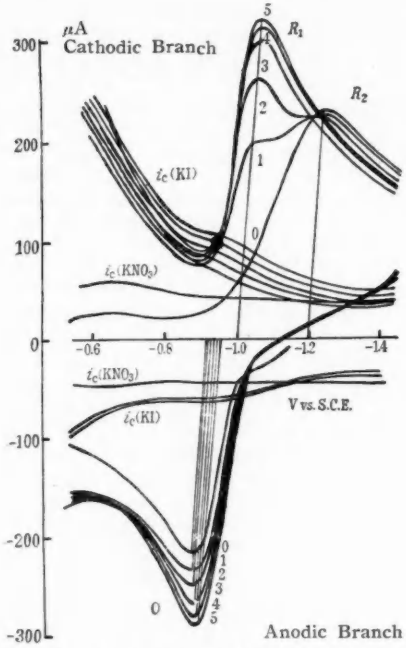

Fig. 1. Current-potential oscillograms of 0.37 mM Zn^{++} in various concentrations of KI (O-oM KI, 1-0.45 M KI, 2-0.9 M KI, 3-1.8 M KI, 4-2.7 M KI, 5-3.6 M KI, i_c-charging current).

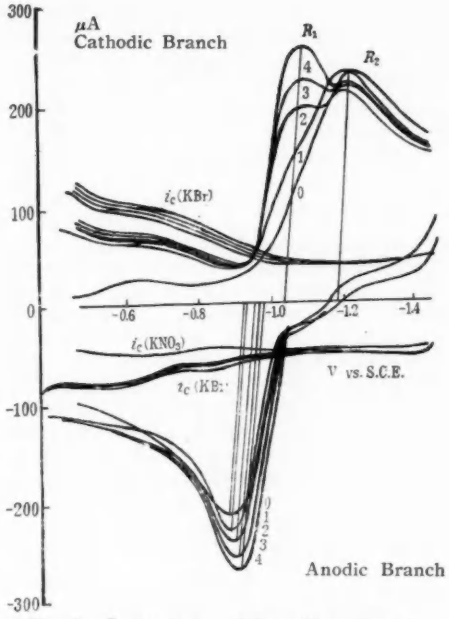

Fig. 2. Current-potential oscillograms of 0.73 mM Zn^{++} in various concentrations of KBr (O-oM KBr, 1-0.59 M KBr, 2-1.77 M KBr, 3-2.95 M KBr, 4-4.0 M KBr, i_c-charing current).

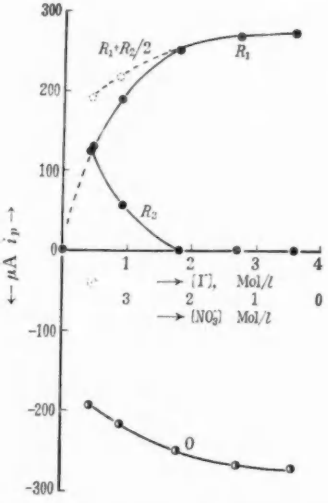

Fig. 3. Variation of the peak current with the concentration of KI.

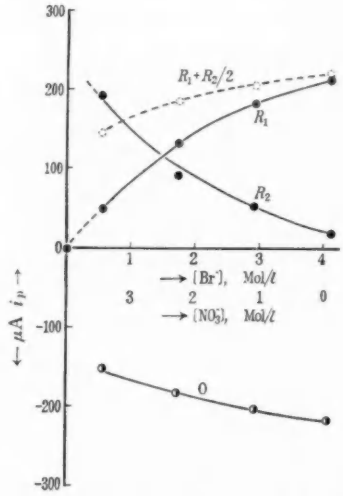

Fig. 4. Variation of the peak current with the concentration of KBr.

tion is better realized in Fig. 4.

From these results it can be reasoned that a half of the irreversible peak current corresponds to the reversible one in yielding

the anodic current. Supposing that the dismutation process proposed by Heyrovský[3] is the case mentioned above, the reversible process, in which the electron transfer is facilitated by the catalytic action of anions such as iodide or bromide ions, results from the repetition of a cycile process, $2Zn^{++}+2e \rightleftarrows 2Zn^{+} \rightarrow Zn^{++}+Zn$, and yields the reduced metal the concentration of which is equivalent to that of the oxidant. Virtually this process is party limited except in the case of the solution containing more than 2 mol./l. I^-, and the residual oxidant is reduced in the second reduction when the applied potential shifts toward the more negative potential.

The irreversible process (R_2), however, is limited in the reaction, $2Zn^{++}+2e \rightarrow 2Zn^{+} \rightarrow Zn^{++}+Zn$. In this case the concentration of the reduced metal will be invariably as much as a half of the concentration of the oxidant. Since the peak current is linearly proportional to the concentration of a depolarizer, it is now easy to see why we obtain the above-mentioned characteristic relation between two cathodic peak currents (R_1, R_2) and the anodic peak current (0). In other words, these results seem to endorse the validity of the dismutation process assumed by Heyrovský. A more detailed investigation is now in progress.

Laboratory of Chemisry, Minami College, Hiroshima University, Hiroshima

* Presented at the discussion on polarography held by the Chemical Society of Japan in November, 1955.

1) M. Shinagawa, H. Imai and H. Sunahara, *J. Chem. Soc. Japan* (in press).
2) B. Breyer, F. Gutman and S. Hacabian, *Australian J. Sci. Resear.*, **3**, 567 (1950).
3) J. Heyrovsky, *Z. Elektrochem.*, **59**, 820 (1955).